Metabolic characterization of the pathogen *Yersinia pseudotuberculosis* and identification of metabolic traits co-regulated with virulence

Von der Fakultät für Lebenswissenschaften

der Technischen Universität Carolo-Wilhelmina zu Braunschweig

zur Erlangung des Grades einer

Doktorin der Naturwissenschaften

(Dr. rer. nat.)

genehmigte

D i s s e r t a t i o n

von Maike Sest
aus Niebüll

1. Referent: Profosseor. Dr. Dietmar Schomburg
2. Referentin: Professorin Dr. Petra Dersch
eingereicht am: 29.05.13
mündliche Prüfung (Disputation) am: 20.08.13

Druckjahr 2013

Vorveröffentlichungen der Dissertation

Teilergebnisse aus dieser Arbeit wurden mit Genehmigung der Fakultät für Lebenswissenschaften, vertreten durch den Mentor der Arbeit, in folgenden Beiträgen vorab veröffentlicht:

Publikationen

Jäger, C., Sest, M. & Schomburg, D.: GC-APCI-MS/MS based identification of metabolites in bacterial cell extracts. (Newsletter-Beitrag) Bruker e-dispatch Separations + Mass Spec July 14 BDAL 24 (2011)

Heroven, A.K., Sest, M., Pisano, F., Scheb-Wetzel, M., Steinmann, R., Böhme, K., Klein, J., Münch, R., Schomburg, D., Dersch, P.: Crp induces switching of the CsrB and CsrC RNAs in *Yersinia pseudotuberculosis* and links nutritional status to virulence. Front. Cell. Inf. Microbio. 2:158 (2012)

Tagungsbeiträge

Sest, M., Schomburg, D.: Identification of growth stage associated metabolite markers in the pathogen *Yersinia pseudotuberculosis*. (Poster) Metabolomics 2010, Amsterdam, Netherlands (2010)

Sest, M., Dersch, P., Schomburg, D.: Revealing insights in metabolic adaptation of *Yersinia pseudotuberculosis* during host colonization. (Poster) Trends in Metabolomics – Analytics and Applications, Frankfurt am Main (2011).

Jäger, C., Sest, M. & Schomburg, D.: GC-APCI-MS/MS based identification of metabolites in bacterial cell extracts. (Poster) Trends in Metabolomics – Analytics and Applications, Frankfurt am Main (2011).

Table of Contents

Abbreviation

A	adenine
Ap	ampicillin
aqua bidest.	double-destilled water
ATP	adenosine triphosphate
bp	base pair
C	cytosine
CDW	cell dry weight
Cm	chloramphenicol
Da	dalton
DNA	desoxyribonucleic acid
EC	enzyme commission number
EI	electron impact ionisation
et al.	and others, lat.: *et alii*
eV	electron Volt
G	guanine
kb	kilobase
kDa	kilo-Dalton
Kn	kanamycin
kV	kilovolt
LB	lysogeny broth medium
LC	liquid chromatography
M	molare
µ	growth rate
mA	milliampere
MeOX	O-Methyloxim group
µg	microgram
mg	milligram
min	minute
µl	microliter
ml	milliliter
mM	millimolare

X

M63	minimal medium 63
MS	mass spectrometer
MSTFA	N-Methyl-N-trimethylsilyl-trifluoracetamid
m/z	mass to charge ratio
NADPH	nicotinamidadenindinukleotid
NCBI	national center for biotechnology information
ng	nanogram
NIST	national institute of standards and technology
nm	nanometer
nM	nanomolare
NMR	nuclear magnetic resonance
nt	nucleotides
dNTP	deoxynucleotide triphosphate
OD	optical density
Ω	ohm
PAGE	polyacrylamide gelelectrophoresis
PCA	principle component analysis
PCR	polymerase chain reaction
PM	phenotyping microarry
pmol	picomol
PPP	pentose phosphate pathway
Q	quadrupol
R	antibiotic resistance
RI	retention index
RNA	ribonucleic acid
rpm	rotations per minute
SDS	sodium dodecyl sulfate
t	time
T	thymine
TCA	tricarboxylic acid
Tet	tetracycline
U	uridine
V	volume

1 Introduction

1.1 The genus Yersinia

Yersiniae are gram-negative rods that belong to the family of Enterobacteriacea and are named after the bacteriologist Alexander Jean Emile Yersin (1863-1943) who discovered *Yersinia pestis* as the causative agent of the bubonic plague. They can be divided into 14 species, whereof three species are pathogenic: *Yersinia pseudotuberculosis*, *Y. enterocolitica* and *Y. pestis*. These three pathogenic species have been completely sequenced (Chain et al. 2004; Thomson et al. 2006; Eppinger et al. 2007; Copeland et al. 2008). The pathogenic bacteria form microcolonies and microabscesses preferentially in the lymphoid tissue of the host. They bypass the host immune response by prevention of lysis by the complement system and inhibition of macrophages and neutrophils (Cornelis 1998).

However, the transmission of the infection and the course of the disease differs greatly between the species. *Y. pestis* is the most infamous of the three, causing the burbonic, septemic and pneumonic plague killing millions of people in the 14th century (Stenseth et al. 2008). The infection is transmitted to humans via flea bites with subsequent proliferation of the bacteria in the lymphatic tissue. *Y. pestis* still causes outbreaks in America, Africa and Asia with hundreds of deaths. It exhibits a rapid clinical course and high mortality if left untreated (WHO 2010).

Several reports indicate that *Y. pestis* originated from *Y. pseudotuberculosis* 1,500 to 20,000 years ago through a process of inactivation and modification of genes resulting in a highly increased virulence and a restricted ability to survive outside the host. The strains carry a high genetic similarity, although *Y. pestis* has two unique plasmids (Achtman et al. 1999; Chain et al. 2004)

Y. pseudotuberculosis and *Y. enterocolitica* have been isolated from environmental samples and domestic and wildlife animals. They are transmitted via the fecal-oral route and cause gut- and lymph-associated diseases known as Yersiniosis, describing enteritis, terminal ileitis and mesenterial lymphadenitis but also autoimmune diseases like reactive arthritis and erythema nodosum (Bottone 1997; Kaasch et al. 2012).

The infections are usually non-lethal for humans, but can spread into the blood stream in immuno-compromised patients causing a sepsis. The infection is fatal for certain animals such as rodents and can lead to losses in cattle (Tauxe 2004). The distribution of the bacteria is worldwide. Very recently a consumer report study found that 69 % of raw pork meat was contaminated with *Y. enterocolitica* in the U.S.A. (Consumer Reports 2013) and an outbreak of *Y. pseudotuberculosis* infections has been reported in Finland (Nuorti et al. 2004)

1.2 The metabolic characteristics of Y. pseudotuberculosis

The pathogenic *Y. pseudotuberculosis* are chemoheterotroph and can also live facultative aerobe. *Yersiniae* can proliferate at low temperatures at 4 °C such as in cold storage of food but also at temperatures up to 43 °C. 30 °C is considered as optimal growth temperature. At temperatures below 30 °C, *Y. pseudotuberculosis* is motile and exhibits flagella (Carniel et al. 2006). Experimental studies and genome annotation confirm, that *Y. pseudotuberculosis* exhibits a complete glycolysis, the pentose phosphate pathway (PPP) as well as the Entner-Doudoroff-pathway, which are all utilized in parallel to different extent depending on the carbon source (Brubaker 1968). A functional citrate cycle is also annotated and also all amino acid biosynthesis pathways, together with the main anapleurotic reactions including the glyoxylate shunt. Under anaerobic conditions the bacteria perform mixed acid fermentation, which is characteristic for *Enterobacteriaceae*. Metabolic features of *Y. pseudotuberculosis* are the lack of lysine decarboxylase, ornithine decarboxylase, arginine dihydrolase and phenylalanine deaminase activities, which can be used to distinguish them from other *Enterobacteriaceae* (Carniel et al. 2006).

Here, the *Y. pseudotuberculosis* serotype O:3 strain YPIII was investigated. Its genome is a circular chromosome consisting of 4,689,441 bp with an average GC content of 47.5 % and 4,313 genes (Copeland et al. 2008, NCBI Genome GenBank NC_010465). Additionally, *Y. pseudotuberculosis* harbors one 70 kb plasmid (pYV), that encodes a type III secretion system as well as several virulence associated genes, but no genes related to metabolic functions (Carniel et al. 2006). The program *Enzyme Detector* (Quester & Schomburg 2011) integrates the annotation of several databases such as KEGG, NCBI, Pedant and SwissProt to generate a consensus annotation. It predicts *in silico* 1280 enzyme encoding genes (with a relevance over 7) in the chromosome of the strain YPIII.

Additionally, the database *Metacyc* (Caspi et al. 2010) 278 genes encoding transport proteins, which catalyze 175 transport reactions. Further, 24 two-component systems are identified in *Yersiniae* by comparison with other species (Marceau 2005). These information suggest, that YPIII possess a variety of uptake system and comprehensive synthesizing abilities.

1.3 Lifestyle of Y. pseudotuberculosis

Y. pseudotuberculosis can live in a multitude of environments and has been isolated from plants, soil and water (Tauxe 2004). The bacteria can survive over several weeks in water and several months in soil (Buzoleva & Somov 2003).

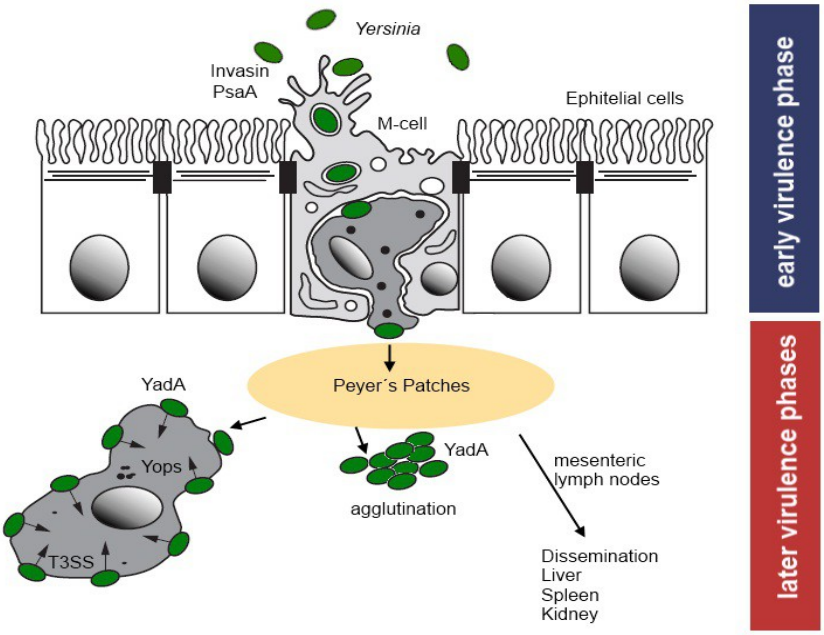

Figure 1.1: Infection route of *Y. pseudotuberculosis* (green) in the ileum. During early phase of infection Invasin and PsaA are used to adhere and invade the M-cells The bacteria cross the intestine epithelial layer through the M-cells from where it reaches the Peyer´s patches. In the later phases of the infection *Y. pseudotuberculosis* surpresses expression of these factors and induces the expression of the adhesion factor YadA and the type three secretion system (T3SS), which translocates the Yop effector proteins into the host phagocytes to prevent phagocytosis and to disseminate into deeper tissues (adapted from Sansonetti 2002).

From food or water it is taken up through the oral route. It passes through the gastrointestinal tract and enters the small intestine, where it adheres in the lowest part, the ileum, to the M-cells (microfold cells) (Isberg & Barnes 2001). M-cells are specialized cells of the host immune system integrated in the epithelial cells of the ileum (figure 1.1).

They take up antigens via endocytosis or phagocytosis to transport them to the Peyer's patches. These are lymphoid follicles located around the ileum. The bacteria proliferate in the Peyer's patches and are able to immigrate from there to the underlying tissue and proliferate extracellularly (Simonet et al. 1990). Usually the infection causes a mesenteric lymphadentitis in patients with intact immune response, which is essentially self-limiting and ceases after several days.
In mice the bacteria spread into the surrounding organs and infect liver, spleen and kidney with subsequent death of the host animal after approximately nine days. An alternative route where liver and spleen infection is independent from colonization of the Peyer's patches and the mesenteric lymph nodes has been proposed (Barnes et al. 2006).

1.4 Virulence effectors of Y. pseudotuberculosis

For initiation and establishment of the infection of *Y. pseudotuberculosis* a set of specific proteins is needed to adhere and invade the host cells and to counter the host immune defense. These proteins are termed virulence factors and the most important ones are shown in figure 1.1. They can be roughly divided into virulence factors present during early stages of infection and factors expressed during later stages of infections. In early stages of the infection when the bacteria enter the ileum in the host, they need to adhere to the M-cells. This is done through the virulence factor **Invasin**, an outer membrane protein encoded by the gene *inv* on the chromosome. Invasin belongs to the adhesins and binds to the β_1-integrins at the luminal side of the M-cells. The binding leads to the uptake of the bacterium into non-phagocytic cells by a zippering mechanism (Dersch & Isberg 2000). The deletion of *inv* leads to a reduced initial colonization of the Peyer's patches, but does not influence the later infection. In later stages of infection Invasin is not expressed to avoid recognition by the immune system (Marra & Isberg 1997). The expression of Invasin is subject to many environmental factors such as pH, temperature, growth phase and nutrient availability, whereas it is maximally expressed at moderate temperatures in late stationary growth phase in complex media (Revell & Miller 2000; Nagel et al. 2001).
During the ongoing infection of the host, *Y. pseudotuberculosis* colonizes the Peyer's patches and mesenteric lymph nodes, from where it penetrates deeper tissues through the action of a different sets of virulence factors (figure 1.1) such as the outer membrane protein **Yersinia adhesin A** (**YadA**). It is encoded by *yadA*, which is located on the

virulence plasmid pYV. The adhesion protein forms oligomers, consisting of 41 to 44 kDa monomers and binds to β_1-integrins of mammalian cells using the extracellular matrix protein fibronectin as bridging molecules. The binding activates signaling pathways of the host immune defense. (Eitel et al. 2005). Additionally, the head domains of YadA mediate autoagglutination and hemagglutination of the bacteria, leading to the formation of microcolonies and resistance of neutrophil attacks (Eitel & Dersch 2002).

Further, *Y. pseudotuberculosis* expresses a **type III secretions system (T3SS)**, which translocates **Yersinia outer membrane proteins (Yops)** from the bacterium into the host cell in the later stages of infections (figure 1.1). The T3SS is assembled through several of the Yersinia secretion (Ysc) proteins (YscC, D, J, N ,Q, R, S, T, U, V), which are well conserved between the three pathogenic *Yersinia* species (Diepold et al. 2010). The aforementioned Yops counteract the defense mechanism of the host. Some of them support the translocation by functioning as secretion channel plugs that open the T3SS needle (YopN, TyeA, LcrG), whereas others show pore forming activity (YopB, YopD). Yops, that are transferred into the host cell, consisting of YopH, E, T, O, J, M, fulfill various functions, primarily to hinder the host immune response and promote survival of the bacteria (Viboud & Bliska 2005; Ruckdeschel et al. 2008). The genes encoding both the T3SS and Yops are located on the virulence plasmid pYV.

The late virulence factors such as YadA, T3SS and the Yops are maximally expressed at 37 °C during exponential phase in minimal medium (Nagel et al. 2001; Eitel & Dersch 2002).

Y. pseudotuberculosis possesses other factors associated with virulence, of which the function is not fully understood. One of them is the **pH 6 antigen (Psa),** an adhesion factor, that induces adhesion to mammalian cells in the absence of Invasin, but no uptake of the bacteria is mediated after adhesion via this factor (Yang et al. 1996). Psa is the product of the gene *psaA,* which requires the expression of *psaBC* and *psaEF,* the transcriptional regulators of *psaA*. It is expressed in *Y. pseudotuberculos*is at 37 °C under acidic conditions. In *Y. pestis* Psa promotes resistance to phagocytosis and its deletion leads to attenuated virulence after intravenous infection and (Price et al. 1995; Huang & Lindler 2004).

The **lipopolysaccharides (LPS)** of *Y. pseudotuberculosis* clearly play an important role in virulence and their composition as well as their regulation is subject to several studies (Bengoechea et al. 2002; Skurnik 2003; Rebeil et al. 2004). They are composed of lipid A

and O-polysaccharides (O-antigens), with most biological effects caused by lipid A. Nevertheless, the O-antigens play an important role in host colonization, serum resistance and resistance to antimicrobial peptides. Mutants, lacking the O-antigen or with altered composition, showed significant attenuated virulence (Skurnik 2003). The O-antigen structure changes in response to temperature and growth stage, thereby it is less expressed at 37 °C in stationary phase (Skurnik 2003).

1.5 Regulatory factors of Y. pseudotuberculosis *controlling virulence*

The *Yersinia* regulatory networks are organized hierarchically with master regulators, that control other regulators which in turn influence subgroups of genes. So far a number of approximately 250 transcriptional regulators has been identified in *Y. pestis* (Marceau 2005). On the following pages the key regulators of virulence in *Y. pseudotuberculosis* are shortly introduced (figure 1.2). The expression of virulence factors is tightly adjusted to the stage of infection, which requires a suitable regulation to react appropriately to the environment. The most prominent stimulus concerning regulation in *Yersinia* is temperature but also other environmental signals as pH, nutrients, osmolarity and oxygen tension. Sensing these stimuli and coordinating the response is the main function of the regulatory network.

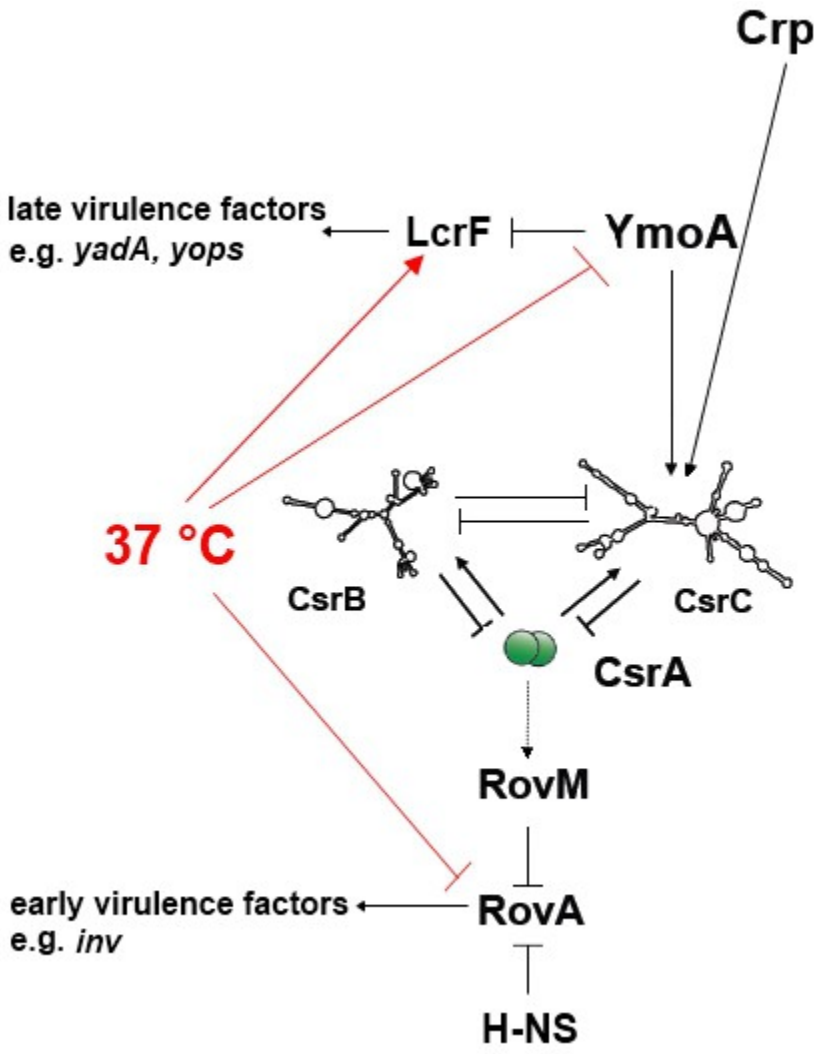

Figure 1.2: Interconnection of the regulatory network controlling expression of virulence factors in *Y. pseudotuberculosis.* Adapted from (Heroven & Böhme et al. 2012)

1.5.1 The virulence regulator RovA

The Invasin expression is regulated by the yersinia specific regulator protein RovA (Nagel et al. 2001). The protein is a homologue to SlyA, which is a global transcriptional activator of the MarR family. RovA is a 15 kDa transcriptional activator with a central helix-turn-helix motive, responsible for DNA binding. The regulator forms a dimer (figure 1.3) and binds in regions within in the *inv* promoter (Nagel et al. 2001). It is also self inducing by binding to its own promoter (Heroven et al. 2004). Its expression is similar to that of Invasin and is dependent on growth phase, nutrition and temperature as well.

The protein is thermosensing and appears to be thermally unstable at elevated

temperatures, which impairs the DNA binding affinity. As a result, transcription of *rovA* and *inv* is reduced at 37 °C. Additionally, RovA is subject to protease digestion, especially during exponential growth (Herbst et al. 2009).

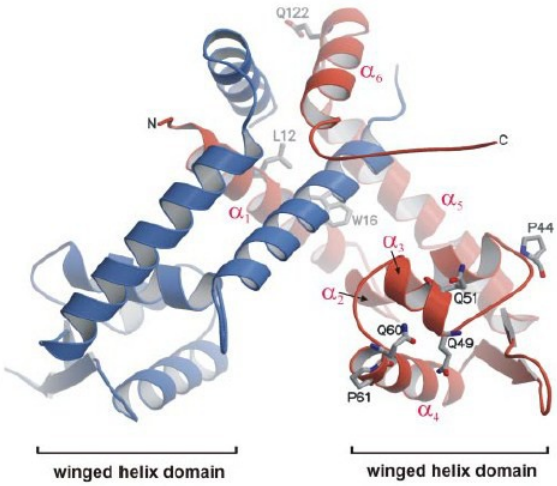

Figure 1.3: Structure of the thermosensing regulator RovA as dimer. One monomer is shown in red and the other in blue. From (Tran et al. 2005)

The deletion of RovA in *Y. pseudotuberculosis* leads to a dramatic loss of virulence, when infection occurred over the Peyer's patches (Dube & Handley 2003). Interestingly mutants, where only *inv* was deleted, showed less attenuated virulence then *rovA* deletion mutants (Revell & Miller 2000; Dube & Handley 2003), which indicates a regulatory effect of RovA to more targets than just *inv*.

1.5.2 The nucleoid-associated protein H-NS

One repressor of RovA is the heat-stable nucleoid-structuring (H-NS) protein, a nucleoid-associated protein, which forms dimers, and is known to organize chromosomal DNA. It acts mostly as a transcriptional repressor (Dorman 2004). H-NS shows an affinity to virtually all bindings sites of RovA in *Y. enterocolitica.* The ability of RovA to replace H-NS is believed to be an important step for derepression of H-NS mediated repression (Ellison & Miller 2006). In most *Yersinia* strains H-NS acts as a repressor for both *rovA* and *inv* (Heroven et al. 2004; Ellison et al. 2004).

1.5.3 The RovA antagonist RovM

Another factor involved in repression of *rovA* is the LysR-type regulator RovM, which

binds prior to the promoter region of *rovA* and down-regulates the expression in cooperation with H-NS. In the absence of H-NS, *rovA* repression through RovM is inhibited, showing that both proteins are required for efficient repression (Heroven & Dersch 2006). RovM shows homology to the PecT/HexA regulator of the *Erwinia* species (Heroven & Dersch 2006) and is maximally expressed in minimal medium, hence mediates medium dependent repression of *rovA*. RovM synthesis is not influenced through temperature or growth state, indicating that *rovA* expression is regulated through other factors under these conditions. The *rovM* deletion mutant is more virulent than the wild type and can be detected in higher numbers in the gut-associated lymphatic tissues and organs. Contrary, overexpression of RovM had a positive effect on flagellar motility. The strain was also less virulent and fewer bacteria were found in both, the Peyer's patches and the mesenteric lymph nodeas. Moreover the strain was not able to disseminate into deeper tissue. These findings suggest that RovM might control more genes besides *rovA* (Heroven & Dersch 2006).

1.5.4 The RNA-binding protein CsrA

The regulator RovM itself is regulated by the carbon storage (Csr) system (Heroven et al. 2008). The Csr system has also been identified in *E. coli* and *Salmonella* where it is known as repressor of stationary phase metabolites (Rsm). The system consists of the RNA-binding protein CsrA and two regulatory RNAs: CsrC and CsrB. The CsrA protein forms a dimer of 18 kDa. It usually binds the Shine-Dalgarno sequence of its target mRNAs and represses the translation initiation. The regulatory RNAs CsrC and CsrB form secondary structures with hairpin loops and are able to bind to the CsrA protein thereby inhibiting its binding to other factors (Majdalani et al. 2005). A scheme of this interaction is displayed in figure 1.4.

In *Y. pseudotuberculosis* CsrA was identified to indirectly upregulate *rovM* expression. Moreover, CsrA is responsible for the medium dependent regulation of *rovA* through RovM (Heroven et al. 2008). CsrC is expressed in complex medium during stationary phase, whereas it is absent in minimal medium. Through this media-dependent expression of CsrC, RovA synthesis is promoted via inhibition of CsrA and RovM (Heroven et al. 2008).

CsrA is a global regulator not only affecting virulence but also flagella synthesis and carbon metabolism. A CsrA lacking mutant exhibits severe attenuation in growth, loss of

flagella and motility. Moreover the morphology is altered: Deletion of CrsA leads to short, thick, rod shaped cells, while overproduction leads to long flagellated filamentous cells (Heroven et al. 2012).

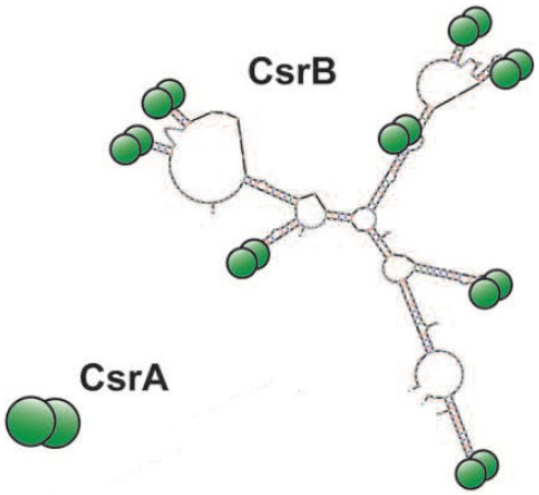

Figure 1.4: Interaction between the CsrA protein (green) and the regulatory RNA CsrB. CsrB and CsrC form highly structured molecules with multiple hairpins and are able to bind several CsrA proteins and prevent them from binding their target site. Modified from Heroven et al. 2012.

In *E. coli* CsrA is essential for growth on glycolytic carbon sources, represses glycogen metabolism, gluconeogenesis and biofilm formation and activates glycolysis and acetate metabolism (Romeo 1998, Timmermans & Van Melderen 2009). A *csrA* deletion mutant is unable to grow on glucose and fructose-6-P as sole carbon source because the carbon flux is directed to glycogen synthesis, yet the mutant grows on pyruvate (Timmermans & Van Melderen 2009).

1.5.5 The histone-like proteine YmoA

Another protein plays a major role in the regulation of virulence, the Yersinia modulator A (YmoA). The 8 kDa histone-like protein of *Yersinia* is homologue to the Hha regulator protein in *E. coli* and *Salmonella* and shares the same functionality (Mikulskis & Cornelis 1994). In *Y. enterocolitica* the deletion of *ymoA* is lethal (Ellison et al. 2003). There, YmoA downregulates the expression of the virulence factor invasin at moderate temperatures, probably together with H-NS as a repression complex (Ellison & Miller 2006). It is proposed that YmoA is responsible for the temperature and growth phase-dependent regulation of the Yersinia-enterotoxin and invasin in *Y. enterocolitica* (Ellison et al. 2003; Mikulskis & Cornelis 1994). In *Y pestis* YmoA is degraded at 37 °C through the proeases

ClpXP and Lon. Deletion of *lon* and *clp* leads to repressed expression of virulence factors at elevated temperatures (Jackson et al. 2004). In *Y. pseudotuberculosis* YmoA deletion leads to an extreme reduction of RovA, Invasin and CsrC expression but to an induction of RovM expression. This effect is probably mediated through indirect repression of CsrC in the absence of YmoA.

In *E. coli* and *Salmonella* the homologue Hha regulator represses the expression of virulence factors in response to environmental signals as low temperature and high osmolarity (Mouriño et al. 1996; Mouriño et al. 1998; Jones 2005).

1.5.6 LcrF and low calcium response

A central regulator of the late virulence factors is LcrF, a transcriptional activator of the AraC family and a homologue of VirF in *Y. enterocolitica*. The *lcrF* gene is located on the pYV plasmid. The regulator protein activates the expression of YadA and the Yops, while itself is subject to repression through YmoA. Additionally to the regulation through YmoA the *lcrF* mRNA undergoes conformational changes at higher temperatures, leading to increased translation at 37 °C.

LcrF is part of the low calcium response, which describes the increased secretion of Yops in Ca^{2+}-poor media at 37 °C. In the absence or millimolar concentrations of Ca^{2+} the T3SS is blocked and no Yops are secreted (Fowler & Brubaker 1994). Additional transcription of Yops is repressed. The calcium concentration in the cytoplasm of a cell is lower than in the extracellular fluid and could therefore be the signal to release the Yops in proximity of a target cell. Besides LcrF at least three other proteins are involved in the low calcium response (Marceau 2005).

1.5.7 The global regulator Crp

One of the global regulators of virulence and metabolism is the cyclic AMP receptor protein (Crp). Crp is activated by the binding of cAMP and controls the transcription of the target genes as a complex. The presence of glucose reduces the levels of cAMP and Crp, thus reducing the activation of controlled genes. This mechanism is known as carbon catabolite repression (CCR).

Crp is the most important regulator of carbon flux under glucose limitation in *E. coli* and controls over 100 promoters (Nanchen et al. 2008). Recent studies indicate that not all

target sites have been recognized and an even higher number of binding sites has been proposed (Shimada et al. 2011). In *Y. pestis* 37 genes or operons are under direct control of Crp, including other regulatory proteins (Zhan et al. 2008). Especially the genes needed for the catabolism of non-glucose carbon and energy sources are activated through Crp.
Crp is also recognized as virulence regulator in several pathogenic bacterial species including *Y. pestis* (Zhan et al. 2008), *Y. enterocolitica* (Petersen & Young 2002), *Vibrio cholerae* (Skorupski & Taylor 1997) and *Mycobacterium tuberculosis* (Rickman & Scott 2005). The deletion of *crp* in all three pathogenic *Yersinia* species results in the massive reduction of virulence (Petersen & Young 2002, Zhan et al. 2008; Heroven et al. 2012). Several genes encoding Yops and compartments of the T3SS were affected through the Crp-cAMP complex and showed regulation in response to glucose. In addition to the attenuated virulence *Y. enterocilitica* Crp deficient mutants were restricted to the Peyer's patches and mesenteric lymph nodes and could not establish infection in deeper tissues (Petersen & Young 2002). In *Y. pseudotuberculosis* Crp also affects RovA and Invasin expression through the Csr-system (Heroven et al. 2012).

1.6 Interplay of metabolism and virulence

1.6.1 Survival in different milieus

Prior and during the infection process, *Y. pseudotuberculosis* is exposed to changing environments and tissues. It has to survive for long terms in cold and nutrient-poor milieus such as water and soil (Buzoleva & Somov 2003). A life-style as saprophyte has also been proposed (Dreyfus & Brubaker 1978). After transmission into the host the pathogen first has to withstand the acidic pH of the stomach for about 2 h and later compete for nutrients in the intestine with resident bacteria (Eckburg et al. 2005; Flint et al. 2007). A successful replication in the intestine appears to be necessary to establish the infection (Barnes et al. 2006). Finally, for long term survival and proliferation in the Peyer's patches and the extracellular space in the lymphatic tissue and organs the bacterium must withstand the host immune response and also adapt its metabolic requirements to its surroundings. There, it has to survive with the nutrients available cytoplasm of host cells or in the lymph, in the intestinal fluid or in plasma. The biosynthesis and secretion of virulence factors as Yops in later stages of infection are highly demanding for the metabolism and result in diminished

growth *in vitro* (Ramamurthi & Schneewind 2002). The metabolism has to be subject to fast regulation and coordination, with a wide capacity for adaption.

1.6.2 Metabolism of pathogenic bacteria in the host

The intestine

The ileum, where *Y. pseudotuberculosis* has to persist and replicate to initiate the infection (Barnes et al. 2006), is considered to be low in oxygen tension. In the intestine most available carbon sources come from mucosal polysaccharides and indigestible polysaccharides (as cellulose and pectin). Further, the mucus contains glycoproteins, glycolipids, proteins and lipids (Conway & Cohen 2006). The polysaccharides are degraded through extracellular glycosyl hydrolases of resident microbes. In *E. coli* several pathways utilizing the mucus-derived saccharides have been identified as crucial for initiation and maintenance of colonization of the mouse intestine. Thereby gluconate, N-acetylglucosamin and sialic acids are important for initiation and glucuronate, mannose, fucose and ribose are important for maintenance (Chang et al. 2004). The study also showed that the glycolysis and the Entner-Doudoroff-pathway were crucial for colonization and maintenance in the intestine, whereas the TCA cycle, the PPP and gluconeogenesis were not (Chang et al. 2004).

Another potential carbon source in the intestine is deoxyribose, derived from DNA degradation of shed colonic epithelial cells. The ability to degrade deoxyribose is encoded on the *deoK* operon which is associated with pathogenicity and an increased ability to colonize the gut (Martinez-Jéhanne et al. 2009).

Intra- and extracellular growth

The cytosol of an average mammalian cell has not been completely characterized for its nutritional content yet. It provides a neutral pH (7.1 – 7.4) (Bright et al. 1987) and a reducing environment. In a typical cell the cytosol contains about 0.5 mM magnesium, 5-15 mM sodium, 10^{-4} mM calcium ions and 140 mM potassium (Ray et al. 2009). Through studies with auxotrophic mutants, the available nutrients were proposed to be serine, proline and glycine as well as hexose phosphates and pyruvate. Aromatic amino acids, threonine and adenine were limiting for bacterial growth of auxotrophic mutants. Also, auxotrophic mutants could not grow in the cytosol if they required guanine, thymine,

histidine, diaminopimelate, phenylalanine, tryptophan, tyrosine or aminobenzoate (Ray et al. 2009).

The interstitial fluid surrounds the cells of multicellular organisms and resembles blood plasma. The concentrations of ions are different from those in the cytosol and less proteins are present. It is established that approximately 2.5 mM calcium and 1.5 mM magnesium ions are contained. The concentration of glucose in biological fluid is proposed to be about 7 mM (Rosso et al. 2008).

Recent studies showed that for the intracellular pathogenic bacterium *Listeria monocytogenes* glycerol may serve as an important carbon source (Eylert et al. 2008). Another study implies that glucose and glucose-6-phosphate might not be the most important carbon source for intra- and extracellular growing *E. coli* and *S. enterica* (Götz & Goebel 2010). However, glycolysis is required for survival of *S. enterica* in macrophages and is essential for systemic infection in mice (Bowden et al. 2009). However, several studies indicate strain specific differences in the carbon source preference of pathogenic bacteria, even if the strains are highly related (Le Bouguénec & Schouler 2011).

Fatty acid degradation is an important carbon and energy source for pathogenic microorganisms in host tissue. Fatty acids are degraded using beta-oxidation and the glyoxylate bypass generating precursor for gluconeogenesis in many species as *S. typhimierium*, *Mycobacterium. tuberculosis* and *Candida albicans* (Somerville & Proctor 2009). Deletion of isocitrate lyase, the key enzyme of the glyoxylate shunt, leads to attenuated persistence and virulence of *M. tuberculosis* (McKinney et al. 2000).

In the enteroinvasive *E. coli, S. enterica* and *L. monocytogenes* most amino acids are taken up from the host and become directly incorporated, when grown intracellular in the cytosol, or in *Salmonella*-containing-vacuole and macrophages (Eylert et al. 2008, Götz et al. 2010). For many intracellular bacteria including *Chlamydiae* and *Mycobacteria*, tryptophan is an essential amino acid, required to be present in the host (Schaible & Kaufmann 2005).

1.6.3 Connection between metabolism and virulence in other pathogenic bacteria

Connections between metabolism and virulence have been noted in several pathogenic

species and can occur in different ways (Rohmer et al. 2011): (I) The acquisition of metabolic pathways can allow colonization of new habitats like the utilization pathway for sialic acids in *Vibrio cholerae* (Jermyn & Boyd 2002). (II) The loss of synthesizing pathways occurs when metabolites are readily available in the host, leading to genome reduction (Sakharkar et al. 2004). Also, the loss of pathways for other reasons can be an advantage for pathogenicity, e.g. the loss of the lysine decarboxylase in *Shigella*. The product of lysine decarboxylase inhibits the enterotoxin activity and thereby attenuates virulence (Maurelli et al. 1998). Similar mechanism, might have occurred in *Y. pestis*, where some metabolic functions are lost in the cysteine and aspartate metabolism, as well as PPP compared to *Y. pseudotuberculosis* (Chain et al. 2004). (III) Metabolic signals can regulate virulence factor expression. Iron depletion is a signal for many pathogensto sense the host surroundings (Skaar 2010). Further, carbon catabolite repression, amino acid and fatty acid limitation can trigger either activation or repression of virulence factors (Poncet et al. 2009; Dalebroux et al. 2010, Le Bouguénec & Schouler 2011). In *Staphylococci* the TCA cycle activity controls the expression of several virulence factors (Somerville & Proctor 2009). (IV) Virulence associated regulators can co-regulate metabolic traits. Recently, a virulence factor in *Y. enterocilitica* has been proposed to directly interact with the regulation of the metabolism. The phosphoenolpyruvate carboxylase (PEPC) interacts with the virulence factor YscM1 (LcrQ in *Y. pseudotuberculosis*), which leads to an inactivation of the PEPC, when the concentrations of YscM1 are high enough. Since PEPC plays an important role in the anapleurotic reaction to refill the oxcaloacetate in the TCA cycle, this results in a significant alteration in the carbon flux (Schmid et al. 2009).

1.6.4 Metabolic processes associated to the pathogenic nature of Y. pseudotuberculosis

As described before, pathogenic bacteria face a challenging environment while colonizing the host. Most pathogens have specialized metabolic traits that are adjusted for in-host survival. *Y. pseudotuberculosis* possesses some metabolic properties that are associated with pathogenicity, which are shortly described in the following sections. Nevertheless, this introduction is far from being complete, since not all features have been fully discovered and understood, yet.

Urease

All *Yersinia* species exhibit urease activity with the exception of *Y. pestis*. The enzyme requires nickel to be functional and is encoded by the genes *ureA*, *ureB* and *ureC*. The incorporation of nickel is mediated via the gene products of *ureE*, *ureF*, *ureG* and *ureD,* which are highly homologous between the *Yersinia* species (De Koning-Ward & Robins-Browne 1996). Urease activity is not induced by the presence of urea or the limitation of nitrogen. The genes are mostly expressed in stationary phase, independent from current temperature. The enzyme exhibits highest activity at acidic pHs and low urea concentration, which resembles the condition in the gastric juice (De Koning-Ward & Robins-Browne 1997). The presence of urease indicates a partial lifestyle as saprophyte, with urea being the most common nitrogen source. It has also been proposed that urease could function as a protection system against the acidic stress in the stomach by raising the pH in a microenviroment (De Koning-Ward & Robins-Browne 1995; Hu et al. 2009).

Iron acquisition

Iron acquisition systems are regularly considered as virulence factors themselves, reflecting their importance regarding the virulence of pathogenic bacteria.

The concentrations of free iron in the mammal body are very low (~ 10^{-18} M), because most iron is bound by the iron storage protein ferritin or is complexed within heme. The available free iron is considerably less than the concentration needed for growth of bacteria (~ 10^{-6}M). The ability to successfully establish an infection in the host depends on the acquirement of iron. Patients with iron-overload can develop systemic infection through *Yersinia* species, that are normally restricted to the intestine (Carniel 2001). Bacteria contain proteins called siderophores with high affinity to iron, that can compete for iron binding with the iron loaded proteins of the host.

Y. pseudotuberculosis synthesizes a siderophore named Yersiniabactin, which is expressed at low temperatures and is positively regulated by the Fur-regulator (Carniel et al. 1996; Carniel 2001). The genetic elements of the siderophores are located in the high pathogenicity island (HPI) of the Y*ersiniae* species and are crucial for virulence (Carniel 2001). Other than its own siderophores, *Y. pseudotuberculosis* is also able to utilize other siderophores as ferrioxamine, enterochelin and deferoxamine produced by other bacteria species.

Polyamine biosynthesis

Yersiniae produce two main polyamines: putrescine and spermidine. These are generated from ornithine and arginine over two independent synthesis pathways (Wortham et al. 2007). Polyamines act in a variety of capacities. They bind RNA and DNA and stabilize them. Additionally, a role in transcription is proposed (Igarashi & Kashiwagi 2010) and the involvement of polyamines in *Y. pestis* biofilm formation has been noted (Wortham & Oliveira 2010).

Sialic acid utilization

Yersiniae can utilize sialic acids as sole source of carbon and energy due to the presence of the *nan* operon (**N**-**a**cetyl**n**euraminate catabolism), which is associated with pathogenic bacteria (Almagro-Moreno & Boyd 2009). Sialic acids are the derivatives of neuraminate and are ubiquitous in human mucus especially in the lung and in the intestine. The ability to access and utilize these sugars is very limited in bacteria and provides them with a selective advantage in the human gut. It was shown for *E. coli* that utilization of sialic acids is essential for colonization of the mouse intestine (Chang et al. 2004).

1.6.5 Temperature as a factor influencing virulence and metabolism

Although bacteria face many environmental stimuli, the greatest influence on the regulation of virulence factors in *Yersiniae* is the temperature (Marceau 2005). Most bacteria sense temperature increase as a signal for the entrance in the host. The sensing of temperature variations can occur in various ways in bacteria: With accumulation of denatured proteins during heat shock, through stalled ribosomes during cold shock and by thermosensing regulators, which have been described as acting on transcriptional, translational and post-translational level.

The influence of temperature completely changes the expression of virulence factors in *Y. pseudotuberculosis*: Invasin, the O-antigen of LPS, flagella and iron scavenging systems are maximally expressed at 25 °C and weakly expressed at 37 °C, to allow fast adherence and uptake of the bacteria into the host, for initiation of the infection.

At 37 °C the pH 6-antigen, T3SS, Yops and YadA are induced, mediating adherence, serum resistance and preparation of the bacterium against the immune response of the host.

RovA, LcrF and YmoA are temperature sensing regulators and undergo conformational changes during temperature shift or, in the case of LcrF, conformational changes of the

mRNA. (Hoe & Goguen 1993; Jackson et al. 2004; Herbst et al. 2009). These regulators are predominantly responsible for the temperature mediated changes, though the presence of so far unrecognized regulators mediating temperature control has been suggested (Marceau 2005). It has been noted that the nutritional requirement may change as a result of temperature elevation in *Y. pseudotuberculosis* (Bochner 2009). This has also been observed in the closely related *Y. pestis* where the bacteria required more additives at 37 °C to promote growth (Hills & Spurr 1952). The changes in the metabolism of *Y. pestis* upon temperature shift from 26 °C to 37 °C involve the inhibition of glycolysis and preference for terminal oxidation of different substrates. Genes involved in nitrogen assimilation, biosynthesis of amino acids and purines were upregulated (Motin et al. 2004).

1.7 Systems biology

This thesis elucidates the connection between virulence and metabolism with the approaches of systems biology. This field of research investigates the composition, structure and dynamic of a cell as a system. The utilized methods are unbiased and therefore not focused on expectations. The investigation of the cell as a system, and not as several, independent processes, is a tribute to the true nature of a cell, where all activities are interconnected. The advantage is, that only through global observations connections between seemingly unrelated fields can be recognized. benefit of

Systems biology uses recent achievements in technologies and computational methods, to raise and evaluate multitudes of data to describe and characterize the dynamic processes in a cell. Commonly applied methods are the investigation of the genome, the transcriptome, the proteome and the metabolome. The advantages and disadvantages as well as recent discoveries with the methods of systems biology have been extensively reviewed (Fiehn 2001; Kell 2004; Barabási & Oltvai 2004). Here, predominantly the analysis of the metabolome and the transcriptome were applied.

1.7.1 Metabolomics

The metabolome describes all metabolites in a cell, under defined conditions, at a single time point. It is known to be highly dynamic, with enzymatic turn-overs on a subsecond timescale and responses sensitively to environmental changes. The metabolome is also

highly diverse, comprising substances with different concentrations as well as chemical and physical properties. It is considered to represent the actual phenotype of the cell since it displays the response to all other "-omes" (Fiehn 2002). The research on the composition of the metabolome is named metabolomics and has recently gained some interest. It has been reviewed several times (Glassbrook et al. 2000; Scholz et al. 2004; Oldiges et al. 2007)

The diversity of the constituents of the metabolome represents a challenge for detection. Even the combination of several technologies does not allow a complete measurement. Therefore, several sub research areas have emerged focusing on metabolites, that are related to known pathways (Metabolite profiling), that are secreted (Metabolite footprinting), that are unpolar (Lipidomics) and that allow designation of the main carbon fluxes (Fluxomics). The most prominent applied technologies are based on mass spectrometric detection and identification with optional combination of chromatographic techniques like gaschromatography (GC-MS), liquidchromatography (LC-MS) as well as nuclear magnetic resonance spectroscopy (NMR) (Dunn et al. 2005).

1.7.2 Transcriptomics

Transcriptomics, also referred to as expression profiling, analyzes the relative abundance of RNAs in a cell population under defined conditions at a specific time point. For the analysis predominantly custom-made DNA microarrays are applied, allowing a high-throughput approach. Knowledge of the complete sequence of the genome is necessary for using this hybridization based method. Due to the more uniform nature of RNAs compared to metabolites the complete detection can be performed with one technology that, however, is constantly further developing (Wang et al. 2009).

1.8 Objectives

The virulence and the virulence regulation in *Y. pseudotuberculosis* and other pathogens, have been subject to many studies and reviews in the past. Through the increasing possibilities to generate and evaluate large quantities of data on genome, transcriptome and proteome level, new regulatory networks have been unraveled. In most of these global studies the interest was focused solely on the virulence associated traits though the

collected data showed many metabolic connections, which not have been regarded as important until now. Only recently, with the emerging possibilities in metabolome and fluxome technologies, this field has gained interest again, showing that in many cases metabolic abilities are as crucial for pathogenicity as virulence effectors.

This study concentrates on the metabolome of the pathogenic bacterium *Y. pseudotuberculosis* under various conditions, with particular interest in its virulence phases. Several environmental stimuli like temperature, growth stage and nutrient availability are known to fundamentally influence the expression of virulence factors and are proposed to also influence the metabolism, which is investigated here.

Further, the study looks into the recently discovered regulation network based on the virulence regulators RovA, RovM, CsrA, YmoA and Crp, analyzing their effect on the metabolome and investigating potential co-regulation of virulence and metabolism.

Through these experiments a general understanding of the catabolic and anabolic properties of the bacterium shall be generated and metabolic traits that are potentially important for virulence are to be identified. The improved understanding of these processes may support the development of more effective therapies against *Yersinia* infections.

2 Material and Methods

2.1 Equipment and Instruments

All Instruments used in this study are listed in table 2.1 Instrument present at the Helmholtz center for infection research are marked with HZI.

Table 2.1: Equipment

Equipment	Manufacturer
Autosampler	
Autosampler AS3000	Thermo Scientific
Autosampler MPS 2XL	Gerstel
Gas chromatograph	
7890 Agilent GC	Agilent Technologies
Finnigan TRACE GC	Thermo Scientific
TRACE GC Ultra	Thermo Scientific
Mass spectrometer	
Leco Pegasus 4D GCxGC-TOFMS	Leco Instruments
DSQII	Thermo Scientific
Finnigan TRACE MS	Thermo Scientific
Centrifuge	
Centrifuge 5424	Eppendorf
Centrifuge 5810R	Eppendorf
Incubator	
Certomat BS-1 (orbit:50 mm)	Sartorius
Incubator BD 53	Binder
Other	
Agilent 2100 Bioanalyzer (HZI)	Agilent Technologies
Autoclave Varioklav 135 S	H + P Labortechnik
3-place manifold	Millipore
Balance Discovery DV214C	OHAUS
G:BOX	Syngene
Heat block	VWR International
Homogenizer Precellys 24	Peqlab
Ice machine Endos AF80	Scotsman Ice Systems
Infinite M200 NanoQuant	Tecan
Magnet stirrer IKAMAG RCT classic	IKA-Werke
Microscope Axiostar plus	Carl Zeiss
Microwave HMT 842C 1300W	Bosch

Equipment	Manufacturer
Mix Mate	Eppendorf
Nanodrop (HZI)	Peqlab
OmniLog-Incubator/Reader	Biolog
pH-Meter inoLab pH 720	WTW
Photometer Genesys 6	Sysmex Digitana
Precellys24 homogenizer	Peqlab
Precicison Balance Adventurer Pro AV2102C	OHAUS
Speed Vac Concentrator 5301	Eppendorf
Sterile bench HERAsafe KS 18	Fisher Scientific
Thermo mixer Comfort	Eppendorf
Turbidimeter	Biolog
Ultra pure water system Arium	Sartorius
Ultrasonic bath Sonorex Digitec DT 255 H	Bandelin electronic
Vacuum pump Laboport SCC840	KNF Neuberger
Vortexer VV3	VWR International

2.2 Consumables

Table 2.2: Consumables

Material	Manufacturer
Agilent gene expression hybridization kit	Agilent Technologies
Affimetrix chips, 8 x 15 K	Agilent Technologies
Ceramic beads, diameter: 5 mm,	Peqlab
Cuvettes Sarstedt	Sarstedt
Kreapure purification columns	Kreatech
Pipettes Research Pro 10/100/1000	Eppendorf
Phenotyping Microarrays: PM1, PM2A, PM3B, PM4A	Biolog
RNA purification Kit	Promega
RNA nano 6000 kit	Agilent Technologies
Silica beads, diameter < 0,1 µm	Kuhmichel
Sterile filters, Isopore 0,2 µm	Millipore
ULS™ Fluorescent Labeling Kit	Kreatech
Vf-5MS column (30 m x 0.25 mm I.D.)	Varian Deutschland
Zebron ZB-5MS + 5 m Guardian column (30 m x 0.25 mm I.D.)	Phenomenex

2.3 Chemicals

If not indicated otherwise, chemicals and reagents of highest quality marked with the term "purest" or "for analytic purpose" were utilized. The substances were purchased from the manufacturers Carl Roth, Sigma-Aldrich, Serva and Fisher Scientific.

2.4 Organism

Table 2.3: Yersinia pseudotuberculosis strains

Strain	Description	Reference
YPIII	pIB1, wild type	(Bölin et al. 1982)
YP3	plB1, rovA::TN10(60)[a;] cm^R	(Nagel et al. 2001)
YP50	pIB1, Δ*ymoA*; Kn^R	A. K. Heroven
YP53	pIB1, Δ*csrA*; Kn^R	(Heroven et al. 2008)
YP72	pIB1, Δ*rovM*	A. K. Heroven
YP89	plB1, Δ*crp*	(Heroven et al. 2012)

2.5 Databases

Table 2.4: Databases

Database	Description
Metacyc	Database for pathways and compounds
BRENDA	Database for enzymes and ligands
KEGG	Database for pathways and compounds
MD Library-2012-04-20	In-house library of EI mass spectra and retention indices (Department of bioinformatics and biochemistry, TU Braunschweig)
NIST08 Mass Spectral Database	Commercial spectra library of EI mass spectra
Golm Metabolome Database	Open source mass spectra library
NCBI	Biomedical and genomic information
Pubmed	Literature research

2.6 Software

Table 2.5: Software

Software	Description
MetaboliteDetector, Version 2.0.7 (2011-09-29) (http://md.tu-bs.de/)	Program for GC-MS analysis and evaluation
Microsoft Office Excel 2007	Spreadsheat program
EnzymeDetector (http://edbs.tu-bs.de/)	Program for comparative pathway prediction based on genome annotation
Microsoft Windows XP	Operating system
MultiExperiment Viewer, Version 4.7.3 (http://www.tm4.org/mev/)	Statistical data evaluation and visualisation
MySQL Workbench, Version 5.2.34 CE	Database administration
OmniLog – OL PM FM, Version 1.20.02	Data evaluation and visualization of kinetic respiration plots (Biolog)
OmniLog – OL PM Par, Version 1.20.02	Program for configuration of evaluation parameter of kinetic respiration plots (Biolog)
OmniLog – PM DC, Version 1.30.01	Administration software of the OmniLog Incubator/ Reader (Biolog)
OpenOffice.org, Version 3.3.0	Office Suite
TargetSearch	R- Package for GC-MS data analysis
OriginPro 8.1G SR1, Version 8.1.13.88 (http://www.OriginLab.com/)	Statistic program for analysis and visualization of scientific data
ChromaTOF (version 4.24)	Vendor software for GC-MS data acquisition and and evaluation (Leco)
R, Version 2.13.0 (http://www.r-project.org/)	Statistical programming language
Vanted, Version 2.0 (http://vanted.ipk-gatersleben.de/)	Visualization of metabolic networks an experimental data
Xcalibur 2.0.7	Vendor software for GC-MS data acquisition and evaluation (Thermo Fisher Scientific)

2.7 Media and Supplements

All water based media and solutions were prepared with salt free, particle filtered and sterile filtered ultra pure water (*aqua bidest)* from an ultra pure water system (Arium, Sartorius). If not indicated otherwise the solutions were autoclaved for 20 min at 121 °C and 1 bar overpressure (Varioklav 135 S; H + P Labortechnik) for sterilization.

2.7.1 LB medium (Luria-Bertani medium)

Yeast extract	5.0 g
Tryptone	10.0 g
NaCl	5.0 g

filled up to 1 l with *aqua bidest* (Sambrook et al. 1989):

Solid medium

For preparation of solid media 15 g of agarose were added to 1 l of liquid media.

2.7.2 M63 Medium

KH_2PO_4	13.6 g
$(NH_4)_2SO_4$	2.0 g
$FeSO_4 \cdot 7H_2O$	0.5 mg

filled up to 1 l with *aqua bidest* and adjusted pH to 7 (Miller 1992).

M63 Medium modified for growth of *Y. pseudotuberculosis* at 25 °C

KH_2PO_4/K_2HPO_4	13.6/17.4 g
$(NH_4)_2SO_4$	5.0 g
$FeSO_4 \cdot 7H_2O$	0.5 mg
$ZnSO_4 \cdot 7H_2O$	0.5 mg
$MgSO_4 \cdot 7H_2O$	0.2 mg
Trace elements	1.0 ml

filled up to 1 l with *aqua bidest*

M63 Medium modified for growth of *Y. pseudotuberculosis* at 37 °C

KH_2PO_4/K_2HPO_4	13.6/17.4 g
$(NH_4)_2SO_4$	5.0 g
$FeSO_4 \cdot 7H_2O$	0.5 mg
$ZnSO_4 \cdot 7H_2O$	0.5 mg
$MgSO_4 \cdot 7H_2O$	0.2 mg
Trace elements	1.0 ml
Vitamin stock solution	1.0 ml
Thiosulfate stock solution	100.0 ml

Calcium stock solution	10.0 ml

filled up to 1 l with *aqua bidest*

Trace element stock solution (1000x)

$FeCl_3 \cdot 6H_2O$	200.0 mg
$MnSO_4 \cdot H_2O$	200.0 mg
$ZnSO_4 \cdot H_2O$	50.0 mg
$CuCl_2 \cdot 2H_2O$	20.0 mg
$Na_2B_4O_7 \cdot 10\ H_2O$	20.0 mg
$NH_4Mo_7O_{24} \cdot 4H_2O$	10.0 mg

filled up to 1 l with *aqua bidest* and sterile filtered. Adjacent stored at 4 °C until usage.

Vitamin stock solution (1000x)

Pantothenate	1.0 mM
Thiamin	1.0 mM
Biotin	0.1 mM

dissolved in *aqua bidest* and sterile filtrated. Aliquoted in 1 ml and stored at -20 °C until usage.

Thiosulfate stock solution

For the thiosulfate stock solution a concentration of 0.25 M Na_2SO_3 was prepared in *aqua bidest*. The final concentration in the media was 0.025 M.

Calcium stock solution

For the calcium stock solution a concentration of 0.25 M CaCl was prepared in *aqua bidest*. The final concentration in the media was 2.5 mM.

Carbon source stock solution

Different carbon sources were added to the minimal media. Every carbon source was added discretely.

Table 2.6: Carbon sources

Carbon source	Stock solution	Final concentration in medium
Glucose	1 M	0.04 M
Mannitol	1 M	0.04 M

Carbon source	Stock solution	Final concentration in medium
Inosine	0.1 M	0.04 M
Adenosine	0.02 M	0.016 M
Thymidine	0.2 M	0.04 M
Uridine	0.4 M	0.04 M

Carbon sources were sterile filtered and stored at room temperature.

2.7.3 Biolog–inoculum solution

Biolog–inoculum solution 1

IF-0a GN/GP (1,2X)	5.0 ml (Biolog, Hayward, CA, USA)
aqua bidest.	1.0 ml

Biolog–inoculum solution 2

IF-0a GN/GP (1,2X)	8.33 ml (Biolog, Hayward, CA, USA)
Redox Dye Mix A (100x)	0.12 ml (Biolog, Hayward, CA, USA)
aqua bidest.	0.55 ml

2.8 Solutions

9% Sodiumchloride stock solution(w/v)

90 g sodiumchloride was dissolved in 1 l *aqua bidest.* The stock solution was diluted (1:10, v/v) and stored at 4 °C.

Ribitol stock solution

0,05 g ribitol were dissolved in 0.25 l *aqua bidest.* The solution was sterile filtered, aliquoted and stored at -20 °C.

Ribitol methanol solution

0.4 ml of the ribitol stocksolution ($c = 0{,}2\ g \cdot l^{-1}$) was mixed with 9.6 ml methanol and stored at -20°C.

Methoxyamin-Pyridin-Lösung

20 mg methoxyamin hydrochlorid was placed in a clean glas vial and dissolved in 1 ml pyridin directly before usage.

Alkane time standard (Calibrationmix)

Decane	17.12 mg
Dodecane	16.67 mg
Pentadecane	16.23 mg
Nonadecane	12.50 mg
Docosane	12.50 mg
Oktacosane	12.50 mg
Dotriacontane	12.50 mg
Hexatriacontane	12.50 mg

The alkanes were dissolved in 20 ml cyclohexan and filled up to 25 ml with cyclohexan. The solution was aliquoted and stored at -20 °C until usage.

2.8.1 Solutions for the determination of the biomass composition

P1 solution

Glucose	50 mM
Tris/HCl	25 mM
EDTA	10 mM

The pH was set to 8.0.

PCI-Solution

Phenol, chloroform and isoamlalcohol were mixed in the relation of 25:24:1 and stored at 4 °C.

RNase

The RNase was suspended in *aqua bidest* (20 $mg \cdot mL^{-1}$) and boiled for 20 min at 95 °C. Adjacent the solution was stored at -20 °C.

High salt solution

Na-Citrate	0.8 M

NaCL	1.2 M

dissolved in 1 l *aqua bidest* and stored at room temperature.

2.9 Microbiological Techniques

2.9.1 Cultivation condition

Strains were routinely stored as glycerol stocks at -80 °C and streaked at solid agar plates for incubation. After the incubation the plates were sealed with parafilm and stored at 4 °C. For liquid cultures a preculture was inoculated from agar plates in complex LB medium. For cultivation in minimal medium an additional preculture in minimal medium was performed, which was used to inoculate the main culture. The initial cell density was always set to 0.1 OD_{600}. *Y. pseudotuberculosis* was grown at 25 °C or 37 °C under aerobic conditions. If cultivated in liquid media, the cells were shaken at 200 rpm in a shaker with an orbit of 50 mm (Certomat BS-1, Satorius).

2.9.2 Measurement of cell density

The cell density was determined photometrically by measuring the optical density (OD) with a spectral photometer (Genesys 6, Sysmex Digitana) at 600 nm. The linear range of this photometer is between 0.05 and 0.5, samples were diluted accordingly. For reference and dilution *aqua bidest.* or corresponding media was used. An OD_{600} of 1 corresponds roughly to a cell density of $1 \cdot 10^9$ cells/ml (Sambrook et al. 1989).

2.9.3 Deriving the characteristic parameters of growth

The growth of cell material is described through the formula 2.1.

$$\frac{dN}{dt} = \mu \cdot N \tag{2.1}$$

Where N is the number of cells or any extensive property thereof and μ is the specific growth rate. Through conversion formula 2.2 is formed.

$$\mu = \frac{(\ln(N) - \ln(N_0))}{(t - t_0)} \tag{2.2}$$

Following this, the maximum growth rate can be obtained from the slope of the growth curve in the exponential phase, when plotted in a half-logarithmic way.
The doubling time of a bacteria can be calculated with the formula 2.3.

$$t_d = \frac{ln2}{\mu} \tag{2.3}$$

2.9.4 Correlation of cell dry weight to optical density

The cell dry weight was determined by filtration of the cells on nitrocellulose filters with 0.2 µm pore size (Millipore). The filters were dried at 80 °C for three days until a constant weight was reached. The weight of each filter was recorded.
Two 100ml main culture of *Y. pseudotuberculosis* was cultivated in 1 l Erlenmeyer flasks and harvested at exponential growth and at stationary growth.
Different dilutions between an OD_{600} of 0.1 and the density of the cells at the point of harvesting were produced in triplicates by mixing with fresh medium. The OD_{600} for every dilution was measured and directly subsequent 10 ml of the mixture was filtered with a 3-place manifold (Millipore) under low pressure. The filters were washed twice with 0.9 % NaCl solution and dried for three days at 80 °C. Afterwards they were weighted again. The difference to the first measurement was correlated to the measured OD_{600}, respectively. As blanks fresh medium was filtered and handled equally to the bacteria samples. The blanks were subtracted from the data. The procedure was repeated twice and the results were averaged.

2.9.5 Determination of the biomass composition

DNA Fraction

For the measurement of the DNA fraction 2 ml of bacteria culture was centrifuged for 3 min at 4629 x g at 4 °C. The pellet was washed twice with 1 ml 0.9 % NaCl (4 °C) and resuspended in 700 µl P1-solution (chapter 2.8.1). The mixture was shaken in a thermomixer (Thermo mixer Comfort, Eppendorf) at 600 rpm for 10 min at room

temperature. 20 µl RNAse (chapter 2.8.1) were added to the sample and the mixture was incubated for another 10 min. Adjacent 700 µl PCI solution (chapter 2.8.1) were added and the sample was vigorously shaken. Subsequently the sample was centrifuged 2 min at 20,000 x g and the supernatant was transferred into a new reaction tube. The washing step was repeated twice. To the supernatant 700 µl chloroform were added and the mixture was centrifuged at 20,000 x g for 2 min. The supernatant was transferred into a new reaction tube and 60 µl 3 M sodiumacetate (pH 5.5) and 700 µl isopropanol were added. The sample was incubated for 20 min at room temperature and adjacent centrifuged for 15 min at 20,000 x g. The pellet was rinsed with 100 µl 70% ethanol, with subsequent centrifugation for 5 min at 20,000 x g. After drying the sample 100 µl *aqua bidest* was used to resuspend the pellet overnight. The quality of the DNA sample was tested by measuring the OD_{260}/OD_{280} ratio. The amount of DNA was determined by measuring the absorbance at 260 nm with a photometer (Infinite M200 NanoQuant, Tecan).

RNA Fraction

For the measurement of the RNA fraction all consumables such as pipette tips, reaction tubes and *aqua bidest* were made RNAse free by doubled autoclaving. 1 ml of the bacteria culture was centrifuged for 3 min at 1 4629 x g at 4 °C. The pellet was washed twice with 500 µL 0.9 % NaCl (4 °C). In the last washing step the centrifugation was carried out for 10 min. The pellet was resuspended in 750 µL TRIZol (Invitrogen) at 50 °C at 600 rpm in a thermomixer (Thermo mixer Comfort). Adjacent the sample was centrifuged for 10 min at 10,000 x g at 4 °C. The supernatant was transferred into a new reaction tube and 150 µl chloroform was added. The mixture was vigorously shaken and subsequently centrifuged for 15 min at 10,000 x g at 4 °C. The upper polar phase was transferred into a new reaction tube and 190 µl isopropanol and 190 µl high salt solution (chapter 2.8.1) were added. The mixture was centrifuged at 10.000 rpm for 10 min at 4 °C and the resulting pellet was washed with ice-cold 75% ethanol. The sample was again centrifuged for 2 min at 10.000 x g and dried. Then the RNA was resolved in 100 µl RNAse-free water. The amount of RNA was determined photometrically with with a the Infinite M200 NanoQuant (Tecan).

Lipid Fraction

The amount of the lipid fraction was measured with the method of Bligh and Dyer (Bligh & Dyer 1959). Therefore 25 ml of a bacteria culture were centrifuged for 5 min at 4629 x g

at 4 °C. The pellet was washed twice with 10 ml 0.9 % NaCl (4 °C) and resuspended in 1 ml *aqua bidest*. Adjacent 3.75 ml of a 1:2 chloroform:methanol mixture were added and the sample was incubated for 10 min at room temperature. Then 1.25 ml *auqua bidest* and 1.25 ml chloroform were added and the mixture was centrifuged for 15 min at 3,000 x g. The nonpolar chloroform phase was transferred into a glass vial and dried under vacuum. The amount of lipid was determined by the weight difference between the empty glass vial and the glass vial with the dried sample.

Protein Fraction

The detection of the protein fraction was performed as described by Bradford (Bradford 1979). 5 ml of bacteria culture was centrifuged for 3 min at 4629 x g at 4 °C. The pellet was washed twice with 2 ml 0.9 % NaCl (4 °C) solution and adjacent resuspended in 1 ml 0.9 % NaCl. Subsequently 1 ml of 1.32 M NaOH was added and the sample was incubated at 80 °C. After 15 min the sample was centrifuged for 10 min at 5,000 x g. 20 µl of the sample were mixed with 800 µl *aqua bidest* and 200 µl Bradford reagent. After incubation of 10 min the absorption of the sample was measured at 595 nm with a photometer. The protein concentration was determined with a calibration curve.

2.9.6 Phenotyping MicroArray

Y. pseudotuberculosis YPIII cells were taken from -80 °C glycerol stocks and streaked on solid LB plates. After incubation at 30 °C for 16 h the bacteria were picked with a sterile cotton stick into a reaction tube with the Biolog-inoculum solution 1 (chapter 2.7.3) until a turbidity of 42 % was reached. Before, the reaction tube with the pure inoculum solution was used to set the turbidimeter (Biolog) to 100 %. Of the bacteria-inoculum solution 2 ml were transferred into 10 ml of the Biolog-inoculum solution 2 (chapter 2.7.3). For plates PM3 and PM4 0.12 ml mannitol (c=1 M) as a carbon source was added. The resulting mixture was used to inoculate the Biolog phenotyping microarrays with 100 µl per well.
The microarrays were incubated for 48-72 h at 25 °C or 37 °C in the OmniLog-Incubator/Reader (Biolog), where they were monitored every 15 min. The resulting data were analyzed with the vendor software OmniLog-PM FM and OmniLog-PM Par (both version 1.20.02, Biolog). In all measurements the negative control was deducted (A1 zero). Each strain was analyzed in duplicate and later averaged. If not indicated otherwise a

significant change between wild type and mutant strain was defined as a difference >1000 in the integrated kinetic curve area.

2.10 Transcriptome analysis

The transcriptome analyses of the *Y. pseudotuberculosis* mutant strains were performed by A. K. Heroven and J. Melzer (Group of P. Dersch, HZI, Braunschweig, Germany). The data processing was performed by J. Klein (Group of D. Jahn, TU Braunschweig, Braunschweig, Germany).

For the transcriptome analysis 16 independent cultures of *Y. pseudotuberculosis* were grown in LB medium. The RNA was isolated with the RNA purification kit (Promega). The RNA concentration and purity was analyzed with an Agilent 2100 Bioanalyzer using the RNA Nano 6000 kit, adjacent the total RNA of four samples was pooled. The ULS™ Fluorescent labeling kit for Agilent arrays (Kreatech) was used for the labeling of 1 µg of the pooled RNA sample with Cy5 (reference/wild type DNA) and Cy3 (sample/mutante DNA). Spare Cy5/Cy3 was removed by KREApure purification columns and the labeling was controlled using a nanodrop (Peqlab). 300 ng of Cy5 labeled RNA and 300 ng of Cy3-labeled RNA were mixed, fragmented and subsequently hybridized to custome-made microarrays (Agilent, 8×15K format) with the Agilent gene expression hybridization kit. Four biological replicates were used for each experiment. The analysis was performed using microarrays with three different 60 nt oligonucleotides for all 4172 chromosomal genes (ORFs >30 codons) of *Y. pseudotuberculosis* YPIII and additionally six probes for the 92 genes of the virulence plasmid pYV of *Y. pseudotuberculosis* strain IP32953. The sequences were obtained from NCBI Genome GenBank (NC_010465 and NC_006153).

The microarray was washed and dried and then scanned using Axon GenePix Personal 4100A scanner. Images were generated using the software package GenePix Pro 6.015.

The data were processed using the software R (chapter 2.6) and the Bioconductor software (Gentleman et al. 2004). The data were preprocessed using the marray package and the read.GenePix function. A Lowess normalization was performed, with adjacent scale normalization between different microarrays if necessary. For the identification of the differentially expressed genes the limma package with the lmFit function was used. Significance was calculated using eBayes (Smyth 2004). For every gene the median value of the fold-change between sample/reference was calculated based on at least three probes.

2.11 Sample preparation for metabolome analysis

2.11.1 Cell harvesting and metabolite extraction with centrifugation and ultrasonic bath

The bacteria culture volume utilized for the harvesting was equivalent to 20 mg cell dry weight. The cells were separated from the medium by centrifugation for 3 min at 4 °C and 4629 xg. The supernatant was discarded and the pellet was resuspended in 20 ml 0.9 % NaCl (4 °C) and centrifuged again for 3 min at 4 °C and 4629 xg. The supernatant was discarded and the washing step was repeated. The resulting pellet was resuspended in 1.5 ml cold methanol (-20 °C) containing ribitol (c = 2 µg/ml). The suspension was incubated for 15 min in an ultra sonic bath at 70 °C and subsequent cooled on ice for 2 min. Afterwards 1.5 ml of *aqua bidest.* was added and the solution was vigorously shaken for 60 s. Then 1 ml of chloroform was added and the mixture was again vigorously shaken for 60 s. The phase separation was obtained by centrifugation (5 min at room temperature, 15800 xg). 1 ml of the upper polar phase was transferred into a clean 2 ml reaction tube. The sample was placed in a vacuum concentrator (Speed Vac-Concentrator plus, Eppendorf) and dried under vacuum for 1 h with rotation and adjacent overnight without rotation. The samples were sealed with parafilm and stored at -20 °C or directly derivatized (chapter 2.11.4) for measurement. For all metabolome data sets control-samples (blanks) were generated. Blanks were produced by centrifugation of fresh medium with a following treatment like a bacteria-containing sample.

2.11.2 Cell harvesting and metabolite extraction with filtration and homogenizer

The bacteria culture volume utilized for the harvesting was equivalent to 5.3 mg cell dry weight. The cells were separated from the medium by filtration with a 3-place manifold (Millipore) utilizing polycarbonate filters with a pore-size of 0.22 µm (Isopore, Millipore). The cells and the filters were washed twice with 4 ml 0.9% NaCl solution to remove remaining medium components and subsequently transferred to a 2 ml reaction tube (Peqlab) containing 600 mg silica beads (diameter <0,1 µm; Kuhmichel) and 3 ceramic

beads (diameter: 5 mm, Peqlab). Afterwards, the tubes were immediately frozen in liquid nitrogen. The cells were resuspended in 0.75 ml cold methanol (-20 °C) containing ribitol (c = 2 µg/ml). Subsequently the cells were disrupted in a homogenizer (Precellys24, Peqlab) at -5 °C with 3 cycles at a speed of 6500 rpm for 30 sec with breaks of 20 sec. Phase separation was obtained by adding 0.4 ml *aqua bidest* and 0.25 ml chloroform with adjacent centrifugation (5 min, 15800 xg). 0.75 ml of the polar phase were taken and dried under vacuum at room temperature and stored at -20 °C until derivatisation. For all metabolome data sets control-samples (blanks) were generated. Blanks were produced by filtration of fresh medium with a following treatment like a bacteria-containing sample.

2.11.3 Sample preparation for supernatant analysis

200 µl from a bacterial culture were harvested into 1 ml reaction tubes and pelleted by centrifugation (2 min, 15800 xg). Afterwards 100 µl of the supernatant was taken into a new reaction tube and mixed with 0,5 ml cold methanol (-20 °C) containing ribitol (c = 2 µg/ml). The sample was then dried under vacuum at room temperature and stored at -20 °C until derivatization.

2.11.4 Derivatization

Samples were dried for 30 min under vacuum prior derivatisation. The pellets were derivatized in 40 µl pyridine containing methoxyamine hydrochloride(c = 20 mg/ml) (2.8) at 30 °C for 90 min under constant mixing. After the addition of 70 µl MSTFA (N-methyl-N-trimethylsilyltrifluoroacetamide), samples were incubated for 30 min at 37 °C followed by 2 h at 25 °C with constant agitation. The samples were centrifuged at 14.000 xg for 5 min and the supernatant was transferred into a glass vial for GC-MS analysis. All samples were analyzed within 24 h after derivatization. An alkane retention index marker(2.8) was used to convert retention times to retention indices.

2.12 Gas chromatography mass spectrometry

2.12.1 Quadrupol mass spectrometry

GC-MS analysis was done on a Thermo GC Ultra coupled to a DSQII mass spectrometer equipped with an AS3000 autosampler (ThermoScientific). In summary, 1 µl of the derivatised sample was injected in split mode (1:25) into a PTV injector (ThermoScientific). After an initial time of 0.2 min at 70 °C, temperature was increased to 330 °C at a rate of 14 °C/s, followed by an additional constant temperature period at 330 °C for 5 min. Gas-chromatography was performed over 60 min on a Zebron ZB-5MS + 5 m Guardian column (30 m x 0.25 mm I.D.) (Phenomenex). Helium flow was set to 1.2 ml/min. After 1 min at 70 °C, temperature was ramped to 76 °C with 1 °C/min and then increased to 325 °C with 6 °C/min followed by an additional constant temperature period at 325 °C for 10 min. The transfer line temperature was set to 275 °C. Ion source temperature was adjusted to 220 °C. Full scan mass spectra were acquired from m/z 40...460 with an acquisition rate of 2.5 scans/s. Data acquisition was done using the Xcalibur software (version 1.4, ThermoScientific).

2.12.2 Time of Flight Mass spectrometry

Additionally, the samples were analyzed using the Leco Pegasus 4D GCxGC-TOFMS in GC-TOF mode (Leco Instruments) equipped with a MPS 2XL autosampler (Gerstel). 1 µl of the samples was injected in splitless mode into a cooled injection system (Gerstel). After an initial time of 0.2 min at 70 °C the temperature was ramped to 280 °C at a rate of 12 °C/s, followed by an additional constant temperature period at 280 °C for 5 min. Gas chromatography was performed with a 7890 Agilent GC over 35 min on a Vf-5MS column (30 m x 0.25 mm I.D.) (Varian). Helium flow was set to constant 1 ml/min. After 1 min at 70 °C the temperature was increased to 330 °C with 10 °C/min followed by an additional constant temperature period at 330 °C for 8 min. The transfer line was set to 275 °C. Ion source temperature was 250 °C. Full scan mass spectra were recorded from *m/z* 45...600 with 20 scans/s. Data acquisition was done using the ChromaTOF software (version 4.24, Leco).

2.13 Data processing

Data analysis was done with MetaboliteDetector (version 2.07, (Hiller et al. 2009)). The software supports automatic deconvolution of all mass spectra from a chromatogram and calculates the retention indices of all analytes based on the alkane time standard (chapter 2.8). For this the retention indices for the alkanes at the time point of elution were calculated by multiplying the number of carbon atoms with 100. Based on the formula displayed below (2.4) the retention indices of all peaks can be calculated by setting them in a relation to the corresponding alkanes.

$$I^{(T)} = 100\left[(y-x)\frac{t_i - t_x}{t_y - t_x} + x\right] \quad (2.4)$$

With:
I = retention index
T = in a temperature gradient
x = number of carbon atoms of the alkane before the analyte
y = number of carbon atoms of the alkane after the analyte
t_d=retention time of the analyte
t_x=retention time of the of the alkane before the analyte
t_y=retention time of the of the alkane after the analyte

Additionally to the retention index calculation with the alkane time standard also the internal standard ribitol was used for a retention index adjustment between a batch of samples. Peaks were identified by comparison of retention index and mass spectrum to a user-defined spectra library (MD Library-2012-04-20) using a cut-off of 70% identity match.

MetaboliteDetector was used for analyzes of GC-MS chromatograms in an untargeted approach, which detected also substances, that could not be identified. The unknown substances were added to the spectra library and termed with an unique name. The compounds were termed “unknowns” and their identifiers were created from the acronym of the experimentalist, the organism, a consecutive number and the retention index. A typical identifier for an unknown was “Unknown#mse-ypy-001_1846.9”.

Quantification was based on selected unique fragment ions for each metabolite individually. Only substances were considered that were detected in at least 50% of the investigated samples. The data were normalized to the peak area of the internal standard ribitol. The blanks were used for the identification of contamination that were manually

removed from the data set. The values of the derivatives of the same substances were added to represent a single substance and used for further evaluation.

2.14 Statistical Data Analysis

All basic statistical calculations were applied, using the standard formulas described elsewhere (Hartung et al. 2005).

2.14.1 Characteristics of a data set

The arithmetic **mean** was used to calculate the average tendency of a series of n measurements. The **median** gives the value that separates the higher half of a data set from the lower half of the data set. The **standard deviation** s was used to describe the variation of a data set around the mean The **standard error** Se was used to calculate the accurateness of the arithmetic mean. The **relative standard error** rel. Se shown allows a direct understanding of the accurateness of a data set (Koschack 2008).

2.14.2 Normalization & Scaling

The generated metabolome data included always a degree of biological and non-biological variation. For an efficient analysis the removal of the non-biological variation was desirable. One way to archive this is a normalization process. In a data matrix were the rows present the metabolites and the columns represent the samples, normalization can be performed row-wise or column-wise. As mentioned previously the data was always column-wise normalized to the **internal standard ribitol** to remove device related fluctuations (Hiller et al. 2009). If necessary the data was also subjected to column-wise **median normalization** to compare data sets from different measurements (Villas-Bôas et al. 2007).

Depending on the further analyzes of the data additional normalization procedures were performed. Row- and column-wise **standardization** was performed for unbiased visualization processes (Villas-Bôas et al. 2007) such as the principle component analysis and the hierarchical clustering (chapter 2.14.5). The information about the magnitude of intensity of a metabolite was important cor certain data sets and desired to maintain present in the data. This was the case for analysis of the supernatant data, that were therefore row-

wise scaled by the **root mean square** (RMS) of the metabolite.
Frequently, the relevant information was the relative comparison of the value of a metabolite between an investigated situation and a control situation. Therefore the samples of interest were divided by the median of the control samples. To avoid different ratios for the same level of up-and downregulation (e.g. 2 and 0.5), the ratios were **logarithmized** to the basis 2 (log_2) which resulted in symmetrically treated data (Scholz & Selbig 2006).

2.14.3 Correlation

For the detection of similarities or dependencies the correlation coefficients were calculated. Mostly the **Pearson coefficient** was applied to detect linear dependencies between two groups. However, for certain data sets a correlation was not expected to be necessarily linear or the correlation was strongly influenced through outliers. In these cases the **Spearman's rank correlation coefficient** was used. The Spearman rank correlation coefficient gives a high grade of correlation for every monotonic relation between data sets and is robust in the presence of outliers.

2.14.4 Significance

The **two-tailed students t-test** was used to investigate whether a metabolite level was significantly for different conditions. The t-test is suited for samples with equal variance , which will be assumed in the following. If more than two conditions were compared an **analysis of variance** (ANOVA) was performed. The method tests if the variance between the conditions is greater than the variance within the conditions.
In certain cases the impact of more then one factor to the metabolome was investigated, generating conditions, that were influenced by more than one factor. Therefore a **two-factor ANOVA** (or two-way ANOVA) was applied. This method reveals the influences of the investigated factors and also their interactions. If not indicated otherwise a significance level of 5 % was used in all significance tests.

2.14.5 Visualization

Since through metabolome analysis large of data sets were generated, visualization was of uttermost importance to allow a intuitive understanding. The method regularly used for

metabolome analysis is the **principle component analysis** (PCA). It is used to visualize data and to reveal discriminating structures in the data (Scholz & Selbig 2006). The method reduces the dimensionally of the data while retaining as much information as possible. Thereby the first principle component represents the linear combination of the variables, that explain the greatest amount of data. The second principle component accounts for the linear combination of the original variables, that explain the greatest amount of remaining data, that is orthogonal to the first principle component. The following principle components are calculated alike.

The classical method for the analysis of metabolic patterns is the **hierarchical clustering** (HCL), which has also been used for gene expression (Bohlin et al. 2009). Hereby metabolites and samples are clustered according to their similarity, which is represented in form of the vertical distance of a dendrogram. For the HCL an average clustering was used. A drawback of HCL is the sensitivity against background noise in the data, which hinders the interpretation of the clustering. An alternative method also developed for the analysis of gene expression patterns is a **self-organizing tree algorithm** (SOTA)(Dopazo & Carazo 1997). This method combines the approach of a HCL with an unsupervised neural network, improving accurateness and robustness of the clustering (Herrero et al. 2001).

3 Results and Discussion

3.1 Characterization of the metabolic properties of Yersinia pseudotuberculosis

A central aspect of this thesis was the characterization of the metabolic properties of the *Yersinia pseudotuberculosis* strain YPIII, which included the collection of data under reference conditions at 25 °C. The intention was to gain a general understanding of the metabolic properties of YPIII, but also to generate a basis for comparison to other situation such as different temperatures or mutant analyses. For this purpose, YPIII was investigated regarding its ability to use different nutrients, its growth in different media and its intra- and extracellular metabolome, which is described in the following chapters.

3.1.1 Analysis of utilizable nutrients and energy sources

In order to gain insight in the uptake abilities of YPIII, the bacterium was tested with phenotyping microarray (PM) analysis (Biolog) at 25 °C. The procedure is described in chapter 2.9.6. The bacterium was tested on 190 carbon sources (PM1 & PM2A), 94 nitrogen sources (PM3B), 59 phosphor sources (PM4A) and 35 sulfur sources (PM4A). The complete list of the tested substances is available online on the Biolog homepage (www.biolog.com).

The PM analysis does not allow direct deduction of the anabolic usability of a compound, as only the respiratory activity is measured by monitoring a color change of a tetrazolium dye. This dye is first colorless and turns violet when it is reduced. The reduction occurs through electrons of reduction equivalents (e.g. NADPH, NADH), which can be directly linked to respiratory activity in a cell and therefore to the uptake and consumption of the provided source. The color change is measured over time, which results in a kinetic curve plot for every tested substance (Bochner et al. 2001; Bochner 2009). A positive result on a substance indicates the presence of both, a transport mechanism and the necessary catabolic enzymes.

The application of the plates, testing for the four major elements important for nutrition (C, N, P and S), allows a global characterization of the catabolic properties of the bacterium.

Utilizable carbon sources

45 carbon sources, out of 190 tested sources on PM1 and PM2A, showed a positive result. These included 6 amino acids, 2 dipeptides, 24 sugars and sugar-derivatives, 5 alcohols, 6 organic acids, 2 glucosides and 2 nucleosides as shown in table 3.1.

Table 3.1: Utilizable carbon source from phenotyping microarray analyses, using PM1 and PM2A

Amino acids/ Dipeptides	Monosaccharides	Di/Poly-saccharides	Sugar-derivatives	Alcohols	Carboxylic acids	Others
L-Glutamic Acid	D-Ribose	D-Trehalose	N-Acetyl-b-D-Mannosamine	D-Arabitol	Melibionic Acid	2'-Deoxy Adenosine
L-Proline	L-Arabinose	Maltose	N-Acetyl-D-Glucosamine	L-Arabitol	Pyruvic Acid	Adenosine
D-Alanine	D-Xylose	D-Melibiose	N-Acetyl-D-Galactosamine	Adonitol	Methyl Pyruvate	Arbutin
L-Asparagine	L-Lyxose	Maltotriose	N-Acetyl-Neuraminic Acid	Glycerol	L-Lactic Acid	b-Methyl-D-Glucoside
L-Histidine	D-Mannose	Pectin	D-Glucosamine	D-Mannitol	Acetic Acid	
Glycyl-L-Glutamic Acid	L-Rhamnose	Dextrin	D-Fructose-6-Phosphate		D-Gluconic Acid	
L-Serine	D-Fructose		D-Glucose-6-Phosphate			
Glycyl-L-Proline	a-D-Glucose					
	D-Galactose					

In total, 17 proteinogenic amino acids were provided on the plates (tryptophan, tyrosine and cysteine were not present), but the majority did not provide respiration. Only D-alanine, L-glutamate and L-serine could be metabolized. Asparagine, proline and histidine promoted weak responses (area < 10000). The majority of the utilizable carbon sources were (poly)saccharides, including pentoses, hexoses, di- and polysaccharides. Many polysaccharides as e.g. pectin are probably present in the intestine, since they cannot be digested by most mammals. The sugars L-arabinose, D-galactose and mannose, that are crucial for the colonization of the mouse intestine for *E. coli* (Fabich et al. 2008), were used as well by YPIII. All four acetylated amino sugars (N-acetyl-D-glucosamine, N-acetyl-D-mannosamine, N-acetyl-D-galactosamine, N-acetyl-neuraminic acid) provided on the PMs showed respiratory activity. These compounds are known to be naturally present in mammals and can also serve as carbon sources for pathogenic bacteria in the intestine (Severi et al. 2007).

Of the tested nucleosides, only adenosine and 2-deoxyadenosine were utilized as carbon source. The tested fatty acids (C_5:0, C_{10}:0) did not support respiration. In *E.coli* and *Salmonella* the C_4-C_{10} fatty acids are not used either (Gutnick et al. 1969).

A similar study was performed with the *Y. pseudotuberculosis* strain 15478 and some differences occurred. In the strain 15478 no proteinogenic amino acid gave a positive signal, but the dipeptides were used as well such as glycyl-L-glutamic acid and glycyl-l-proline (Bochner 2009). Furthermore, the strain 15478 did not produce a signal on the carbon sources rhamnose, melibiose, lyxose and adonitol, but showed an additional signal on inosine. This indicates a high variability of carbon usage properties between the *Y. pseudotuberculosis* strains.

In *Y. pestis* the activation of the glycolysis at 25 °C has been proposed (Motin et al. 2004). Further, glycolysis and the Entner-Doudoroff pathway are crucial for *E. coli* for infection of the intestine, implying that sugars are the main source of carbon and energy in the intestine for pathogenic bacteria (Chang et al. 2004). Overall the carbon sources used by *Y. pseudotuberculosis* YPIII at 25 °C are similar to those compounds proposed to be important for colonization of the intestine. Since the bacteria express their virulence effector Invasin at 25 °C, in order to be prepared to adhere and invade the M-cells, it seems likely that also their metabolic equipment is prepared to efficiently proliferate in the ileum. Nevertheless, some utilized carbon sources such as alanine, serine, fructose-6-P, glucose-6-P, glycerol, lactate and pyruvate are rather associated with nutrients in the cytosol or the intestinal fluid (Ray et al. 2009).

Utilizable nitrogen sources

In addition to the carbon sources, nitrogen sources were tested on the plate PM3B. 34 out of 95 tested substances showed a positive response during incubation at 25 °C, comprising 14 amino acids, 11 dipeptides, 2 nucleosides, 3 sugar derivatives and 1 purine as shown in table Fehler: Referenz nicht gefunden. Additionally, urea and ammonium were also used as sole nitrogen sources. A functional urease is present in *Y. pseudotuberculosis* YPIII, which allows the use of urea. This is probably the most important nitrogen source during its lifestyle as saprophyte (chapter 1.6.4).

Table 3.2: Utilizable nitrogen source from phenotyping microarray analyses, using PM3B

Amino acids	Amides	Dipeptides	Others	Nucleosides
L-Alanine	D-Glucosamine	Ala-Asp	Xanthine	Adenosine
L-Arginine	N-Acetyl-D-Galactosamine	Ala-Gln	a-Amino-N-Valeric Acid	Cytidine
L-Asparagine	N-Acetyl-D-Mannosamine	Ala-Glu	Ammonia	
L-Aspartic Acid		Ala-Gly	Urea	
L-Glutamic Acid		Ala-His		
L-Glutamine		Ala-Thr		
Glycine		Gly-Asn		
L-Histidine		Gly-Gln		
L-Leucine		Gly-Glu		
L-Proline		Gly-Met		
L-Serine		Met-Ala		
L-Threonine				
D-Alanine				
L-Ornithine				

Of the 21 provided proteinogenic amino acids, 12 could be used as nitrogen sources. The organism had a clear preference for L-amino acids, which occur naturally. All provided dipeptides supported respiration. Dipeptides including methionine could be utilized, but not methionine alone, indicating that only the alanine and glycine groups of the dipeptides were used. Several amino acids could be used as sole nitrogen source, but not as sole carbon source (e.g. glutamine, glycine, threonine, see also table 3.1). The reason for this discrepancy is probably an insufficient expression of degradation enzymes or transporters, which has been observed in *E. coli* (McFall & Newman 1996).

Two of the amino sugars, that were used as carbon source, were also used as N-source: N-acetyl-D-galactosamine and N-acetyl-D-mannosamine. These compounds are ubiquitously present on mucus rich surfaces and therefore associated with a pathogenic lifestyle.

Some substances on the PM plates (valine, lysine, putrescine) could not be used as nitrogen source, despite the fact that the corresponding transporters are annotated in the genome. Probably, the expression of the transporters or degrading enzymes is to low to allow sufficient nitrogen supply.

Interestingly, of all nucleosides on the PM3B plate only adenosine and cytidine could be used as nitrogen sources. For both substances a deamination step yields two other nucleosides: inosine and uridine, respectively. Since none of the other nucleosides or nucleobases could be utilized, this indicates that YPIII can only use the nitrogen from the deamination step, but not the ring nitrogen. This is in accordance with the genome annotation. The same observation has been made in *Salmonella* (Gutnick et al. 1969). The only exception was the purine xanthine, which also showed a positive signal in YPIII.

Utilizable phosphor and sulfur sources

Finally, the usable phosphor and sulfur sources were tested with the plate PM4A. YPIII was able to utilize 24 out of the 59 provided phosphor source, and 12 out of the 35 tested sulfur sources (table 3.3). In general the signals of the PM4 plate were less intense, than on the other arrays.

Table 3.3: Utilizable phosphor and sulfur source from phenotyping microarray analyses, using PM4A

Nucleotides as phosphor source	Other phosphor sources	Amino acids as sulfur sources	Other sulfur sources
Adenosine- 2'-Monophosphate	Phosphate	L-Cysteine	Sulfate
Adenosine- 3'-Monophosphate	Pyrophosphate	D-Cysteine	Thiosulfate
Adenosine- 5'-Monophosphate	Trimetaphosphate	L-Cysteinyl-Glycine	Tetrathionate
Adenosine- 2',3'-Cyclic Monophosphate	Tripolyphosphate	L-Cysteine Sulfinic Acid	L-Djenkolic Acid
Adenosine- 3',5'-Cyclic Monophosphate	D,L-a-Glycerol Phosphate	L-Methionine Sulfoxide	Taurine
Cytidine- 2',3'-Cyclic Monophosphate	D-2-Phospho-Glyceric Acid	Glycyl-L-Methionine	
Uridine- 2'- Monophosphate	Phosphoenol Pyruvate	N-Acetyl-D,L-Methionine	
Uridine- 5'- Monophosphate	D-Glucosamine-6-Phosphate		
Uridine- 2',3'- Cyclic Monophosphate	O-Phospho-D-Tyrosine		
Uridine- 3',5'- Cyclic Monophosphate	Inositol Hexaphosphate		
Thymidine 3',5'- Cyclic Monophosphate			
Guanosine- 3'-Monophosphate			
Guanosine- 3',5'-Cyclic Monophosphate			
Thymidine- 5'-Monophosphate			

The bacterium was able to use the phosphate of all nucleotides, as well as all phosphorylated amino acids and phosphorylated sugars.
D- and L-forms of the amino acids cysteine and methionine as well as their derivatives were used as sulfur sources by YPIII. Further sulphate and reduced sulfur in the form of thiosulfate provided positive signals.
Since *Y. pseudotuberculosis* lives in mammalians as well as in soil, it encounters environments were both organic and inorganic compounds are present. The ability to use inorganic phosphate and inorganic sulfate as well as phosphor and sulfur sources from organic compounds (DNA, proteins) reflects its broad habitat.

Catabolic properties at 25 °C

The reference temperature of 25 °C used for the phenotyping microarrays is a signal for YPIII for early virulence or an outer-host environment (chapter 1.6.5). This can range from very nutrient poor (soil, water) to nutrient rich surroundings (feces, meat). The obtained data suggests broad catabolic abilities on all four tested elements, which is beneficial for these diverse conditions. The range of compounds, that can be utilized as carbon and nitrogen source, by YPIII is comparable with *E. coli* and *Salmonella* (Gutnick et al. 1969) but somewhat limited in comparison with *Pseudomonas* (Stanier et al. 1966).
Moreover, the results show the ability to use many of the nutrients, present in the intestine as carbon and nitrogen source. The results provided by the phenotyping microarrays and their implications are used to interpret the metabolome data and serve as reference for other conditions and mutant strains tested in the following chapters (chapter3.2.1 and chapter 3.3.2). Additionally, the data is used for validation and refining of an *in-silico* metabolic network model (I. Hartwig, unpublished data) as it has been done for other organisms already (Oberhardt et al. 2008).

3.1.2 Characteristics of growth and morphology

The cultivation parameters for the strain YPIII are described in chapter 2.9.1, if it is not indicated otherwise. The reference medium was lysogeny broth (LB) medium. In this medium YPIII reached a maximum optical density (OD) of 3.9 ±0.1 after 12 h as displayed in figure 3.1.a.

a. **b.**

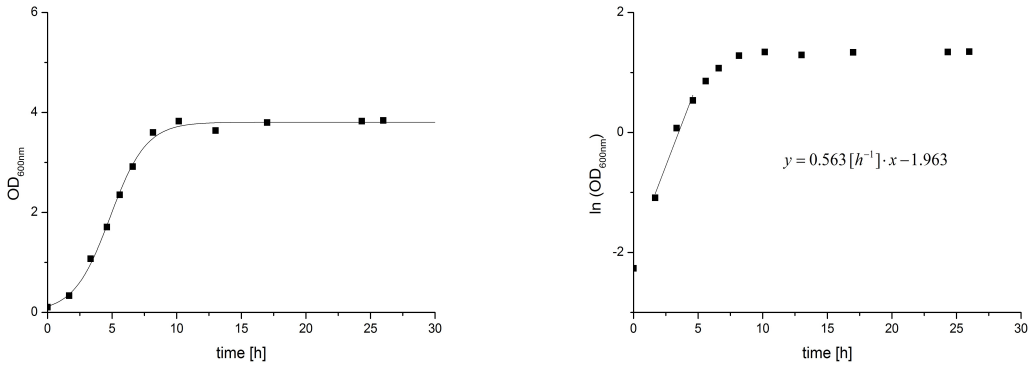

Figure 3.1: (a) Growth curve of *Y. pseudotuberculosis* YPIII in LB medium at 25 °C, (b) graphical designation of the exponential growth rate and maximum growth rate μ by a half-logarithmic plot.

As can be seen in figure 3.1.b the cells grew instantly in the exponential phase without a lag phase with a maximal growth rate μ_{max} of 0.563 h^{-1} and a doubling time t_d of 1.23 h.

A pH of 7 was measured in the beginning of the cultivation and increased to pH 8 during cultivation.

In the beginning of this work no minimal medium for *Y. pseudotuberculosis* was known without a complex factor such as yeast extract or a multitude of amino acids (Schmid et al. 2009; Heroven et al. 2004; Rosso et al. 2008). However, the annotation of the genome and the positive results of the phenotyping microarrays without further supplements (chapter 3.1.1) suggested synthesizing capabilities for all amino acids and no auxotrophies. In cooperation with R. Bücker (Group of Prof. Wittmann, IBVT, TU Braunschweig) a minimal medium was developed, that was based on the classic M63 medium (Miller 1992). A phosphate buffer system with KH_2PO_4/K_2HPO_4 was used to set the pH to 7.0. Some additional salts and trace elements were added and the ammonium component was increased from 2 $g \cdot L^{-1}$ to 5 $g \cdot L^{-1}$ (chapter 2.7.2). The growth in this modified M63 medium with glucose as carbon source is displayed in figure 3.2.

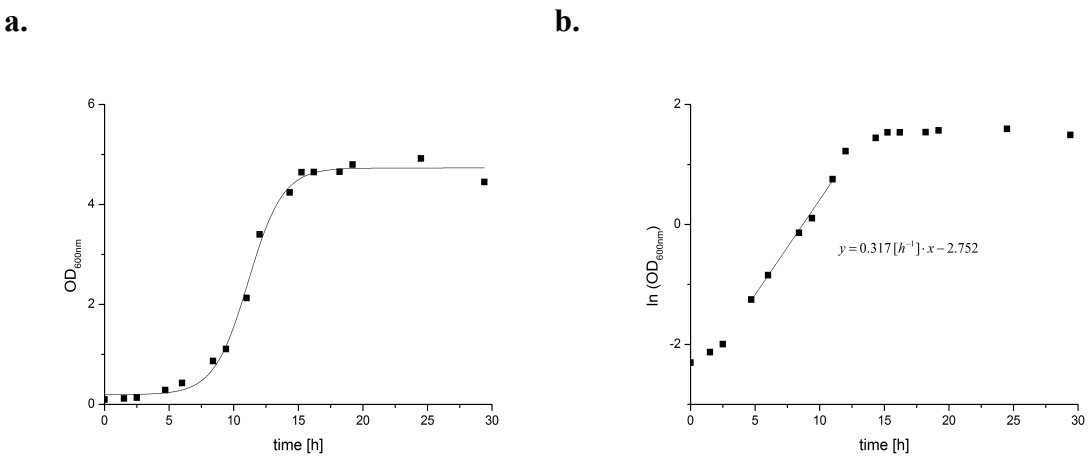

Figure 3.2: (a) Growth curve of *Y. pseudotuberculosis* YPIII at 25 °C in minimal medium with 40 mM glucose as C-source, (b) graphical designation of the exponential growth rate and maximum growth rate μ by a half-logarithmic plot.

The lag phase in the minimal medium is with five hours considerably longer than in the LB medium (figure 3.1). The maximum OD_{600} reached by YPIII after 17 h is 4.8±0.2 and the μ_{max} is 0.314 h^{-1} with a t_d of 2.21 h. Compared to the growth in LB medium the cells reached a higher density in the minimal medium, but grew significantly slower. The pH did not change during the cultivation and was constant at pH 7.

The LB medium contains many precursor molecules and vitamins, that can be directly utilized by the cell and that are expensive to synthesize otherwise. The reduced growth rate of YPIII in minimal medium is probably a result of the increased energy requirements for the biosynthesis of all required components, although a slightly higher end-OD was reached. This might be due to less toxic side-effects resulting from the rich medium or a higher energy content of the glucose concentration in the minimal medium. The high amount of ammonia required for growth in minimal medium could be a result of the poor ability to assimilate low ammonium concentrations into organic linkage, as reported for *Y. pestis* (Brubaker & Sulen 1971).

3.1.2.1 Correlation of cell dry weight to optical density

The cell dry weight (CDW) is an important parameter for the quantification and comparability of metabolites and biomass components. Since it is time-consuming to determine the CDW for every experiment, a correlation factor for optical density (OD_{600}) is useful to determine. The detailed description of the procedure is described in chapter 2.9.4. The cells were grown in LB medium at 25 °C and harvested in the mid exponential phase

after four hours at an OD_{600} of 1.4-1.6 and a μ of 0.56 h^{-1}. The averaged results are displayed in figure 3.3.

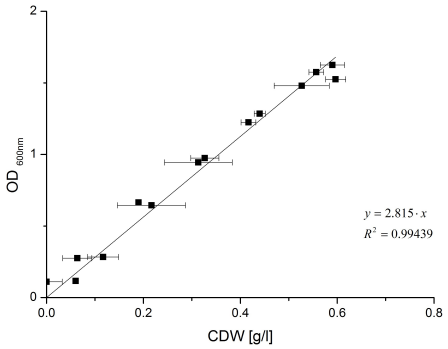

Figure 3.3: Correlation of cell dry weight (CDW) to optical density (OD) of YPIII at 25 °C during exponential growth in LB medium.

The linear regression from figure 3.3 leads to a formula, that describes the correlation between CDW and OD_{600}.

$$CDW_{\,Y.\,pseudotuberculosis\ \ 25\,°C}\,[g/l] = 0.355 \cdot OD_{600\,nm} \qquad (3.1)$$

The formula 3.1 can be used for calculating the CDW by measuring the OD_{600} and therefore allows comparison between organism with different morphology and different CDW/OD_{600} relation.

3.1.2.2 Composition of the biomass

A subject of bioinformatic research and systems biology (chapter 1.7) is to generate *in-silico* models of the metabolic network of bacteria based on the genomic annotation. In order to be a useful tool for predicting metabolic states, the model has to represent conditions close to nature. Therefore additional information is required, that cannot be gained from the genomic annotation, but experimentally. The composition of the biomass of an organism holds valuable information for the metabolic characteristics, and needs to be determined experimentally in order to generate a realistic model.

The methods were adapted for quantitative analysis in our group by N. Bill and C. Nienhagen. The necessary experiments were done by J. Grimm in the context of her bachelor thesis.

The molecular composition of a bacterium is dependent on the growth rate, the applied medium and the cultivation temperature (Neidhardt 1963; Hanegraaf & Muller 2001), therefore these parameters were kept constant throughout the experiments. YPIII was

grown in LB medium in cultivation flasks to avoid effects created by shortages of nutrients during growth. LB medium consists of yeast extract and tryptone. The combination of both substances are regarded as good medium, which contains all necessary sources and co-factors for growth of YPIII. The temperature was set to 25 °C and the bacteria were always harvested in mid-exponential state after four hours of growth, resulting in an OD of 1.2-1.5 and a μ of 0.56 h^{-1}. The concentration of the biomass components (DNA, RNA, proteins, lipids) was determined experimentally and normalized to the respective CDW.
The concentrations were determined with at least two biological replicates and at least three technical replicates, resulting in a minimal number of six samples as described in chapter 2.9.5.

a. *Y. pseudotuberculosis* 25 °C **b.** *E. coli* 37 °C

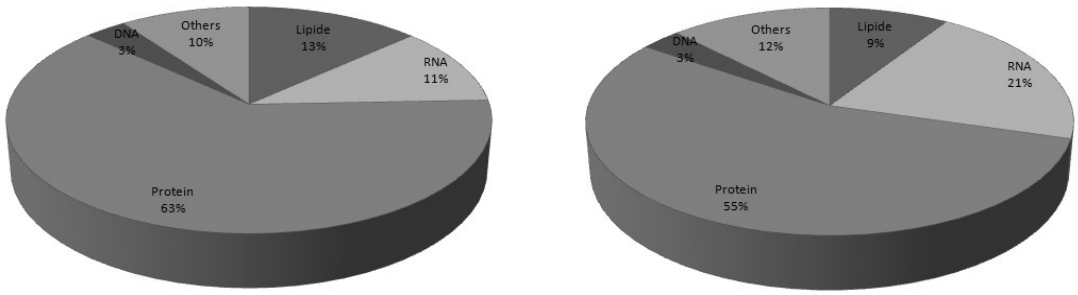

Figure 3.4: (a) Composition of biomass of *Y. pseudotuberculosis* YPIII at 25 °C in LB medium as determined experimentally with 63 ± 7% protein, 3 ± 0.3 % DNA, 11 ± 1 % RNA and 13 ± 4% lipids .(b) Composition of biomass for *E. coli* at 37 °C (Neidhardt 1990). Numbers are calculated relatively to the CDW. The values for *E. coli* were obtained with the *E. coli* strain B/r in balanced growth at 37 °C in glucose minimal medium and a μ of 1.04 h^{-1} and a t_d of 0.67 h (Neidhardt 1990).

The results for *Y. pseudotuberculosis* YPIII at 25 °C in LB medium (figure 3.4.a) were similar to the published results of *E. coli* (figure 3.4.b) with the exception of the RNA value, which was only 50% of the *E. coli* value. This deviation might be due to the biochemical differences between the two organisms or due to differences in the culture conditions. It is also possible that the different growth rates ($\mu_{Y.pseudotuberculosisis}$=0.56 h^{-1}, $\mu_{E.coli}$=1.04 h^{-1}) have a major influence on the composition of the biomass as indicated in figure 3.37. It is proposed that the RNA fraction is increasing with the growth rate, while the protein fraction is decreasing (Neidhardt 1990). This could explain the rather drastic differences in the RNA amount and the increase of the protein fraction. Most cellular compositions are a function of the growth rate and can vary considerably. It has been

reported, that the RNA amount shifts up to 10-fold only due to changes in growth rate (Neidhardt 1990).

The difference in the applied media (minimal medium for *E. coli* and LB medium for YPIII) probably also accounts for differences in the protein fraction. LB medium contains many amino acids and peptides, that probably favor the generation of proteins.

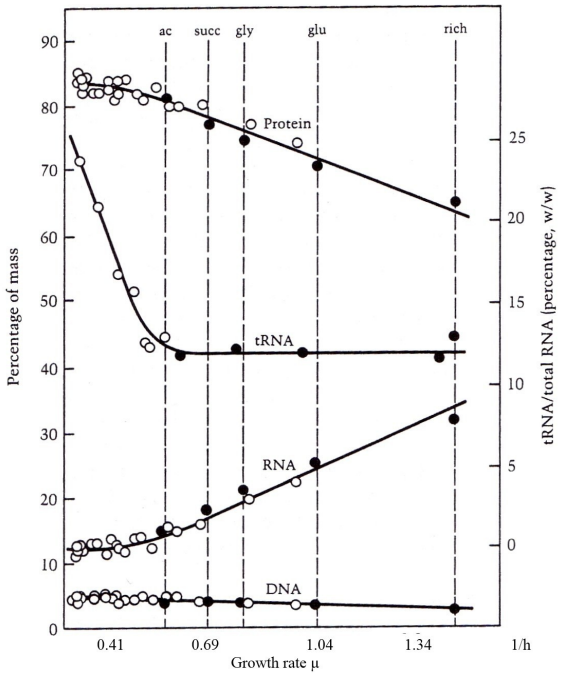

Figure 3.5: Effect of growth rate on the cellular proportions of protein, RNA, and DNA. Filled circles refer to results from *E. coli* B/r cultures undergoing balanced growth in batch cultures in various media, open circles are from cultures growing in a glucose-limited chemostat. Adapted from (Neidhardt 1990).

3.1.3 Growth phase and nutrient dependent changes in the metabolome

Naturally, growth phases significantly influence the metabolism. The cells grow at maximal growth rate while sufficient nutrients are present in the medium during exponential growth phase. The metabolism is focused on proliferation and anabolism. Growth decreases when the nutrients are depleted, a high cell density is reached or toxic side products impair the metabolism. During stationary growth, the growth rate is approximately zero and the metabolism is occupied with maintenance. Energy generation is limited and stress protection systems are expressed.

The growth phase is also one of the most important factors influencing the expression of virulence effectors and regulators. During exponential growth the virulence regulator RovA is degraded by proteases and the adhesion protein Invasin is less expressed (Herbst et al.

2009), whereas virulence effectors of the late virulence (YadA, T3SS, Yops, chapter 1.4) are more expressed during exponential growth.

Nutrient availability is an important signal for the cell influencing metabolism and virulence. Carbon catabolite repression is active in the presence of glucose, thereby repressing the activation of the cyclic AMP receptor protein (Crp). Crp is globally influencing catabolic enzymes and virulence factors (chapter 1.5.7). As a consequence, the global virulence factor RovA, is repressed in minimal medium, which impairs the expression of the adhesion factor Invasin. In contrast, during growth in rich medium with low glucose levels, RovA and Invasin are expressed (Herbst et al. 2009).

In order to gain a general understanding of the metabolism of YPIII during different growth phases and different media, the metabolome in exponential and stationary growth phase was analyzed in minimal medium with glucose as carbon source (chapter 2.7.2) and in rich LB medium (chapter 2.7.1). Further metabolic footprinting was performed, analyzing the supernatant for consumption of substrates and secretion of side products for a complete analysis of the metabolism.

3.1.3.1 Supernatant analysis in minimal medium

The supernatant of cells in minimal medium was analyzed during exponential growth and stationary growth, in parallel to the metabolome analysis after 10 h and 16 h. A summary is shown in table 3.4.

Table 3.4: Summary of the results of the extracellular metabolome analysis of growth phases in minimal media

Experiment	**Detected compounds**	**Identified metabolites**	**Relative standard error** (n= 6, biological replicates)
Exponential phase supernatant:	29	22	7.8%
Stationary phase supernatant:	23	17	12.1%

The composition of the minimal medium was defined (chapter 2.7.2) and the only measurable components in the beginning of the cultivation were glucose and phosphate. In the culture supernatant of YPIII during exponential and stationary phase, 30 compounds could be measured. 24 of these were significantly altered between the growth conditions. The significantly changed metabolites are shown in figure 3.6 and the complete list is given in supplement A.1.

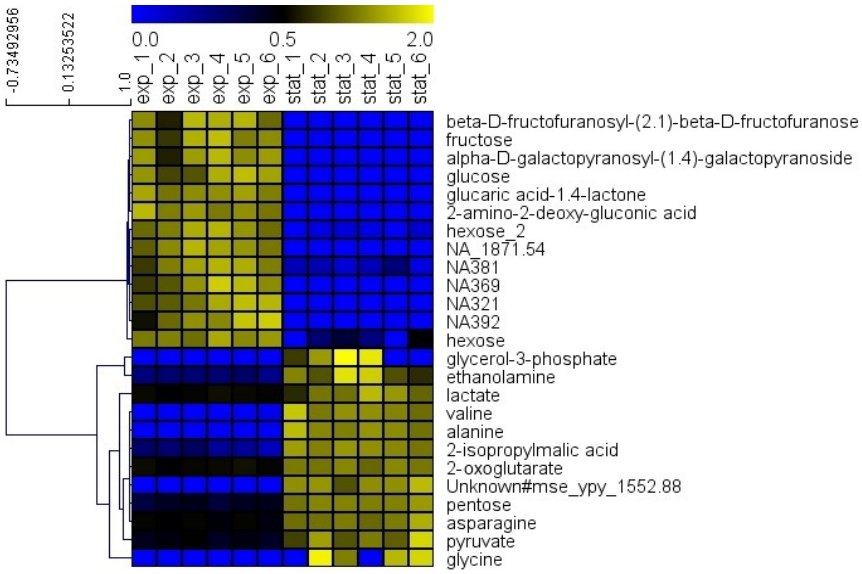

Figure 3.6: Heat map with hierarchical clustering of extracellular metabolites in the supernatant of cells grown in minimal medium at 25°C with glucose as carbon source. Only metabolites are shown, that were significantly altered between exponential state and stationary phase (p-value < 0.01, two paired t-test). The shown data is root-mean-square normalized over the rows. Hierarchical clustering was performed with average linkage and euclidean distance.

The extracellular metabolites with the highest abundance were glucose and phosphate in supernatant from exponential phase, as expected. While phosphate was not significantly altered over time, glucose was consumed after 16 h and was only detected in traces in the stationary phase.

The hierarchical clustering clearly divided the data in figure 3.6 into two groups: The first group contained glucose and a number of sugar derivatives, that were consumed in the stationary phase. All other compounds in this group, other than glucose, were detected in low concentration close to the detection limit. One can assume, that these compounds were other forms or debris of glucose, since they decrease simultaneously. Glucose is known to undergo interconversion processes in aqueous solutions forming small amounts of its isomers (Speck 1958).

The second group is more heterogeneous and consists of compounds, that were detected in both exponential and stationary samples (lactate, asparagine, pyruvate, 2-oxoglutarate) and compounds, that were only detected in stationary phase samples (ethanolamine, alanine, valine, 2-isopropylmalate). This result indicated, that the compounds from the latter group were only secreted in later phases of cultivation or leaked from broken cells in stationary phase.

Since the glucose was depleted in stationary phase the transition into stationary phase was probably due to carbon limitation. To assure that the transition was not due to nitrogen limitation, the amount of $(NH_4)_2SO_4$ was raised from 5 $g \cdot L^{-1}$ to 10 $g \cdot L^{-1}$, which did not alter

the growth. The pH was constant at pH 7 during the cultivation and therefore not growth limiting. Further, an experiment in the nutrient rich Brain Heart Infusion (BHI) medium showed that the bacteria can grow to ODs of 9, the cell density was therefore not limited due to quorum sensing. These results suggested that the transition into stationary phase was due to shortage of the carbon and energy source.

3.1.3.2 Intracellular metabolome analysis in minimal medium

The samples for the metabolome analysis of YPIII in minimal medium at 25 °C were prepared as described in chapter 2.11.1 with adjacent measurement as described in chapter 2.12.1. The samples grown from the exponential phase were harvested after 10 h at an OD of 1.67 ± 0.1 and a $\mu = 0.314\ h^{-1}$ and the samples from the stationary phase were taken after 16 h at an OD of 4.83 ± 0.08 and a $\mu \sim 0\ h^{-1}$. An overview of the detected and identified compounds in the metabolome analyses is shown in table 3.5.

Table 3.5: Summary of the results of the intracellular metabolome analysis of growth phases in minimal media

Experiment	**Detected compounds**	**Identified metabolites**	**Relative standard error** (n= 6, biological replicates)
Exp. phase metabolome minimal medium	98	72	12,90%
Stat. phase metabolome minimal medium	91	66	19.1%

A complete list of all detected substances is given in supplement A.2.

In the metabolome of the exponential phase 10 substances were detected that were not detected in the stationary phase and one substance was detected only in the stationary phase (table 3.6).

Table 3.6: Compounds found only in the metabolome of one growth phase of YPIII in minimal medium with glucose as sole carbon source at 25 °C

Exponential phase	Stationary phase
Not detected	Unknown#mse-ypy-036_1981.10
1,6-anhydro-glucose	Not detected
2-hydroxy-glutarate	Not detected
2,6-diamino-pimelate	Not detected
adenosine-3'-monophosphate	Not detected
cytosine	Not detected
galactose-6-phosphate	Not detected
guanosine	Not detected
phosphoenolpyruvate	Not detected
ribose	Not detected
Unknown#sst-cgl-119_2551.5	Not detected

Several of these metabolites participate in the nucleotide metabolism (ribose, cytosine, guanosine, adenosine-3-P). Some were also sugar derivatives (galactose-6-P, 1,6-anhydro-glucose). A comparison of the amounts of the metabolites detected in both growth phases is presented in a scatterplot in figure 3.7. Some amino acids (cysteine, lysine) were increased in stationary phase, while sugar derivatives (mannose-6-P, glucose-6-P) and nucleobases (uracil, hypoxanthine) were decreased.

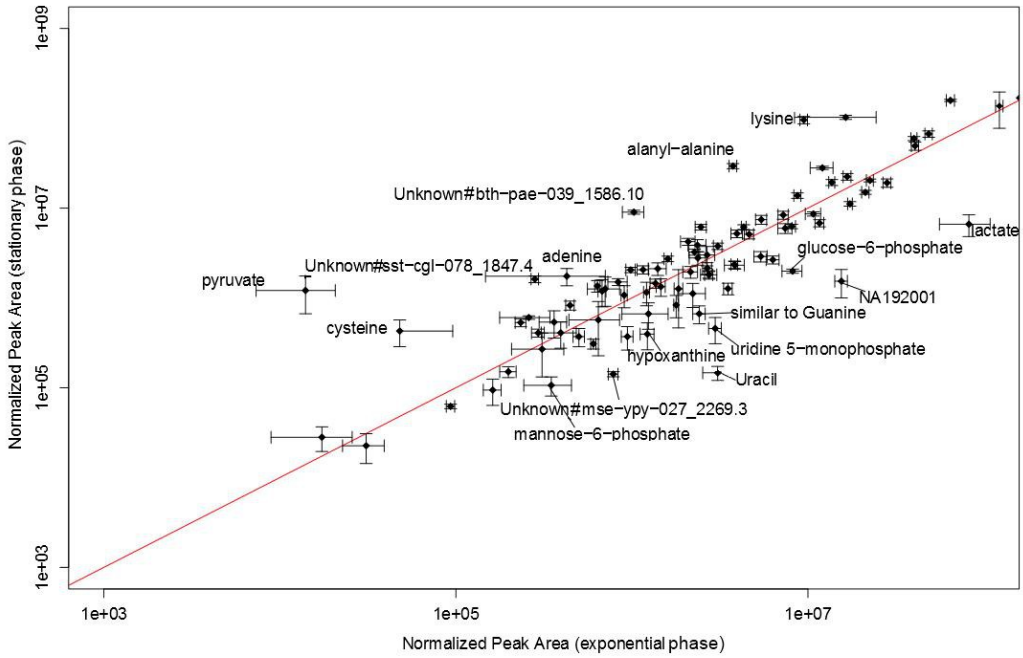

Figure 3.7: Scatterplot of the metabolome of YPIII in exponential phase (X-axis) and stationary phase (Y-axis) in minimal medium with glucose as sole carbon source plotted with logarithmic axes. Metabolites are indicated with names, if they differ more than 3-fold from the bisecting line.

In total, 43 compounds showed significant differences between the growth conditions (p-value < 0.01) as shown in figure 3.8. 22 compounds were decreased in stationary phase, and 21 were increased, showing an even distribution in each direction of the changes in the metabolome. From these results one can summarize that the metabolome of the stationary phase showed several decreased metabolite pools, that belong to the main energy pathways: The glycolysis (glucose, glucose-6-P, glycerate-3-P, glycerate-2-P), the PPP (xylulose-5-P) and the TCA cycle (succinate, malate). Phosphoenolpyruvat (PEP), a key intermediate from the glycolysis, and 2-oxoglutarate were both not detected in stationary phase. This suggests that the glucose was metabolized via the glycolysis and the Entner-Doudoroff-pathway since the corresponding metabolites were decreased, when glucose was depleted. The decrease of the TCA cycle intermediates, except citrate, suggest further a lower energetic state of the cell in stationary phase.

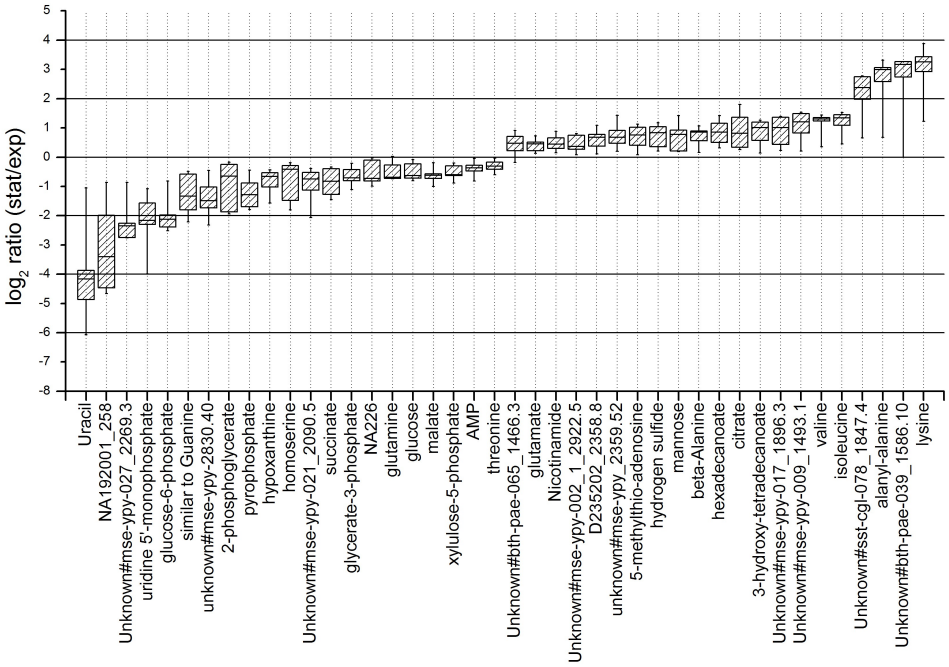

Figure 3.8: Alteration between the metabolites of the exponential and the stationary phase of YPIII grown on minimal medium with glucose as sole carbon source. The boxplots represent $\log_2$ ratios of peak-area$_{exponential}$/ peak-area$_{stationary}$. The displayed metabolites were significantly changed with a p-value < 0.01 (two paired t-test).

The metabolites from the nucleotide metabolism AMP, UMP; cytosine, uracil, hypoxanthine and a compound, that was similar to guanine, were decreased (figure 3.7 and 3.8). Guanosine and ribose were not detected in stationary phase. The lower amounts of nucleobases, nucleotides and nucleosides suggest a decreased DNA and RNA biosynthesis, which was no longer required as growth ceased.

Some amino acids and amino acid precursors were decreased in stationary phase such as glutamine, homoserine, threonine and 2,6-diaminopimelate a precursor of lysine biosynthesis from aspartate.

Interestingly, certain amino acid pools (lysine, cysteine, valine, isoleucine, glutamate) were strongly increased. The decrease of precursors of amino acid biosynthesis and the increase of amino acids in the metabolome of the stationary phase suggest, that the protein biosynthesis was slowed down or that proteins were degraded to fuel the metabolism.

The fatty acids 3-hydroxy-tetradecanoate ($C_{14:0}$) and hexadecanoate ($C_{16:0}$) were increased in stationary phase as well. Long chain beta-hydroxy acids are often part of lipopolysaccharides (LPS) in Gram-negative bacteria. The increase of fatty acids in the

metabolome of stationary cells could be due to changes in the cell wall. Moreover the accumulation of citrate suggests that fatty acids were degraded to fuel the TCA cycle.

Pyruvate was secreted into the supernatant and accumulated intra- and extracellularly over the time. In contrast, lactate was intracellularly reduced in stationary phase, but increased in the supernatant of the stationary phase (chapter 3.1.3.1). The two metabolites are indicators for a partly fermentative metabolism and oxygen limitation. The high amount of lactate in exponential phase cells suggests a higher need for oxygen due to faster growth.

Y. pseudotuberculosis is known to apply mixed acid fermentation under conditions with insufficient oxygen supply. Under these conditions, glucose is degraded to pyruvate, which is then metabolized to lactate, succinate, acetate, ethanol, CO_2 and H_2O. However, it was not expected that the oxygen supply was insufficient since the cultures were vigorously shaken. Also no succinate was detected in the supernatant. Acetate and ethanol could not bet detected with the utilized methods.

Another phenomenon that might have caused these results is the “glucose overflow metabolism”, which was indicated by previous transcriptome analysis in *Y. pseuodtuberculosis* (Rosso et al. 2008). This variant of glucose metabolism occurs at high glucose consumption rates, where the carbon flow is channeled towards acetate formation to prevent the accumulation of NADPH. This was also investigated in *E. coli,* where genes in the TCA cycle and respiration were repressed at high glucose consumption rates (Vemuri et al. 2006).

A similar mechanism or a combination of both might have channeled the carbon flow in YPIII in the direction of pyruvate formation. This could also explain the secretion of valine, alanine, 2-isopropylmalate and glycine into the medium (chapter 3.1.3.1), which are amino acids or amino acid precursors, that can be produced from pyruvate. A secretion of acetate would also be expected under these conditions.

Although this explains the secretion of pyruvate during exponential phase, it is not clear why pyruvate was not consumed again in stationary phase. It was shown previously that YPIII can use pyruvate as sole energy and carbon source (chapter 3.1.1). A possible explanation is the suppression of catabolic enzymes through carbon catabolite repression (chapter 1.5.7), since experiments with a *crp* deletion mutant showed, that the presence of Crp is required to consume pyruvate as sole carbon source (chapter 3.3.9.2). Because traces of glucose could be detected in the supernatant of the stationary phase, it is possible that Crp is repressed trough carbon catabolite repression.

3.1.3.3 Supernatant analysis in LB medium

The analysis in rich medium was used to investigate a physiological state of YPIII closer to the natural conditions, that enteropathogenic *Yersiniae* face outside their host e.g. in raw meat, than the rather unnatural condition in minimal medium. LB medium meets these requirements and is well studied, since it is used for decades in laboratories. Further, it promotes the expression of the global virulence regulator RovA (chapter 1.5.1). Nevertheless, the choice for LB medium is a difficult one, since it is undefined and the composition can vary slightly from batch to batch. To antagonize these effects, all experiments for one analysis were done with the same batch of LB medium to avoid deviations in the composition. Further, the supernatant was carefully monitored to take consumption and secretion patterns into account, when interpreting the corresponding intracellular metabolome data.

The medium was made from yeast extract, tryptone and NaCl (chapter 2.7.1). Yeast extract is derived from the water-soluble portion of autolyzed yeast and tryptone is made from digested casein. The medium consists of peptides, amino acids, sugars, alcohols, nucleotides, vitamins, trace elements, fatty acids and minerals.

Three pure LB medium samples were analyzed with the standard GC-MS method (chapter 2.12.1). The main components detected in the LB medium are shown with their normalized peak-areas in figure 3.9, the complete list of detected substances is presented in supplemental B.1.

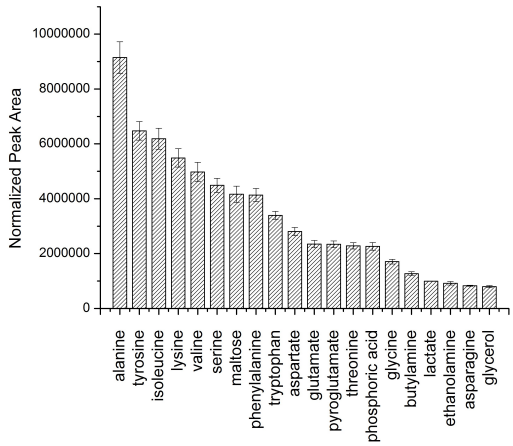

Figure 3.9: The most abundant components of LB medium. 90% of the summarized peak-area of the analysis is described by these components.

The analysis of the medium showed that roughly 2/3 of the detectable components of the summarized peak-area were amino acids and 1/10 were sugars. A smaller part consisted of

nucleotides and nucleobase and organic acids. Due to limitations in the detection method, peptides and vitamins were not measured. Nevertheless, the detected substances are in accordance with previous analysis (VanDusen et al. 1997; Hanko & Rohrer 2000; Hanko & Rohrer 2004). In a study with auxotrophic *E. coli* mutants, the composition of utilizable components was determined as approximately 89.8 mM amino acids (including accessible oligopeptides), 0.5 mM purine and pyrimindines and approximately 0.1 mM carbohydrates (Sezonov et al. 2007).

The supernatant samples of the YPIII cultivation were taken in three biological replicates at five different time-points after 0 h, the pure medium samples, 2.5 h and 5.5 h, which both represent the exponential phase and 12 h and 15 h, which represent the stationary phase. The growth of YPIII in LB medium is shown in figure 3.5. The summary of the analyses is shown in table 3.2 and the complete results are given in supplemental B.1.

Table 3.7: Summary of the results of the supernatant analysis of YPIII in LB medium during growth

Sample time-point [h]	**Detected compounds**	**Identified metabolites**	**Relative standard error** (n= 3, biological replicates)
0	75	57	9.0%
2.5	75	58	11.9%
5.5	67	51	14.6%
12	67	49	13.5%
15	68	50	16.8%

It can be observed, that the number of detected compounds decreased from the first to the last time-point by 7, probably through the consumption of compounds. Figure 3.10 shows the significantly changed metabolites from the supernatant. The hierarchical clustering of figure 3.10.a differentiates the metabolites in six cluster. The clustering reveals that YPIII had different preferences for nutrients. While the sugars glucose and fructose as well as glycerate and adenosine were rapidly consumed in the first cluster, the amino acids from the second and third cluster were taken up more slowly and only after the sugars were depleted. These clusters were very similar according to the hierarchical clustering, but while the second cluster contained metabolites that were completely consumed before 5.5 h, the metabolites of the third cluster were diminished but not depleted after 5.5 h. The fourth cluster included extracellular metabolites that were detected after 2.5 h, and were directly consumed after this time-point. This concerned inosine, uracil and hypoxanthine, which are involved in nucleoside metabolism. Pyruvate was also found in this cluster. The fifth cluster consisted of metabolites, that showed a significant increase after 2.5 h with

adjacent consumption, that inclosed mostly intermediates of the TCA cycle such as fumarate, succinate and malate. Finally, the sixth cluster included metabolites, that were secreted during the cultivation. While the putrescine concentration raised directly after 2.5 h, the other metabolites increased steadily like 2-hydroxyglutarate or only in the stationary phase like N-acetyl-serine.

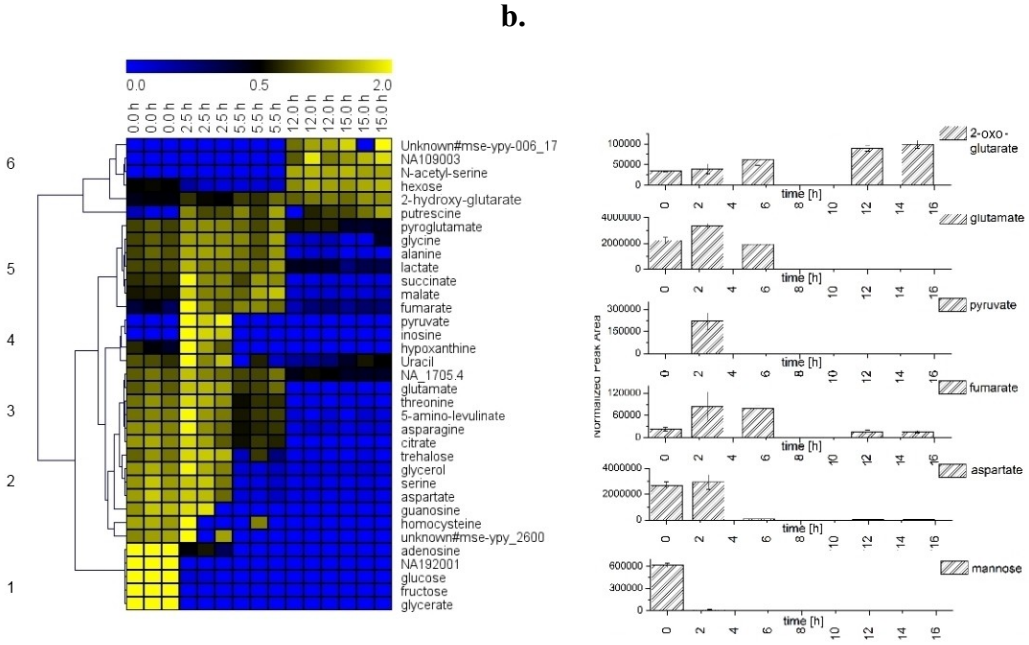

Figure 3.10: Time resolved extracellular metabolite values from cultivation in LB medium at 25 °C. (a) extracellular metabolites, that showed significant changes over the time of cultivation, root-mean-square normalized over the rows and displayed in a heatmap with hierarchical clustering. Sample time-points are indicated above. (b) selected extracellular metabolites, that represent distinguishable groups, identified by the hierarchical clustering, with their ribitol-normalized peak-areas.

The analysis also reveals that amino acids YPIII had different up-take preferences for amino acids: Aspartate and serine were nearly depleted after 5.5 h, but glutamate, asparagine and threonine were consumed to a lesser extent and were still present in the supernatant after 5.5 h. The consumption of glycine, alanine and pyroglutamate did not start before 5.5 h. For cysteine, isoleucine, leucine, lysine, methionine, ornithine, phenylalanine, tryptophan, tyrosine and valine no consumption was measured during the cultivation (supplement B.1). These findings are in accordance with the results of the phenotyping microarray analysis, as these did also not provide respiration as carbon or nitrogen source (chapter 3.1.1). The proteinogenic amino acids glutamine, arginine, proline and histidine could not be detected in the medium. The sequential consumption of amino acids has also been observed in *E. coli* (Baev et al. 2006) and some of them have been

tested in *Y. pseudotuberculosis* PB1 cells (Dreyfus & Brubaker 1978). The results concerning uptake and utilization of amino acids are summarized in table 3.7.

Table 3.8: Summary of usability of proteinogenic amino acids as determined experimentally. Utilizable carbon sources are marked bold, weak signals are shown in brackets.

Amino acid	Digestible as C-source[1]	Digestible as N-source[1]	Consumed from medium[2]	Rate of destruction[3] [nmol amino acid/min/mg dry weight]
Serine	yes	yes	xxx	53.1
Aspartate	no	yes	xxx	31.0
Alanine	yes	yes	xx	9.3
Glycine	no	yes	xx	5.8
Glutamate	yes	yes	x	10.2
Asparagine	(yes)	yes	x	46.6
Threonine	no	(yes)	x	10.1
Lysine	no	no	no	
Cystein	Not tested	no	no	
Isoleucine	no	no	no	
Leucine	no	no	no	
Methionine	no	no	no	
Ornithine	no	(yes)	no	
Tyrosine	Not tested	no	no	
Valine	no	no	no	
Phenylalanine	no	no	no	
Tryptophan	Not tested	no	no	
Proline	(yes)	yes	Not detected	11.3
Glutamine	no	yes	Not detected	2.2
Histidine	(yes)	yes	Not detected	
Arginine	no	yes	Not detected	

The medium included small amounts of nucleosides, that were consumed very fast. Adenosine and guanosine were depleted after 2.5 h and 5.5 h, respectively (first and second cluster). The phenotyping microarray analysis showed that adenosine can be used as carbon source and as nitrogen source (see chapter 3.1.1). The desamination of adenosine leads to inosine, which was increasingly detected in the supernatant after 2.5 h. Inosine can be further cleaved to yield hypoxanthine, which was also increased after 2.5 h. Uracil is a by-product of uridine catabolism as discussed later in chapter 3.3.7. Its increased detection

1 Results from phenotyping Microarrays (Chapter 3.1.1)

2 xxx = depleted before 2.5 h of cultivation in LB medium supernatant, xx = before 5.5 h, x = after 5.5 h

3 Rates from resting *Y. pseudotuberculosis* PB1 in 0.033 M MOPS buffer, pH 7 from (Dreyfus & Brubaker 1978)

after 2.5 h indicates the consumption of urdinine. In *E. coli*, the enzymes for uridine utilization are up-regulated in exponential growth in LB medium (Baev et al. 2006), encouraging this assumption. Nevertheless, uridine could not be detected in the supernatant, maybe because the concentration was under the detection limit.

In an additional experiment, two-times concentrated LB medium was added to the cells in stationary phase. As a result, the growth of YPIII was instantly reestablished and optical density increased further (data not shown). Hence, the growth phase transition from exponential to stationary phase in the LB medium was due to nutrient limitation, like in the minimal medium (chapter 3.1.3.1). Since ethanolamine and putrescine increased in the supernatant during cultivation of YPIII in LB medium, an excess of nitrogen can be assumed. This would indicate that the transition was not due to nitrogen limitation, suggesting rather a carbon- or energy source limitation. Carbon limitation is also the reason for growth phase transition in *E. coli* in LB medium (Baev et al. 2006).

3.1.3.4 Intracellular metabolome analysis in LB medium

The metabolome samples for the exponential phase of YPIII cells grown in LB medium were harvested after 5.5 h at an OD of 1.2 ± 0.1 and a $\mu = 0.56\ h^{-1}$. The samples for stationary growth were harvested after 15 h at an OD of 3.9 ± 0.1 and a $\mu \sim 0\ h^{-1}$. An overview of the number of detected and identified compounds in the metabolome analyses is shown in table 3.1 and the complete results are given in supplement B.2.

Table 3.9: Summary of the results of the intracellular metabolome analysis of growth phases in LB medium

Experiment	**Detected compounds**	**Identified metabolites**	**Relative standard error** (n= 6, biological replicates)
Exponential phase	93	60	12.2%
Stationary phase	106	64	13.2%

13 compounds were only detected in the metabolome of the stationary phase. Additionally, 2 compounds were only measured in the exponential phase metabolome (table 3.8).

Table 3.10: Compounds found only in one growth stage of cultivation in LB medium at 25 °C

Exponential phase	Stationary phase
Unknown#mse-ypy-026_2236.8	Not detected
Unknown#mse-ypy-037_2590.9	Not detected
Not detected	3-amino-propane-1,2-diol
Not detected	heptadecanoate
Not detected	homocysteine
Not detected	N,N-dimethylglycine
Not detected	NA184
Not detected	NA411
Not detected	NA438
Not detected	Unknown#bth-pae-038_1567.3
Not detected	Unknown#mse-ypy_2600
Not detected	Unknown#mse-ypy-028_2276.9
Not detected	Unknown#mse-ypy-030_2498.7
Not detected	Unknown#mse-ypy-036_1981.9
Not detected	Unknown#sst-cgl-094_2097.4

The metabolites, that were detected in the metabolome of both growth phases, are compared in a scatterplot in figure 3.11.

Several metabolites from the TCA cycle were decreased in stationary growth (succinate, fumarate, citrate, 2-oxoglutarate), while the majority of increased metabolites were amino acids or amino acid degradation products (2-aminoadipate, tryptamine, asparagine, ornithine, phenylalanine, tyrosine).

44 compounds were significantly altered between the growth in exponential and stationary phase (p-value < 0.01). The $\log_2$ ratios of the peak-areas are shown as boxplots in figure 3.12. 29 metabolites of these were decreased in the stationary phase and 15 were increased. This fact, together with the observation of the scatterplot (figure 3.11), shows a reduction of metabolite pools in the stationary phase, although more compounds were detected, compared to the exponential phase (table 3.8). Most of these compounds, solely detected in the stationary phase, were unknown and remained to be elucidated further.

The intracellular metabolite pools belonging to the glycolysis or gluconeogenesis (glucose, glucose-6-P, fructose-6-P) and the TCA cycle (fumarate, malate, citrate, 2-oxoglutarate) were significantly decreased in the stationary phase, hence a lowered energy generation was likely. Only fructose-1,6-bisphosphate was increased, which indicated more gluconeogenesis activity in stationary phase. This is in accordance with the supernatant

analysis of the culture, which showed that all sugars were depleted from the medium during the stationary phase (chapter 3.1.3.3).

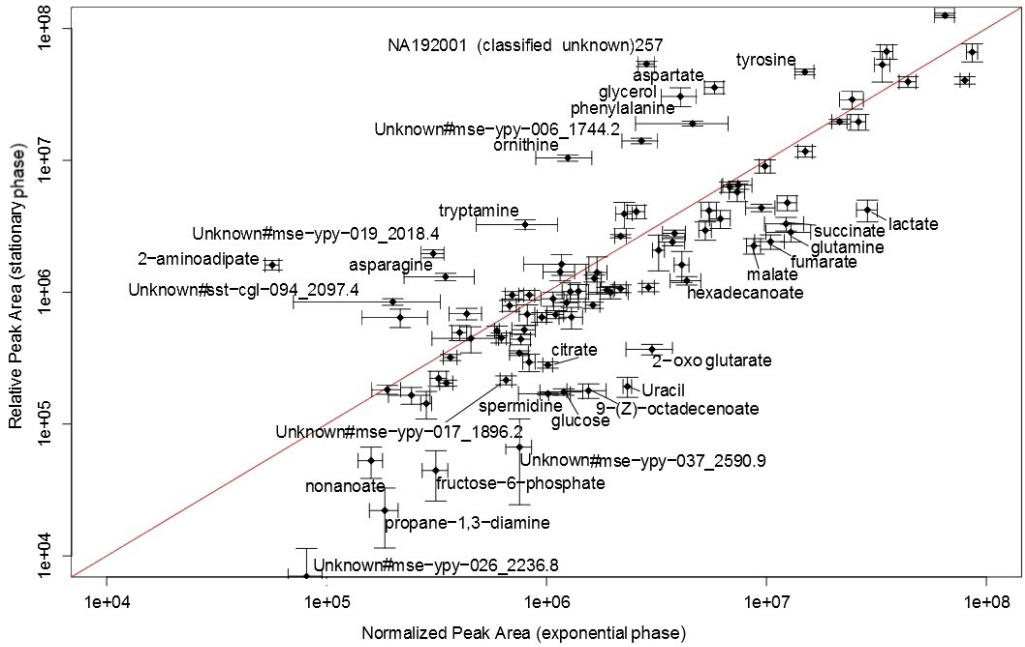

Figure 3.11: Scatterplot of the metabolome in exponential phase (X-axis) and stationary phase (Y-axis) in LB medium plotted with logarithmic axes. Metabolites are indicated with names, if they differ more than three-fold from the bisecting line.

The most striking change in the stationary phase was the increase of the amino acids pools (tyrosine, ornithine, phenylalanine, asparagine, aspartate, valine, lysine). The compound 2-aminoadipate was also about 30-fold heightened. It participates in the degradation of lysine *via* pipecolate in some organisms, but the corresponding enzymes are not identified in YPIII. Tryptamine concentration was also raised in stationary phase. The metabolite is formed from tryptophan and is a precursor for secondary metabolites. Though tryptophan was under the detection limit and therefore not measured, it can be assumed from tryptamine, that it was also increased in stationary phase. The majority of the amino acids enhanced in the stationary phase were the product of biosynthesis and not incorporated from the medium (tyrosine, ornithine, phenylalanine, valine, lysine), since they were not consumed from the medium (chapter 3.1.3.3). Only asparagine and aspartate were both, enhanced in stationary phase and consumed from the medium. Amino acids such as phenylalanine and tyrosine need to be synthesized from gluconeogenesis indicating that some flux was required through this pathway, which was supported by the increase of

fructose-1,6-bisphosphate in stationary phase. Studies with *E. coli* grown in LB medium showed that most amino acid biosynthesis pathways are increasingly expressed in late exponential phase and stationary phase (Baev & Radek et al. 2006). However, alternative to enhanced biosynthesis, increased protein degradation might have caused the higher amino acid pools.

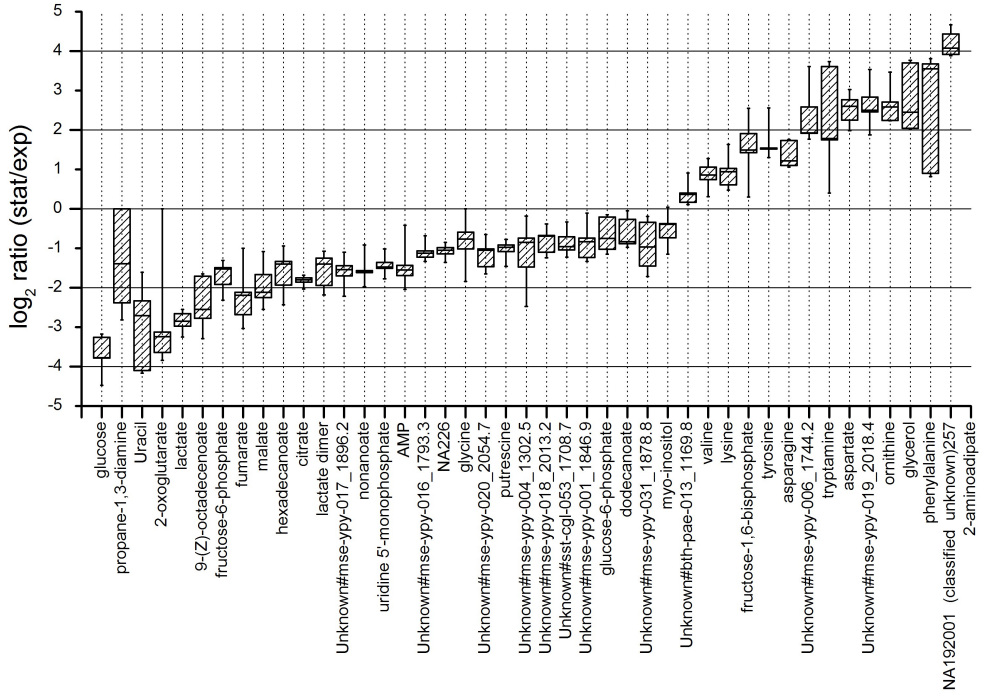

Figure 3.12: Alteration between metabolites from *Y. pseudotuberculosis* grown on LB medium during exponential and stationary phase. The boxplots represent $\log_2$ ratios of peak-area$_{stationary}$/ peak-area$_{exponentiel}$. The displayed metabolites were significantly changed with a p-value < 0.01 (two paired t-test).

The majority of the detected fatty acids was decreased in the stationary phase (dodecanoate ($C_{12:0}$), 9-Z-octadecenoate($C_{18:1}$) , nonaoate ($C_{9:0}$), hexadecanoate ($C_{16:0}$)), which pointed to a reduced lipid biosynthesis. Since citrate, which is the entry point of fatty acid degradation to the TCA cylcle, was also decreased in stationary phase, a reduced cell wall biosynthesis due to reduced doubling time is rather likely than the degradation of fatty acids.

The decreased metabolites of the nucleoside metabolism (uracil, AMP, UMP) in the stationary phase metabolome, suggest a down-regulated DNA and RNA biosynthesis, probably due to ceased proliferation.

The polyamines spermidine and putrescine as well as the polyamine cleavage product propane-1,3-diamine decreased in stationary phase (figure 3.11, 3.12). Putrescine was

secreted into the medium in the beginning of the cultivation and was not reused later (chapter 3.1.3.3). Polyamines have various roles in the metabolism of bacteria and are known to be generated as stress response or as energy storage. In *Y. pestis* they are associated with biofilm formation (Wortham & Oliveira 2010). Putrescine was influenced by the ammonium concentration of the medium in YPIII (data not shown). It decreased under high nitrogen availability suggesting no nitrogen limitation present in the stationary phase in LB medium.

Intracellular pyruvate and lactate decreased in stationary phase, but the compounds were secreted during exponential growth the cells (chapter 3.1.3.3). The secretion could be a result of an incomplete TCA cycle and suggests a mixed acid fermentation or glucose overflow to avoid accumulation of NADPH. This matter has been observed in the minimal medium supernatant over the whole cultivation time (chapter 3.1.3.1). It is possible that a similar mechanism also occurred during the first hours of cultivation in LB medium, when predominantly sugars were consumed. Potentially, the bacteria were performing an incomplete mixed acid fermentation, where not only the common end-products (lactate, succinate, acetate, ethanol, CO_2, H_2O) were secreted but also fumarate, malate and pyruvate. When the sugar pools were depleted, the bacteria started to consume the by-products and therefore their concentrations decreased again in the supernatant. This is in line with other observation such as that the expression of enzymes involved in lactate utilization are increasingly expressed in *E. coli* during late exponential and stationary phase in LB medium, indicating the use of lactate in later stages of growth (Baev et al. 2006). Further, a similar secretion and uptake pattern has been reported in the supernatant of *Staphylococcus aureus*, when grown on glucose minimal medium supplemented with amino acids (Liebeke et al. 2011). Only cells grown in LB medium were secreting TCA cycle intermediates in the exponential phase (fumarate, malate, succinate). These substances were not detected in the minimal medium supernatant, thus the secretion was not the result of glucose consumption and probably rather due to amino acid consumption.

Rosso *et al* (Rosso et al. 2008) performed a transcriptome study with the *Y. pseudotuberculosis* strain IP32953 where they investigated different conditions regarding besides other the growth stages (exponential vs. stationary) in LB medium at 28 °C. The results of this analysis are available online under www.genoscript.pasteur.fr. These data were used for a comparison of the here-described metabolome analyses. Several transcripts encoding ribosomale proteins (*rplC, rplD, rplE, rplP, rplQ, rplW, rpsC, rpsE,*

rpsS) were down-regulated in stationary phase, indicating a reduced protein biosynthesis as suggested in the metabolome through increased amino acid pools.

The transcripts for the glycerol kinase, the glycerol-3-P dehydrogenase and the glycerol uptake facilitator protein (*glpK, glpD, glpF*) were down-regulated. These enzymes are responsible for the uptake, phosphorylation and degradation of glycerol. Glycerol can serve as carbon and energy source or as precursor for phospholipid synthesis. Since the uptake protein was also down-regulated in stationary phase, the detected glycerol was probably the result of the degradation of phospholipids. Since the glycerol-3-P in the intracellular metabolome was not increased, the down-regulation of the transcripts of the glycerol kinase and the the glycerol-3-P dehydrogenase, responsible for the degradation of glycerol, was the probable reason for the intracellular accumulation of glycerol.

The uridine phosphorylase (*udp*) was likewise down-regulated, which is in accordance with the decreased UMP and uracil in the metabolome. The transcriptome results further show that the pH 6 antigen (*psaA*) was up-regulated in stationary phase in LB medium.

3.1.3.5 Media dependent differences in the metabolism

The previous investigation of the intracellular metabolome in chapter 3.1.3.2 and 3.1.3.4 showed that 38 metabolites in the metabolome of cells grown in minimal medium and 47 in the metabolome of cells grown in LB medium were unique for these conditions while 59 compounds were detected in both conditions (figure 3.13).

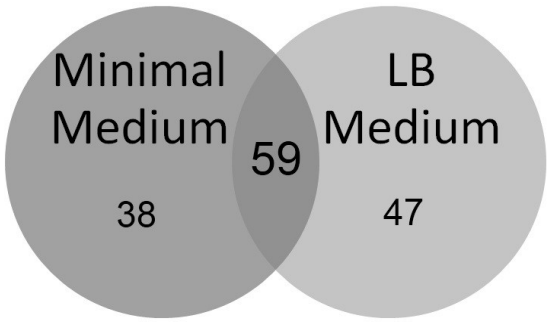

Figure 3.13: Venn diagram of metabolites found in the metabolome of cells grown on LB medium and minimal medium.

This shows that the metabolism is greatly altered between growth in minimal medium and LB medium. In the cells grown in minimal medium, several metabolites belonging to the central carbon pathways (6-phosphogluconate, xylulose-5-P), nucleoside metabolism (guanosin-6-P, guanosine, ribose, hypoxanthine, cytosine, adenosine), precursors for cell

wall and amino acid biosynthesis (2-amino-2-deoxy-glucose-6-phosphate, 2,6-diaminopimelate, alanyl-alanine), tetrapyrrole biosynthesis (5-aminolevulinate) and certain amino acids (serine, cysteine, tryptophan) were detected, that were not measured in samples from LB medium.

The cells grown in LB medium contained some odd-numbered fatty acids (heptadecanoate ($C_{17:0}$), nonanoate ($C_{9:0}$)), degradation products of amino acids and polyamines (homocysteine, tryptamine, spermidine, propane-1,3-diamine, 2-aminoadipate, urea), which were not detected in cells grown in minimal medium. The sugar derivatives fructose-6-P and fructose-1,6-bisphosphate were also not detected in the cells grown in minimal medium. Nevertheless, since most of the above described metabolites are essential for bacterial growth, they were probably present in the investigated bacteria but their concentration was below the detection limit.

The 59 metabolites that were found in both conditions, were used for a principal component analysis (PCA) of the metabolome samples (figure 3.14).

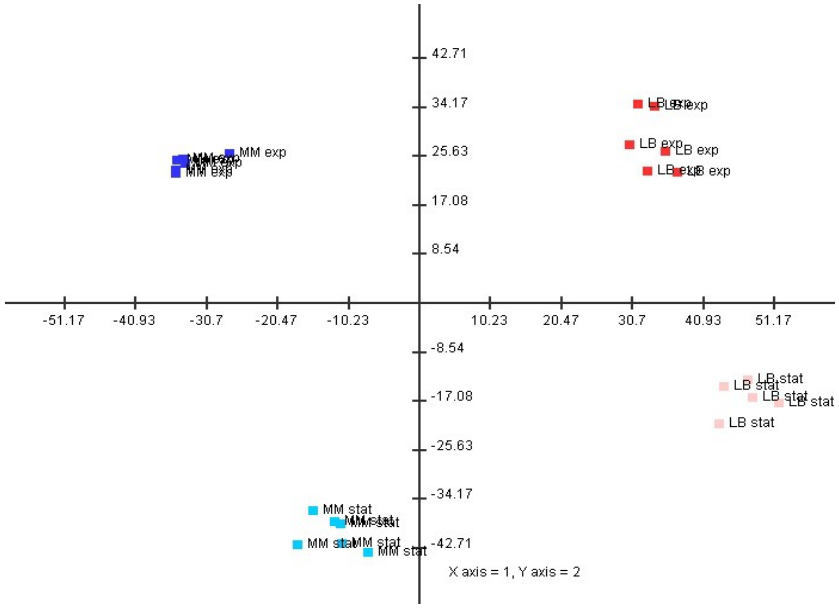

Figure 3.14: Principal component analysis of the metabolic profiles of cells grown in LB medium and minimal medium (MM) in exponential and stationary phase. Every condition is displayed with six biological replicates. X-axis (PC1) accounts for 32.4 % of the total variance, while the Y-axis (PC2) accounts for 24.5 %. The analysis is based on 59 metabolites that were detected in all conditions.

The PCA is used to reduce the variance and information of a data set to a minimum of components and to visualize the connection of the data, as explained in chapter 2.14.5.

The PCA displays 56.9 % of the total variance of the data set, whereas the first principle component (PC1) accounts for 32.4 % and the second principal component (PC2) accounts for 24.5 %. The samples can be divided into four groups according to their growth phase

and medium. The separation of the samples of the different media occurs predominately on the X-axis (PC1), whereas the separation of the growth phases occur mostly over the Y-axis (PC2). This indicates that several changes in the metabolism between exponential and stationary phase were similar, despite the different nutrition. The supernatant analyses in the previous chapters 3.1.3.1 and 3.1.3.3 suggest that the transitions from exponential to stationary phase in minimal medium and LB medium were both due to the depletion of carbon sources, which might account for similar metabolic mechanisms during transition.

To point out the influences of the media to the dynamic of the metabolome, metabolites that were detected under both conditions are shown in their metabolic context in figure 3.15. Metabolites are highlighted in red, if they showed a similar tendency between exponential and stationary phase metabolome. Additionally metabolites are highlighted in blue, if they show different tendencies during cultivation in different media.

In both media, a decrease of intermediates of the energy generating pathways glycolysis and TCA cycle was observable (with the exception of pyruvate and citrate) as well as reduced pools of nucleotides in stationary phase. Both phenomenons have been reported in *P. putida* and *S. aureus* in minimal medium (Jäger 2011; Liebeke et al. 2011) and can be interpreted as signals for low energy and carbon source availability and slow dell division independent from the medium. Lactate was decreased in stationary phase in both media suggesting insufficient oxygen supply in exponential phase during maximum growth rate.

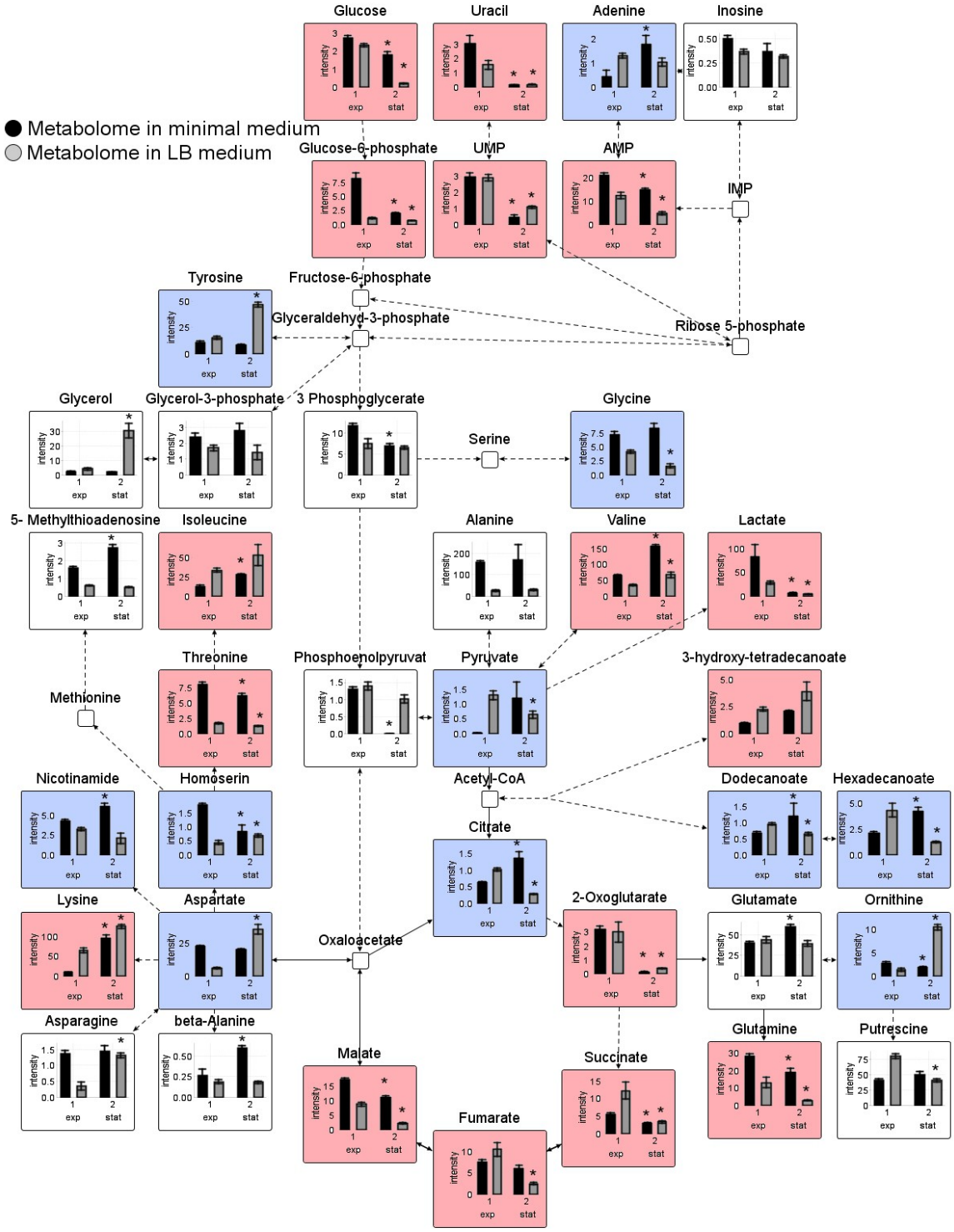

Figure 3.15: Visualization of intracellular metabolite concentrations in minimal medium (black) and LB medium (light grey) bars. The first time-point represents the exponential phase, the second time-point represents the stationary phase. The asterisk above the bars represent significance between growth phases. Metabolites are highlighted in red, if they change alike between the growth phases in both media (LB medium ratio$_{exp/stat}$ ≈ minimal medium ratio$_{exp/stat}$) and in blue, if they change inversely. The metabolites with a white background do not show changes in both media. Interrupted connections represent a conversion of metabolites *via* more than one step. Image created with the Vanted software (Junker et al. 2006).

The amino acids that increased in stationary phase in both media, were lysine, isoleucine and valine, while glutamine and threonine both decreased (figure 3.15). The increase of

lysine in stationary phase has also been observed in *S. aureus,* when grown on glucose minimal medium supplemented with amino acids (Liebeke et al. 2011). Proteome data were included in the study and no increase in the synthesizing enzymes was noted. Since lysine was non consumed from either media, the increase was probably the result of the digestion of intracellular proteins and a reduced protein biosynthesis leading to accumulation of the amino acids. The decrease of glutamine in both media during growth, might be linked to the reducing ammonia content of the medium. Another capacity occurring in both media was the continuous secretion of 2-hydroxyglutarate. This was unexpected since the metabolite is closely connected to 2-oxoglutarate, an intermediate of the TCA cycle important for energy generation and carbon flux. *Y. pestis* extracts showed modest ability to convert 2-oxoglutarate to succinate (Brubaker 2006), hence a similar mechanism can be suspected, leading to the formation of 2-hydroxyglutarate from 2-oxoglutarate with adjacent secretion. However, no further indicators for such a process were detectable in the analysis.

Only the minority of detected metabolites showed contrary tendencies between the growth phases in both media (marked blue in figure 3.15). Adenine, pyruvate, citrate, dodecanoate, hexadecaonate, nicotinamide and glycine were all increased in stationary phase in minimal medium but were decreased in LB medium. Aspartate, homoserine, tyrosine and ornithine were decreased in the in stationary phase in minimal medium and increased in LB medium. The considerable increase of ornithine, tyrosine and aspartate in stationary phase in LB medium was not the result of degradation of compounds from the medium, since aspartate was depleted in the supernatant and ornithine and tyrosine cannot be utilized by YPIII (table 3.7). Therefore it is likely, that the increase is due to different protein degradation or biosynthesis rates. From earlier studies it is known that YPIII expresses Invasin in the stationary phase in LB medium but not in minimal medium (Herbst et al. 2009), which could have caused the different sizes of amino acid pools. Further, it is known that Invasin is anchored in the outer membrane. The protein is therefore translocated through the inner membrane, which requires the formation of specific pores altering the membrane (Tsai et al. 2010). The different tendencies of fatty acids and glycerol in the metabolome of the two media could be a sign for this.

Strikingly, two metabolites of the central carbon pathway were differently altered between the media. Pyruvate and citrate were increased in stationary phase in minimal medium and decreased in stationary phase in LB medium. Through the analysis of the supernatant also

the continuous secretion of pyruvate and lactate in the minimal medium was measured and an incomplete degradation of glucose could be suspected.

Taken these information together, one can assume that there are some universal changes in the metabolome between exponential and stationary growth phase independent nutrition, that can shortly be described as, decrease of metabolites in the central carbon and biosynthetic pathways and increase of amino acid pools in the stationary phase.

However, despite these general aspects some differences between the metabolic profiles grown in different media were notable. In the minimal medium, the glycolysis and the PPP were more active than in the LB medium. This was indicated by the presence of several higher concentrated glycolytic intermediates. Further, several compounds that are synthesized from precursors from glycolysis or PPP are higher concentrated in cells grown in minimal medium (e.g. nucleosides, nicotinamide, serine, cysteine, tryptophan).

Another difference was, that in the cells grown in minimal medium heightened concentrations of biosynthesis intermediates were detected. Especially compounds involved in peptidoglycan biosynthesis (alanyl-alanine, 2-amino-2-deoxyglucose-6-P, 2,6-aminopimelate) were exclusively found in the metabolome of cells grown in minimal medium, indicating an increased cell wall biosynthesis. Congruently, heightened concentrations of fatty acids were detected in minimal medium in stationary phase.

In cells grown in LB medium more fructose-6-P and fructose-1,6-bisphosphate were detected indicating gluconeogenesis activity, which is in coherence with the analysis of the LB supernatant in chapter 3.1.3.3, where most sugars are exhausted very early.

Also, more intermediates of degradation processes were detected in LB medium (2-aminoadipate, propane-1,3-diamine, urea). Since the organism was grown mostly on amino acids in LB medium an excess of nitrogen was expected, which might have caused an increase of the mentioned metabolites and could be disposed though conversion in urea and subsequent degradation through urease activity to NH_4^+ and CO_2. The increase of certain compounds (ornithine, tyrosine, aspartate, glycerol) only in stationary phase of LB medium could be linked to the increased Invasin expression.

3.2 Influence of the temperature on the physiology of Y. pseudotuberculosis

Temperature is the most important indicator for bacteria to sense their environment as previously discussed in chapter 1.6.5. The elevation of the temperature to 37 °C is generally understood as a signal for entrance into the mammalian host. The expression of several virulence f actors of *Y. pseudotuberculosis* is regulated through the regulator proteins YmoA, RovA and LcrF in response to the temperature (Hoe & Goguen 1993, Herbst et al. 2009).

Since 25 °C represents the situation outside the host, the virulence factors of the early virulence (Invasin, motility) are expressed, while at 37 °C they are repressed and virulence factors of the later stage of infection are expressed (Yops, YadA, T3SS, pH 6-antigen).

Several studies indicate a drastic influence of the temperature on the metabolism of *Yersiniae* (Hills & Spurr 1952, Motin et al. 2004, Bochner 2009b), which includes increasingly complex nutritional requirements and differences in energy generation during temperature elevation.

Since it was also observed during this work that the form and motility of the bacteria change between the two investigated temperatures, it was supposed that the morphology of the bacteria may alter. Consequently, several of the experiments for characterization of the cell that were performed at 25 °C, were also performed at 37 °C. The experiments were done analogously to the experiments described earlier. The only differing parameter was the cultivation temperature of 37 °C. The results are mainly discussed with regard to the differences to the analysis at 25 °C, since all basic conclusions at 25 °C have been discussed in the previous chapters. The objective of this part of my thesis was to characterize and interpret the changes in the metabolism and nutritional requirements of YPIII at 37 °C compared to 25 °C to derive detailed information on how the metabolism might adapt to the intra-host lifestyle.

3.2.1 Catabolic abilities at 37 °C

It is supposed that nutrient availability changes drastically between the inside of the host and the outside (as discussed in chapter 1.6.2). Therefore the bacteria need to adapt its nutritional requirements to the varying environment. To investigate the way of adaption,

phenotyping microarrays from BIOLOG were applied. The arrays have been previously used at 25 °C to characterize the general catabolic abilities at 25 °C in chapter 3.1.1. Their handling is described in chapter 2.9.6.

The investigations at 37 °C included testing 190 carbon sources (PM1 and PM2A), 59 phosphor sources (PM4), 35 sulfur sources (PM4) and 95 supplemental substances (PM5). The test for utilizable nitrogen sources (PM3) did not provide any positive signal at 37 °C.

Utilizable carbon sources

From the190 offered carbon sources 10 could be utilized at an incubation temperature of 37 °C. These were one alcohol, two organic acids and seven saccharides and saccharide derivatives. The comparison to the results at 25 °C are displayed in figure 3.16.

The results differ vastly from each other, since at 37 °C 31 less compounds gave a positive signal. Also, many respiration curves reached a lower intensity at 37 °C than at 25 °C. Only for four substances similar intensities were obtained: mannitol, methyl pyruvate, N-acetyl-β-D-mannosamine and β-methyl-glucoside. Six substances showed a lower respiratory signal compared to 25 °C: Fructose, D-trehalose, maltotriose, lactate, N-acetyl-neuraminic acid and arbutin. Most of these substances are degraded *via* the glycolysis except for lactate and methyl pyruvate. No amino acids could be consumed as carbon source at 37 °C.

a.

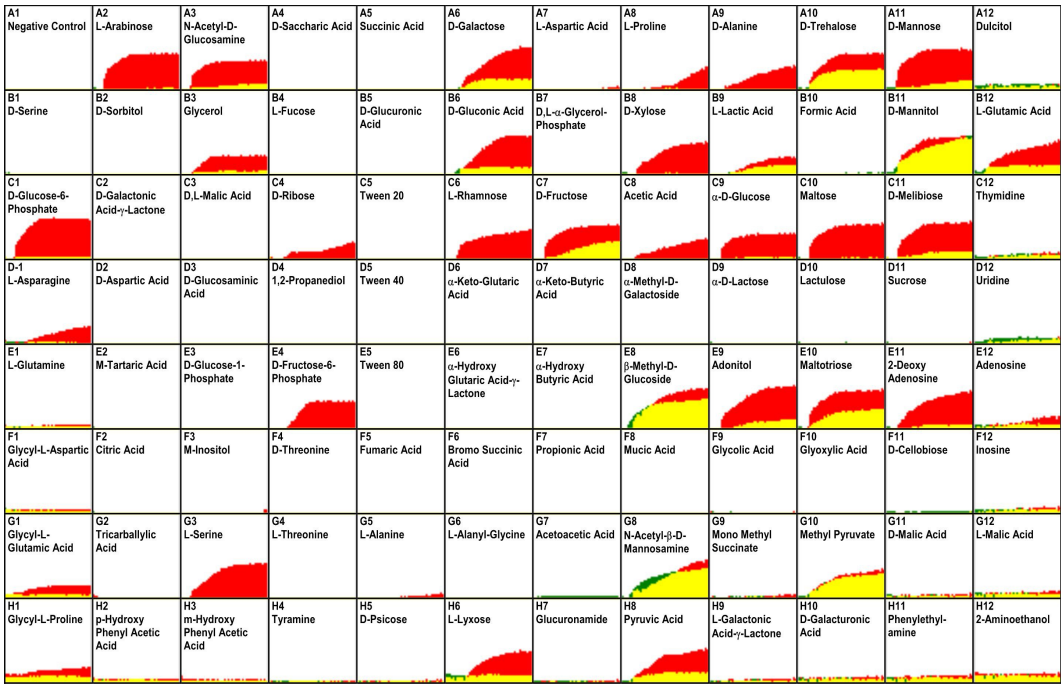

b.

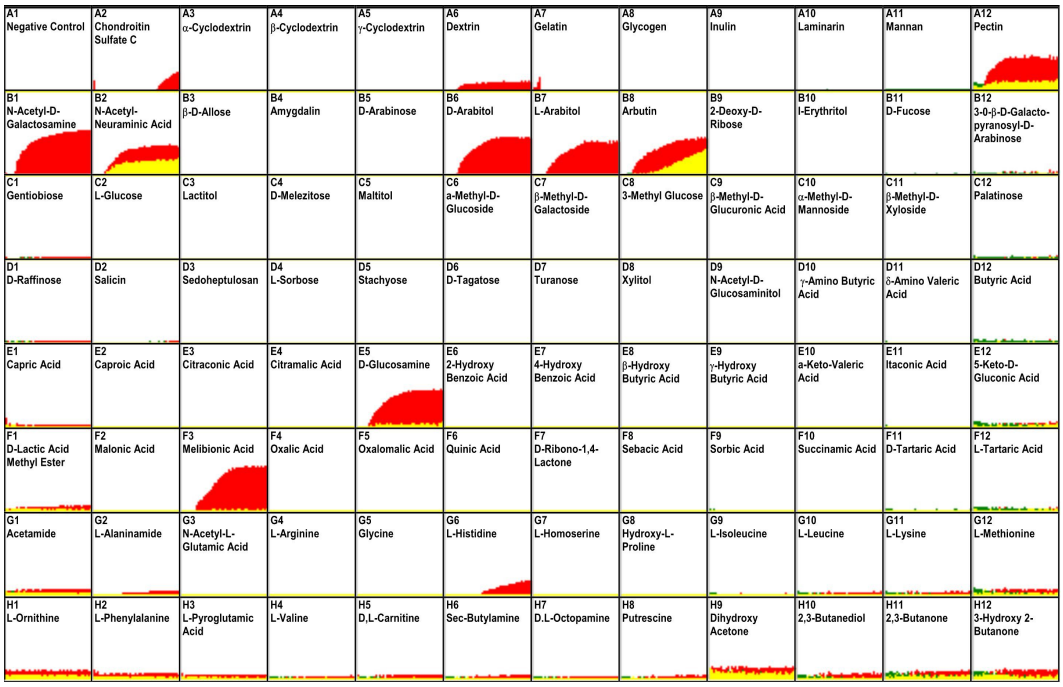

Figure 3.16: Phenotyping microarray analysis of carbon sources at 37 °C (green) compared to 25 °C (red): (a) PM1, (b) PM2A. Overlaps are displayed as yellow areas. Each well represents one carbon source. The curves indicate the time courses of the color changes of the tetrazolium dye and therefore respiratory activities. The orthogonal scale in the graphs has a maximum of 500.

In a similar study the *Y. pseudotuberculosis* strain 15478 was tested under different temperature conditions (Bochner 2009). The experiments were done at 26 °C and 33 °C. Deviating from the results here, the study found some increased respiratory activities at the

higher temperature. Nevertheless, at 33 °C no respiratory activity occurred on fructose-6-P and glucose-6-P and was also reduced on arabinose. In general, the effects observed in the study with the strain 15478 were milder than in the present investigation with the strain YPIII. This could be due to differences in the strains and in the temperatures. Since a smaller temperature difference was investigated, a less extreme effect can be expected.

The lack of activity at glucose, glucose-6-P, fructose-6-P, alanine, serine and glycerol at 37 °C is unexpected since these compounds are known to be available in the cytosol and the intestinal fluid, and it is generally believed that hexose phosphates are important energy sources for intracellular growth (Ray et al. 2009).

Utilizable phosphor and sulfur sources

The microarray containing 59 phosphor and 53 sulfur sources was also tested at 37 °C. The comparison of the results 37 °C vs. 25 °c is shown in figure 3.17.

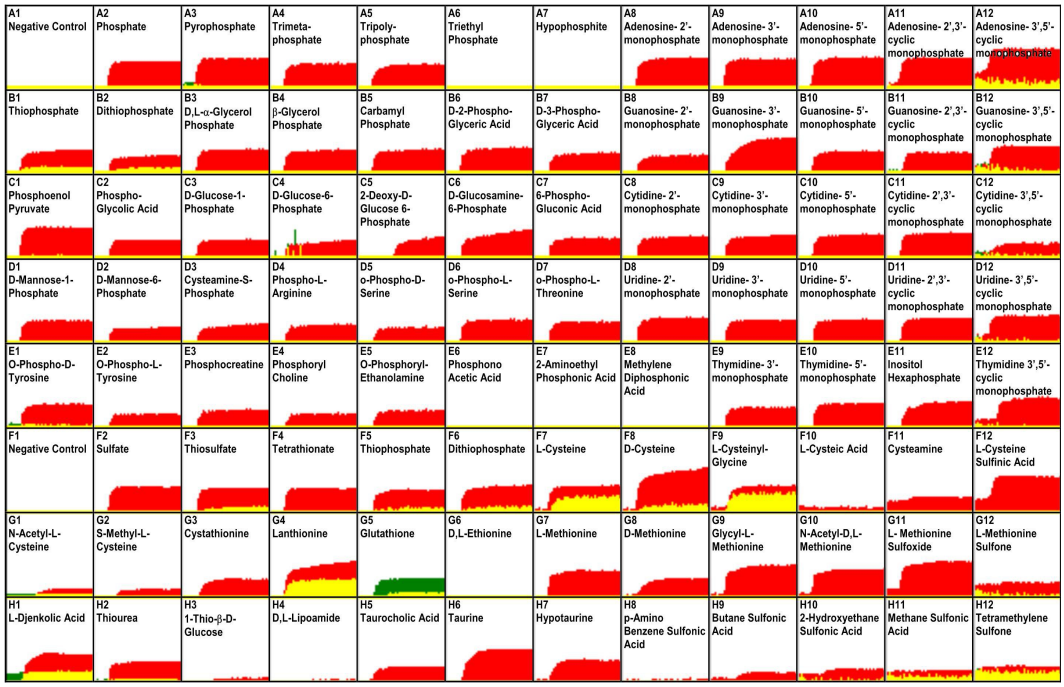

Figure 3.17: Phenotyping microarray analysis of phosphor (well A1-E12) and sulfur (well F1-H12) sources in PM4B at 37 °C (green) compared to 25 °C (red). Overlaps are displayed as yellow areas. Each well represents one sulfur or phosphor source, respectively. For better comprehensibility the orthogonal scale was set to a maximum of 250.

No phosphor source was able to promote any respiratory signal at 37 °C, indicating a crucial lack of an additional substance in the medium available in the plates.

4 out of the tested 35 sulfur sources gave a positive signal. Again the higher temperature lead to a profound decrease in the ability of using different sulfur sources. At 25 °C 21 sources could be utilized to produce a respiratory signal. In the PM4 plate one source was

utilized at 37 °C and not at 25 °C. The ability to utilize glutathion was gained at 37 °C. Together with the signals on L-cystein, L-cysteinyl-glycine and lanthionine the results suggest the need for reduced sulfur at 37 °C. The environment in the cytosol is considered to be reducing and glutathion is omnipresent, which might explain the ability of the bacteria to use it at 37 °C.

Additional supplements

As it became clear that growth requirements were more complex at 37 °C than at 25 °C an additional microarray was used, which tested for 94 supplemental substances (PM5). The results of this particular array are not compared to 25 °C, since every source, including the negative control, gave the same high signal at 25 °C, indicating that no supplements were needed at 25 °C. The result for 37 °C is displayed in figure 3.18.

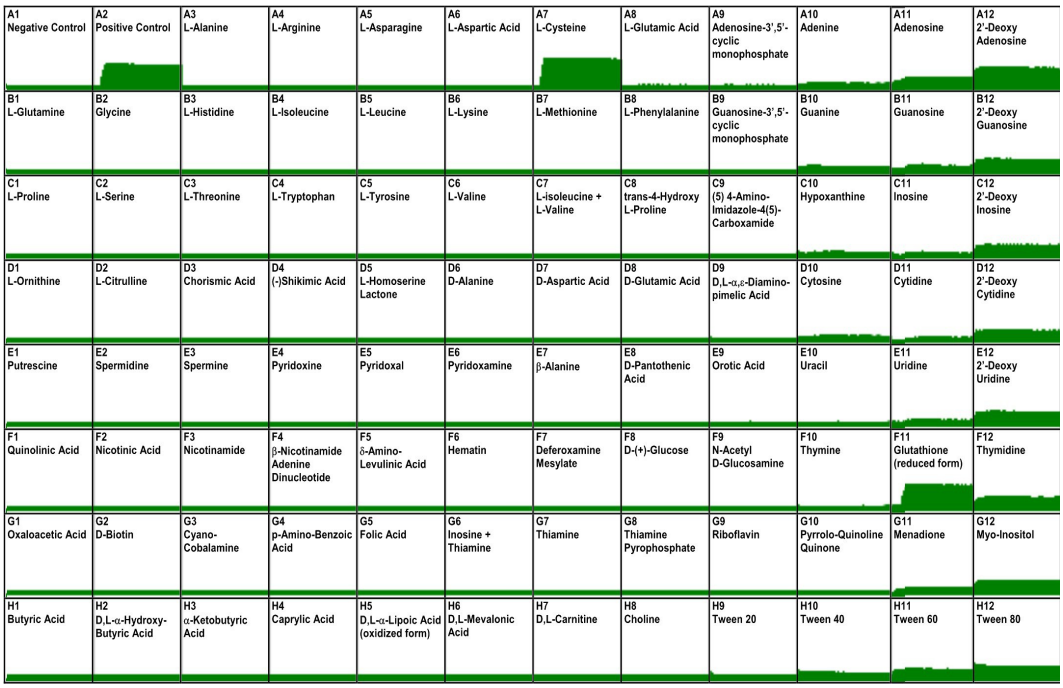

Figure 3.18: Phenotyping microarray of additional supplements (PM5) of *Y. pseudotuberculosis* at 37 °C. Each well represents one supplement. The green curve represents respiratory activity. For better comprehensibility the orthogonal scale was set to a maximum of 250.

Two of the 94 investigated substances showed a signal: L-cysteine and the reduced form of glutathion. Together with the results of the PM4 a need for L-cystein or reduced sulfur is observable.

Catabolic abilities at 37 °C in comparison to 25°C

The results obtained with the phenotyping microarrays show a drastic decrease of utilizable carbon, phosphor and sulfur sources at 37 °C under the tested conditions. In addition, the bacteria may require some additional unknown substance to promote growth at 37 °C. While the bacteria showed a broad catabolic ability with considerable synthesizing capability at 25 °C (chapter 3.1.1) these properties were extremely limited at 37 °C.

The causes for these findings can be various. The drastic reduction might be a result of reduced expression or activity of uptake systems or catabolic enzymes of YPIII. It is probable that many of the tested substances can still be utilized, but they are not sufficient as sole source of the respective element. Another possible explanation could be an extreme specialization to avoid synthesizing costs for a broader enzyme repertoire. This would be in line with the Freter's nutrient-niche theory, which concerns colonization of the intestine and postulates that species in the intestine have a strong preference for one or very few nutrients taking advantage of an ecological niche (Freter 1983)

3.2.2 Correlation of cell dry weight to optical density

Since morphology of YPIII changes at 37 °C, e.g. flagella synthesis stops, the correlation between optical density and dry weight was determined for YPIII grown at 37 °C. The experiment was performed just as the previous investigation at 25 °C and according to the description in chapter 2.8.4. The cells were grown in LB medium at 37 °C until mid-exponential state and harvested with an OD of 1.4-1.6.

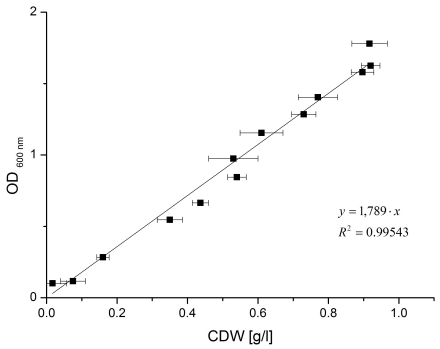

Figure 3.19: Correlation of cell dry weight (CDW) to optical density (OD) at 37 °C during exponential growth in LB medium.

Already through a rough observation under the microscope, the result of the lack of flagella was visible on the cells of YPIII. The bacteria were non-motile and aggregated to small

clumps of several cells.The linear regression from figure 3.19 leads to the formula, that describes the correlation between CDW and OD_{600} at 37 °C.

$$CDW_{\,Y.\,pseudotuberculosis\ 37\,°C}[g/l]=0.559 \cdot OD_{600\,nm} \qquad (3.2)$$

The results show a significant difference between the temperatures, as the correlation factor at 25 °C was 0.355. This might be a result of the observed aggregate formation that was only seen at 37°C under the microscope. While the cells grew as single rods at 25 °C, they agglomerated at 37 °C and grew as clumps of several rods together. This phenomenon was probably caused by the increased expression of adhesin molecules at this temperature (Bliska et al. 1993). However, since there was a linear correlation between the OD_{600} and the CDW, this phenomenon does not interfere with reproducible measurements, but it could be a reason for the bigger OD deviations observed at 37 °C and the different maximal OD in LB medium.

3.2.3 Characteristics of growth at 37 °C in LB medium

The culture condition were the same as at 25 °C. The growth was also measured in LB medium and a typical growth curve is displayed in figure 3.20.a. The maximal optical density after 12 h was 2.8±0.1 for YPIII in LB medium at 37 °C.

a. **b.**

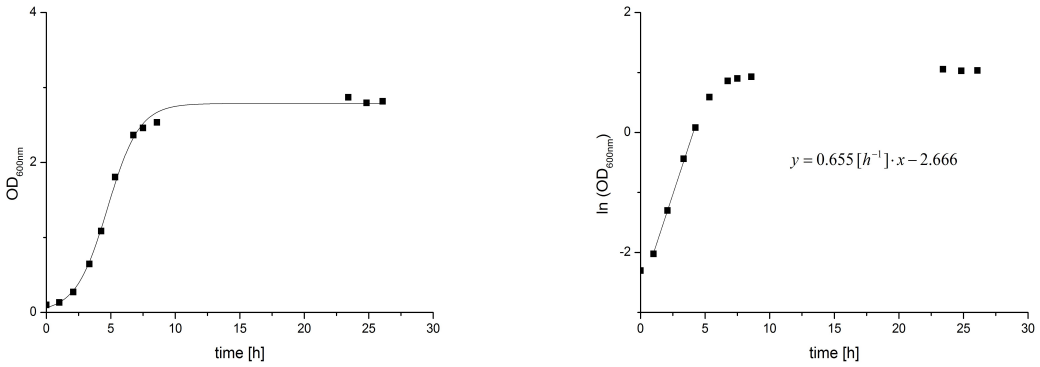

Figure 3.20: (a) Growth curve of *Y. pseudotuberculosis* in LB medium at 37 °C, (b) Graphical designation of the exponential growth rate and maximum growth rate μ by a half-logarithmic plot.

From figure 3.20.b. it can be seen that the cells grow with a maximal growth rate μ_{max} of 0.655 h^{-1} and a doubling time t_d of 1.06 h. Compared to the parameters at 25 °C in the same

medium (OD_{max}= 3.9, μ_{max}=0.563 h^{-1}) it can be observed, that the cells grew faster but reached a lower OD at 37 °C. If the maximum cell dry weight is calculated from the OD_{max} with the formulas 3.1 and 3.2, the maximum cell dry weight concentration at 25 °C was 1.38 $g \cdot L^{-1}$ and 1.57 $g \cdot L^{-1}$ at 37 °C. This points to a higher biomass yield of approximately 14% at 37 °C.

This was unexpected since the phenotyping analysis in chapter 3.2.1 showed that YPIII had reduced abilities to use available energy sources at 37 °C. Nevertheless, the growth in rich medium was not impaired.

3.2.4 Characteristics of growth of Y. pseudotuberculosis *at 37 °C in minimal medium with different additives*

It has been mentioned before, that no minimal medium for *Y. pseudotuberculosis* at the beginning of this thesis was known. The adjusted M63 medium described in chapter 3.1.2 provided growth at 25 °C but not at 37 °C. The results from the phenotyping microarrays in chapter 3.2.1 show that YPIII had extremely different nutritional requirements at 37 °C compared to 25 °C. The bacteria were not able to utilize glucose at 37 °C and a source of reduced sulfur was needed (chapter 3.2.1). Congruently, the study of Hills and Spurr showed that also *Y. pestis* has different nutritious requirements above 32 °C than below (Hills & Spurr 1952). Based on previous works (Higuchi & Carlin 1957) and the results of the PM analysis several medium compositions were tested and their influences to the growth behavior are discussed in the following sections.

Carbon sources

The carbon sources glucose and mannitol were tested at a concentration of 40 mM at 37 °C. The PM analysis in chapter 3.2.1 indicated that mannitol could serve as sole carbon source rather than glucose. Mannitol is a hexitol that also occurs naturally. It is transferred into the cell by a specific PTS system and converted to mannitol-1-P. Adjacent it is transformed to fructose-6-P and metabolized in the central metabolism.

Each carbon source was tested with and without thiosulfate as source of reduced sulfur at a concentration of 2.5 mM. The experiments were performed in the adjusted M63 medium introduced in chapter 3.1.2. Its composition is described in detail in chapter 2.7.2.

Glucose failed to provide growth with and without a source of reduced sulfur. Mannitol could only be utilized with the addition of reduced sulfur. The need for reduced sulfur is

discussed in the following sections. With mannitol as carbon source and addition of thiosulfate the cells reached a maximal OD of 1.5 after 40 h. The pH dropped from 7 to 5.5 after 20 h, indicating the secretion of acids into the medium. The results led to the use of mannitol as main carbon source with the addition of thiosulfate for the experiments at 37 °C in minimal medium and confirmed the crucial need for reduced sulfur at 37 °C.
Interestingly, a *crp* deletion mutant was able to grow on glucose as sole carbon source in 37 °C minimal medium without thiosulfate (chapter 3.3.9.2), indicating a repression of glucose catabolism through catabolite repression at 37 °C in the wild type.

Reduced Sulfur

The previous experiments showed a requirement of YPIII for reduced sulfur to grow at 37 °C in minimal medium. The PM analysis of the usable sulfur sources in chapter 3.2.1 indicated that cysteine and glutathione were able to provide respiration at 37 °C. For the cultivation in shaking flasks, cysteine could be substituted by thiosulfate and both substances proved to have a positive effect on growth.
Further, it was tested which other forms of sulfur could be used in liquid cultures. This included inorganic forms such as sulfide, thiosulfate and sulfite (figure 3.21). No growth occurred when natriumsulfite (2.5 mM) was added to the medium. Natriumsulfide (2.5 mM) and natriumthiosulfate (2.5 mM) both provided growth, indicating that a reduced form of sulfur was indeed necessary.

a. **b.**

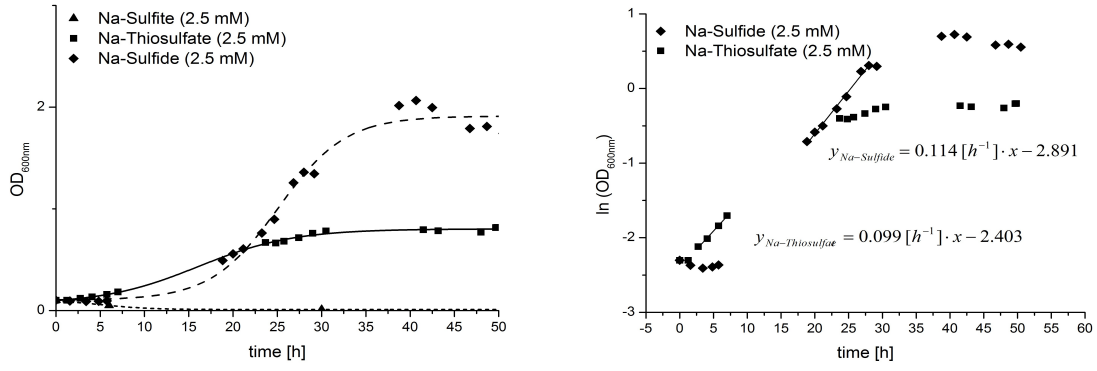

Figure 3.21: (a) Growth curve of YPIII in minimal medium with 2.5 mM thiosulfate (squares) or 2.5 mM sulfide (diamonds) and 2.5 mM sulfite (triangles) at 37 °C. 40 mM mannitol as sole carbon source in all curves. (b) Graphical designation of the exponential growth rate and maximum growth rate μ by a half-logarithmic plot for sulfide (diamonds) and thiosulfate (squares) experiment.

Interestingly, natriumsulfide led to a higher maximal OD compared to thiosulfate. However, the maximum growth rate was comparable (figure 3.21.b). This effect might be

caused by the greater reducing power of sulfide and confirms again the need for reduced sulfur. Natriumthiosulfate was established as medium additive for experiments at 37 °C due to its less complicated handling, despite the higher OD reached with sulfide.

To understand the role of reduced sulfur as growth promoting factor, it was examined, if thiosulfate was the only necessary sulfur source that was needed during cultivation. Therefore, all sulfate containing components in the minimal medium were substituted with phosphate-analogues. The bacteria were not able to grow in this medium with thiosulfate as sole sulfur source, but when 37.8 mM $(NH_4)_2SO_4$ were added, growth could be established to normal densities, proving that thiosulfate did not satisfy the cells complete need for sulfur and that sulfate was used as sulfur source at 37 °C.

Since the reducing power clearly was important to promote growth, another reducing agent without sulfur was added to the medium. Ascorbate (2.5 mM) was tested as additive instead of thiosulfate but failed to promote growth, indicating the importance for reduced sulfur.

When 0.7 % yeast extract was added to the medium, the cells were able to grow without thiosulfate at 37 °C. However, when thiosulfate was added to a culture with 1 % yeast extract, it still had a growth promoting effect leading to higher maximal ODs (figure 3.22.a).

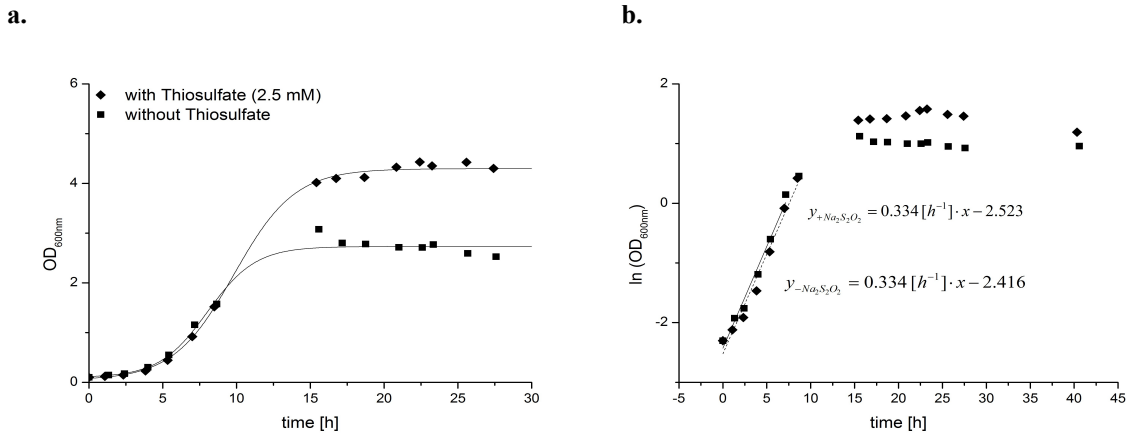

Figure 3.22: (a) Growth curve of YPIII in minimal medium with 0.7 % yeast extract with the addition of 2.5 mM thiosulfate (diamonds) and without (squares) at 37 °C. 40 mM mannitol as sole carbon source in all curves. (b) Graphical designation of the exponential growth rate and maximum growth rate μ by a half-logarithmic plot for addition of thiosulfate (diamonds) and without (squares).

It is obvious from figure 3.22.b that the maximal growth rate was identical between the two conditions, but the culture without thiosulfate stopped growing earlier and reached a lower maximal OD. These findings indicate a limitation in the culture without thiosulfate. The growth with yeast extract was probably promoted due to small amounts of cysteine

and glutathione in the medium that satisfied the need for reduced sulfur. They were probably depleted after approximately 10 h leading to a limitation and ceased growth, while in the culture with the addition of thiosulfate, the cells continued growing.
Interestingly, at 25 °C the addition of thiosulfate to the minimal medium did not show any effect (data not shown).
Taken together, these results demonstrated that YPIII has a requirement for a reduced form of organic or inorganic sulfur at 37 °C for growing in minimal medium. Similar requirements have been noted before: Some earlier studies of the nutritional requirements of *Y. pestis* stated that a reduced form of sulfur is required for growth that could be satisfied with cysteine, methionine or thiosulfate (Hills & Spurr 1952; Englesberg 1952). Additional genes necessary for sulfur uptake and metabolism are frequently regulated in *Y. pestis* in studies with environmental stresses, indicating the importance of these pathways to metabolic adaption (Han et al. 2007). Nevertheless, a connection of the need for reduced sulfur to temperature has not been noted. Reduced sulfur is a component in many important metabolites such as methionine, cysteine and coenzyme A, crucial for the metabolism. One can speculate that the synthesis of reduced sulfur from sulfate is down-regulated at 37 °C, which leads to the need for direct uptake of reduced sulfur. Possible candidates for down-regulated genes are *cysG*, *cysJ* and *cysI* encoding an enzyme of siroheme biosynthesis and subunits of the sulfite reductase, respectively. In *E. coli*, mutants lacking these genes are unable to utilize sulfate and sulfite as sole sulfur source but grow on thiosulfate, cysteine and sulfide (Kredich 1996), which is comparable to the phenotype of YPIII at 37 °C. This phenomenon might be a consequence of the fact, that a source of reduced sulfur is available in the host, since glutathione is omnipresent in mammalian cells.

Amino acids, vitamins and yeast extract

It was suggested in the literature that the addition of amino acids to the culture medium could increase growth (Higuchi & Carlin 1957). Several amino acids and amino acid mixtures were added to the preciously described M63 medium with mannitol (40 mM) and thiosulfate (2.5 mM) and the effect on the maximal OD of YPIII was tested. Glutamate (0.2 $g \cdot L^{-1}$), glutamine (0.2 $g \cdot L^{-1}$), alanine (0.2 $g \cdot L^{-1}$) as well as a mixture of alanine, tyrosine and aspartate (0.2 $g \cdot L^{-1}$) were separately added to the medium but failed to increase growth (data not shown). The addition of 1% casamino acids, which contains all a mixture of all 20 amino acids (except glutamine and asparagine), improved the growth yield slightly (data not shown).

The addition of the vitamins pantothenate (1 mM), thiamin (1 mM) and biotin (0.1 mM) had mild growth promoting effects. The addition of nicotinamide (5 mM) showed no effect on growth of YPIII.

The addition of 1% yeast extract improved growth yield considerably, indicating that other compounds than the previously tested had a major influence on growth of YPIII at 37 °C. The amount of yeast extract used was proportional to the maximal OD as can be seen in figure 3.23.

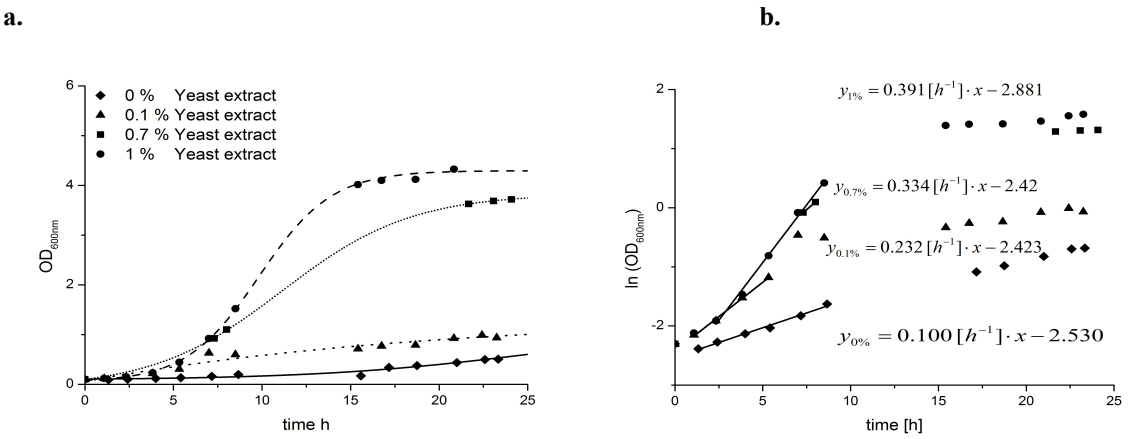

Figure 3.23: (a) Growth curve of *Y. pseudotuberculosis* in minimal medium at 37 °C with 40 mM mannitol as sole carbon source, 2.5 mM thiosulfate and 1 %, 0.7 %, 0.01 %, 0 % yeast extract, respectively. (b) Graphical designation of the exponential growth rate and maximum growth rate μ by a half-logarithmic plot.

The YPIII cultures grew with different maximal growth rates and reached different maximal ODs depending on the amount of added yeast extract. This behavior indicates the presence of one or more growth promoting factors in the yeast extract. However, these factors are not yet identified. The good growth in LB medium at 37 °C (chapter 3.1.2) was probably due to the high concentration of yeast extract in the composition. Despite the growth enhancing effect, yeast extract was not used as supplement in minimal medium for further experiments at 37 °C because of its undefined composition.

Calcium

Calcium is known to influence growth and virulence of *Yersiniae*. To investigate the effect of Ca^{2+} on growth YPIII, 2.5 mM $CaCl_2$ was added to the minimal medium with 40 mM mannitol and 2.5 mM thiosulfate. The addition proved to have a positive effect on growth of YPIII at 37 °C (figure 3.24) and no effect at 25 °C (data not shown).

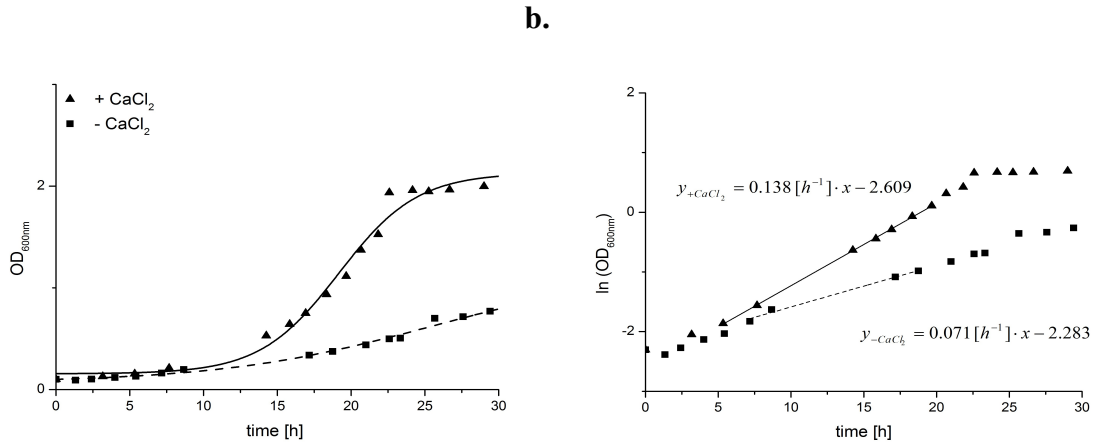

Figure 3.24:(a) Growth curve of *Y. pseudotuberculosis* in minimal medium with 40 mM mannitol as sole carbon source, 2.5 mM thiosulfate (squares) and additional 2.5 mM $CaCl_2$ (triangles) at 37 °C. (b) Graphical designation of the exponential growth rate and maximum growth rate μ by a half-logarithmic plot.

Figure 3.24.b shows, that both the μ_{max} and the maximal OD were increased in the presence of Ca^{2+}-ions. It is assumed that Ca^{2+}-ions in concentrations of 2.5 mM repress the expression of genes encoded on the virulence plasmid pYV such as YOPs. This leads to reduced energy costs for protein synthesis resulting in better growth (Fowler & Brubaker 1994; Higuchi et al. 1959). Consequently, 2.5 mM $CaCl_2$ was added to the minimal medium for experiments at 37 °C.

Minimal Medium for 37 °C

In the previous sections several substances were tested for their growth stimulating effects on YPIII at 37 °C. Taken the results together, a minimal medium for 37 °C was created, which is described in chapter 2.7.2. The medium was similar to the minimal medium used at 25 °C (chapter 3.1.2) but 40 mM mannitol were used instead of glucose as carbon source, and 2.5 mM thiosulfate, 2.5 mM CaCl and vitamins were added. The growth of YPIII at 37 °C and at 25 °C in the designated minimal medium is shown in figure 3.25.

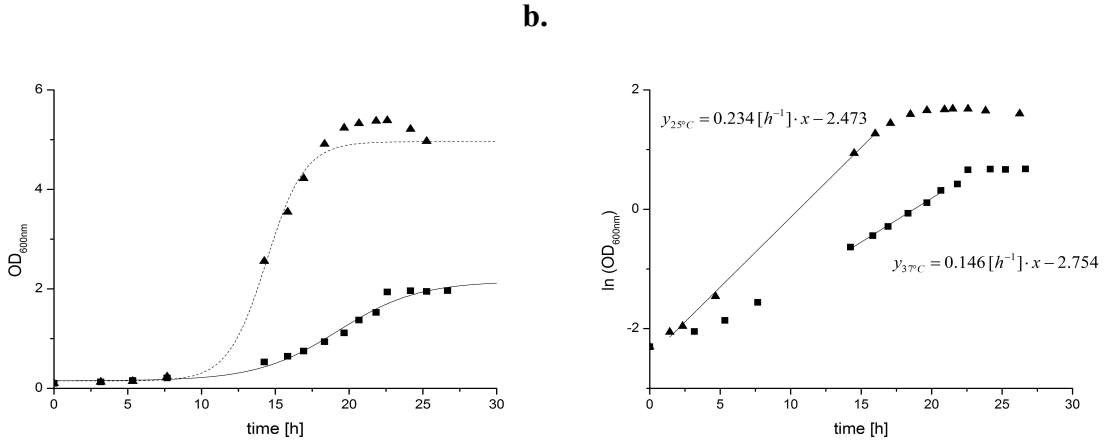

Figure 3.25: (a) Growth curve of *Y. pseudotuberculosis* in minimal medium with 40 mM mannitol as sole carbon source, 2.5 mM thiosulfate and 0.25 mM $CaCl_2$ at 37 °C (squares) and 25 °C (triangles), (b) Graphical designation of the exponential growth rate and maximum growth rate μ by a half-logarithmic plot.

The maximal optical density of YPIII in the optimized minimal medium at 37 °C was 2±0.2 with a maximum growth rate μ_{max} of 0.146 h^{-1} and the maximum doubling time t_d of 4.74 h. For growth at 25 °C in the same medium the maximal OD reached was 5.2±0.1 with a μ_{max} of 0.234 h^{-1} and a doubling time t_d of 2.96 h. Previously, it was shown that the correlation between OD and CDW were different between 25 °C and 37 °C (chapter 3.2.2) leading to a maximal CDW of 1.12 $g \cdot L^{-1}$ at 37 °C and 1.85 $g \cdot L^{-1}$ at 25 °C. This shows that the formulated medium provided sufficient growth rate and maximal cell density at 37 °C. Nevertheless, the growth in this optimized minimal medium was still diminished compared to 25 °C. In comparison growth in complex LB medium was similar at 25 °C and 37 °C (chapter 3.2.3). It can be assumed that a still unidentified factor was present in the yeast extract that enhanced growth of YPIII at 37 °C considerably.

3.2.5 The metabolism of YPIII at 37 °C

Since severe changes in nutritional requirements, morphology and growth of YPIII were observed in the previous chapters, the temperature difference was expected to have a major influence on metabolism too. To evaluate this phenomenon on a comprehensive level the culture supernatant, the intracellular metabolome and the transcriptome were analyzed from YPIII grown in LB medium at 25 °C and 37 °C. Further, YPIII was grown in mannitol minimal medium at 25 °C and 37 °C and the culture supernatant as well as the intracellular metabolome were measured during several time-points resulting in a time-resolved metabolic profile. The samples grown at 25 °C were handled analogously to the

samples at 37 °C and were thereby regarded as reference to highlight the differences due to the temperature difference.

3.2.5.1 Culture supernatant analysis in LB medium

The culture supernatant of YPIII grown in LB medium at 37 °C was analyzed over the course of time and samples were taken as described before in chapter 2.11.3 after 3 h, 5.5 h, 9.5 h, 14.5 h and 23.5 h. These time-points represent exponential phase (3.5 h and 5.5 h), transitional phase (9.5 h) and stationary phase (14.5 h and 23 h) conditions. An additional blank medium sample was analyzed in parallel, representing the time-point 0 h. The complete list of compounds detected in the analysis can be found in supplemental data C.1 and a summary is shown in table 3.9.

Table 3.11: Summary of the results of the supernatant analysis of YPIII in LB medium at 37 °C and 25 °C during growth

Sample time-point [h]	**Growth temperature**	**Detected compounds**	**Identified metabolites**	**Relative standard error** (n= 3, biological replicates)
0	-	107	73	12,17%
3	25 °C	104	72	11,80%
5.5	25 °C	99	67	9,80%
9.5	25 °C	91	60	12,11%
14.5	25 °C	90	61	11,37%
23.5	25 °C	90	60	8,59%
3	37 °C	106	72	18,30%
5.5	37 °C	102	71	13,12%
9.5	37 °C	91	63	8,53%
14.5	37 °C	92	64	10,14%
23.5	37 °C	95	67	11,54%

The summary of the supernatant analysis showed that the number of detected compounds in the supernatant decreased during ongoing cultivation at both temperatures. Interestingly, at 37 °C 5 components less than at 25 °C were measured after 23.5 h, indicating a lessened uptake of compounds by the bacteria.

The composition and the consumption of the LB medium over the time at 25 °C was previously described in chapter 3.1.3.3. Here, the characteristics of consumption at 37 °C are analyzed and compared to the results at 25 °C. For an unbiased analysis the samples

were subjected to an unsupervised clustering algorithm. The result is shown in form of a dendrogram in figure 3.26.

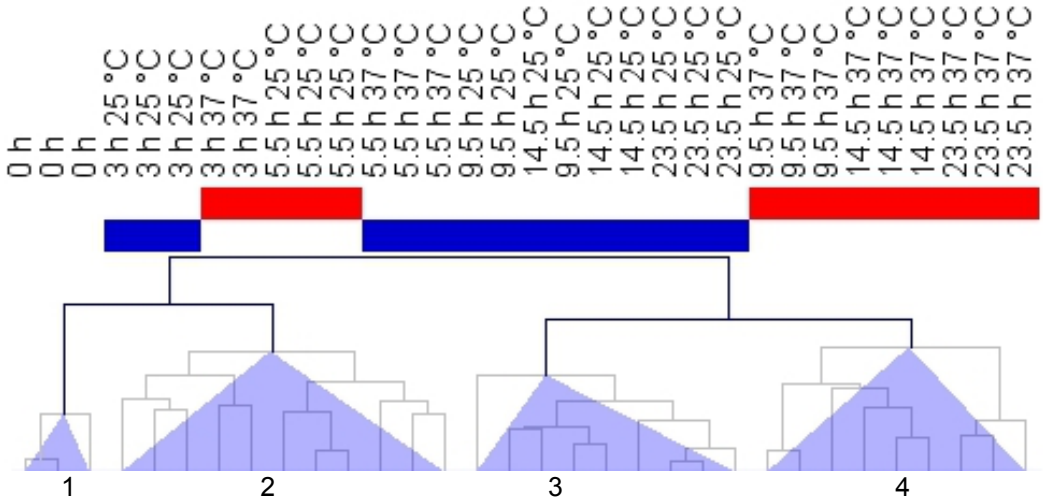

Figure 3.26: Hierarchical cluster of supernatant samples taken over the time of cultivation at 25° C and 37°C in LB medium. Clustering is based on all detected metabolites. For the clustering of the samples euclidean distance and average linkage was used.

The dendrogram is ordered according to the similarity of the investigated samples. 4 major clusters can be observed. The samples of pure medium (0 h) form the first cluster. The samples from exponential phase (3 h, 5.5 h) cluster together independently from the cultivation temperature in the second cluster and are separated by the clustering according to the harvesting time-points. The samples of the transition (9.5 h) and stationary phase (14.5 h, 23.5 h) are located in the third and fourth cluster and divided by the temperature. This indicates that the differences between the supernatant samples from the two temperatures increased over the time of cultivation.

A two-factor ANOVA (chapter 2.14.4) of the supernatant analyses was performed analyzing the influence of the time and the temperature (figure 3.27). It showed that 36 metabolites were significantly changed between the temperatures and 61 metabolites were significantly changed over the 5 time-points. Most amino acids, that were known to serve as C-source at 25 °C (see table 3.7), were not significant altered between the temperatures and varied only over time: Serine, alanine, glutamate show the same up-take process between both temperatures. No significant differences between the temperatures was also detected in the consumption of trehalose, aspartate, asparagine and glycine. It seems that the uptake of nitrogen and carbon sources was similar between 25 °C and 37 °C. These results are contrary to the findings of the phenotyping microarray (chapter 3.2.1). The heat map in figure 3.27 shows the compounds, that detected as significantly changed between

the temperatures. The samples were not subjected to the hierarchical clustering in figure 3.26, but ordered for clarity purposes according to the time and to the temperature.

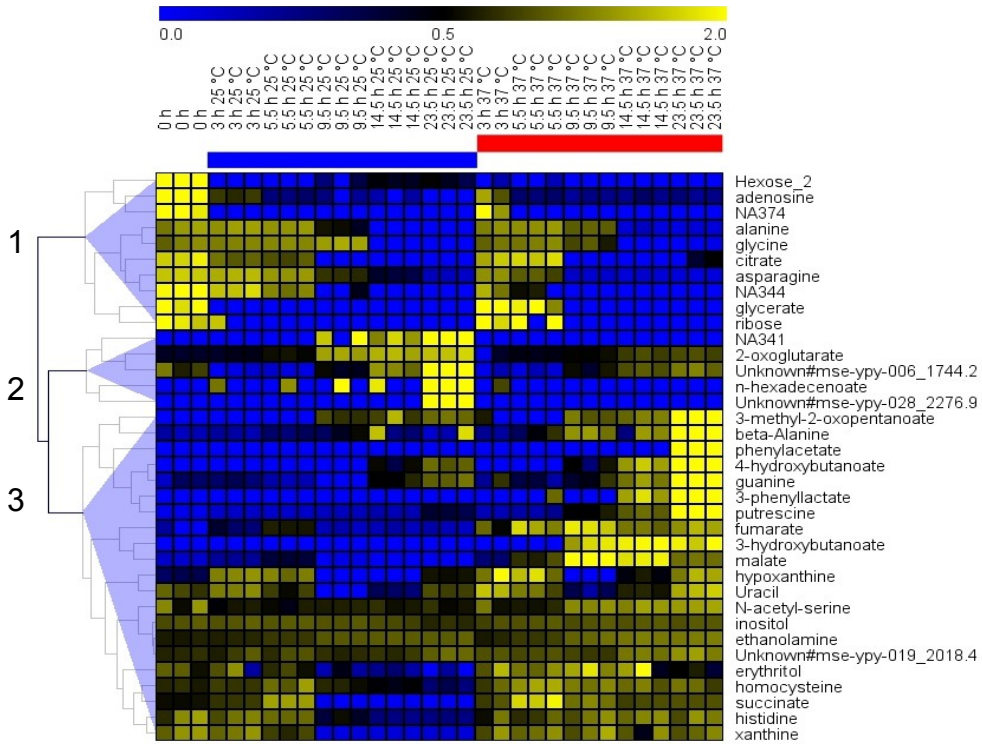

Figure 3.27: Heat map with hierarchical clustering of the extracellular metabolites over time of YPIII cells grown in LB medium at 25 °C and 37 °C. Only metabolites are shown that were significantly altered in response to the temperature (p-value < 0.01, two factor ANOVA). Data is RMS-normalized over the rows. Euclidean distance and average linkage was used to cluster the metabolites.

The metabolites can be divided into three groups according to the clustering in figure 3.27. The first group contains the compounds, that were consumed over the time at both temperatures but with different rates. Here, carbon and nitrogen sources such as citrate, alanine, asparagine, glycine, glycerate and ribose are contained. The differences between the temperatures in this cluster are rather mild. Asparagine and alanine were consumed faster at 37 °C, while glycerate and ribose were taken up slower than at 25 °C.

The second cluster is more heterogeneous and is formed from substances that were secreted differently, e.g. 2-oxoglutarate, which was secreted to lesser extent at 37 °C, and also hexadecenoate, which was only secreted at 25 °C. 3-methyl-2-oxopentanoate, 4-hydroxybutanoate, 3-hydroxybutanoate, beta-alanine and guanine were more secreted at 37 °C. Another abundant difference is the secretion of putrescine into the medium during stationary phase, which was considerably higher (~ 8 times) at 37 °C than at 25 °C. Phenylacetate and phenyllactate were exclusively secreted at 37 °C, probably as by-products of the degradation of aromatic amino acids or other aromatic compounds.

The third cluster includes metabolites, that were only consumed under one condition. Some nucleobases are included such as hypoxanthine and uracil, which were both consumed from the medium at first and secreted later, but to a greater extent at 37 °C than at 25 °C. The secretion of uracil, hypoxanthine and guanine has been noted in LB medium at 25 °C in chapter 3.1.3.3 and was interpreted as side-product of the degradation of the corresponding nucleoside uridine, adenosine and guanosine, respectively. The increased secretion at 37 °C indicates an increased degradation of nucleosides probably due to DNA and RNA degradation. Xanthine was consumed from the medium only at 25 °C but was unchanged at 37 °C. Also histidine, homocysteine and erythritol were not consumed at 37 °C but at 25 °C, showing reduced catabolic abilities at 37 °C as indicated in chapter 3.2.1. The increase of aromatic compounds (phenylacetate, phenyllactate) in the medium together with the inability to consume histidine and xanthine at 37 °C may suggest a lack in the catabolism of aromatic structures.

The most striking observation in the third cluster of figure 3.27 is the course of the TCA cycle intermediates malate, fumarate, and succinate. These were secreted at 37°C at a significant higher extent compared to 25 °C and were not completely consumed afterwards (figure 3.28).

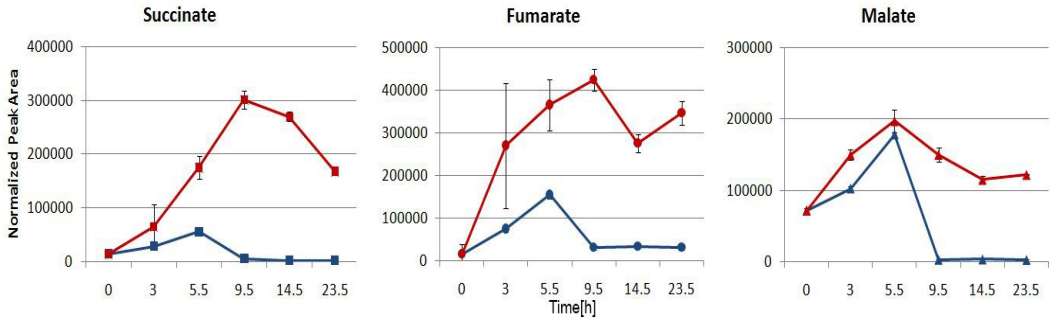

Figure 3.28: Time resolved comparison of extracellular TCA intermediates measured in the LB supernatant of *Y. pseudotuberculosis* YPIII over the time at 25 °C (blue) and 37 °C (red).

The supernatant analysis in LB and minimal medium at 25 °C indicated that the secretion of TCA cycle intermediates occur predominantly as a result of amino acid consumption (chapter 3.1.3.5). The pathogenic bacterium *S. aureus* is known to secrete different organic acids as acetate, fumarate and succinate in the exponential phase and to reuse them later (Liebeke et al. 2011). Different *S. aureus* strains are known, that have a diminished ability to reuse acetate, which results in lower growth yield (Somerville et al. 2003). It was shown that the down-regulation or the knock-out of certain enzymes of the TCA cycle could lead to the effect of diminished acetate resumption. Therefore the increased secretion and the

reduced ability to reuse the organic acids could indicate a down-regulation of TCA cycle enzymes.

3.2.5.2 Intracellular metabolome analysis in LB medium

The samples for the intracellular metabolome analysis of YPIII in exponential phase at 37 °C and 25 °C in LB medium were harvested after 5 h at an OD of 1.2±0.1 and a μ=0.66 h^{-1} in 3 biological and 3 technical replicates each. The samples of the stationary phase were harvested after 16 h at an OD of 2.75±0.05 and a μ~0 h^{-1}. The samples were prepared as described before (chapter 2.11.2) and measured at the GC-MS (chapter 2.12.2). A summary of the results is shown in table 3.9 and the complete analysis is given in supplemental C.2.

Table 3.12: Summary of the results of the metabolome analysis at 25 °C and 37 °C in LB medium

Experiment	**Detected compounds**	**Identified metabolites**	**Relative standard error** (n= 9, 3 biological replicates, 3 technical replicates)
Exponential phase 25 °C	78	65	22.10%
Stationary phase 25 °C	87	68	14.28%
Exponential phase 37 °C	83	66	18.86%
Stationary phase 37 °C	89	69	17.31%

The metabolic profiles from both growth phases at 37 °C were compared to the corresponding profiles at 25 °C. The results are shown in the following section. During exponential phase 10 compounds were only detected at one of the temperatures (table 3.10).

Table 3.13: Compounds found only at one temperature when YPIII was cultivated in LB medium at 25 °C and 37 °C in exponential phase

Exponential phase 25 °C	**Exponential phase 37 °C**
Not detected	trehalose
Not detected	pantothenate
Not detected	methionine
Not detected	Unknown#mse-ypy-002_1_2922.4
Not detected	Unknown#mse-ypy-023_2128.1
Not detected	Unknown#mse-ypy-002_2_2955.1
Not detected	tyrosine
heptadecanoate	Not detected
pentadecanoate	Not detected

Besides 3 unknown components as well as pantothenate, methionine and tyrosine, trehalose was only present in the metabolome of exponentially growing cells at 37 °C. Trehalose can serve as a sole carbon source at 25 °C and 37 °C (chapter 3.1.1 and 3.2.1). Trehalose is normally consumed from the medium via a PTS system, thereby phosphorylated with adjacent conversion into glucose-6-P and directed to the glycolysis. It was present in the LB medium and consumed alike at 25 °C and 37 °C (chapter 3.2.5.1). It is known as a stress protection compound in *E. coli* and other bacteria (Strøm & Kaasen 1993). At 25 °C trehalose was neither found in the metabolome of cells grown in LB medium or minimal medium at any investigated time-point (chapter 3.1.3.2 and 3.1.3.4). The presence at 37 °C in the exponential phase suggested inhibited degradation.

The metabolites, that were found under both temperatures in the metabolome of the exponential phase in LB medium, were compared in a scatterplot (figure 3.29). The correlation of the metabolites of YPIII at 25 °C and 37 °C was 0.89 after Spearman and 0.93 after Pearson in the exponential phase.

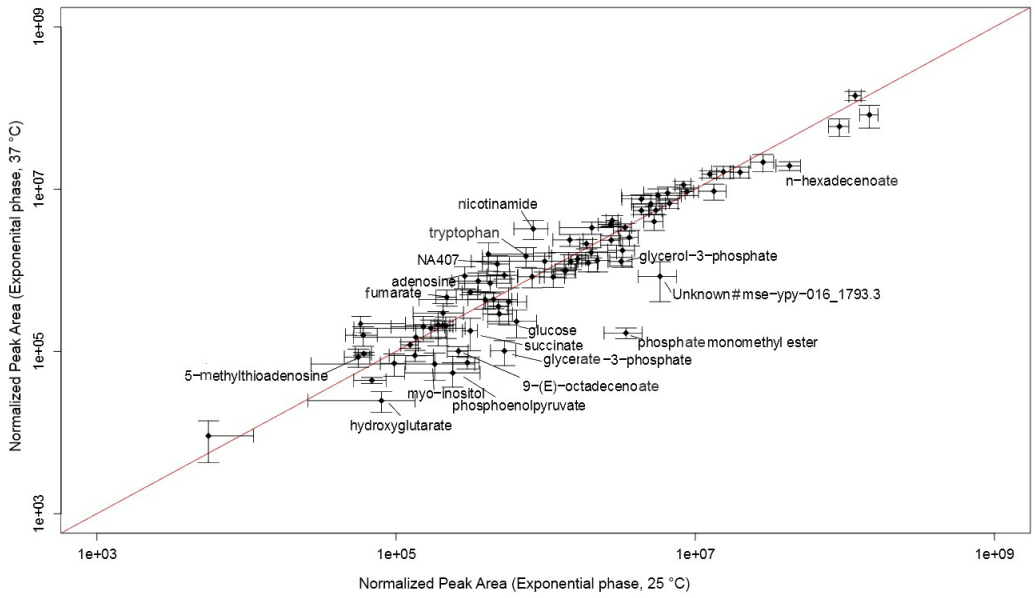

Figure 3.29: Scatterplot of the metabolome at 25°C (X-axis) and at 37 °C (Y-axis) from YPIII cells grown in LB medium and harvested during exponential growth. The metabolites are plotted with logarithmic axes. Metabolites are indicated with names if they differ more than 2-fold from the bisecting line.

Some intermediates from the glycolysis (glycerate-3P, PEP) and an intermediate from the TCA cycle (succinate) were decreased at 37 °C. Together with the higher concentration of the sugar trehalose, this points to reduced glycolytic activity, where surgars were slowlier consumed than at 25 °C. Certain unsaturated fatty acids as octodecenoate ($C_{18:1}$) and

hexedecenoate ($C_{16:1}$) were present in lower amounts at 37 °C fitting to the observation, that heptadecenaote and pentadecanoate were not detected at 37 °C at all.

Only few metabolites were increased at 37 °C in exponential phase such as nicotinamide, adenosine, methylthioadenosine and tryptophan.

The comparison between the metabolites of the stationary phases showed that 4 compounds were only detected at one temperature (table 3.11).

Table 3.14: Compounds detected only at one temperature when YPIII was cultivated in LB medium at 25 °C and 37 °C in stationary phase

Stationary phase 25 °C	Stationary phase 37 °C
Not detected	nicotinate
Not detected	Unknown#bth-pae-038_1567.3
Not detected	Unknown#sst-cgl-001_1746.7
Unknown#mse-ypy-028_2276.9	Not detected

These were 3 unknown compounds and nicotinate. In both exponential and stationary phase more compounds were detected at 37 °C than at 25 °C, although these compounds were different between the growth phases.

The direct comparison of the metabolomic profiles of the stationary phase at 25 °C and 37 °C showed a correlation of 0.87 after Spearman and 0.95 after Pearson (figure 3.30).

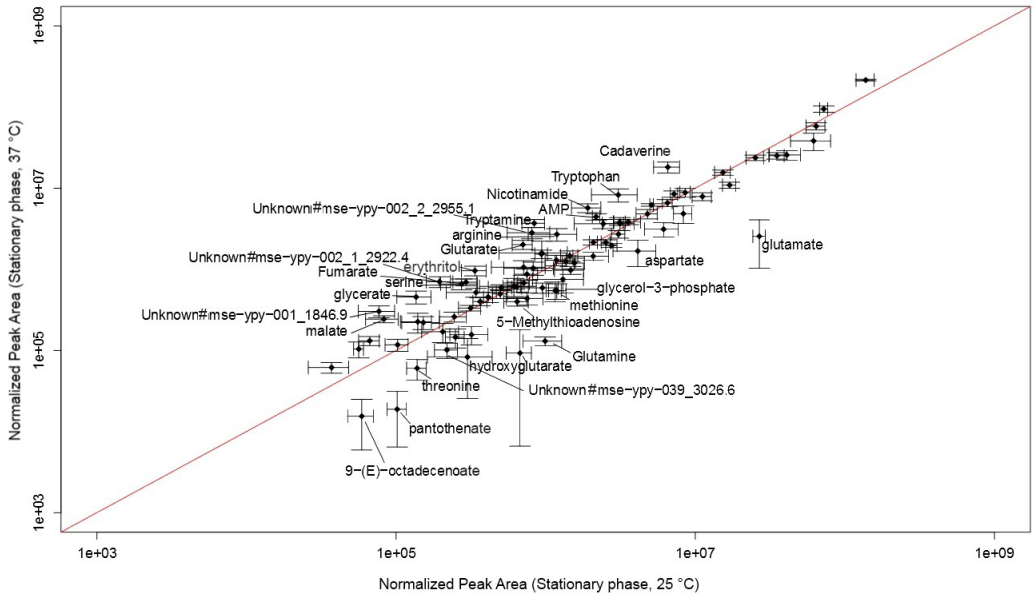

Figure 3.30: Scatterplot of the metabolome at 25°C (X-axis) and at 37 °C (Y-axis) from YPIII cells grown in LB medium and harvested in stationary phase. The metabolites are plotted with logarithmic axes. Metabolites are indicated with names if they differ more than 2-fold from the bisecting line.

The most prominent change was the decrease of amino acids (glutamate, glutamine, aspartate, threonine) in stationary phase at 37 °C. These metabolites were all present in the medium and were similarly consumed from the supernatant during the cultivation at both temperatures (chapter 3.2.5.1). A degradation product (3-methyl-2-oxopentanoate) of the threonine metabolism was detected in increased concentrations in the supernatant at 37 °C (chapter 3.2.5.1) and indicated changes in the degradation of this amino acid at higher temperatures. Erythritol was increased in the metabolome of YPIII grown at 37 °C. This compound was also detected in the supernatant and was completely consumed at 25 °C after 9.5 h. However, it was present over the whole cultivation time in the supernatant at 37 °C and the concentration declined only in stationary phase, explaining the increased presence in the intracellular metabolome. Similar, glycerate was also consumed slower from the supernatant at 37 °C and was increased in the corresponding intracellular metabolome in stationary phase.

Arginine and cadaverine were both increased at 37 °C in the metabolome of the stationary phase. Putrescine and cadaverine are polyamines and are build from arginine. The intracellular metabolite concentration of putrescine varies only slightly but the extracellular concentration increases 8-fold compared to 25 °C. Like trehalose, cadaverin and putrescine have a multitude of functions in a microbial cell and are known as stress responses or biofilm formation (Wortham et al. 2007).

Some intermediates from the TCA cycle (malate, fumarate) were increased at 37 °C. It is known from the supernatant analysis (chapter 3.2.5.1), that the TCA cycle intermediates fumarate, malate and succinate were secreted in the exponential phase at both temperatures but only consumed at 25 °C.

In both growth phases the concentrations of the aromatic compounds tryptophan and nicotinamide were increased. Nicotinamide is part of an essential redox cofactor for the cell. It is also an important for ADP-ribosylation, which occurs as a regulatory event in DNA repair. Nicotinamide is synthesized from aspartate, but aspartate was decreased at 37 °C. The cleavage product nicotinate was exclusively found in the stationary phase at 37 °C. The aromatic amino acid tryptophan was increased at 37 °C in the metabolome of both the exponential and stationary phase. An increased expression of the synthesizing enzymes of tryptophan has been shown in *Y. pestis* during temperature elevation with transcriptome analysis (Motin et al. 2004). Additionally, serine and tryptamine were increased in stationary phase, both substances from biosynthesis and degradation of

tryptophan. These findings are in line with the increased aromatic compounds detected in the culture supernatant at 37 °C (chapter 3.2.5.1).

From the metabolome analysis a change in fatty acid metabolism can be deduced. The fatty acid 3-hydroxytetradecanoate was increased at 37 °C in both growth phases, which is the most common fatty acid constituent of the lipid A component of LPS and therefore a a key component of bacterial endotoxins (Rebeil et al. 2004). Glycerol-3-P, hexadecenoate and octadecenoate were decreased at 37 °C during both growth phases and hexadecenoate was exclusively secreted at 25 °C (chapter 3.2.5.1). Further, pentadecanoate and heptadecanoate were only detected at 25 °C in exponential phase. This indicates a changed concentration of fatty acids in the metabolome at 37 °C and suggests an alteration of the cell membrane composition at elevated temperatures.

3.2.5.3 Transcriptome analysis at 25 °C and 37 °C in LB medium

For a comprehensive analysis the transcriptome of YPIII at 37 °C was compared to the transcriptome at 25 °C. The samples for the analysis were taken during stationary growth after 15 h of cultivation in LB medium and handled as described in chapter 2.10. The time-point was chosen for analysis, since many virulence factors of *Y. pseudotuberculosis* are only produced in stationary phase (Nagel et al. 2001). The experiments for the analysis were performed by A.K. Heroven and J. Melzer (Group of P. Dersch, HZI, Braunschweig, Germany), the statistical evaluation was done by J. Klein (Group of D. Jahn, TU Braunschweig, Braunschweig, Germany).

In total 166 genes showed significant alterations between the temperatures as defined with a students t-test with a p-value < 0.01 and a ratio > 1.8. Of these genes, 62 were up-regulated and 104 genes were down-regulated at 37 °C (supplement C.3).

Most of the identified up-regulated genes belong to virulence-associated proteins, like Yop regulators and type III secretion systems. The most abundant changes were detected in genes coding for hypothetical proteins.

Transporter

A number of genes encoding transport proteins were regulated. In total 11 genes involved in transport functions were regulated, but only 2 were upregulated at 37 °C. The gene for the gluconate transporter *gntP* and a monosaccharid-transporting ATPase were both up-regulated. A greater number of genes were down-regulated at 37 °C, this include a mannose-specific PTS system (*manZ, manY*), an ABC transporter for oligo peptides (*oppA,*

oppB, oppC), a polar amino acid transporter for glutamate/aspartate (*gltl*) as well as *actP* coding for an acetate permease, and *afuA* coding for an iron(III)transport system. The relatively few regulated transporter were in accordance with the observed similar uptake rates of nutrients from the medium between the temperatures (chapter 3.2.5.1).

Metabolism

In total 29 genes were regulated that are involved in metabolism. Interestingly, the majority of these genes were down-regulated at 37 °C. Only seven genes were up-regulated. The results are summarized and compared to the metabolome analysis in figure 3.31. One up-regulated gene was *rpiB* coding for the ribose-5-phosphate isomerase. The enzymes participates in the PPP, where it catalyzes the conversion of ribulose-5-P to ribose-5-P.
Several genes encoding enzymes of the TCA cycle were down-regulated, such as succinate dehydrogenase (*sdhA*, *sdhB, sdhC*), 2-oxoglutarate decarboxylase, (*sucA, sucB*), succinyl-CoA synthetase (*sucC)*, fumarate reductase (*frdD*). Further, the gene for the succinate semialdehyde dehydrogenase (*gabD*), the glyoxylate shunt enzyme isocitrate lyase (*aceA*) and the glycolysis/gluconeogenesis enzyme glyceraldehyde 3-phosphate dehydrogenase (*gapA*) were down-regulated. Additionally, several transcripts encoding enzymes of the energy generation and respiration such as the ATP synthase subunit C (YPK_4221) and several enzymes that generate reducing equivalents such as the formate dehydrogenase (*fdoH*, *fdoI*) as well as genes encoding subunits of cytochrome C (*napB, cyoC*) were down-regulated. The data suggests a reduced energy generation through oxidative phosphorylation, since some cytochrome C genes were down-regulated, as well as several NADH yielding reactions (e.g. in the TCA cycle). In the metabolome, an increase of nicotinamide and nicotinate was observable, which could be due to less NADH in the cell.
Many of the genes altered between the temperatures belonged to the central carbon metabolism, especially the TCA cycle and the glyoxylate shunt. These genes and particularly the isocitrate lyase are known to be involved in virulence and persistence in several pathogenic microorganisms including *Mycobacterium tuberculosis* as well as *E. coli*, *S. typhimurium* and *fungi* (McKinney et al. 2000, Lorenz & Fink 2001). Further, the down-regulation of the acetate permease and the acetyl CoA synthetase indicate reduced uptake of acetate at 37 °C. The opposite regulation, an increase of acetate permease and acetyl-CoA synthetase, has been observed in *Y. pestis* upon temperature downshift (Vadyvaloo et al. 2010). These proteins are also known to play a crucial role in the resumption of organic acids in stationary phase in *S. aureus* (Somerville et al. 2003).

There, the lack of acetate catabolism resulted in diminished growth yields, but did not influence virulence or persistence. The down-regulation of these genes could be the reason for the observed lack of TCA cycle intermediates re-consumption in stationary phase at 37 °C (chapter 3.2.5.1).

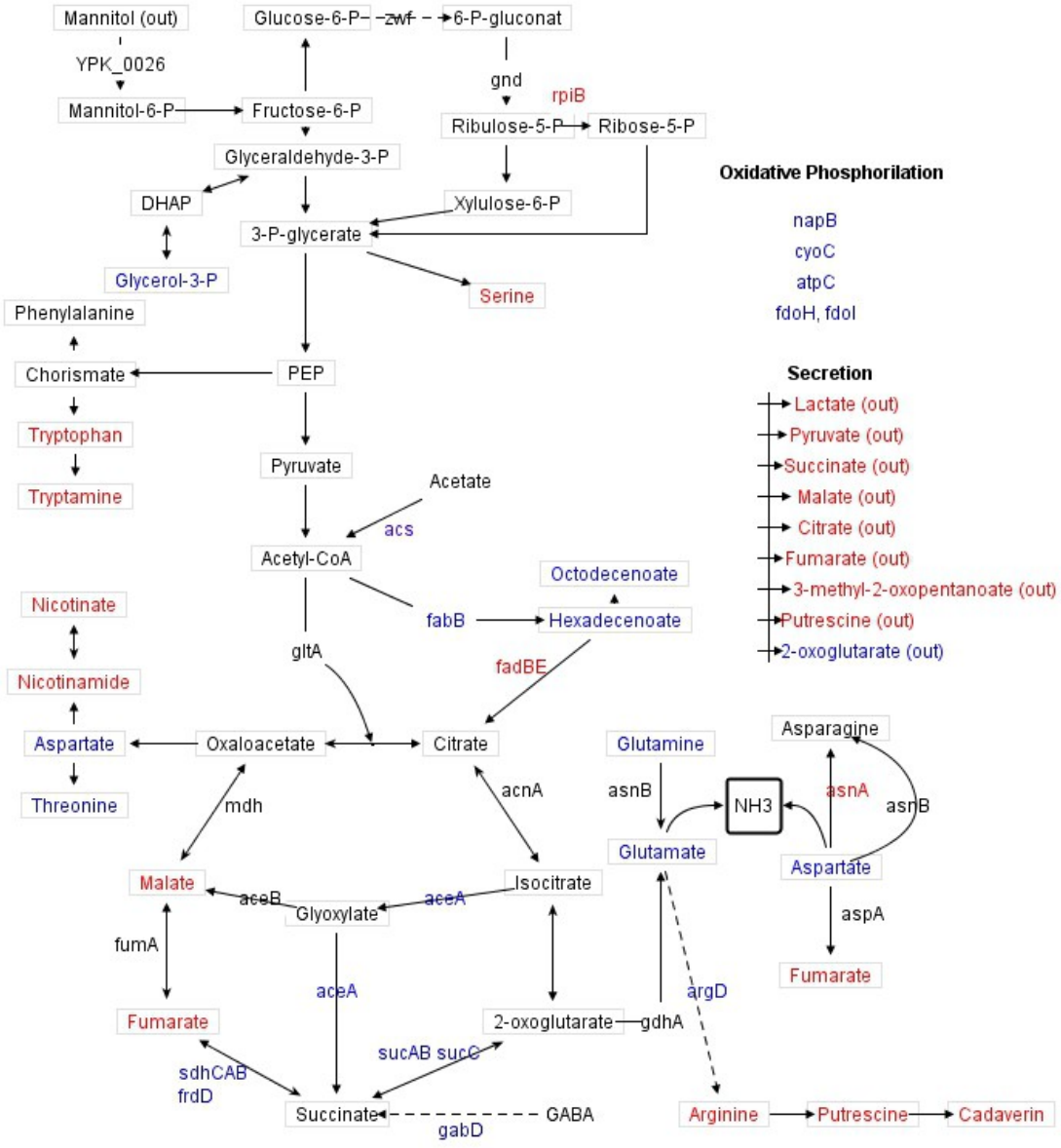

Figure 3.31: Central metabolism of *Y. pseudotuberculosis* YPIII during growth in LB medium in stationary phase at 37 °C compared to 25 °C. Changes in the transcriptome and the metabolome are indicated through colors, whereas red indicates an up-regulation of a gene or a higher concentration of the respective metabolite at 37 °C and blue indicates a down-regulation or a lower concentration at 37 °C. The metabolites and the secreted compounds correspond to the measurements in stationary phase in LB medium (chapter 3.2.5.2 and 3.2.5.1).

The level of the transcript of *asnA*, a gene coding for asparagine synthetase, was elevated at 37 °C. The enzyme catalyzes the conversion of aspartate to asparagine under ATP and

ammonia usage. This is in line with the reduced concentrations of aspartate in the metabolome of the stationary phase at 37 °C. The reduced level of the *argD* transcript, which encodes the acetylornithine transaminase, indicates an alteration of arginine and polyamine biosynthesis. Nevertheless, arginine was higher concentrated in the metabolome and putrescine was more secreted during the stationary phase at 37 °C.

The transcript *luxS* coding for the ribosylhomocysteinase is also reduced. It catalyzes the reverse reaction of S-ribosyl-L-homocysteine to L-homocysteine and 4,5-dihydroxy-2,3-pentanedione and could responsible for the missing uptake of homocysteine at 37 °C. Further it is involved in the synthesis of autoinducer-2 and a regulation through temperature has been noted in *E. coli* (Kim et al. 2005). Further LuxS is widely conserved in pathogenic bacteria and plays a crucial role in virulence in *Streptococcus*, *Vibrio* and *E. coli* (Vendeville et al. 2005).

Additionally, several genes involved in fatty acid metabolism were altered. Genes encoding enzymes of the fatty acid oxidation (*fadB*, *fadE*) were up-regulated at 37 °C. On the other hand the gene for the 3-oxoacyl-acyl carrier protein synthase *fabB* was significantly down-regulated. It is involved in fatty acid biosynthesis, where it elongates fatty acids. Also *acs*, encoding the acetyl-CoA synthetase, is down-regulated, which is involved in the formation of acetyl-CoA from acetate and coenzyme A and catalyzes the first committed step in fatty acid biosynthesis. These results indicate that at host temperatures the degradation of fatty acids is promoted, while synthesis is repressed, which is in accordance with the lower concentrations of fatty acids in the metabolome at 37 °C. A study of transcriptional alteration under temperature shift to 37 °C in *Y. pestis* observed similar effects in lipid metabolism (Motin et al. 2004).

Cell wall

The outer membrane pore protein, encoded by the gene *ompF* was strongly down-regulated at 37 °C. A similar observation has been reported for *Y. pestis* (Han et al. 2005, Pieper et al. 2009;), where additionally *ompC* was repressed at lower temperatures. It has been proposed, that the pore forming protein OmpF is the preferred expressed protein at lower temperatures, while OmpC is the preferred pore at higher temperatures. This is thought to be because OmpF forms larger pores than OmpC and therefore counterbalance the reduced diffusion through the decreased temperatures at lower temperatures (Han et al. 2005).

Transcription and translation

The genes for 12 ribosomal proteins were down-regulated at 37 °C and one was up-regulated. This is in accordance with other studies in *Y. pseudotuberculosis* (Rosso et al. 2008). The regulation of ribosomal proteins to temperature is diverse between species. While in *E. coli* ribosomal proteins are down-regulated in response to cold temperatures (Kim et al. 2005), they are up-regulated in *B. subtilis* (Beckering et al. 2002). However, the meaning of these results is not clear, yet.

Additionally some transcriptional regulators were down-regulated at the higher temperature including *crp,* coding for the cAMP-regulatory protein, and *trpR,* coding for the binding protein WrbA, which induces inhibition of tryptophan biosynthesis when bound to tryptophan. The protein WrbA was detected in an increased concentration in *Y. pestis* at 37 °C compared to 26 °C (Chromy et al. 2005).

Temperature shock proteins and general stress responses

Interestingly, several cold- and heatshock proteins were regulated. A well known cold shock protein was decreased at 37 °C: *cspE*, which has been described for *E. coli* to be involved in low temperature survival of the cell (Phadtare et al. 2002; Phadtare & Inouye 2004). *cspD* is also down-regulated but known to be induced upon nutrient starvation, especially glucose starvation, and not as a response to cold shock (Yamanaka & Inouye 1997). Additionally the genes for universal shock protein UspA and the RNA polymerase sigma factor RpoS were down-regulated at 37 °C. It is supposed that in *E. coli* the CspE and CspC proteins are involved in the control of the expression of the universal stress response proteins RpoS and UspA (Phadtare & Inouye 2001). However, *cspC*, coding for another cold-shock protein, was up-regulated at 37 °C maybe indicating a different role in YPIII. It has been shown that decreased expression of the *cspC* gene leads to increased fitness in *E. coli* (Rath & Jawali 2006). Several heat shock proteins were up-regulated at 37 °C including the heat shock chaperone genes *ibpA*, *ibpB* and *dnaK*. IbpA/B are small heat shock proteins that can cooperate with the DnaK system to reverse protein aggregation, supporting correct protein production under elevated temperatures (Mogk et al. 2003). These results indicate that heat and cold shock genes were regulated antagonistically in YPIII. Since several unspecific stress proteins were down-regulated (e.g. UspA, RpoS), it seems that the temperature of 37 °C did not represent a stress situation for YPIII and that the observed changes contributed to a normal adaption process to the environment.

Pathogenity

Consistently with previous results (Nagel et al. 2001; Herbst et al. 2009) the *rovA* gene and also some known RovA-regulated genes such as *invA* and *ail* were down-regulated at 37 °C. The gene of the histone like DNA-binding protein H-NS is decreased at 37 °C. The regulator is known to act as RovA antagonist (Heroven et al. 2004, chapter 1.5.2), but is also associated with cold stress in *E. coli* and is known as a regulator for several cold-shock genes (White-Ziegler & Davis 2009). Several genes involved in the later virulence phase, coding for effector proteins and type III secretion systems were up-regulated at 37 °C (*yopE, yopH, yopK, yopD, yopN, yopN, yscB, yscO. yscC, yscX, lcrV, lcrG*). Further, the type VI secretion system (*hcp*) was decreased at 37 °C, which has also been observed in *Y. pestis* (Pieper et al. 2009). In general the transcriptome showed a state of late virulence, where the later early virulence factors (*rovA, inv, ail*) are repressed and the late virulence factors (*yops*) are expressed and proved that temperature is extremely important factor in the control of virulence.

3.2.5.4 Time-resolved metabolome analysis at 37 °C compared to 25 °C in minimal medium

For a more detailed understanding of the metabolism of YPIII at 37 °C, a time resolved analysis of the metabolome in the exponential, transient and stationary phase in mannitol minimal medium at 25 °C and 37 °C was performed. The mannitol medium was developed for growth at 37 °C as described in chapter 3.2.4. The minimal medium was used to avoid disturbance in the analysis through the multitude of degradable components in the LB medium.

The experiments were performed at both temperatures for comparability according to the descriptions in chapter 2.11.2 and 2.12.2. Four time-points were chosen representing the above mentioned phases. Corresponding supernatant samples were taken as described before (chapter 2.11.3). To get representative intracellular metabolome data from different time-points without inducing stress to the cultures, separate cultures for every harvesting time-point were generated and harvested. Every biological sample originated from a separate culture. For every time-point 2 biological and 2 technical replicates were analyzed.

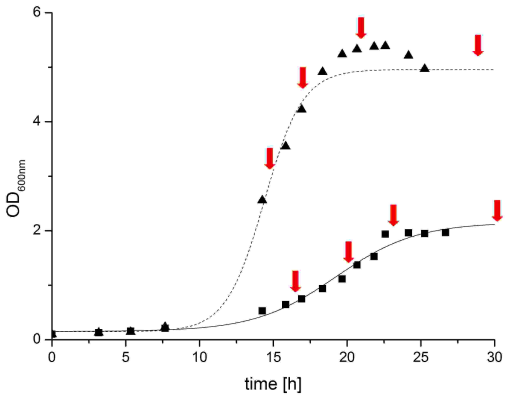

Figure 3.32: Growth curve of *Y. pseudotuberculosis* in minimal medium with 40 mM mannitol as sole carbon source, 2.5 mM thiosulfate and 0.25 mM $CaCl_2$ at 37 °C (squares) and 25 °C (triangles). Arrows indicate sampling time-points for metabolome and supernatant analysis.

The harvesting time-points for 25 °C samples were after 15 h, 19 h, 22 h and 30 h of cultivation at an OD of 2.6±0.07, 4.89±0.06, 5.12±0.05 and 4.73±0.08, and a specific growth rate μ of 0.23 h^{-1}, 0.08 h^{-1}, 0.01 h^{-1} and -0.01 h^{-1}, respectively (figure 3.32). At 37 °C the samples were harvested after 17 h, 20 h, 23 h and 31 h of cultivation at an OD of 0.88±0.1, 1.1±0.02, 1.76±0.06 and 1.79±0.02 and a μ of 0.15 h^{-1}, 0.14 h^{-1}, 0.04 h^{-1} and 0.00 h^{-1}, respectively (figure 3.32). The experiments were performed by J. Grimm in the context of her bachelor thesis.

3.2.5.5 Culture supernatant analysis in minimal medium

The supernatant samples were each taken from separate cultures. In total 36 samples were analyzed at 5 different time-points, including the sample taken at the time-point of inoculation. The summary of these experiments is given in table 3.12 and the complete list of metabolites can be found in supplement D.1.

Table 3.15: Summary of the results of the supernatant analysis of YPIII in minimal medium at 25 °C and 37 °C

Sample time-point [h]	**Growth temperature**	**Detected compounds**	**Identified metabolites**	**Relative standard error** (n= 4, 2 biological replicates, 2 technical replicates)
0	-	11	10	11,39%
15	25 °C	19	18	15,40%
19	25 °C	17	16	14,52%
22	25 °C	20	19	15,11%
30	25 °C	18	17	12,04%

Sample time-point [h]	Growth temperature	Detected compounds	Identified metabolites	Relative standard error (n= 4, 2 biological replicates, 2 technical replicates)
17	37 °C	22	19	18,19%
20	37 °C	22	19	14,62%
23	37 °C	22	20	15,37%
31	37 °C	24	21	16,31%

As can be seen in table 3.12 an increase of the measurable components over the time was detected, which indicates secretion of substances into the medium. Notably, more compounds were secreted at 37 °C than at 25 °C.

The supernatant samples were subject to a hierarchical clustering analysis and the resulting dendrogram clearly divides between the 25 °C and 37 °C samples (figure 3.33).

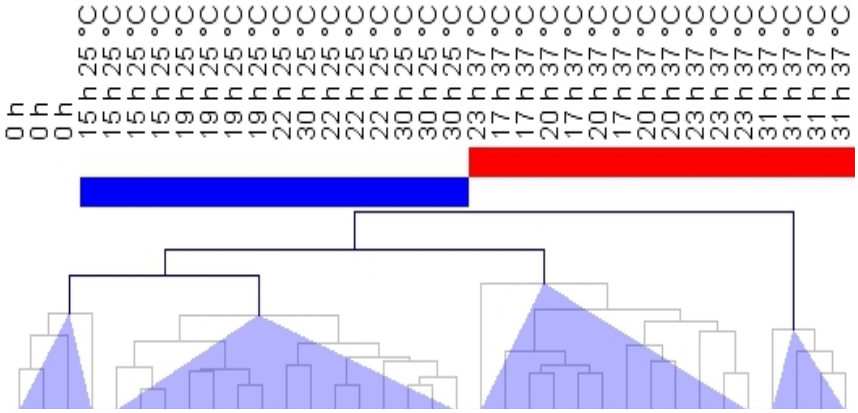

Figure 3.33: Hierarchical cluster analysis of supernatant samples taken over the time of cultivation at 25°C and 37°C in minimal medium. Clustering is based on all detected compounds. For the clustering of the samples euclidean distance and average linkage was used.

All samples of the 25 °C cultivation cluster together, which can be further separated into early and late exponential phase (15 h, 19 h) and early and late stationary phase (22 h, 30 h). The samples of the 37 °C culture show one cluster, which includes samples of early exponential, late exponential and early stationary phase (17 h, 20 h, 23 h), while the samples from late stationary phase (31 h) were separated, indicating a reduced similarity to the other samples.

The compounds detected in the supernatant, were also analyzed with a hierarchical cluster analysis and are displayed as a heatmap in figure 3.34.

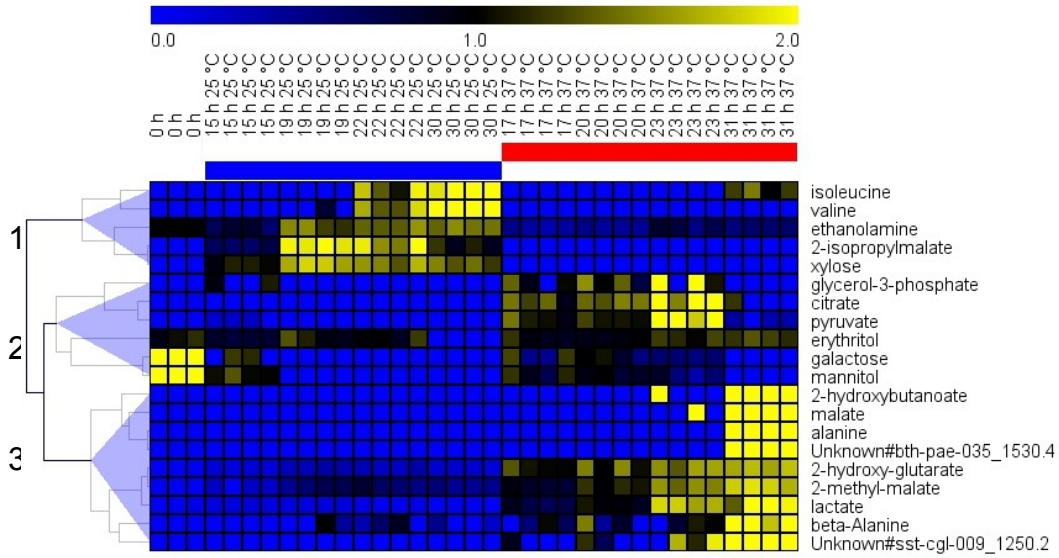

Figure 3.34: Heat map with hierarchical clustering of the extracellular metabolites over time of cells grown in minimal medium at 25 °C and 37 °C. Only metabolites are shown that were significantly altered in response to the temperature (p-value < 0.01, two factor ANOVA). Data is RMS-normalized over the rows. Euclidean distance and average linkage was used to cluster the metabolites.

The hierarchical cluster divides the metabolites into 3 major clusters. The first cluster includes compounds that were secreted at 25 °C. This includes amino acids (isoleucine, valine), ethanolamine, 2-isopropylamalate and a pentose. These substances are similar to those secreted during growth in glucose minimal medium at 25 °C (chapter 3.1.3.1) and belong predominantly to the biosynthesis of branched chain amino acids (valine, isoleucine, 2-isopropylmalate). These compounds were not detected in the supernatant at 37 °C. The second cluster was more heterogeneous and contained substances secreted during growth at 37 °C like glycerol-3-P, citrate, pyruvate, that were consumed at later stages of growth at 37 °C, and also the carbon source mannitol, which was consumed slower at 37 °C. The third cluster revealed by the hierarchical clustering, includes compounds that were secreted at 37 °C. The substances 2-hydroxybutanoate, malate and alanine were secreted at the end of the cultivation and were only detectable after 31 h of cultivation. During the whole course of cultivation a secretion of 2-hydroxyglutarate, 2-methylmalate, lactate and beta-alanine was measured at 37 °C. At 25 °C also smaller amounts of 2-methylmalate and 2-hydroxyglutarate were secreted. In the supernatant analysis in LB medium (chapter 3.2.5.1) and minimal medium the secretion of hydroxybutanoate compounds (4-hydroxybutanoate, 3-hydroxybutanoate, 2-hydroxybutanoate) and beta-alanine was noted at 37 °C, indicating a nutrient independent response to the elevated temperature.

Mannitol is taken up into the cell by a mannitol-specific phosphotransferase system,

entering the cell as mannitol-1-P. This is converted by a single dehydrogenase reaction to fructose 6-P and enters the central carbon metabolism. Since the catabolism of mannitol and glucose are similar, a similar metabolism can be expected. Nevertheless, an increased lag phase has been noted with mannitol at 25 °C compared to growth on glucose at 25 °C. Interestingly, during growth on glucose at 25 °C also lactate, pyruvate and alanine were secreted, which does not appear with mannitol as carbon source at 25 °C but at 37 °C. Only small amounts of pyruvate were detected in the supernatant at 25 °C after 15 h of cultivation similar to the phenomenon that has been noted in LB medium (chapter 3.1.3.3). This further confirms that the continuous secretion of pyruvate during growth in glucose minimal medium in chapter 3.1.3.5 was the effect of carbon catabolite repression mediated through presence of glucose in the medium. This could explain why mannitol provides slower growth but allows higher biomass yields ($OD_{max\ mannitol}$ = 5.2, $OD_{max\ Glucose}$ = 4.8, $\mu_{max\ Mannitol}$ = 0.234 h^{-1}, $\mu_{max\ Glucose}$ = 0.314 h^{-1}).

The analysis showed an enhanced secretion of several substances at 37 °C. Lactate was the most abundant metabolite in the supernatant of the stationary phase at 37 °C. It was secreted while mannitol was consumed (figure 3.35).

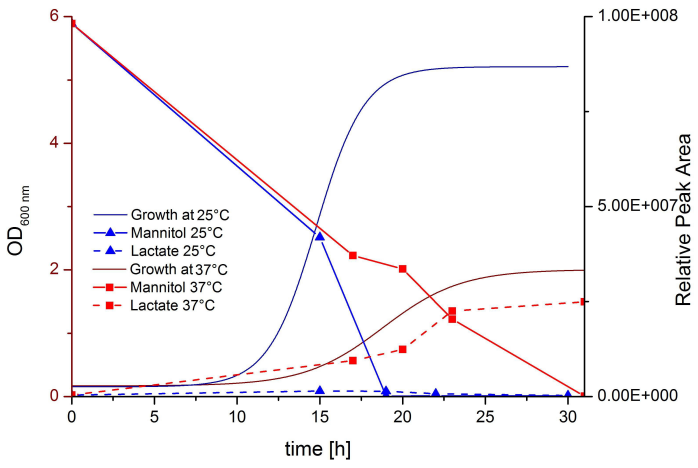

Figure 3.35: Growth curves of YPIII grown at 25 °C and 37 °C in mannitol minimal medium. The relative peak-areas of mannitol and lactate are shown over the course of cultivation.

The high amounts of secreted lactate might indicate an incomplete catabolism of mannitol, which leads to the reduced biomass yield at 37 °C compared to 25 °C. From the concentration curve of mannitol one can assume that carbon limitation led to cease of growth at 25 °C. However, carbon limitation does not cause the cease of growth at 37 °C. At 37 °C the YPIII cells entered the stationary phase after 22 h before mannitol was completely consumed. This indicates that the growth is limited in another way.

3.2.5.6 Intracellular metabolome analysis in minimal medium

The samples for the intracellular metabolome analysis were harvested as described previously (chapter 2.11.2 and 2.12.2). The summary of these experiments is given in table 3.13 and the complete list of metabolites can be found in supplement D.2.

Table 3.16: Summary of the results of the intracellular metabolome analysis at 25 °C and 37 °C in mannitol minimal medium

Sample time-point [h]	Growth temperature	Detected compounds	Identified metabolites	Relative standard error (n= 4, 2 biological replicates, 2 technical replicates)
15	25 °C	81	61	17.54%
19	25 °C	83	62	17.54%
22	25 °C	81	62	18,60%
30	25 °C	79	61	19,31%
17	37 °C	87	64	18.93%
20	37 °C	87	64	13,47%
23	37 °C	86	64	20,98%
31	37 °C	78	59	20,85%

In the samples similar numbers of compounds were detected, independent from temperature and harvesting time-point. To determine how alike the metabolome samples from 25 °C and 37 °C cultures were to each other, a hierarchical clustering was performed and is displayed as a dendrogram (figure 3.36).

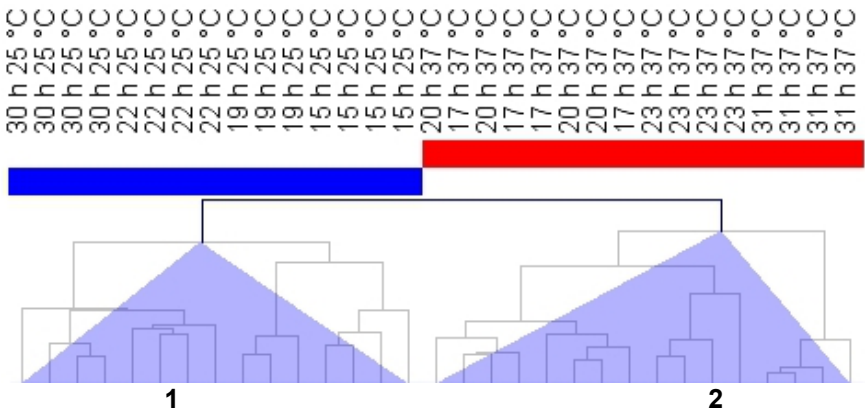

Figure 3.36: Hierarchical cluster analysis of the metabolome samples taken over the time of cultivation at 25 °C and 37 °C in minimal medium. Clustering is based on all detected compounds. For the clustering of the samples euclidean distance and average linkage was used.

The hierarchical clustering in figure 3.36 divides the samples by the temperatures. The first cluster consists of the samples grown at 25 °C and is further divided into samples from each time-point: The samples from early and late stationary phase (22 h, 30 h) cluster together and also from early and late exponential phase (15 h, 19 h). The second cluster contains the samples grown at 37 °C. Here, the samples from 17 h and 20 h show high similarity and are not separated by the clustering. The samples from 23 h are similar to the samples from 17 h and 20 h but form a subcluster, while the samples from 31 h are more distant. A similar clustering was observed when analyzing the corresponding supernatant (chapter 3.2.5.5). The proximity of the samples from 17 h, 19 h and 23 h at 37 °C can be explained through the high mannitol concentrations present in the medium (chapter 3.2.5.5) and the resulting similar growth rates of the cells.

In order to get a detailed insight into the differences between the temperatures and the growth phases the metabolites were analyzed with a two-factor ANOVA. The analysis showed, that 70 metabolites were significantly (p-value > 0.01) changed due to the temperature and 56 metabolites were significantly changed due to time. The metabolites, that were significant for the temperature, are subjected to an hierarchical clustering and are displayed as a heatmap (figure 3.37). The heatmap can be roughly divided into 4 clusters, whereas the first two clusters show metabolites that were increased at 25 °C and the third and fourth cluster consist of metabolites, enhanced at 37 °C.

The first cluster contains metabolites, that were present in increased concentrations in stationary phase at 25 °C. These were aromatic amino acids (phenylalanine, tyrosine) and intermediates from biosynthesis pathways (beta-alanine, 2-aminoadipate). The second cluster consists of a multitude of metabolite classes. Most of them were increased in the metabolome samples after 19 h of cultivation at 25 °C. These were mostly amino acids (aspartate, threonine, homoserine) and polyamines (putrescine). Further, several metabolites were constantly lower concentrated at 37 °C than at 25 °C, which included fatty acids and their precursors (heptadecanoate, octadecenoate, tetradecanoate, dodecanoate, glycerol-3-P) as well as amino acids (methionine, valine, leucine, cysteine, glycine, glutamate). In the third and fourth cluster many compounds were increased at 37 °C that belong to the central carbon pathways (glucose, glucose-6-P, mannitol-6-P, xylulose-5-P, lactate, pyruvate). Also the cofactor nicotinamide and its precursor nicotinate were increased at 37 °C as well as some fatty acids (3-hydroxy-dodecanoate, decanoate) and amino acids (lysine, alanine).

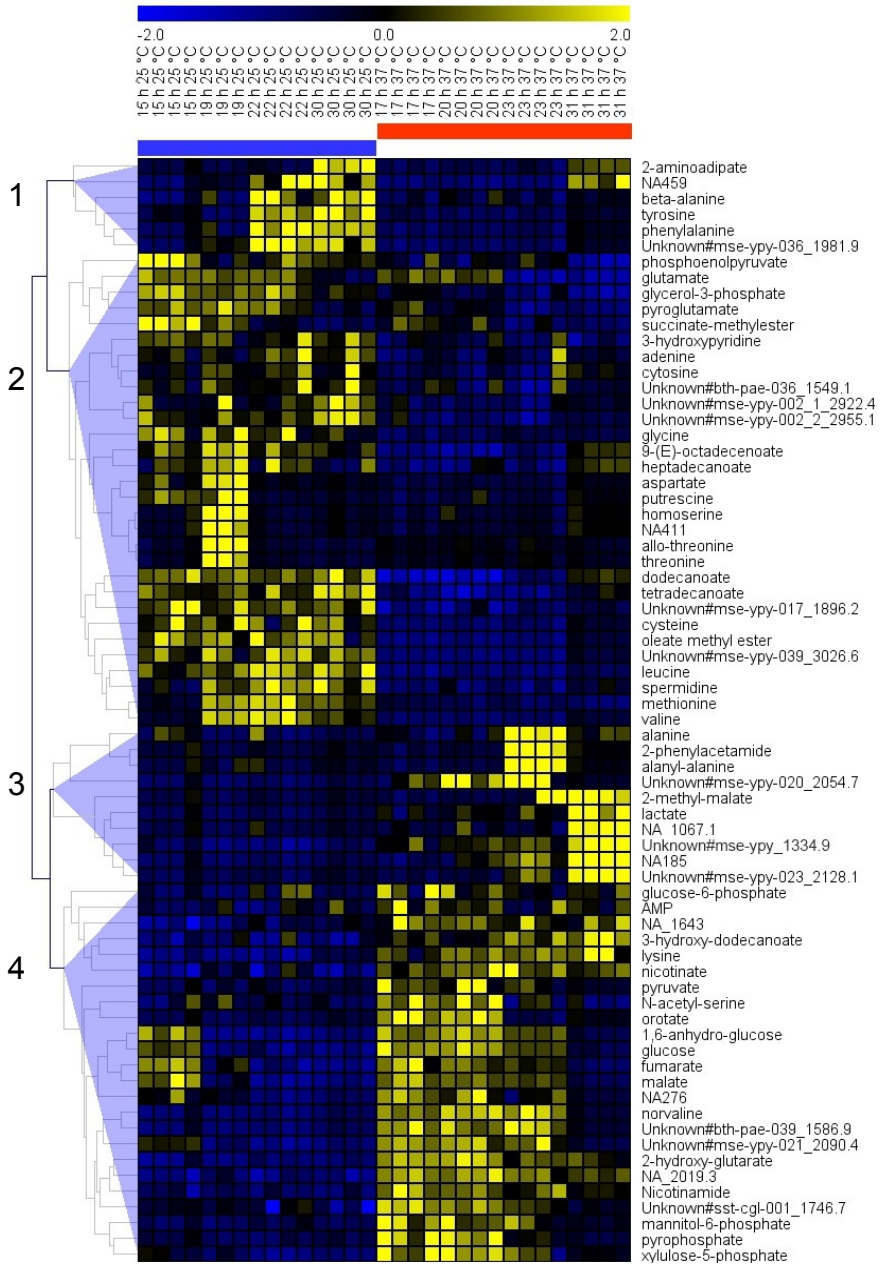

Figure 3.37: Heatmap with hierarchical clustering of the metabolites that were significantly altered between 25 °C and 37 °C in minimal medium (p-value < 0.01, two factor ANOVA). Data is z-score normalized over the rows and for the clustering euclidean distance and average linkage were used.

To further understand these changes, some of the detected metabolites are displayed in their metabolic context with their dynamic profile obtained at the two temperatures (figure 3.38). It seems that the main carbon pathways were mostly unaffected by the temperature. The dynamic profile of the TCA intermediates correlates roughly with the growth rates of the cells during the cultivation and decreased during stationary phase at both temperatures. The observed differences in the metabolite concentrations were therefore probably not caused by the the temperature difference.

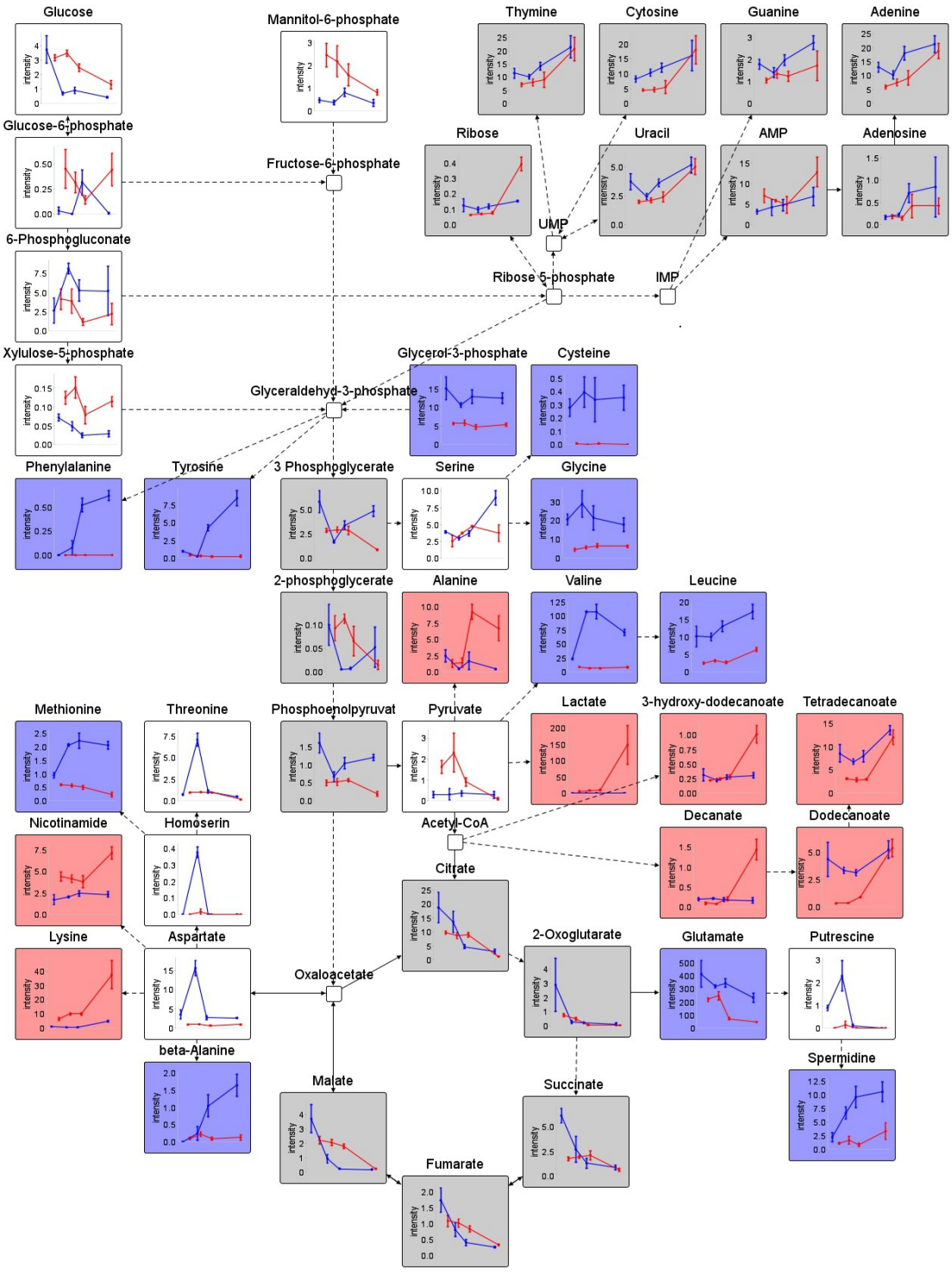

Figure 3.38: Visualization of time-resolved intracellular metabolite concentrations in minimal medium at 25 °C (blue line) and 37 °C (red line). The X-axis in the charts represents the time from 15 h to 31 h of cultivation. Metabolites unchanged by the temperature, have a grey background, metabolites increased at 25 °C have a blue background and metabolites increased at 37 °C have a red background. The metabolites, that could not be assigned to one of the previous groups were left with white background. Interrupted connections between the metabolites represent conversion of metabolites via more than one step. Error bars indicate the relative standard error. Image created with the Vanted software (Junker et al. 2006).

The metabolites from the nucleotide metabolism showed similar tendencies and concentrations at both temperatures, and the previously performed ANOVA showed that none of the intermediates was significantly altered between the temperatures.

The carbon source mannitol enters the cell via a PTS as mannitol-6-P. While the intracellular concentration of mannitol-6-P was similar to the concentration of mannitol outside the cell at 37 °C, the mannitol-6-P concentration at 25 °C was very low and independent from the mannitol in the supernatant (figure 3.35, chapter 3.2.5.5). This indicates a slower processing of mannitol-6-P with increased intracellular accumulation at 37 °C compared to 25 °C where it seems to be directly converted. The carbon source is further processed to fructose-6-P to enter the central carbon pathways. The metabolome data showed no evidence for the activity of gluconeogenesis (e.g. fructose-6-P, fructose-1,6-bisP) neither at 25 °C nor at 37 °C, but showed signs for the use of the PPP (xylulose-5-P, 6-phosphogluconate). Despite the fact that these metabolites show a great deviation, the constant higher concentration of xylulose-6-P at 37 °C might indicate an increased flux through the PPP at 37 °C. This is strengthened through the up-regulation of the ribose-5-phosphate isomerase in the transcriptome in LB grown cells (chapter 3.2.5.3). Consistently, Chromy et al. found that the ribulose-5-phosphate epimerase, the 6-phosphogluconate dehydrogenase and the glyceraldehyde 3-phosphate dehydrogenase were increased in the proteome of *Y. pestis* upon temperature shift from 26 °C to 37 °C during growth on gluconate (Chromy et al. 2005). However, in a transcriptome analysis under similar conditions the genes *gnd* and *gapA* encoding the 6-phosphogluconate dehydrogenase and the glyceraldehyde 3-phosphate dehydrogenase were down-regulated upon temperature shift from 26 °C to 37 °C (Motin et al. 2004; Ansong et al. 2012). This might indicate a posttranscriptional regulation of these enzymes. A down-regulation of most enzymes of glycolysis has been noted in the transcriptome of *Y. pestis* cells grown at 37 °C (Motin et al. 2004). If enzymes of the glycolysis were also down-regulated in YPIII, this could explain the slower degradation of the mannitol 6-P pool at 37 °C.

Another regulation between the temperatures occurred on the level of pyruvate: Pyruvate was increased at 37 °C after 20 h and subsequently the neighboring metabolites alanine and lactate increased. Further, the fatty acids, that are synthesized from acetyl CoA, showed a similar pattern and were increased after 31 h. In the supernatant, pyruvate was secreted at 37 °C during 17 h, 20 h and 23 h and was consumed after 31 h from the medium. This resumption was probably responsible for the increase of metabolites, that originated from pyruvate after 31 h at 37 °C.

The constant secretion of lactate and other organic acids (malate, citrate, 2-hydroxyglutarate) into the medium indicates a partial fermentative metabolism at 37 °C. This is encouraged by the fact, that the gene encoding cytochrome C *cyoC* was down-regulated in the transcriptome of LB medium grown cells at 37 °C (chapter 3.2.5.3). This down-regulation was also observed in the study of Ansong *et al.* (*cyoECD*) at 37 °C in YPIII (Ansong et al. 2012). This might be a mechanism induced by the reduced oxygen in the medium at elevated temperatures. The down-regulation of cytochrome C genes was also observed in *Y. pestis*, when shifted from 37 °C to 45 °C (Han et al. 2005).

Despite the fact, that in transcriptome analyses (chapter 3.2.5.3 and Motin et al. 2004; Han et al. 2005) several enzymes of the TCA cycle were regulated by the temperature, the metabolic intermediates did not show significant differences between the temperatures.

Several amino acids were lower concentrated at 37 °C, such as the branched chain amino acids valine and leucine. Valine, isoleucine and the intermediate isopropylmalate were also secreted into the supernatant at 25 °C but not at 37 °C confirming decreased branched chain amino acid biosynthesis at 37 °C. Motin et al. found that the genes *ilvC,* encoding an enzyme from isoleucine and valine biosynthesis, and *leuABCD*, encoding enzymes of the leucine biosynthesis, were down-regulated at 37 °C in *Y. pestis* (Motin et al. 2004). Further, aromatic amino acids increased over time in the metabolome at 25 °C (phenylalanine, tyrosine). Interestingly, the compound 2-phenylacetamide was increased at 37 °C (figure 3.37), which is an degradation product of aromatic amino acids. In the transcriptome of *Y. pestis* the genes *aroFAK*, encoding enzymes from aromatic amino acid biosynthesis, were down-regulated at 37 °C. Similarly, glycine and serine were decreased at 37 °C compared to 25 °C and so were their corresponding biosynthetic enzymes in *Y. pestis* (*glyA, serA*) (Motin et al. 2004). These findings indicate a decreased biosynthetic activity at 37 °C compared to 25 °C in YPIII, with the exception of lysine and alanine biosynthesis. It seems that the lysine biosynthesis is perturbed at 25 °C in mannitol minimal medium since the precursor 2-aminoadipate was increasing in stationary phase at 25 °C whereas lysine was not.

The compound 2-methylmalate was increased in the metabolome at 37 °C over the whole cultivation time and was also secreted into the medium. This might be a degradation product of glutamate via the methylaspartate pathway. In *Y. pestis* several deamination promoting enzymes are up-regulated at 37 °C including the asparaginase (*ansB*), serine deaminase (*sdaA*) and amino acid dehydrogenase (*dadA*) (Motin et al. 2004). In general a

reduction of amino acid biosynthesis and an increase of degradation seems to occur upon temperature elevation to 37 °C.

The reduced levels of methionine and cysteine in YPIII at 37 °C might be a consequence of the impaired sulfur reduction observed and discussed in chapter 3.2.4. In a study were *Y. pestis* was shifted from 37 °C to 45 °C genes from the cysteine regulon (c*ysB*, *cysM*, *cysA*, *cysW*, *cysT, cysP*, *cysH*, *cysI* and *cysJ*) were down-regulated at 45 °C (Han et al. 2005). These genes encode enzymes involved in the uptake of sulfate and the reduction to sulfide. This indicates, that with increasing temperatures the ability to reduce sulfur is further repressed.

The fatty acids detected in the metabolome, suggest an alteration of the membrane fluidity at 37 °C as less odd-fatty acids (hepta-, pentadecaonate) and less unsaturated fatty acids (octa- and hexadecenoate) were present compared to 25 °C. However, the fatty acids simultaneously increase in stationary phase of cultivation at 37 °C. This has been also observed in the metabolome of YPIII under conditions where thiosulfate was depleted (data not shown). A possible explanation is that coenzyme A cannot be synthesized in a functional form under limitation of reduced sulfur, which leads to perturbation in the fatty acid metabolism. Since it is known that cease of growth at 37 °C occurred not primarily due to depletion of the carbon source mannitol in the presented experiment (chapter 3.2.5.5), it is likely that the thiosulfate was exhausted causing the growth limitation. This was further supported through the fact that sulfide promoted increased growth yield compared to thiosulfate (chapter 3.2.4).

3.2.5.7 The influence of the temperature on the metabolism of YPIII independent from nutrition

Several studies have been performed utilizing the omics-technologies to analyze the changes during temperature transition of *Y. pestis* (Motin et al. 2004, Chromy et al. 2005, Chauvaux et al. 2007, Han et al. 2007, Pieper et al. 2009) and *Y. pseudotuberculosis* (Bölin et al. 1982, Rosso et al. 2008, Ansong et al. 2009). Although these studies revealed a major influence of the temperature on metabolic enzymes, only few studies concerned the meaning of these changes. Up to date no study provided comprehensive metabolomic data to my knowledge. Despite the fact that the studies were performed with different bacterial strains in different media and different conditions, some general mechanism can be deducted. Temperature elevation from room temperature (23 °C–28 °C) to the temperature

of the mammalian host (37 °C) does always influence the TCA cycle, the fatty acid metabolism and amino acid biosynthesis. A summary of the mechanisms is shown in figure 3.39 together with the metabolome data of the exponential phase of cells grown in mannitol minimal medium at 25 °C and 37 °C.

Since in cell grown in LB medium only 45% of the detected metabolites were altered in response to temperature in YPIII, while it was 77% in the minimal medium, the differences in the metabolism due to the temperature seem to be more severe in minimal medium than in LB medium. This was probably due to different nutritional requirements at 37 °C that led to a limitation of some sort. While at 25 °C carbon limitation was responsible for the cease of growth in minimal medium, this was not the case at 37 °C (chapter 3.2.5.5).

The phenotyping microarray analysis showed extremely reduced carbon source uptake capabilities at 37 °C compared to 25 °C (chapter 3.2.1), whereas the uptake of nutrients from LB medium was only slightly altered between the temperatures (chapter 3.2.5.1). Since it was also shown that yeast extract contains an unknown factor that promotes growth considerably (chapter 3.2.4), it is possible that this factor stimulates the uptake of nutrients and its lack in the phenotyping analysis was responsible for the reduced number of utilizable carbon sources. Further, this factor was probably also lacking in the minimal medium, which led to the observed limitation of growth. A possibility is the lack of reduced sulfur in the minimal medium that occurs during cultivation.

The transcriptome analysis showed that the majority of regulated transporters was down-regulated at 37 °C compared to 25 °C in LB medium (chapter 3.2.5.3), including transporters for acetate, mannose, polypeptides, iron, and polar amino acids (chapter 3.2.5.3). This is in accordance with the observations in other studies in minimal medium (Motin et al. 2004; Ansong et al. 2012).

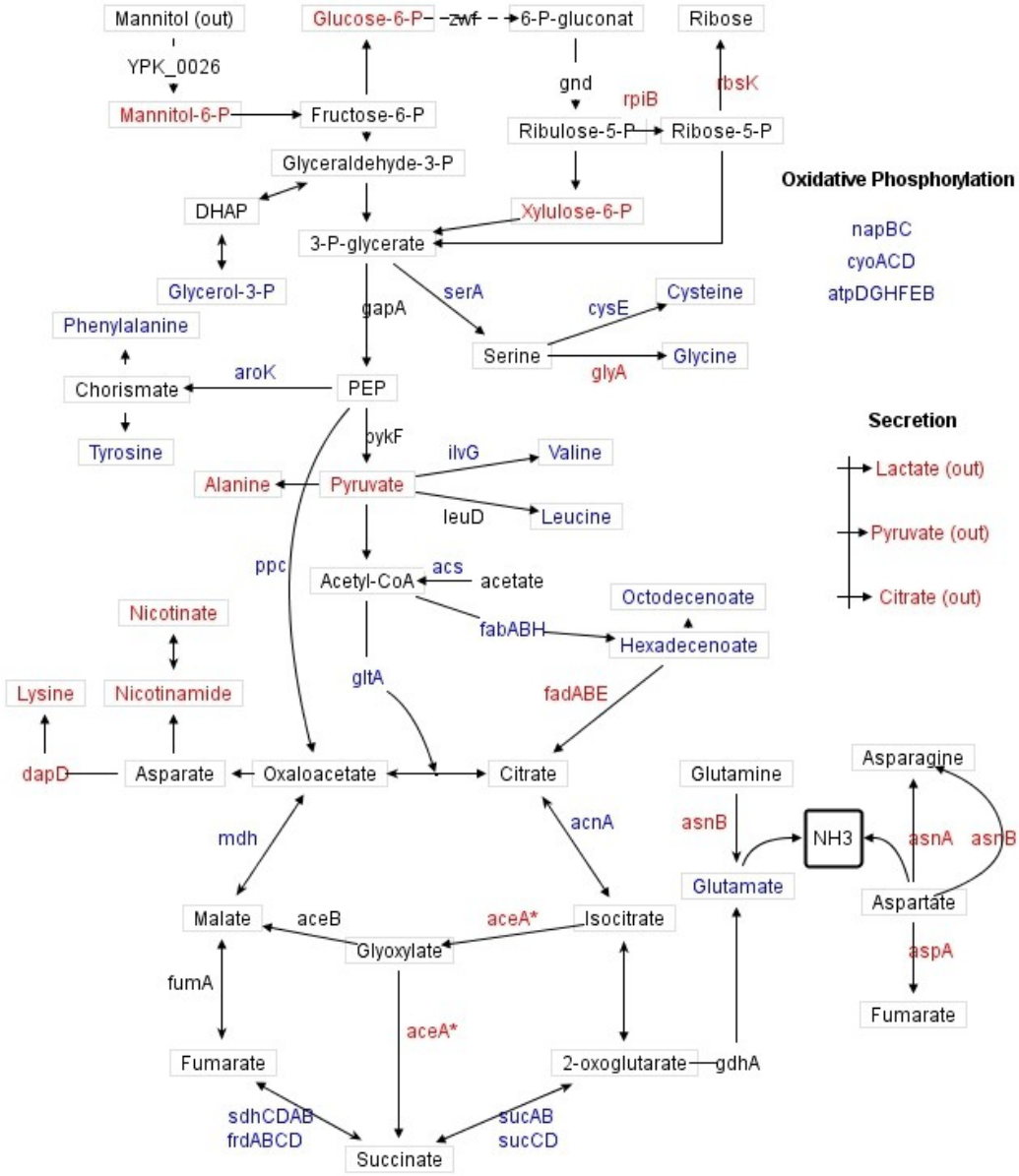

Figure 3.39: Central metabolism of *Y. pseudotuberculosis*. Significant alterations between cells grown at 25 °C and at 37 °C in the metabolome and the transcriptome are indicated through colors, whereas red indicates an up-regulation or a higher concentration at 37 °C and blue indicates a down-regulation or a lower concentration at 37 °C. The metabolites correspond to the measurements in exponential phase in minimal medium with mannitol as sole carbon source (chapter 3.2.5.6). The transcriptome data is merged from data measured in the study of Ansong et al. and Rosso et al. with the *Y. pseudotuberculosis* strains PB1/+ and IP32953 in amino acid supplemented medium with gluconate (Rosso et al. 2008; Ansong et al. 2012). Except for the isocitrate lyase gene *aceA* the data is in accordance with the transcriptome data in LB medium (chapter 3.2.5.3). Transcripts from Ansong et al: *aroK, cyoAECD, fabFGAH, aspA, gdhA, gltA, cys*E. Transcripts from Rosso *et al*: *atpDGHFED, cyoAD, mdh, ppc, napC, asnAB, ilvG, dapD, serA, fabHB, frdABCD, sdhABCD, fumA, suCD, aceA*. The transcripts *atpE, cyoC, napB, fadBE, fabB, rpiB, sdhCDAB, sucAB, sucC, frdD, asnA, acs, aceA* were obtained from the transcriptome analysis in LB medium (chapter 3.2.5.3).

aceA*= up-regulated at 37 °C in the study of Rosso et al. and down-regulated in the transcriptome in LB medium.

The energy metabolism of YPIII seems to be influenced by the temperature elevation (figure 3.39). The transcriptome in chapter 3.2.5.3 showed a down-regulation of cyctochrome C, ATP synthase subunits and TCA cycle enzymes at 37 °C. This is confirmed through the studies of Rosso and Ansong (Rosso et al. 2008, Ansong et al. 2012) (figure 3.39). Rosso further shows an up-regulation of the pyruvate formate lyase (*pflB*) at 37 °C, which is a central enzyme of the anaerobic metabolism. Since at 37 °C several fermentation products were increasingly secreted in minimal (lactate, pyruvate, citrate, malate) and LB medium (succinate, fumarate, malate), a partly fermentative metabolism with reduced energy generation through oxidative phosphorylation was suggested. The increase in nicotinate and nicotinamide at 37 °C in both media was in line with a reduced level of NAD^+ through degradation or an reduced recycling of nicotinamide through the salvage pathways.

The amino acid biosynthesis was down-regulated at 37 °C on transcriptome level, which leads to reduced amino acid pools in the metabolome in minimal medium. This effect is less evident in LB medium, since several amino acids were taken up from the medium. The transcriptome in LB medium (chapter 3.2.5.3) further showed the increase of amino acid degradation enzymes, which is supported by the increased detection of degradation products in the metabolome and supernatant at 37 °C in minimal medium (2-methylmalate, beta-alanine, 2-hydroxybutanoate) and LB medium (tryptamine, putrescine, cadaverin, 4-hydroxybutanoate, 3-hydroxybutanoate). The degradation of aromatic compounds seems to be impaired at 37 °C since several aromatic compounds were secreted into the LB medium (phenylacetate, phenyllactate, phenylpyruvate) and increased in the minimal medium metabolome (phenylacetamide, orotate). The down-regulation of *gabD*, encoding the succinate semialdehyde dehydrogenase, which catalyzes the last step in 4-hydroxyphenylacetate degradation, a common product of aromatic amino acid degradation, could be involved in this effect.

Several fatty acids were initially lower concentrated in the metabolome of YPIII at 37 °C (octadecenoate ($C_{16:1}$), dodecanoate ($C_{12:0}$)), which might indicate an alteration in lipid A composition. It has been reported in *Y. pestis* that the LPS structure is altered in response to temperature (Kawahara et al. 2002, Knirel et al. 2005, Suomalainen et al. 2010). This leads to reduced biological activity of lipid A towards the mammalian immune system at 37 °C reducing the immune response of the host (Kawahara et al. 2002). This includes a reduction of the O-antigens and a reduced level of acylation of the lipid A moiety at 37 °C

compared to 26 °C. The lipid A of *Y. pestis* contains reduced amounts of $C_{16:1}$ and $C_{12:0}$ at growth temperatures of 37 °C, which is in agreement with the present observations in the metabolome. The decreased amounts of unsaturated fatty acids (hexadecenoate ($C_{16:1}$), octadecenoate ($C_{18:1}$)) may also indicate a decrease in fluidity of the membrane at 37 °C, which has also been observed in *E. coli* (Cronan & Rock 1996). Further, glycerol-3-P was decreased in YPIII grown at 37 °C. Glycerol-3-P is a precursor of phospholipids and is directly synthesized from dihydroxyaceton phosphate, an intermediate from glycolysis. The decrease of branch chained amino acids (valine, leucine, isoleucine) at 37 °C indicates reduced synthesis of branched fatty acids, which has been described for *B. subtilis* at low temperatures (Klein et al. 1999). These effects in fatty acid metabolism seem to be independent from the growth medium since they have been observed in LB medium and minimal medium. The transcriptome data in chapter 3.2.5.3 and the study of Ansong et al. indicates an up-regulation of the fatty acid beta-oxidation at 37 °C (Ansong et al. 2012).

Several studies with *M. tuberculosis* indicate the importance of fatty acid metabolism as carbon and energy source for intracellular growth. Other components such as amino acids and hexoses are predominantly used as building blocks for anabolic purposes (Muñoz-Elías & McKinney 2006). A similar mechanism might occur in YPIII upon temperature elevation, which is supported by the reduced transcription of genes encoding enzymes of biosynthesis pathways and increased transcription of genes encoding enzymes of degradation pathways. Also the energy generation from hexoses seems to be limited due to the down-regulated oxidative phosphorylation. However, the use of fatty acids as energy and carbon source is unlikely since the crucial enzyme isocitrate lyase (*aceA*) of the glyoxylate shunt was down-regulated in the transcriptome of cells grown in LB medium. Nevertheless, other studies show an up-regulation of isocitrate lyase at 37 °C when *Y. pseudotuberculosis* was grown on gluconate supplemented with most amino acids (Rosso et al. 2008, Ansong et al. 2009).

In several pathogenic organisms, a down-regulation of synthesizing activity after colonization of the host has been noted. The surroundings in the host provide a broader spectrum of organic compounds than the outer-host environment, making synthesizing not longer necessary (Schaible & Kaufmann 2005). In intracellularly growing *Listeria monocytogenes* 50 - 100% of the amino acid content was obtained from the host cell (Eylert et al. 2008). Also, several obligatory intracellular pathogens have lost synthesizing pathways completely (Sakharkar et al. 2004). A down-regulation of biosynthesis and an up-regulation of defense mechanisms against the host immune system induced through

temperature elevation is likely in YPIII, since genes encoding Yops and T3SS were up-regulated in the transcriptome (chapter 3.2.5.3).

3.3 Influences of virulence regulators on metabolism of Y. pseudotuberculosis

In the previous chapters only the influence of abiotic factors like nutrition and temperature on the metabolism of the *Y. pseudotuberculosis* strain YPIII was examined, but in order to gain further understanding of the interlinkage of metabolism and virulence, the influence of virulence regulators on the metabolism needs to be addressed. Previous studies indicated that several virulence traits, such as invasin, are co-regulated with metabolism (Nagel et al. 2001; Heroven et al. 2008). The regulation of virulence is complex and depends on a multitude of factors as described earlier (chapter 1.4 and 1.5). In cooperation with the group of P. Dersch (HZI, Braunschweig, Germany) five regulatory proteins were selected, that belong to the recently discovered virulence regulation network (chapter 1.5). Mutants of the respective regulators (chapter 2.4) were investigated for their impact on the metabolism of YPIII. The resulting mutant strains are described in table 3.18.

Table 3.18: The investigated *Y. pseudotuberculosis* mutant strains and the regulators

Mutant strain	Regulator	Homologue	Description
YP3 (*rovA*$^-$)	RovA	SlyA (*E. coli*)	Chapter 1.5.1
YP72 (r*ovM*$^-$)	RovM	LrhA (*E. coli*), HexA/PecT (*Erwinia*)	Chapter 1.5.3
YP53 (*csrA*$^-$)	CsrA	RsmA (*Pseudomonas*)	Chapter 1.5.4
YP50 (*ymoA*$^-$)	YmoA	Hha (*E. coli*)	Chapter 1.5.5
YP89 (*crp*$^-$)	Crp	Crp (*E. coli)*	Chapter 1.5.7

The mutant strains were investigated for their growth characteristics (chapter 3.3.1) and subjected to phenotyping microarray analysis (chapter 3.3.2), transcriptome analysis (chapter 3.3.3), supernatant analysis (chapter 3.3.4.1) and metabolome analysis (chapter 3.3.4.2). Depending on the results of the analysis, further experiments were performed to confirm the interpretation.

The regulation of the virulence factors is nutrient and growth phase dependent. The regulator of early virulence genes, RovA, is repressed in minimal medium and is mostly expressed during stationary phase (Nagel et al. 2001). Hence, most experiments were

performed in LB medium in stationary phase at 25 °C. The harvesting time-point was defined in the stable stationary phase two hours after cell density had reached maximal OD. At that time-point a maximum effect of the mutation in comparison to the wild type strain was expected. Since the deleted regulators participate in the same network and affect each other, overlapping and opposed effects were expected. To identify those, the results of the analyzes are summarized and the most frequent incidents are discussed. For a more detailed understanding of the impact of mutation on the metabolism, the mutant strains YP3 (*rovA*$^-$), YP72 (*rovM*$^-$) and YP89 (*crp*$^-$) are discussed in detail in the later sections (chapter 3.3.9.1 - 3.3.9.2).

3.3.1 Growth characteristics

To characterize the phenotype of the *Y. pseudotuberculosis* mutant strains, they were cultivated in LB medium at 25 °C as described earlier (chapter 2.9.1) and the growth was monitored. The results are shown in figures 3.41 and 3.42.

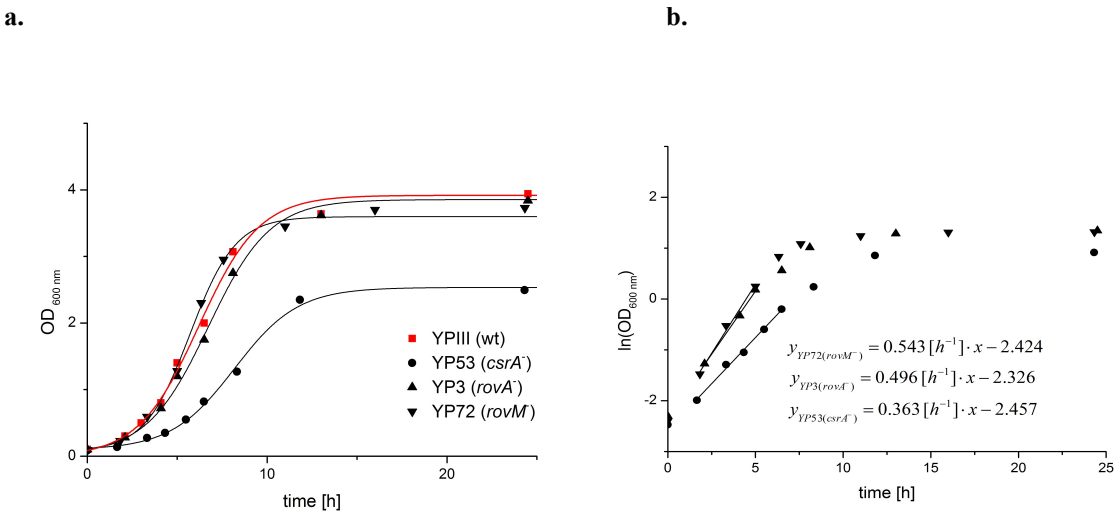

Figure 3.41: (a) Growth curve of *Y. pseudotuberculosis* wild type YPIII and mutant strains YP3 (*rovA*$^-$), YP72 (*rovM*$^-$), YP53 (*csrA*$^-$) in LB medium at 25 °C (b) Graphical designation of the exponential growth rate and maximum growth rate μ by a half-logarithmic plot.

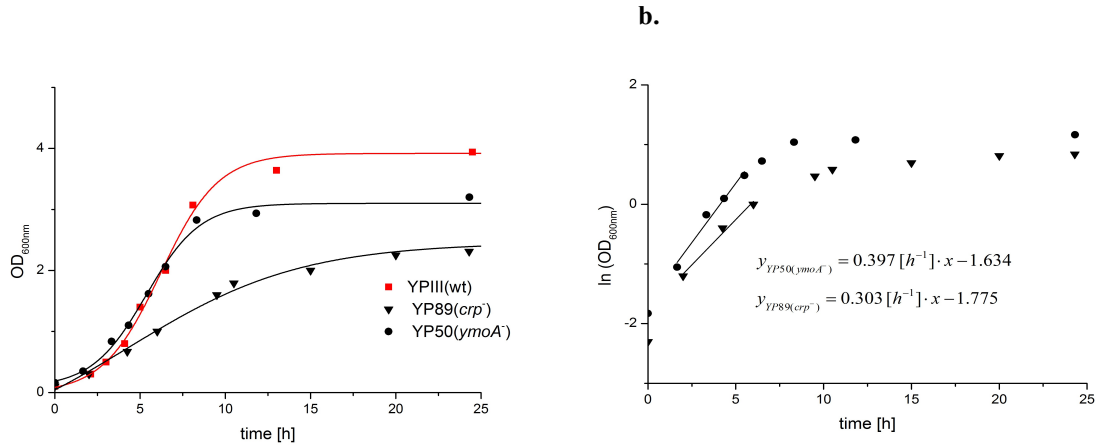

Figure 3.42: (a) Growth curve of *Y. pseudotuberculosis* wild type YPIII and mutant strains YP89 (*crp*$^-$) and YP50 (*ymoA*$^-$) in LB medium at 25 °C (b) Graphical designation of the exponential growth rate and maximum growth rate µ by a half-logarithmic plot.

The deletion of the regulatory elements resulted in different effects on growth behavior. The summarized characteristics are presented in table 3.19.

Table 3.19: Growth characteristics of the examined *Y. pseudotuberculosis* mutant strains

Mutant strain	Maximal growth rate µ [h^{-1}]	Maximal OD
YP3 (*rovA*$^-$)	0,5	3,8
YP72 (r*ovM*$^-$)	0,54	3,7
YP53 (*csrA*$^-$)	0,36	2,5
YP50 (*ymoA*$^-$)	0,4	3,2
YP89 (*crp*$^-$)	0,3	2,4
YPIII	0,56	3,8

The results showed influences of the mutation on the growth behavior of 3 mutant strains, indicating an effect of the mutation on metabolism. The mutant strains YP3 (*rovA*$^-$) and YP72 (*rovM*$^-$) showed no significant difference compared to the wild type. The mutant strain YP50 (*ymoA*$^-$) showed a decreased growth rate and reached a lower maximal OD. Finally, the mutant strains YP53 (*csrA*$^-$) and YP89 (*crp*$^-$) grew considerably slower and reached only 2/3 of the biomass of the wild type, indicating that these mutations had the most severe effects on the organism. The pH was measured during growth and was the same between all cultivations, starting at pH 7 and slowly rising to pH 8-8.5 during cultivation of all mutant strains.

3.3.2 Catabolic uptake differences

For a more accurate characterization of the effects of the mutations on the metabolism of *Y. pseudotuberculosis*, the mutant strains were subjected to phenotyping microarray analysis (chapter 2.9.6). Since carbon sources are known to influence virulence factor expression (Nagel et al. 2001), the utilizable carbon sources were of particular interest. Hence, the plates PM 1 and PM 2 with 190 different carbon sources were tested at 25 °C and the results were compared to the results of the wild type at 25° C (chapter 3.1.1). The summary of the experiments is shown in table 3.20.

Table 3.20: Summary of the results of the mutant strain on the carbon sources phenotyping microarrays (PM1 & PM2) compared to the wild type strain at 25°C

Mutant strain	Utilization ability gained	Utilization ability lost
YP3 (*rovA*$^-$)	3	1
YP72 (r*ovM*$^-$)	0	1
YP53 (*csrA*$^-$)	0	9
YP50 (*ymoA*$^-$)	0	4
YP89 (*crp*$^-$)	3	32

The detailed results are discussed in the integrative consideration of the single mutant strains (chapter 3.3.9.1 - 3.3.9.2). Notably, only the *crp* and *rovA* mutants gained abilities to utilize carbon sources. In both cases the mutants were able to grow on nucleosides (thymidine, uridine, inosine, adenosine), that could not be used by the wild type. This phenomenon is further investigated in chapter 3.3.7. Nevertheless, the *crp* mutant was highly impaired in carbon source utilization and 32 carbon sources less than the wild type were used. Since the cyclic AMP receptor protein (Crp) is involved in the utilization of alternative carbon sources this result was expected. However, also the *csrA* and the *ymoA* mutant showed reduced abilities to use the offered carbon sources, but the effects were less profoundly than in the *crp* mutant. The most frequent changes were the disability to utilize D-alanine (*rovM, csrA, ymoA, crp* mutants) and L-lyxose (*rovA, csrA, ymoA, crp* mutants). Hereby, L-lyxose is known as a frequent false-positive result and was not considered as meaningful (personal communication, Biolog). Interestingly, the *ymoA* and the *crp* mutant were both not able to use N-acetyl-D-mannosamine and D-glucose-6-P. Both substances are ubiquitously present in the mammalian host and the ability to degrade N-acetyl-mannosamine is associated with virulence (Almagro-Moreno & Boyd 2009).

3.3.3 Comparative transcriptome analysis

The transcriptome analyses of the *Y. pseudotuberculosis* mutant strains were performed by A. K. Heroven and J. Melzer (Group of P. Dersch, HZI, Braunschweig, Germany). The sampling and adjacent handling is described previously (chapter 2.10). The data processing was performed by J. Klein (Group of D. Jahn, TU Braunschweig, Braunschweig, Germany), as described in chapter 2.10. Transcripts were regarded as significant if they were altered more than 1.75-fold from the wild type. The results were compared and a summary is given in table 3.21, while the complete data is available in supplement E.1.

Table 3.21: Summary of transcriptome analyses of the mutant strains. Results comprise changed genes compared to the wild type strain (ratio > 1.75)

Mutant strain	Metabolism	Transcription factors	Transporter	Virulence & Stress	other	Total Σ
YP3(*rovA*$^-$)	20	2	5	11	7	44
YP72 (r*ovM*$^-$)	18	3	7	20	64	112
YP53 (*csrA*$^-$)	95	16	50	36	303	500
YP50 (*ymoA*$^-$)	87	26	52	106	442	713
YP89 (*crp*$^-$)	123	24	43	44	306	540

The transcriptome analyses data were correlated with each other to obtain information about similarity of the impact of the mutations. In order to gain further information about the similarity to other conditions, the transcriptome data of the temperature experiment in LB medium (chapter 3.2.5.3) was included (figure 3.43).

The most noteworthy result is the strong positive correlation of 0.77 of the *ymoA* mutant with the 37 °C transcriptome. The correlation is based on 83 transcripts, whereas most of them were similarly altered. The YmoA protein is degraded by proteases at 37 °C , hence it mediates temperature-dependent control (Jackson et al. 2004, chapter 1.5.5). The deletion of the *ymoA* gene seems to cause similar changes in the transcriptome like growth at 37 °C. This is further discussed in chapter 3.3.5. RovA is also known to be degraded by the Lon protease upon temperature elevation (Herbst et al. 2009), but the transcriptome of the *rovA* mutant shows no correlation to the transcriptome at 37 °C. Only 6 transcripts were altered in both *rovA* mutant and 37 °C. One of them was *invA* encoding Invasin, required for cell adhesion in the early stage of infection (Isberg et al. 1987).

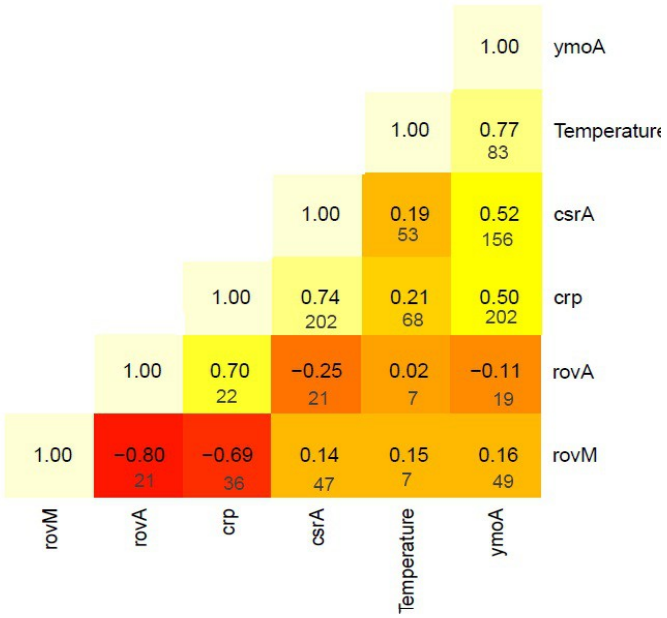

Figure 3.43: Correlation analysis of the transcriptome data, based only on the significantly changed transcripts. Pearson correlation was calculated based on all transcripts that were significantly altered in both conditions. The result is indicated by the color of each square and the black number in the square. Red indicates a strong negative correlation and white indicates a strong positive correlation. The number of transcripts used to calculate the correlation is indicated in smaller gray numbers in each square. The temperature sample consists of the transcriptome data 37 °C vs. 25 °C discussed in chapter 3.2.5.3..

The correlation analyses revealed further that the *rovA* and *crp* mutants exhibited a strong negative correlation to the *rovM* mutant. Since RovM suppress RovA transcription an antagonistically effect is expected. Also, the regulator Crp interacts with the small regulatory RNAs of the Csr-system and indirectly suppresses the activation of RovM. Further, it has been proposed that Crp represses RovM independently of CsrA (Heroven et al. 2012). The high positive correlation of the *crp* and the *csrA* mutant was based on a multitude of similarly regulated genes, which will be the subject of discussion in a later chapter (chapter 3.3.6).

The comparison of the transcriptomic profiles of the mutant strains showed that 308 genes were altered in at least exact 2 strains compared to the wild type, 99 were altered in 3 strains, 18 in 4 strains and 6 in all 5 mutant strains. In order to identify cluster of similar regulated genes the 92 most frequently altered transcripts, that were at least altered in 3 mutant strains and had a known function, were organized with a self organizing tree algorithm (SOTA). SOTA is an algorithm that combines the hierarchical clustering with

self organizing maps, allowing a clustering based on global decision rather than local decision (Dopazo & Carazo 1997, chapter 2.14.5). The analysis identified six main clusters (figure 3.44).

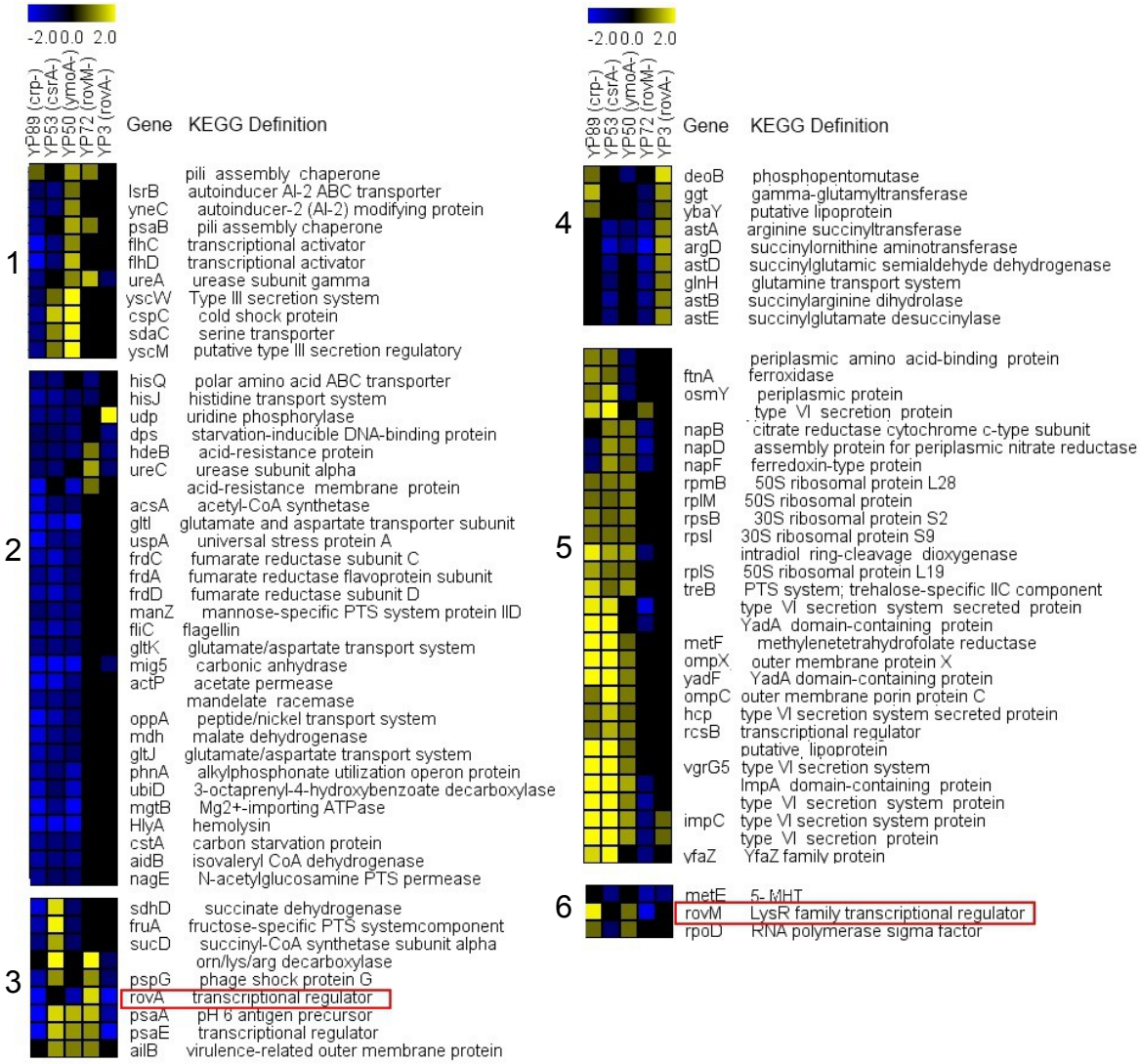

Figure 3.44: Cluster analysis of the most frequently differently expressed genes in response to the mutations. The analysis was performed using SOTA, which identified 6 main clusters. Each square represents the mean value of the $\log_2$ mutant/wildtype ratio, where blue indicates a down-regulation and yellow indicates an up-regulation. Black squares indicate no change compared to the wild type. Only transcripts with known function are displayed.

5-MHT = 5-methyltetrahydropteroyltriglutamate-homocysteine methyltransferase

The first cluster comprised genes of several regulatory proteins (*flhDC*), autoinducer and type three secretion system components. The genes encoding regulatory proteins might account for some regulatory differences in other genes, themselves. This led to complications in the evaluation whether regulations were caused by the investigated

mutation and its implication on the virulence network or by other regulators that have global impacts on the transcriptome.

The second cluster included genes that were predominantly down-regulated in the mutants. This concerned several genes encoding proteins that are involved in stress response (*hdeB, dps, uspA, mig5, cstA*). HdeB is an acid resistance protein. Urease encoded by *ureABCDEFGD* is also associated with acid resistance in *Yersinia* (Koning-Ward & Robins-Browne 1995). The similarly altered transcript *mig5* encodes a carbonic anhydratase conserved between many prokaryotes. A comparison showed a close similarity between the carbonic anhydratase of *Y. pestis* and *S. typhimurium* (Smith et al. 1999). The carbonic anhydratase is important for survival of *S. typhimurium* in the host and is extremely up-regulated in macrophages (*mig* = macrophage inducible gene) (Valdivia 1997). A possible function of the carbonic anhydratase in the macrophage is to mediate acid resistance as in *Helicobacter pylori* (Marcus et al. 2005). Since *Y. pseudotuberculosis* has the ability to survive and proliferate in macrophages (Tsukano et al. 1999, Pujol & Bliska 2003), a similar role for the carbonic anhydratase might apply. The analogous regulation compared to acid resistance proteins supports the involvement of the carbonic anhydratase in acid resistance.

Notably, also genes encoding enzymes of the TCA cycle (*frdACD, mdh*) and amino acid degradation pathways clustered here. The *aidB* gene encodes the isovaleryl-CoA dehydrogenase, which is involved in the degradation of valine, leucine and isoleucine. The mandelate racemase is a protein involved in the aromatic acid metabolism. Another group of genes in the second cluster encodes for transporters of amino acids, acetate, peptides, magnesium ions and sialic acids (*hisQJ, gltJLK, actP, oppA, mgtB, nagE*). The down-regulation of *nagE* results probably in the disability to use N-acetyl-D-mannosamine, which was noted earlier through the phenotyping microarrays for the *ymoA* and *crp* mutants (chapter 3.3.2).

The third cluster contained the gene for the transcriptional regulator *rovA*. The transcriptional regulator is up-regulated in the *rovM* mutant strain, which is its repressor, and down-regulated in the *ymoA* and *crp* mutant. The genes encoding the phage shock protein *pspG* and the components from the pH 6 antigen (*psaA, psaE*) follow a similar pattern and cluster closely together. The transcripts *psaA* and *psaE* are encoding the pH 6 antigen and its transcriptional regulators (chapter 1.4). It is known that RovA affects the transcription of the *psa* locus (Cathelyn et al. 2006).

The fourth cluster was regulated oppositely to the third cluster and in particular all transcripts in the cluster were up-regulated in the *rovA* mutant. The cluster predominantly encompasses genes encoding enzymes from arginine degradation (*astABDE, argD*), which participate in the ammonia-producing arginine succinyltransferase (AST)-pathway of arginine degradation. The AST-pathway is induced upon nitrogen limitation and growth on aspartate and arginine in *E. coli* (Schneider et al. 1998). Further, it is important for virulence in *P. aeruginosa*, but the mechanism still remains unclear (Feinbaum et al. 2012). ArgD is a bifunctional enzyme also catalyzing amination steps in the biosynthesis of lysine, ornithine and arginine. Notably an ornithine/lysine/arginine decarboxylase was located in the third cluster and regulated oppositely, suggesting an involvement in the arginine metabolism.

The phosphopentomutase encoded by *deoB* was regulated to a similar extend as the AST-pathway. It is necessary to use nucleosides as carbon sources in *E. coli* (Leer 1976). The ability to utilize nucleosides as sole carbon sources was improved in the *rovA* and *crp* mutant as shown through the phenotyping microarrays (chapter 3.3.2).

The fifth cluster was directly opposed to the second cluster and compromised mainly of up-regulated transcripts. Here, genes encoding components of anaerobic respiration (*napBDF*) and ribosomal proteins were arranged. NapB is a periplasmatic nitrate reductase, while NapD is required for Nap enzyme activity. NapF is probably an iron-sulfur protein and not required for Nap activity. The Nap nitrate reductase is induced by anaerobiosis and through low concentrations of nitrate. It does support anaerobic respiration of various carbon sources in *E. coli* (Stewart et al. 2002).

However, the majority of the 5. cluster contained genes encoding membrane proteins (*ompC, ompX, yadF*) and parts of the type VI secretion system (*impA, imC, hcp*). The type VI secretion system might play a role in the colonization of the flea vector in *Y. pestis* and its expression is influenced by temperature (Rosso et al. 2008; Pieper et al. 2009). Interestingly, the transcriptional regulator RcsB was also placed in the cluster. It was up-regulated in the *ymoA*, *csrA* and *crp* mutant and regulates cell division and motility. It is a repressor of the transcriptional activator FlhD (Krin et al. 2010), from the first cluster cluster. The FlhC/D regulators are the master regulators of the flagella gene expression (Prüß et al. 1997) and are involved in the regulation of several metabolic processes involving anaerobic respiration and the Entner-Doudoroff pathway (Prüß et al. 2001; Prüß et al. 2003). Among other, the fumarate reductase, encoded through *frdABCDE* and

arranged in the 2. cluster, is repressed through FlhD. FlhD is stabilized by binding of the CsrA protein (Wei et al. 2001; Heroven et al. 2008). Although it is not clear why RcsB is up-regulated in the three mutant strains, the perturbation in the CsrA levels might account for inconsistent response of FlhD: It is down-regulated in the *crp* and *csrA* mutant probably through the increased RcsB but up-regulated in the *ymoA* mutant. The deletion of *rovA* and *rovM* showed no effects on this system.

The sixth cluster finally exhibits similarities to the fourth cluster and was opposed to the third cluster, which contained *rovA*. Consistently, the sixth cluster contained the gene of the RovA repressor RovM (*rovM*). The gene *metE* is coding for a 5-methyltetrahydropteroyltriglutamate-homocysteine methyltransferase, which catalyses the conversion of homocysteine to methionine, and was significantly regulated.

Since neither RovA nor RovM are known to influence their master regulators CsrA or Crp, the genes changed in the *rovA* and *rovM* mutant were probably directly controlled through RovA or RovM. Further, regulations occurring in more mutant strains including RovA or RovM were probably mediated at least partly through RovA for the same reasons. Therefore it is likely that genes from the third, fourth and sixth cluster are influenced through RovA or RovM.

The investigated regulatory network consisting of the transcriptional regulators Crp, CsrA, YmoA, RovM and RovA, seems to influence, among others, acid resistance, anaerobic respiration, the type VI secretion system and amino acid degradation as can be judged on the basis of the transcriptome analyses. Interestingly, the majority of the altered transcripts encode membrane associated proteins or proteins, located in the periplasma.

3.3.4 Comparative metabolome analysis

3.3.4.1 Culture supernatant

In order to determine the metabolic status of the mutant strains at the time point of investigation, samples of the supernatant were taken also during stationary phase from cells grown in LB medium. The supernatant was investigated *via* GC-MS as described in chapter 2.11.3. From every mutant strain and the wild type strain YPIII 3 biological replicates were measured. The results were compared to the wild type and the results of the phenotyping microarrays, as well as to the transcriptome analysis. The summary of the

analyses is shown in table 3.22. The complete list of metabolites can be found in supplemental E.2.

Table 3.22: Summary of supernatant analysis of the different mutant strains

Supernatant of mutant and wild type strain	**Compounds**	**Identified metabolites**	**Mean relative standard error** (n=3, biological replicates)	**Significant changes to wild type** (two-paired t-test p-value < 0.05)
YP3 (*rovA*$^-$)	58	42	9.9 %	6
YP72 (r*ovM*$^-$)	55	38	7.7 %	7
YP53 (*csrA*$^-$)	74	58	14.2 %	27
YP50 (*ymoA*$^-$)	63	47	13.7 %	18
YP89 (*crp*$^-$)	72	53	8.7 %	39
YPIII	56	40	11.2 %	-
Medium	79	64	11.4 %[1]	-

[1] technical replicates

Looking at the significant changes between the supernatants of the mutants compared to the wild type (table 3.22), it is obvious that the absence of Crp had the biggest influence on the utilization of nutrients, while the absence of RovA showed the mildest influence. This was in accordance with the phenotyping microarray analyses (chapter 3.3.2).

The 18 most frequently altered compounds were compared in a heatmap (figure 3.45).

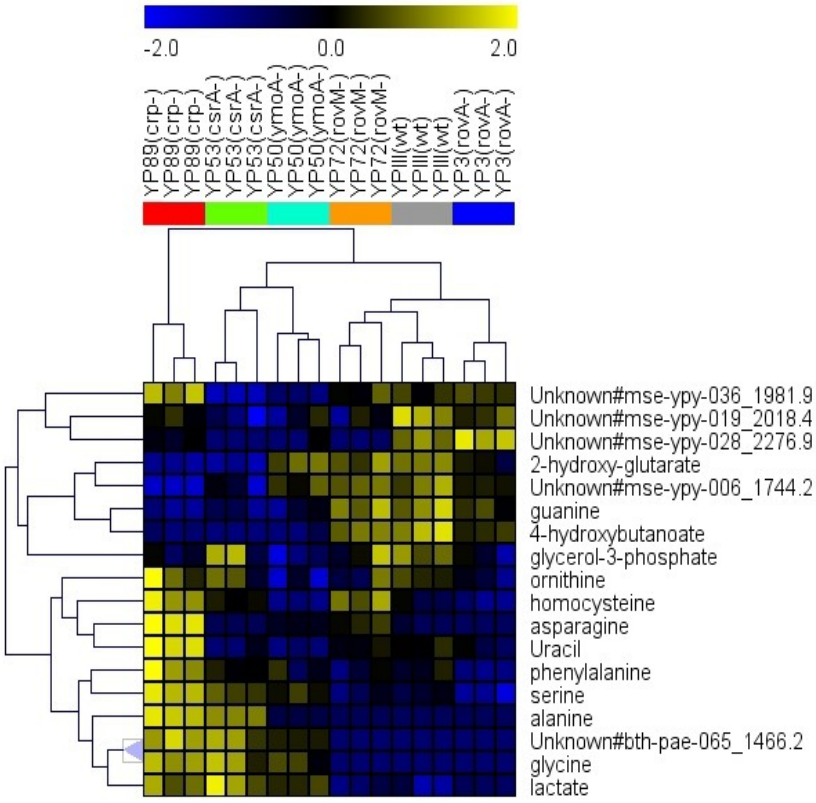

Figure 3.45: Heatmap with hierarchical clustering of the culture supernatant analysis of the five mutant strains and the wild type YPIII during stationary growth in LB medium at 25 °C. Sample names are indicated above. Each square represents the relative peak area of a compound. Data is z-score normalized over the rows. The clustering was performed with euclidean distance and average linkage.

The supernatant samples are separated into each mutant strain and the wild type by the hierarchical cluster, whereas the *rovA* and *rovM* mutants show the highest similarities to the wild type. From the supernatant it is obvious that the *csrA* and *crp* mutants and, to a lesser extent, the *ymoA* mutant were impaired in the nutritional uptake as most substances were still present in the medium. This might result in the observed slower growth and the reduced biomass yield of the *crp* and *csrA* mutants (chapter 3.3.1). Interestingly, 2-hydroxy-glutarate was secreted under all investigated conditions (e.g. different temperature, different media, chapter 3.1 & 3.2) but not in the *csrA* and the *crp* mutant. The absence of 2-hydroxyglutarate was not the result of reduced growth rates in the mutants ($\mu_{max\ crp}$=0.3 h^{-1}, $\mu_{max\ csrA}$=0.36 h^{-1}), since the YPIII wild type strain grew even slower in minimal medium at 37 °C (μ_{max}=0.146 h^{-1}) and regardlessly secreted 2-hydroxy-glutarate. Hence the difference must be due to the mutation.

3.3.4.2 Intracellular metabolome

The bacterial cells were grown in 6 biological replicates and harvested with technical duplicates for the intracellular metabolome analysis and measured as described previously (chapter 2.11.2 & 2.12.2). For every mutant strain the same number of wild type replicates were produced and were used for the determination of the significant changed metabolites in the mutant compared to the wild type (table 3.23). A complete list of all measured metabolites can be found in supplement E.3.

Table 3.23: Summary of metabolome analysis of the mutant strains with corresponding wild type strain YPIII samples

Mutant strain	**Compounds**	**Identified metabolites**	**Mean relative standard error** (n=6, biological replicates)	**Significant compounds** (p-value < 0.05)
YP3 (*rovA*$^-$)	94	72	15.5%	32
YPIII (wt)	93	71	17.2%	
YP72 (*rovM*$^-$)	98	71	14.7%	15
YPIII (wt)	98	71	15.3%	
YP53 (*csrA*$^-$)	92	63	12.8%	47
YPIII (wt)	94	63	14.4%	
YP50 (*ymoA*$^-$)	84	57	15.0%	29
YPIII (wt)	86	57	13.9%	
YP89 (*crp*$^-$)	96	62	12.2%	46
YPIII (wt)	97	63	14.6%	

The data was normalized to the median of the corresponding wild type YPIII reference samples (chapter 2.14.2) and analyzed with a hierarchical clustering of the samples (figure 3.46). The clustering showed a clear separation of the metabolome samples from each mutant strain based on the detected metabolites. This indicates an influence of all mutations on the metabolism of the bacterium *Y. pseudotuberculosis*.

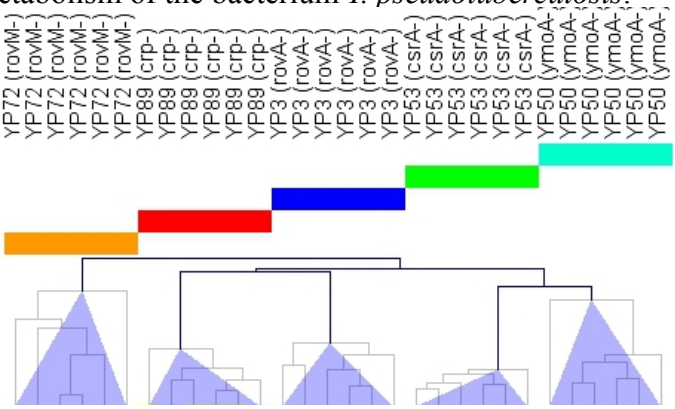

Figure 3.46: Hierarchical cluster of the metabolome samples generated on 70 compounds, that were detected in at least 50% of the samples. The hierarchical clustering is based on Pearson correlation and average clustering.

The 29 most frequently altered metabolites in response to the mutations were subjected to a hierarchical clustering in a heatmap in figure 3.47. The first cluster of the heatmap consists predominantly of components of fatty acid metabolism (hexadecenoate, octadecenoate) and its degradation (2-methylcitrate). The fatty acids hexadecenoate and octadecenoate were altered similarly to each other but the odd-numbered fatty acids heptadecanoate and pentadecanoate in the third cluster were altered differently. The main difference was located in the *csrA* mutant. The compound 2-methylcitrate is a degradation intermediate of odd-numbered fatty acid in the step from propionyl-CoA to succinyl-CoA, hence a correspondence to the odd-numbered fatty acid was expected. Since 2-methylcitrate differed from the odd-numbered fatty acids only in the *csrA*-mutant, a regulation of the degradation can be expected through the lack of CsrA.

Several metabolites from the glycolysis/gluconeogenesis were altered in a similar pattern in the second cluster (fructose-1,6-bisP, PEP, glycerate-3-P) as well as some amino acids (asparagine, glycine, glutamate, glutamine, arginine, ornithine). The most prominent changes were the increased concentrations in the *crp* mutant. Notably, most of these amino acids (asparagine, glycine, glutamate, glutamine) were all taken up from the LB medium by the wild type YPIII (chapter 3.1.3.3). Their concentration might therefore be correlated to the regulation of transporters. Since glutamate can be used as carbon source, the glycolysis/gluconeogenesis activity might be connected to its concentration. The amino acids arginine and ornithine were regulated differently to the other metabolites since they were the only ones less concentrated in the *rovA*, *rovM* and *csrA* mutant in the second cluster. Their degradation pathway was one of the most affected in the transcriptome (*astABDE, argD*, chapter 3.3.3, figure 3.44, cluster 4), indicating a special importance of arginine degradation to the virulence network.

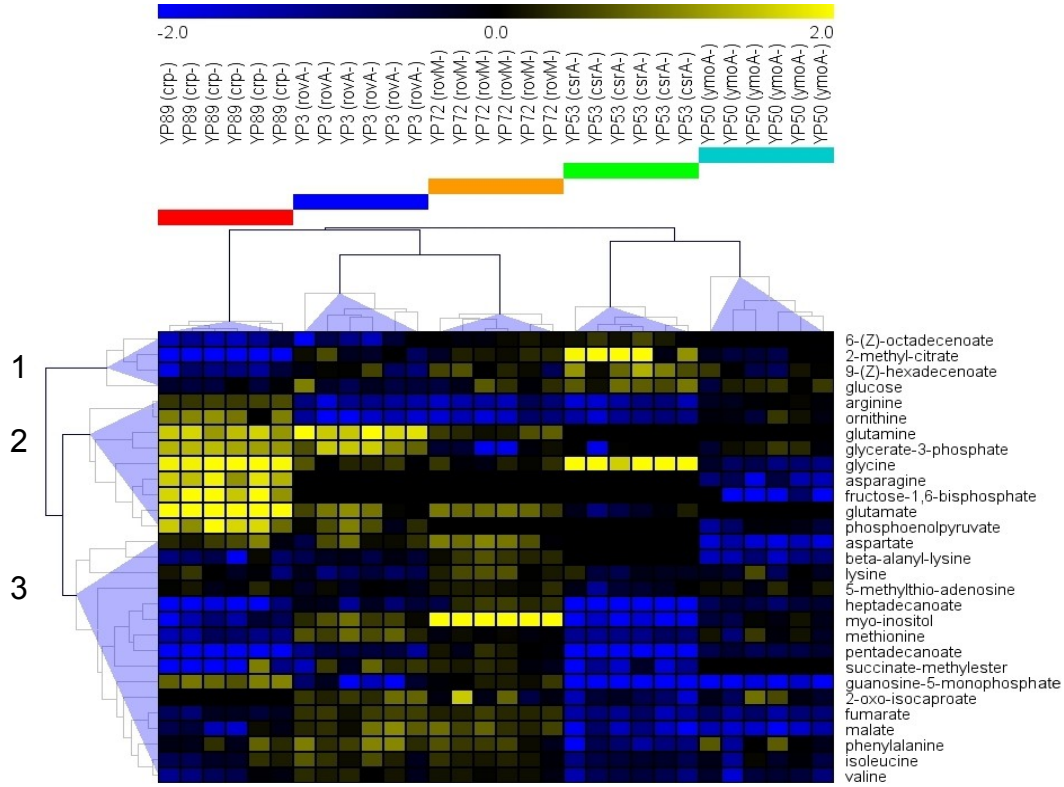

Figure 3.47: Heatmap with hierarchical clustering of the most frequently altered, identified metabolites in response to the mutations. Each square represents the $\log_2$ mutant/wild type ratio of the relative peak areas of a metabolite. Black squares indicate that no significant difference to the wild type was measured. The hierarchical clustering is based on Pearson correlation and average clustering.

In the third cluster the amino acids phenylalanine, isoleucine, valine and the leucine synthesis/degradation intermediate 2-oxo-isocaproate were altered similarly to the TCA cycle intermediates fumarate and malate. These amino acids were not taken up from the LB medium (chapter 3.1.3.3) but were synthesized, hence their concentration was probably linked to the TCA cycle activity. The genes of TCA cycle enzymes, malate dehydrogenase and fumarate reductase, were down-regulated in the transcriptome of the *csrA*, *crp* and *ymoA* mutant (supplement E.1), which was in accordance with the reduced concentration of fumarate and malate in these mutants.

Myo-inositol was altered similarly to the odd-numbered fatty acids heptadecanoate and pentadecanoate in the third cluster. Myo-inositol is the most common stereoisomer from inositol and forms phosphatidylinositol together with two fatty acids, an important component of phospholipid membranes, which might explain the similar regulation pattern to fatty acids. The enzyme phosphatidylinositol 3-kinase catalyzes the phosphorylation of phosphatidylinositol and is involved in the YadA promoted uptake of *Y. pseudotuberculosis* into mammalian cells (Eitel & Dersch 2002). Interestingly, myo-inositol and the transcript of YadA show inverse concentration patters in the mutants (myo-inositol concentration was

decreased in the *crp* and *csrA*-mutant, while it was increased in the *rovM* mutant. Contrary YadA was up-regulated in the *crp* and *csrA* mutant and down-regulated in the *rovM* mutant, chapter 3.3.3).

Interestingly, the regulation in the transcriptome of the pathway does not always show the same pattern as the metabolites (e.g. arginine pathway enzymes, arginine). The lack of coherence between metabolome and transcriptome does not necessarily represent the biological reality since transcriptomics is not able to detect post-transcriptionally regulated processes. Ansong and co-workers found several significant differences between mRNA and protein responses to temperature upshift in *Y. pseudotuberculosis*, including ribosomes, purine and pyrimidine metabolism, peptidoglycan metabolism and amino acetyl-tRNA biosynthesis (Ansong et al. 2012).

3.3.5 Comparison of temperature and ymoA *mutant*

A high correlation of 0.77 was observed earlier between the transcriptome of YP50 (*ymoA*$^-$) strain and the transcriptome measured at 37 °C (chapter 3.3.3). This was mostly due to transcripts associated with virulence factors (*yopBEDHKO*, *yscABDHMN*, *sycEN*, *lcrGHV*) that were regulated similarly (supplement E.1). But also the heat shock (*ippBA*, *dnaK*), cold shock (*cdpDE*) and stress responses (*uspA*, *rpoS*) were regulated alike. Also some genes encoding transporters (*gltL, manY, actP*) and metabolic enzymes involved in the riboflavin synthesis (*ribB*), the TCA cycle (*frdD*), amino acid degradation (*argD*) and fatty acid metabolism (*fabB*) were similarly regulated through mutation and temperature. The transcriptional regulator RovA was down-regulated under both conditions. This indicated that these effects were probably mediated through degradation of YmoA at 37 °C in the wild type YPIII (Jackson et al. 2004). Nevertheless, some ribosomal proteins were oppositely regulated on the transcript level (*rpsSMTP*, *rplKOT*, *rpmHKL*) between the *ymoA* mutant at 25 °C and YPIII grown at 37 °C. Further, some metabolic enzymes were differently regulated including the asparagine synthetase (*asnA*), the nitrate reductase (*napB*) and the glyceraldehyde-3-P dehydrogenase (*gapA*).

However, the supernatant and the metabolome shared very few similarities between the *ymoA* mutant and the analysis at 37 °C. Under both conditions lactate, putrescine and 2-oxopenatonate were secreted. One can assume that at 37 °C not only regulatory differences occurred, but also physiological differences like reduced dissolved oxygen in the medium.

3.3.6 The similar effects of the crp *and* csrA *mutation*

No alteration in *csrA* transcription was detected in the transcriptome of the *crp* mutant, but many direct targets of CsrA were decreased in the absence of Crp, like the gene *flhDC* (chapter 3.3.3), indicating a reduced amount of functional CsrA through increased expression of CrsB (Heroven et al. 2012). This is strongly supported by the high correlation of the transcriptomes of the *csrA* and the *crp* mutant of 0.7 after Pearson (chapter 3.3.3). To further investigate this, the $\log_2$ mutant/wildtype ratios of the transcriptome, metabolome and supernatant of the *csrA* and the *crp* mutant were plotted against each other (figure 3.48). The deficiency of CsrA or Crp had the same effect on many transcripts, intra- and extracellular metabolites. This concerned enzymes and metabolites from the TCA cycle (*mdh, frdABCD, aceAB,* fumarate, malate), amino acid transport and degradation (*metF, lysP, cysK, ddc, aroA, hisQJ, gltLKJI, oppABC, sstT*, methionine, valine, glycine), acetate metabolism (*acs, actP*) and type VI secretion system components. These similarities indicated a positive interaction between Crp and CsrA or many overlapping targets of these regulators.

Besides the strong positive correlation of many transcripts and metabolites, also an anticorrelation was observed, showing that certain traits were antagonistically regulated in the mutants. The transcripts, that were altered differently, included the TCA cycle enzymes (*sucABCD*, *sdhABCD*), that have been recently identified as directly controlled by Crp (Zhan et al. 2008) and potential targets of RovA such as the pH 6 antigen (*psaAEF*) and the phage shock protein (*pspG*). This supports the idea of an interaction between Crp and the RovM-RovA-Invasin cascade independent of the Csr-system. Although no regulation of *rovM* was observed in the transcriptome, a *lacZ* indicator fusion showed that RovM levels were strongly increased in a *Y. pseudotuberculosis crp* mutant and an interaction of Crp with the expression of *rovM* has been proposed (Heroven et al. 2012).

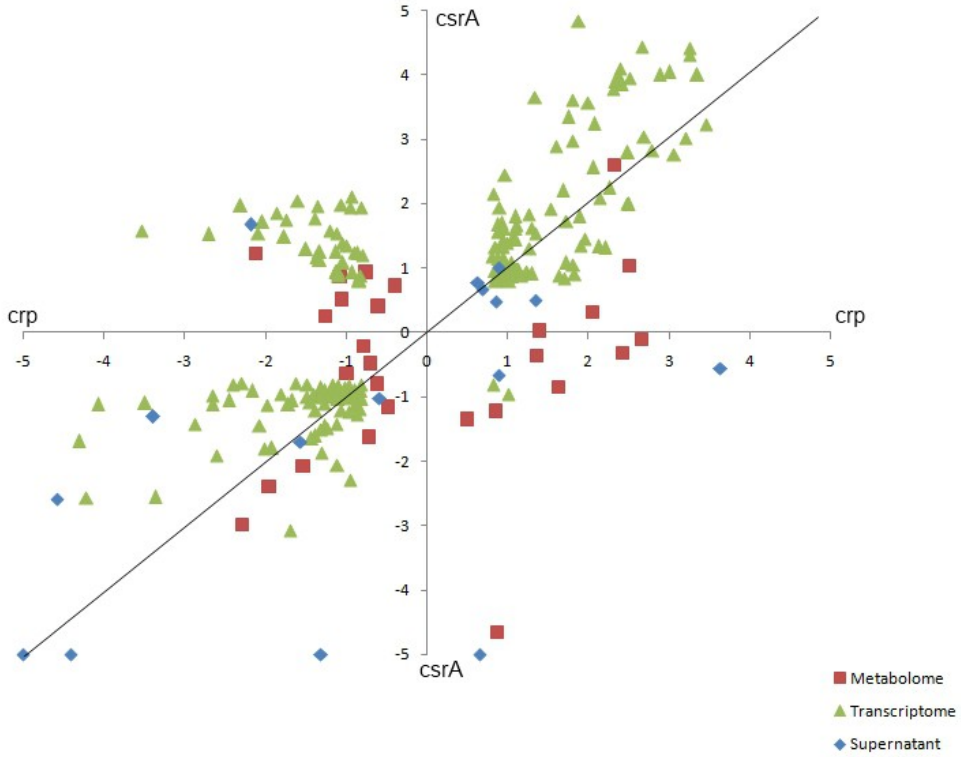

Figure 3.48: Plot of the $\log_2$ mutant/wild type ratios of the transcripts (green), the metabolites (red) and the compounds from the supernatant (blue) for the *crp* mutant (X-axis) and the *csrA* mutant (Y-axis). The figure is based on traits, that were altered and detected in both mutant strains and included 202 transcripts, 27 intracellular metabolites and 15 compounds from the supernatant.

This indicates that Crp can act as a master regulator in *Y. pseudotuberculosis* and impairs the regulatory effects of CsrA as response to carbon source availability, underlining the importance of appropriate regulation of virulence and metabolic traits in response to nutrient sensing in YPIII.

*3.3.7 Growth on nucleosides as sole carbon source in YPIII (wt) and YP3 (*rovA$^-$*)*

One of the most prominent influences of the mutations on the phenotype of *Y. pseudotuberculosis* was the increased usability of nucleosides as sole carbon source in the strains YP3 (*rovA*$^-$) and YP89 (*crp*$^-$). The phenotyping microarray analysis showed that the YP89 mutant could use uridine, adenosine and inosine and the YP3 strain could use uridine, inosine and thymidine as sole carbon sources (chapter 3.3.2). A direct comparison

of the transcriptome of the two mutant strains revealed that several transcripts involved in nucleoside metabolism were affected by the mutations (supplement E.1). Especially the NupC1 nucleoside (*nupC1*) transporter was up-regulated in both mutants and also the *deoB* transcript encoding a phosphopentomutase, which converts ribose-1-P into ribose-5-P during nucleoside degradation.

To investigate the meaning of these observations the mutant strain YP3 and the wild type strain were grown in minimal medium with one nucleoside (thymidine, inosine, adenosine, uridine) as sole carbon source at 25 °C in the adapted M63 minimal medium (chapter 2.7.2). The cells were grown overnight in LB medium and washed twice with fresh minimal medium before inoculation in nucleoside minimal medium. The resulting growth curves are presented in figure 3.49.

a. 40 mM Thymidine **b. 16 mM Adenosine**

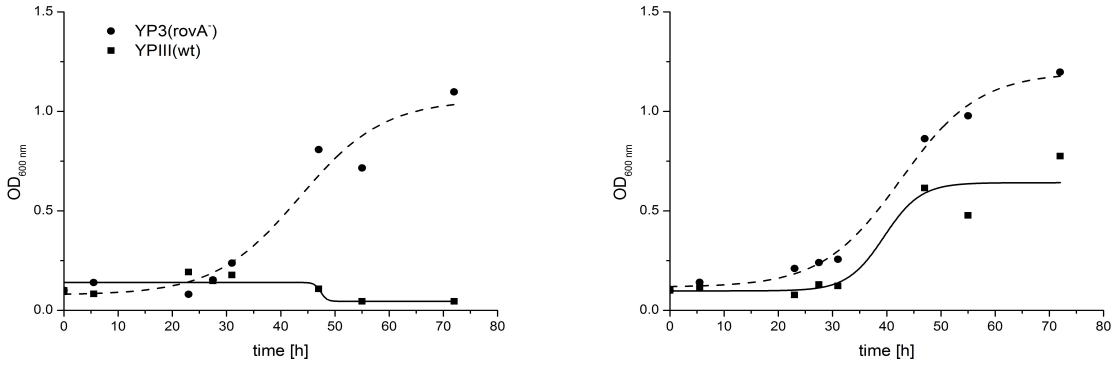

c. 40 mM Inosine **d. 40 mM Uridine**

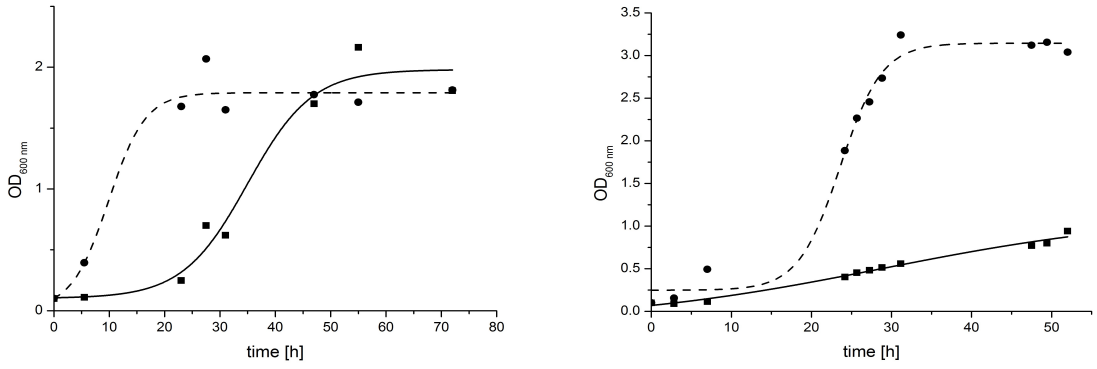

Figure 3.49: a.-d. Growth curves of YP3 (*rovA*⁻) (dashed line) and YPIII (wt) (continuous line) strain on nucleosides as single carbon source.

The growth curves show a better growth of the YP3 (*rovA*⁻) strain on all tested nucleosides. The difference was most pronounced on thymidine and uridine, where the wild type showed only very slow growth and reached low densities. Contrary to the phenotyping

microarray analysis from chapter 3.1.1, the wild type was able to grow on adenosine and inosine as sole carbon source, but grew slower or to lower cell density than the YP3(*rovA*$^-$) mutant strain.

For further insights supernatant samples were taken after 48 h of cultures of the YP3 (*rovA*$^-$) mutant grown on the four investigated nucleosides. The samples were taken in biological triplicates and handled as described previously (chapter 2.11.3). The supernatant samples were investigated regarding the nucleosides and their degradation products (figure 3.50).

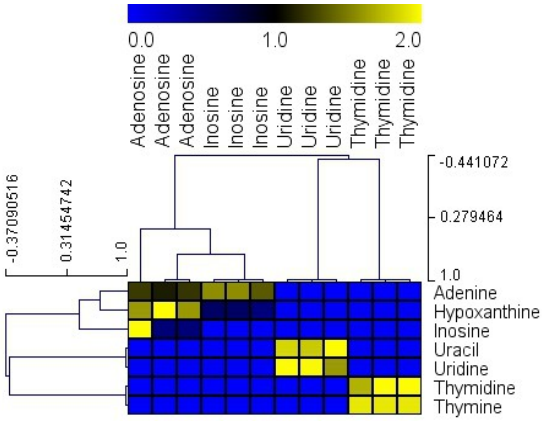

Figure 3.50: Heatmap of the nucleosides and their degradation products in the supernatant of the YP3 (*rovA*$^-$) mutant after cultivation with one nucleoside as carbon source. The used nucleoside is indicated above the sample. The data is RMS normalized over the rows and the clustering is based on Pearson correlation and average linkage.

The samples grown on uridine and thymidine contained uracil and thymine, respectively. This indicated a cleavage into a nucleobase and a ribose-1-phosphate, while the nucleobase is secreted and the ribosephosphate moiety is catabolized. This step is catalyzed by the uridine phosphorylase encoded by *udp* and the thymidine phosphorylase encoded by *deoA*, which were both up-regulated in the YP3 (*rovA*$^-$) mutant.

Adenosine was not detected in the supernatant, but considerable amounts of inosine, hypoxanthine and adenine were detected. This indicated that adenosine is cleaved into adenine and ribose-1-P but the majority is deaminated into inosine and then cleaved into hypoxanthine and ribose-1-P. Consequently, adenosine can probably also serve as sole nitrogen source as indicated by the phenotyping microarray analysis of the wild type YPIII (chapter 3.1.1).

The supernatant of the cultivation with inosine showed that no inosine remained in the supernatant but hypoxanthine and adenine, indicating that the inosine is partly converted into IMP and AMP. The cleavage of inosine and adenosine into hypoxanthine and adenine

is catalyzed by the purine nucleoside phosphorylase encoded by *deoD* which was also up-regulated in the transcriptome analysis of the YP3 (*rovA*$^-$) mutant. The conversion of adenosine into inosine is catalyzed by the adenosine deaminase, which was not altered in the transcriptome analysis of the mutant. The results of adenosine and inosine indicated that the metabolites are not fed completely into the PPP but are also used as nitrogen source (in the case of adenosine) and as precursor for IMP and AMP synthesis, where no regulation through RovA in the transcriptome was observed, which diminished the difference in the growth comapred to the wild type.

Thymidine and uridine showed the most prominent growth differences between the YP3 (*rovA*$^-$) mutant and the wild type, which was probably due to the direct and complete degradation into the energy generating pathways PPP and glycolysis. The up-regulated enzymes may be rate limiting in the wild type.

The results strongly indicate a repression of the degradation of all four investigated nucleosides to serve as carbon and energy source through RovA. Further, the results show that only the ribose-phosphate moiety serves as carbon source while the nucleobase is secreted and the majority is not utilized further.

The similar phenotype regarding nucleoside utilization detected in the *crp* mutant suggests that a regulation might occur through available carbon sources or a combination of carbon source and temperature, rather than temperature alone, since the wild type YPIII grown at 37 °C was not able to utilize nucleosides as carbon sources (chapter 3.2.1). This points towards a tight regulation of nucleoside utilization fitted to a specific environment and emphasizes the importance of these metabolic pathways.

Recent reports suggest a limitation of available nucleosides in the mammalian blood, leading to a crucial need for biosynthesis of nucleosides in pathogenic bacteria (Samant et al. 2008). A similar observation has been made in the intestine for *E. coli*, where colonization requires synthesis of purines and pyrimidines (Vogel-Scheel et al. 2010). The down-regulation of nucleoside degradation could therefore channel the nucleoside usage towards anabolism rather than catabolism during early stages of infection. Studies with infected mice showed that mutants lacking the nucleoside transporters $NupC_{1/2}$ caused slightly higher survival rates compared to the wild type. The mutant was also detected in significantly reduced numbers in the Peyer's patches, mesenteric lymph nodes and spleen of infected mice (A. K. Heroven, unpublished data), demonstrating a need for the uptake of nucleosides during later stages of infection.

*3.3.8 Acidic resistance in YPIII (wt), YP72 (*rovM$^-$*) and YP3 (*rovA$^-$*)*

Several transcripts altered in all 5 mutants indicated a relation to acid resistance (*hdeB*, *ureAC*, *mig5*) and an involvement of the virulence network. Overcoming the acidic stress in the stomach is crucial for colonization of the host-intestine. Many species have different acid resistance systems, which have been best investigated in *E. coli* (Gorden & Small 1993; Lin et al. 1995; Castanie-Cornet & Penfound 1999). The acid-resistance systems identified in *E. coli* have not been found in *Y. pseudotuberculosis*, but besides others the bacteria posses an aspartase-dependend acid resistance system based on AspA, an aspartase. This system protects against mild acidic conditions (pH 4.5) (Hu et al. 2010). Further, an involvement of urease in acidic survival has been suggested in *Yersinia* (Koning-Ward & Robins-Browne 1995; Hu et al. 2009, Hu et al. 2011). Urease catalyzes the hydrolysis of urea to ammonia and carbon dioxide, which could be used to raise the pH in a microenviroment to a tolerable level, which has also been observed for *Helicobacter pylori* (Athmann et al. 2000).

The *Y. pseudotuberculosis* YPIII strain is not able to grow at a pH below 4.0 (Hu et al. 2009). Since amino acid decarboxylases like GadA, CadB and AdiA play an important role in the amino acid dependent acid resistance of *E. coli* (Iyer et al. 2003, Richard & Foster 2004), it was assumed that the lysine/ornithine/arginine decarboxylase encoded by YPK_2860 and the arginine:agmantine antiporter (*adiC*) might account for a similar system in *Y. pseudotuberculosis*. The transcripts were up-regulated in the *csrA* and *rovM* mutants while they were down-regulated in the *rovA* mutant (chapter 3.3.3). In addition, two subunits encoding for urease (*ureA* and *C*) and an acid stress chaperone (*hdeB*) were antagonistically regulated in the *rovA* and *rovM* mutant strains (chapter 3.3.3).

In order to compare the acid resistance of the YP3 (*rovA*$^-$) and the YP72 (*rovM*$^-$) strain to the wild type, the strains were incubated in LB medium at 25 °C at pH 7 overnight and then transferred into LB medium at 25 °C where the pH was adjusted with phosphoric acid to 4.0. The bacteria were adjacently incubated for 72 h. The growth and the pH over time were measured and are displayed in figure 3.51.

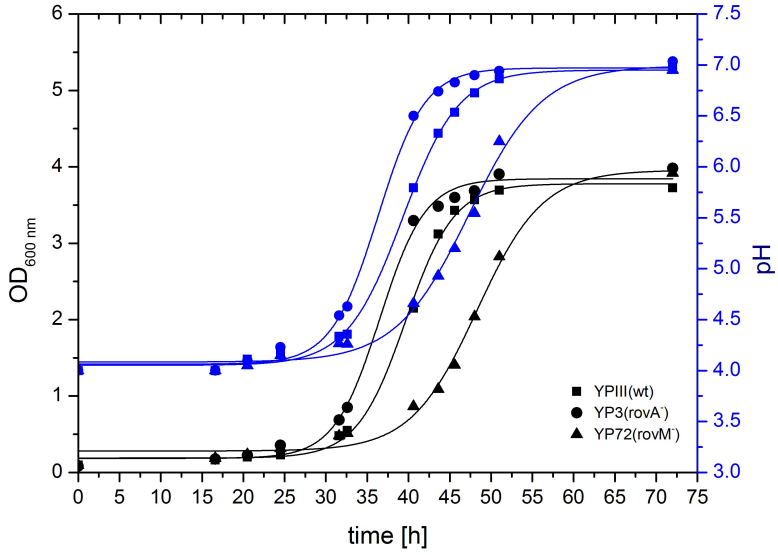

Figure 3.51: Growth of YPIII (wt), YP3 (*rovA*$^-$) and YP72 (*rovM*$^-$) in LB medium with an initial pH of 4. The pH is displayed on the second vertical axis in blue.

The 3 investigated strains showed very similar growth characteristics at pH 7 (chapter 3.3.1) but exhibited considerable differences at pH 4. The YP3 (*rovA*$^-$) strain showed a reduced lag phase compared to the wild type before growth started, while YP72 (*rovM*$^-$) had a longer lag phase. This indicated an improved adaptation to the acidic environment in the absence of RovA and a decreased adaption in the excess of RovA. Over the time of cultivation the pH was constantly elevated in relation to growth. It is probable that the pH elevation was due to secreted ammonia. Since overnight grown cells were used, they were in stationary phase when inoculated at pH 4 and most acid protection systems should have been active (Foster 2001).

Samples of the supernatant have been taken in biological duplicates during the cultivation after 0, 32, 33, 41, 44, 46, 48, 51, and 72 h of all three strains as described preciously (chapter 2.11.3). The uptake and secretion pattern of all three strains was similar, as shown in figure 3.52.

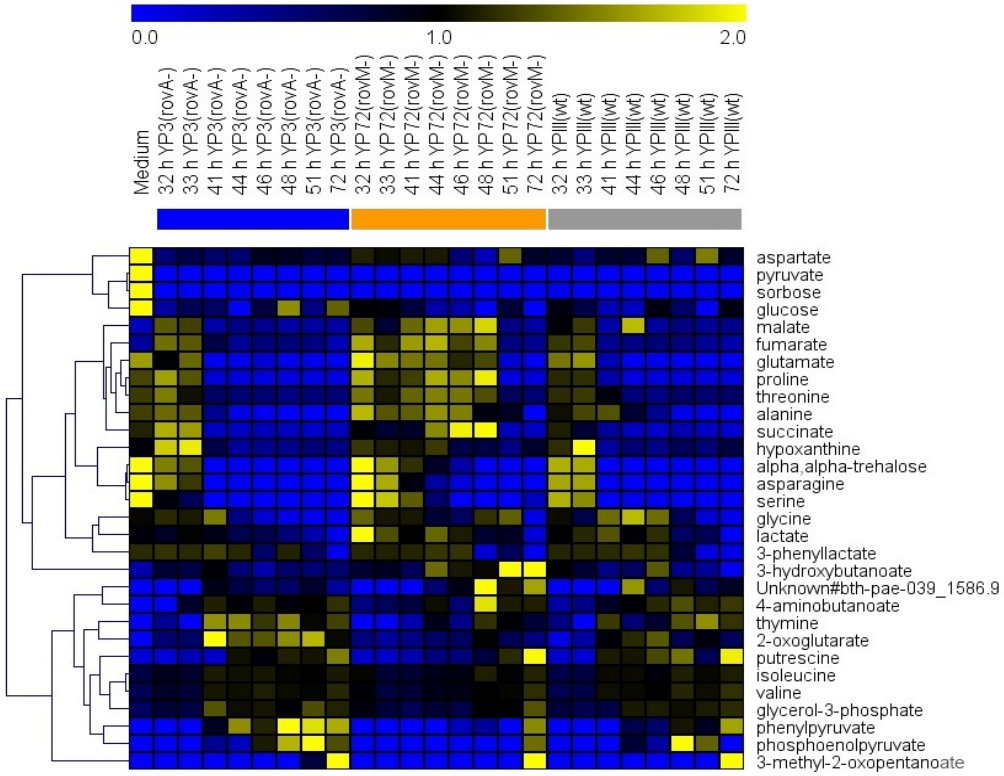

Figure 3.52: Hierarchical clustering of a heatmap of the mean of 30 selected metabolites from the supernatant of YP3 (*rovA*$^-$), YP72 (*rovM*$^-$) and YPIII (wt) under acidic stress. Hierarchical clustering is based on Pearson correlation and average linkage. Data is RMS normalized.

The analysis showed no significant differences in the supernatant except a time-shift between the three strains. The YP3 (*rovA*$^-$) mutant started faster to consume amino acids from the medium and secreted compounds into the supernatant earlier than the wild type. The YP72 (*rovM*$^-$) strain showed a decelerated uptake in comparison to the wild type.

When the metabolites from the supernatant are compared to the results of the wild type YPIII grown in LB medium at pH 7 in chapter 3.1.3.3, some notable differences could be regarded. In the supernatant of all three strains the secretion of 4-aminobutanoate (GABA) was observed. This phenomenon has not been measured before under any conditions and could be a reaction to the acidic environment. In *E. coli,* an amino acid dependent acid resistance system, known as AR2, consists of a glutamate:GABA antiporter GadC and a glutamate decarboxylase (GadA and B). It requires extracellular glutamate and secretes its decarboxylated product GABA to elevate the intracellular pH (Castanie-Cornet & Penfound 1999, Richard & Foster 2004). However, no corresponding system has been annotated in *Y. pseudotuberculosis* yet, but the finding of extracellularly increased GABA in response to acidic environment suggests its presence.

No secretion of agmantine could be measured for any strain. This could be due to levels lower than the detection limit or due to a different functionality other than proposed for arginine:agmantine antiporter AdiC.

The reason for the difference in the growth behavior under acidic stress between the strains can only be superficially explained by the analysis of the supernatant, since the supernatant indicated different speeds of metabolism in the strains. The supernatant allowed some conclusions about the general nature of acidic resistance in YPIII. Nevertheless, it seems that the three strains differ mainly in the speed of adaptation to the acidic environment while the mechanism remains unaltered through the mutation. This shows that the factor RovA is involved in the speed of regulation of acid resistance mechanisms in *Y. pseudotuberculosis* but other factors might also be important.

3.3.9 Integrative consideration of the impact of the mutations on the metabolism

*3.3.9.1 YP3 (*rovA$^-$*) & YP72 (*rovM$^-$*)*

The *rovA* mutant and the *rovM* mutant represent two opposed situations: In the mutant YP3 (*rovA*$^-$) the regulator RovA is nearly absent and in the mutant YP72 (*rovM*$^-$) RovA is over-expressed due to the lack of its repressor RovM. To determine the effects of RovA on the metabolism, the results of these two mutants were regarded in comparison.

Both mutant strains showed rather moderate alterations compared to the wild type: The growth was not significantly changed in both strains. In the transcriptome 44 genes were altered in the *rovA* mutant, 28 transcripts were up-regulated, while 16 were down-regulated. In the transcriptome of the *rovM* mutant 112 transcripts were altered, of which 50 were up-regulated, while 62 were down-regulated. Interestingly, these were more alterations than in the *rovA* mutant. The proposed function of RovM is the repression of *rovA* expression in cooperation with the nucleoid-associated protein H-NS (Heroven & Dersch 2006, chapter 1.5.2) but the transcriptome analysis suggested other functions too. The transcriptome analysis showed 68 regulated genes in the YP72 (*rovM*$^-$) strain that were not altered in the YP3 (*rovA*$^-$) strain. This could be caused by the elevated RovA concentrations but could also be influenced directly through RovM.

The correlation of the transcriptome of the *rovA* and the *rovM* mutant showed that 21 transcripts were altered in both mutants with a Pearson correlation of -0.8 (chapter 3.3.3), which is in accordance with the expected opposed situation described earlier.

Transport & Supernatant

As discussed earlier, the deletion of *rovA* led to the increased usability of nucleosides as carbon source as shown by the PM analysis and in minimal medium (chapter 3.3.2 and 3.3.7). This is in accordance with the results of the transcriptome, where the transcripts *nupC(1)* and *nupC(2)*, which code for nucleoside transporters, were significantly up-regulated. Two transporters were regulated oppositely in the mutants. The genes for the alanine permease (*cycA*) and the glutamine ABC transporter *(glnH*) were down-regulated in the *rovM* mutant and up-regulated in the *rovA* mutant, which was in accordance with transcriptome analysis in *Y. enterocolitica* (Cathelyn et al. 2007). Further, the genes coding for the amino acid transporter for histidine and polar amino acids *(hisJ*, *hisQ*) were also down-regulated in the *rovM* mutant, but the arginine:agmantine antiporter *(adiC*) was up-regulated, as discussed before in the context of the acid resistance (chapter 3.3.8). The *rovM* mutant did not utilize alanine as sole carbon source in the phenotypting microarray analysis (chapter 3.3.2).

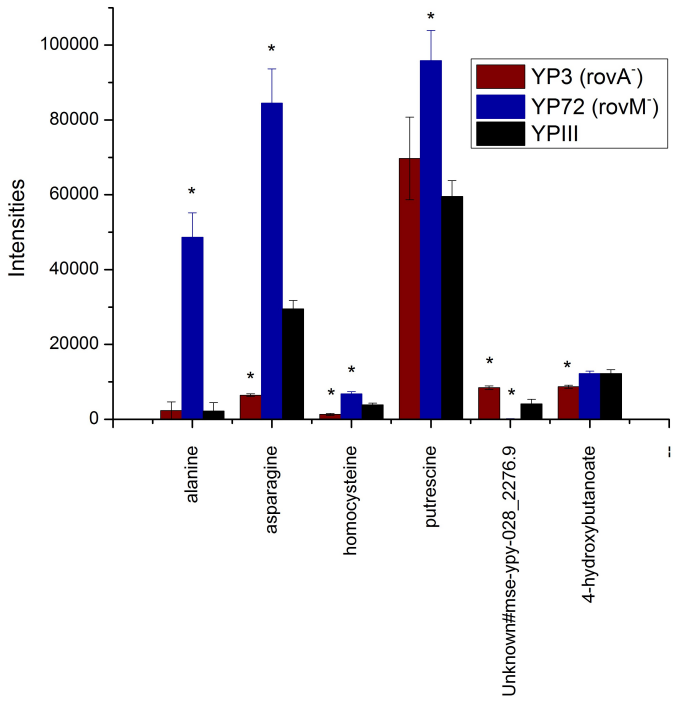

Figure 3.53: Compounds that were altered in the supernatant between the wild type strain YPIII (wt), the mutant strains YP3 (*rovA*$^-$) and YP72 (*rovM*$^-$) in stationary phase after 15 h of growth in LB medium. Significant differences to the wild type ($p > 0.05$, two-paired t-test) are indicated with an asterisk.

In the supernatant 6 and 7 metabolites were significantly changed in the *rovA* and the *rovM* mutant (chapter 3.3.4.1), whereas most changes occurred in both mutants (figure 3.53). The *rovM* mutant showed reduced ability to consume alanine, asparagine and homocysteine from the LB medium, which is corresponding to the phenotyping microarray analysis concerning alanine. Further, the mutant secreted more putrescine. In contrast, the *rovA* mutant showed increased consumption of asparagine and homocysteine and secreted less 4-hydroxybutanoate.

Central Carbon & Energy metabolism

On the transcriptome level, 20 altered genes were involved in metabolism in the *rovA* mutant, of which 15 were up-regulated and only 5 were down-regulated. In the *rovM* mutant only 18 regulated genes were involved in metabolism, from which 7 were up-regulated and 11 were down-regulated. This might explain the lower numbers of changed metabolites in the *rovM* mutant, compared to the higher number of overall changed transcripts: In the metabolome 32 and 15 metabolites were altered in the *rovA* and the *rovM* mutant, respectively (figure 3.54). The scatterplots of the metabolites of the mutants compared to the wild type showed tight correlations, indicating few changes on the metabolite level (supplemental E.4). The only metabolite detected exclusively in the *rovA* mutant and not in the wild type was 2-aminoadipate. In the *rovM* mutant the same metabolites were detected as in the wild type.

The transcriptome showed no changes in the central carbon pathways of both mutants but the metabolome showed an increase of the TCA cycle intermediates fumarate and malate (figure 3.54). In the strain YP3 (*rovA*$^-$) also the levels of the glycolytic intermediates glycerate-3-P, PEP and glucose-6-P were enhanced (figure 3.54.b), whereas glycerate-3-P was decreased in the *rovM* mutant (figure 3.54.a).

Several genes coding for subunits of a predicted periplasmatic nitrate reductase were down-regulated in the *rovM* mutant (*napB,D,F*). In *Y. enterocolitica* a nitrate reductase was up-regulated in a *rovA* mutant (Cathelyn et al. 2007), which indicates a repression through RovA rather than interaction with RovM. Further, one transcript of the oxidative phosphorylation (*cydB*) was up-regulated, indicating together with the down-regulated nitrate reductase an increased aerobic metabolism in the strain YP72 (*rovM*$^-$).

a.

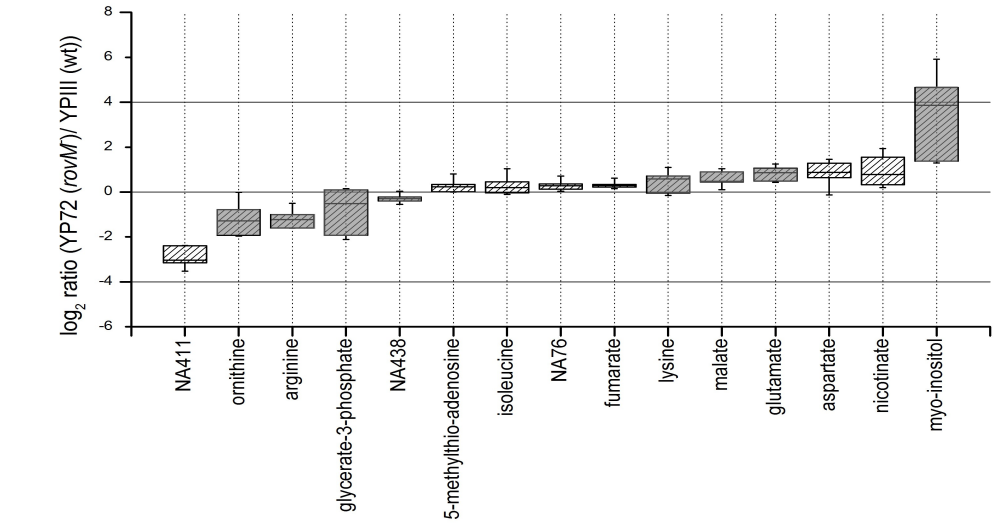

b.

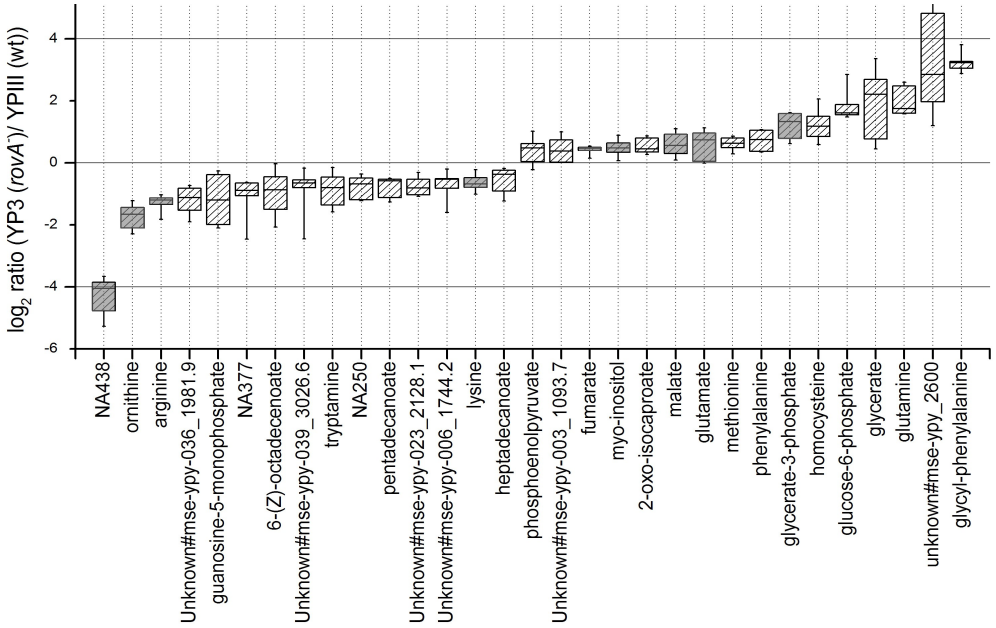

Figure 3.54: Boxplot of the $\log_2$ ratio of the relative metabolite intensities of the mutant strains (a) YP72 (*rovM*$^-$) and (b) YP3 (*rovA*$^-$) compared to YPIII (wt). Only significantly altered metabolites are shown (p-value < 0.05, two-paired t-test). Metabolites altered in both mutants are indicated with filled gray areas.

Amino acid metabolism

The amino acid metabolism was probably the part of the metabolism mostly affected by the mutations. On the transcriptome level the genes encoding enzymes involved in the degradation of arginine were up-regulated (*astA,B,D,E* and *argD*) and the lysine/ornithine/arginine decarboxylase (YPK_2860) was down-regulated in the *rovA*

mutant and vice versa in the *rovM* mutant. These findings might correspond to the decreased pools of arginine and ornithine in the metabolome of both mutants. Since the arginine decarboxylase catalyzes the first step in putrescine synthesis, these changes could be involved in the increased putrescine levels in the culture supernatant of the *rovM* mutant. Additionally, transcripts encoding urease were regulated oppositely in both mutants (*ureA,B,C* up in YP72*, ureA,C* down in YP3). Urease is suspected to be involved in acid resistance (chapter 3.3.8) but also in nitrogen metabolism. An influence on the nitrogen metabolism of the mutations is further strengthened through enhanced levels of glutamate in both mutants as well as through more glutamine in the *rovA* mutant and more aspartate in the *rovM* mutant. In both strains also the gene of the gamma-glutamyltranpeptidase (*ggt*) was regulated (up in the *rovM* mutant, down in the *rovA* mutant). The enzyme encodes the degradation of glutathione and is important for *Campylobacter jejuni* to colonize the mouse intestine (Hofreuter et al. 2006; Hofreuter et al. 2008).

Some amino acids related intermediates were increased in the *rovA* mutant (phenylalanine, glycyl-phenylalanine, 2-oxoisocaproate- a precursor metabolite of leucine synthesis, 2-aminoadipate -a lysine precursor). Also the gene *ansB* encoding the asparaginase was up-regulated, which correlates with the increased uptake of asparagine from the medium by the *rovA* mutant. This fits to observations in *C. jejuni*, which exhibits an heightened requirement for asparagine and asparaginase in later phases of infection in the liver, where in YPIII *rovA* is repressed (Hofreuter et al. 2008).

The gene *metE* coding for an enzyme converting L-homocysteine into methionine was the only transcript that was down-regulated in both mutants. The corresponding metabolites methionine and homocysteine were increased in the *rovA* mutant but not altered in the *rovM* mutant.

Purine and Pyrimidine metabolism

The purine and pyrimidine metabolism was only affected in the *rovA* mutant as already noticed on the phenotyping microarray analysis, the up-regulated nucleoside transporters and the ability to grow on nucleosides as carbon sources (chapter 3.3.7). Several genes encoding enzymes involved in degradation of purines and pyrimidines were up-regulated the *deoCABD* operon (Lomax & Greenberg 1968) as well as *cdd, udp* and *cpdB* (O'Donovan & Neuhard 1970). No effect was observable in the supernatant of the YP3 (*rovA*$^{-}$) strain. Small amounts of nucleosides could be detected in the LB medium

(chapter 3.1.3.3) but they were consumed early during cultivation by the wild type, probably to serve as precursor or nitrogen source as indicated by the phenotyping microarray analysis (chapter 3.1.1). In the metabolism also no effect was observable. Only GMP was reduced in the *rovA* mutant, which might be a result of the increased degradation of nucleosides.

Lipid metabolism

Several fatty acids such as octadecenoate, pentadecanoate and heptadecanoate were decreased in the metabolome of the *rovA* mutant, although there were no corresponding changes in the fatty acid metabolism in the transcriptome. The *rovM* mutant was not affected.

Virulence & Stress

As previously noted (chapter 3.3.3), the gene of RovA (*rovA*) was regulated contradictory in the mutants (up in the *rovM* mutant, down in the *rovA* mutant). The *rovM* gene was only down-regulated in the *rovM* mutant. The RovA controlled genes *psaAEF* encoding the pH 6 antigen and *pspG* encoding the phage shock protein (Cathelyn et al. 2006; Cathelyn et al. 2007) were regulated in the same way as *rovA*. Additionally, the transcript *hdeB* encoding the acid resistance protein follows the same pattern and indicates a regulation through RovA, as discussed previously (chapter 3.3.8).

Several transcripts from the type VI secretion system were influenced through the mutations, but of these only the gene *impC* was regulated in both strains. Opposed to the general pattern, it was down-regulated in the *rovM* mutant and up-regulated in the *rovA* mutant, which indicates that RovA can also act as a repressor of virulence genes.

Considering all results, the deletion of *rovM* had a mild effect on the metabolism of *Y. pseudotuberculosis*. The conditions tested might not have been sufficient to induce expression of RovM and therefore the deletion led only to few significant differences compared to the wild type. However, some effects were regulated oppositely to the *rovA* mutant and can be regarded as RovA-dependent. This included the amino acid uptake (*cycA*, *glnH*, *ggt*), arginine degradation (*astDABE*, *argD*, *adiA*), type VI secretion (*impC*), pH 6 antigen (*psaAEF*) and acid resistance (*ureACF*, *hdeB*). Despite the differently regulated transcripts, several metabolites showed the same changes in both mutants (arginine, ornithine, fumarate, malate, glutamate). This could be due to unnoticed post-

transcriptional regulation or due to similar results of different effects (e.g. up-regulation of the different arginine degradation pathways results in lower arginine levels in all cases). Further, it becomes clear that RovA may also act as repressor of so far undetected targets (type VI secretion system, nucleoside degradation, AST -arginine degradation pathway), which emphasizes the importance of these targets for later stages of infection.

*3.3.9.2 YP89 (*crp$^-$*)*

The YP89 (*crp*$^-$) mutant strain exhibited the most differential phenotype in contrast to the wild type of all investigated mutants. The growth rate was strongly diminished in LB and the biomass yield was reduced (chapter 3.3.1). 540 genes were altered in the transcriptome, thereof 248 genes were down-regulated, while 292 were up-regulated.

Transport & Supernatant

54 significantly changed genes encoded for transporters, of which 42 were down-regulated and 12 were up-regulated. This observation fits to the decreased uptake of compounds from the medium (chapter 3.3.4.1), where 38 metabolites were significantly changed (figure 3.55). Most of these were due to reduced uptake. This is in accordance with the reduced ability of the mutant to utilize carbon sources in the phenotyping microarray analysis, which showed that the *crp* mutant used 33 carbon sources less and 3 carbon sources more in comparison to the wild type (table 3.24).

Table 3.24: Result of the phenotyping microarray analysis of the carbon source assays PM1 & PM2 for YP89 (*crp*$^-$) compared to YPIII (wt) as reference

Utilization ability gained	Difference to wild type[4]	Well #, Plate #
Uridine	13052	D12, PM1
Adenosine	15092.5	E12, PM1
Inosine	17807	F12, PM1
Utilization ability lost	**Difference to wild type[1]**	**Well #, Plate #**
L-Arabinose	-32503.5	A2, PM1
D-Galactose	-28204	A6, PM1
D-Alanine	-13158	A9, PM1
D-Gluconic Acid	-27289	B6, PM1
D-Xylose	-22146	B8, PM1
D-Mannitol	-31609	B11, PM1
L-Glutamic Acid	-19994	B12, PM1
D-Glucose-6-Phosphate	-36823.5	C1, PM1
L-Rhamnose	-22180	C6, PM1
D-Fructose	-16419.5	C7, PM1
Acetic Acid	-11180	C8, PM1
Maltose	-30786	C10, PM1
D-Melibiose	-31467	C11, PM1
D-Fructose-6-Phosphate	-20698	E4, PM1
b-Methyl-D-Glucoside	-30375	E8, PM1
Adonitol	-33069	E9, PM1
Maltotriose	-33582	E10, PM1
L-Serine	-27061.5	G3, PM1
N-Acetyl-b-D-Mannosamine	-17574,5	G8, PM1
Methyl Pyruvate	-19075	G10, PM1
L-Lyxose	-16937.5	H6, PM1
Pyruvic Acid	-22188	H8, PM1
Pectin	-21745.5	A12, PM2
N-Acetyl-D-Galactosamine	-35902	B1; PM2
N-Acetyl-Neuraminic Acid	-24084	B2; PM2
D-Arabitol	-31547.5	B6; PM2
L-Arabitol	-26849	B7, PM2
Arbutin	-13960.5	B8, PM2
D-Glucosamine	-17578.5	E5, PM2
Melibionic Acid	-33160.5	F3, PM2

4 Diffrences calculated by comparison of the area under the curve between mutant and wild type, with two replicates for each plate

The majority of provided carbon sources on the PM1 and PM2 arrays could not be utilized by the mutant. The strain lost the ability to utilize several amino acids, pentoses, sugar phosphates, and carboxylic acids (table 3.24). Congruently, several genes encoding sugar transporters were down-regulated such as for arabinose, fructose, mannose, galactoside (*araF, fruAB, manXY, mglABC)*. Arabinose, fructose and N-acetyl-galatosamine could not be used as sole carbon source by the mutant in the phenotyping microarray analysis. Mannose was still used as sole carbon source, indicating uptake through an alternative transporter e.g. glucose transporter. Also, the genes for the cellobiose PTS transporter (*celA*), the fatty acid transporter (*fadL*), the ribose transporter and kinase (*rbsA, rbsB, rbsD, rbsK*) were down-regulated. Several substances were not taken up by the mutant from the medium (allo-threonine, homoserine, erythriol, histidine, alanine, citrate, histidine and alanine) that were consumed by the wild type strain (figure 3.55).

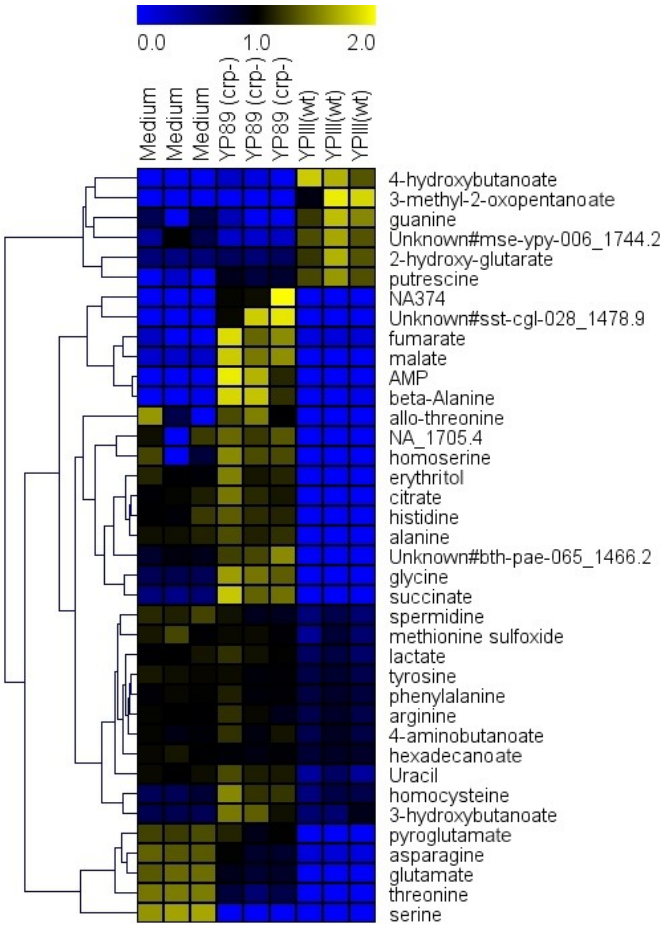

Figure 3.55: Heatmap with hierarchical clustering of the significantly altered compounds in the LB supernatant of YP89 (*crp*$^-$) compared to the wild type YPIII. Additionally, 3 pure medium samples are shown. Data is RMS normalized. Average linkage and Euclidean distance were applied for the hierarchical clustering.

Some substances were taken up from the medium by the mutant but not to the same extent as by the wild type (asparagine, glutamate, threonine, serine, spermidine, lactate, tyrosine, phenylalanine, arginine, 4-aminobutanoate), which is in accordance with the down-regulated amino acid transporters in the transcriptome such as those for glutamate/aspartate, histidine, serine/threonine and peptides (*gltJKL, hisJQ, sstT, sdaC, oppABCD).*

Despite the multitude of changes, the mutant still consumed several substances like the wild type from the LB medium (glycerol, aspartate, proline, glucose, fructose, trehalose, glycerate, inosine, uridine, guanosine, xanthine), which was in agreement with the results of the phenotyping microarray analysis. The other utilizable carbon sources in the phenotyping microarray analysis were alpha-D-glucose, D-trehalose, N-acetyl-D-glucosamine, 2'-deoxy adenosine, adenosine, inosine and uridine. The increased utilization of nucleosides, as shown in the phenotyping microarray analysis, has also been observed in the YP3 (*rovA*$^-$) mutant (chapter 3.3.9.1). Further, the nucleoside transporter (*nupC1*) was up-regulated in the *crp* mutant on the transcriptome level. This phenomenon has been further investigated with the YP3 (*rovA*$^-$) strain and it was shown that the *rovA* mutant gained the ability to grow on nucleosides as sole carbon source (chapter 3.3.7). Similar experiments were performed with the *crp* mutant, which indicated the same abilities but the results were less significant due to general decreased growth of the *crp* mutant (data not shown).

The supernatant shows that the mutant strain secreted certain substances in higher concentrations than the wild type (fumarate, malate, AMP, beta-alanine, glycine, succinate, 3-hydroxybutanoate, uracil, homocysteine), while some secretion products of the wild type were less concentrated in the supernatant of the mutant (4-hydroxybutanoate, 3-methyl-2-oxopentanoate, guanine, 2-hydroxyglutarate, putrescine).

Central Carbon & Energy metabolism

46 intracellular metabolites were altered significantly in the metabolome of the *crp* mutant compared to the wild type (figure 3.56). The scatterplot showed a low degree of correlation between the metabolic profiles of the mutant and the wild type strain (supplemental E.4). 4 substances were not detected in the metabolome of the *crp* strain that were present in the wild type, while 3 substances were only detected in the metabolome of the mutant (table 3.25).

Table 3.25: Metabolites detected exclusively in the mutant YP89 (*crp*$^-$) or in the wild type YPIII

YP89 (*crp*$^-$)	YPIII(wt)
Not detected	2-methyl-citrate
Not detected	pentadecanoate
Not detected	Unknown#mse-ypy-019_2018.4
Not detected	NA229001428
ribose	Not detected
alanyl-alanine	Not detected
NA163015_(classified_unknown)_1642.75	Not detected

The most prominent changes in the metabolome of the *crp* mutant were the lower or even lacking concentrations of fatty acids (pentadecanoate, heptadecanoate, octadecenoate, hexadecenoate) and their degradation product (2-methyl-citrate) in comparison to the wild type. Several metabolites involved in the synthesis of membrane components were also reduced (myo-inositol, beta-alanine-lysine).

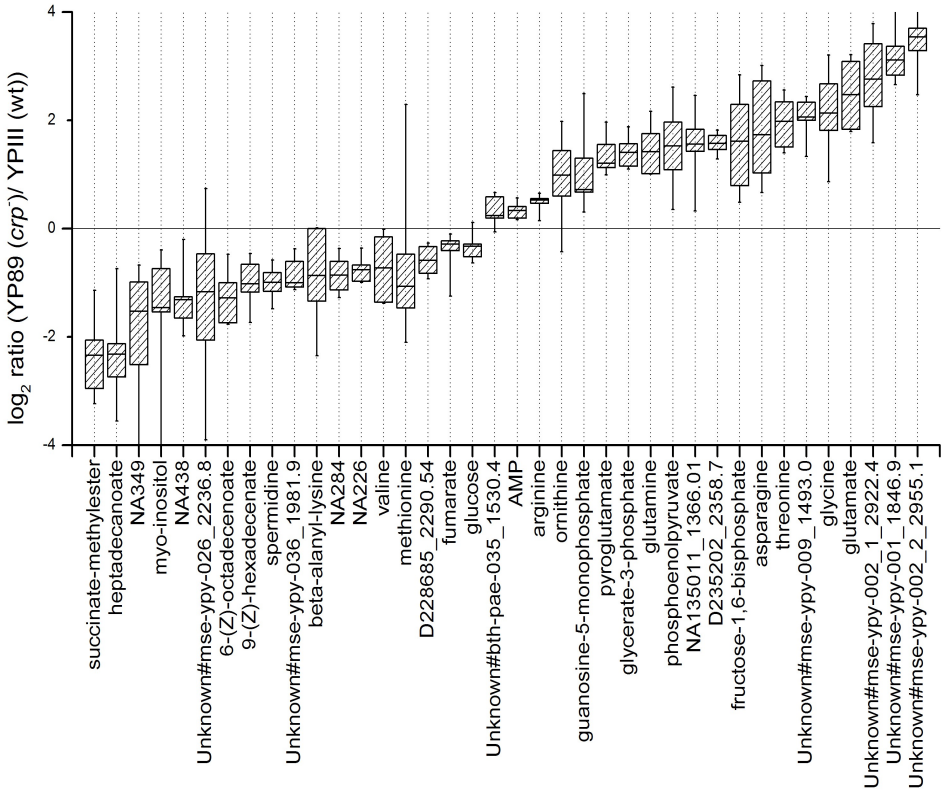

Figure 3.56: Boxplot of the $\log_2$ ratio of the relative metabolite intensitiesYP89(*crp*$^-$)/YPIII (wt). Only significant altered metabolites are shown (p-value<0.05, two-paired t-test).

115 significantly changed genes of the *crp* mutant were involved in metabolism as revealed by the transcriptome analysis, whereof 68 were down-regulated and 47 were up-regulated,

indicating a strong influence of Crp on the metabolism of *Y. pseudotuberculosis*. Some regulated genes are shown in their metabolic context in combination with intra- and extracellular metabolome data of the *crp* mutant compared to the wild type in figure 3.57. The first step of gluconeogensis (*pckA*), the conversion of oxaloacetate and ATP to PEP and ADP, was up-regulated. Also, *eno,* was up-regulated, encoding enolase, which catalyzes the reversible conversion of 2-phosphoglycerate to PEP. The transcript *pykF* was up-regulated, encoding pyruvate kinase. Pyruvate kinase is strongly activated by fructose-1,6-bisP, which was increased in the metabolome. The enzyme catalyzes the reversible conversion of pyruvate and ATP to PEP and ADP. One enzyme from the PPP was down-regulated in the transcriptome of the mutant, the ribose-5-phosphate isomerase (*rpiA*), which catalyzes the reversible conversion of ribose-5-P in ribulose-5-P.

Several metabolites of the glycolysis/gluconeogenesis were increased (fructose-1,6-bisphosphate, PEP, glycerate-3P), while glucose was decreased in the metabolome of the mutant. This points towards increased glycolysis activity rather than gluconeogenesis. The genes encoding TCA cycle enzymes and the glyoxylate bypass were partly down-regulated (*aceAB*). While the first part of the TCA cycle from oxaloacetate to 2-oxoglutarate remained unaltered, the enzymes 2-oxoglutarate dehydrogenase, succinyl-CoA synthetase, succinate dehydrogenase, fumarate reductase, fumarase and malate dehydrogenase (*sucA, sucCD, sdhABC, frdABCD, fumA, mdh,*) were down-regulated. Also fumarate was decreased, while 2-oxoglutarate and glutamate were increased (figure 3.57).

Some genes encoding for different cytochrome oxidases (*cydA, cyoAB*) were down-regulated, which might result in the reduced generation of the proton motive force. Together with the reduced ATP synthase (*atpEFI*), a reduced energy generation through respiration can be suggested and the enhanced level of AMP in the metabolome of the *crp* mutant and the secretion of AMP into the medium could be a result of the reduced ATP generation leading to diminished growth.

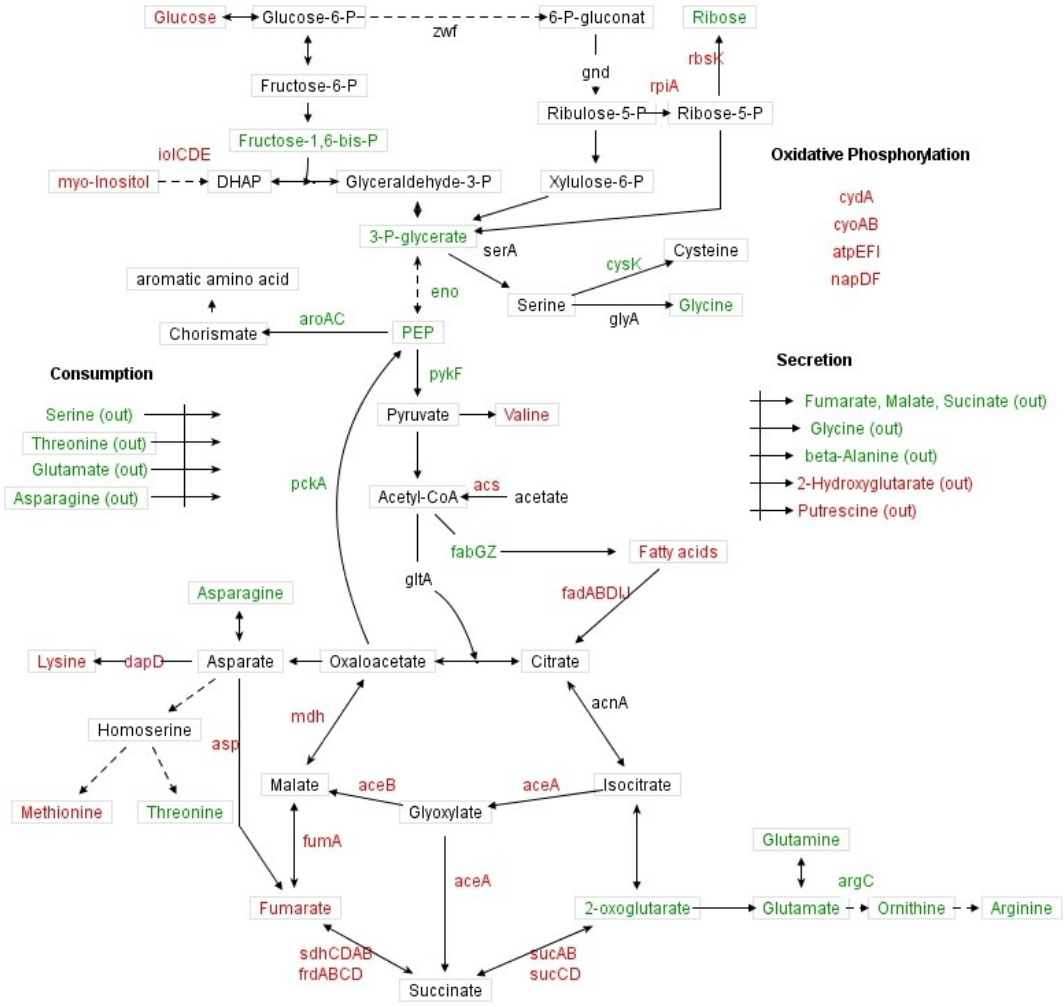

Figure 3.57 Central metabolism of YP89 (*crp*⁻) compared to YPIII. Significantly increased transcripts and higher concentrated metabolites are marked green, while decreased traits are red.

Other fermentative processes such as the fermentative lactate dehydrogenase (*ldhA*) and the formate dehydrogenase (*fdoG*) were both down-regulated. The down-regulation could be involved in the reduced uptake of lactate from the medium. The periplasmatic nitrate reductase (*napDF*) and the acetyl-CoA synthetase (*acs)* were also down-regulated.

An enzyme of the ubiquinone biosynthesis (*ubiA*) was up-regulated, while the menaquinone biosynthesis was down-regulated (*menD*), which rather supports the activation of aerobic respiration and was also observed in the transcriptome of the *csrA* mutant (chapter 3.3.6). Several genes involved in sugar conversion were up-regulated such as the glycogen synthase and the glycogen phosphorylase (*glgAP*), that are involved in glycogen synthesis.

Amino acid metabolism

The majority of amino acid biosynthesis and degradation pathways was down-regulated in the absence of Crp (figure 3.57), although certain amino acids were higher concentrated in the mutant (glutamate, glycine, threonine, asparagine, glutamine) than in the wild type. Exceptions were the arginine biosynthesis (*argC*), cysteine biosynthesis (*cysK*), aromatic amino acid biosynthesis (*aroAC*) and aromatic amino acid degradation (*ddc*), which were all up-regulated. Congruently, also arginine and ornithine levels were increased in the metabolome of the mutant, while no changes in the aromatic compounds or cysteine were detected.

The D-amino acid dehydrogenase (*dadA*) was down-regulated, which catalyzes the second step in alanine degradation. The enzyme has broad substrate specificity and can degrade more D-amino acids. In *E. coli dadA* mutants could not longer use alanine as sole carbon source (Beelen et al. 1973). Although alanine was not altered in the metabolome, it was not consumed from the medium and could not serve as sole carbon source in the PM analysis.

The aspartate ammonia-lyase encoded by *aspA* was down-regulated. The enzyme catalyzes the reversible conversion of aspartate to fumarate and ammonia. Aspartate was consumed from the medium and its levels were elevated in the metabolome. Lysine biosynthesis (*dapD*) was down-regulated and also lysine was decreased. Valine and isoleucine biosynthesis (*ilvB*) and threonine degradation (*mmsA, tdh*) were down-regulated, as a consequence threonine consumption from the medium was impaired. The levels of threonine and glycine were increased in the metabolome, while valine was lesser concentrated.

The serine deaminase SdaA involved in serine degradation to pyruvate and ammonia was down-regulated. Additionally, the serine transporter (*ssT*) was down-regulated, and serine could not serve as sole carbon source in the phenotyping microarray analysis. However, serine was still consumed from the medium. The *hutHI* genes were down-regulated, both encoding enzymes participating in the degradation of histidine, which was not consumed from the medium.

The reduced secretion of amino acid degradation products (3-methyl-2-oxopentanoate, 4-hydroxybutanoate) into the supernatant by the mutant further supports a general down-regulation of amino acid degradation through the absence of Crp.

In total, the down-regulation of amino acid degradation and transporters as well as the reduced uptake of non-glycolytic substances from the medium suggests that the impaired

growth of the *crp* mutant in LB medium was predominantly due to fewer utilization of nutrients. Since the absence of Crp reduces the ability of *Y. pseudotuberculosis* to use non-glycolytic substances but enhances uptake of glycolytic substances, the *crp* mutant strain was grown on glucose as sole carbon source to test if growth was also impaired when enough utilizable carbon source was provided. Therefore, the mutant strain was grown in glucose minimal medium (chapter 2.7.2) at 25 °C and the growth was compared to the wild type strain YPIII (figure 3.58).

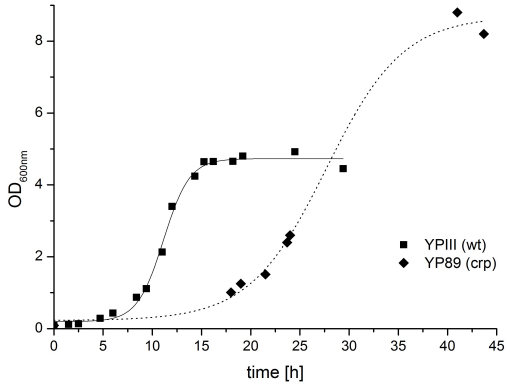

Figure 3.58: Growth curve of YPIII (wt) and the YP89 (*crp*$^-$) mutant strain in minimal medium with 40 mM glucose at 25°C.

The experiment showed that the mutant strain could reach a higher maximal OD than the wild type. That proves that Crp is crucial for growth on non-glucose carbon sources but not on glucose. Since a *crp* deficient mutant of *Y. enterocolitica* is unable to colonize deeper tissues and is restricted to the mesenteric lymph nodes (Petersen & Young 2002), the uptake and degradation of other nutrients than sugars in deeper tissues seems to be of extreme importance.

Sulfur metabolism

Methionine was decreased in the metabolome of the *crp* mutant but the metabolite was measured with high deviation. Elevated levels of homocysteine were detected in the supernatant, although the enzyme catalyzing the conversion from homocysteine to methionine, the methylenetetrahydrofolate reductase (*metF*), was strongly up-regulated in the mutant. This might point towards a posttranscriptional inactivation of the enzyme.

Further, γ-glutamate-cysteine ligase (*gshA*) was up-regulated, which is involved in glutathione synthesis from glutamate and cysteine, but the cysteine desulferase (*icsS*) was down-regulated. The enzyme is critical for iron-sulfur cluster formation and repair.

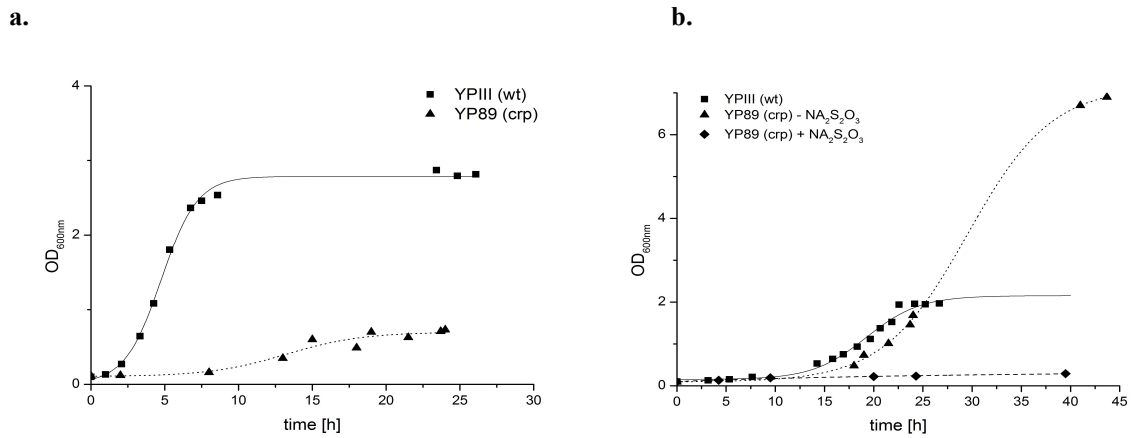

Figure 3.59: Growth curve of YPIII and YP89 (*crp*$^-$) at 37 °C in (a) LB medium and (b) minimal medium, where the wildtype was grown on 40 mM mannitol with the addition of 2.5 mM thiosulfate and the YP89 (*crp*$^-$) mutant was grown on 40 mM glucose with (diamonds) or without (triangles) thiosulfate.

A high number of transcripts involved in sulfur metabolism and transport was affected by the absence of Crp. The cysteine regulon (*cysK, cysPUWAM, cysDNC, cysE, cysQ, cysG, cysH, cysJ, cysN)* was up-regulated. These enzymes encoded by this genes are involved in sulfate uptake, sulfate reduction to sulfite and sulfide as well as the synthesis of cysteine and homocysteine. The deletion of subsets of these genes leads to altered sulfur requirements in *E. coli* (Kredich 1996). The transcription of most of these genes is temperature-regulated in *Y. pestis* and repressed at higher temperatures (Han et al. 2005). Previous experiments indicated that this down-regulation might result in the requirement for reduced sulfur such as thiosulfate at 37 °C (chapter 3.2.4). To my knowledge, no regulation of the sulfur metabolism through Crp is known so far, but the promoters of NADH-sulfite reductase (*cysJ*) and O-acetylserine reductase (*cysM*) exhibit a very weak similarity to CRP-dependent promoters in *E. coli* (Kredich 1996). Since *crp* was also influenced in YPIII by temperature (chapter 3.2.5.3), it is possible that the requirement for reduced sulfur was due to repressed sulfur metabolism through Crp at 37 °C. In order to further investigate this, the YP89 (*crp*$^-$) mutant strain was grown in LB medium to test the general growth behavior at 37 °C (figure 3.59a), where the mutation had a growth

inhibiting effect similar to 25 °C. Because the mutant strain was not able to grow on mannitol neither at 25 °C nor at 37 °C, the growth on glucose was tested at 37 °C with and without the addition of thiosulfate (figure 3.59b). Astonishingly, thiosulfate had a growth inhibiting effect at 37 °C and was not needed to reach high cell densities. This strongly indicates an involvement of Crp in the need for reduced sulfur at 37 °C. This phenomenon emphasizes an important role of sulfur metabolism during host adaption of *Y. pseudotuberculosis* but clearly needs more investigation to be fully understood. The regulation of sulfur metabolism is also essential for virulence and persistence in the host for other pathogenic bacteria such as *Mycobacterium tuberculosis*. The enzymes of *M. tuberculosis* are currently investigated as promising new drug targets, particularly since bacteria sulfur metabolic pathways are absent in humans (Bhave et al. 2007). Therefore this might be applicable for *Y. pseudotuberculosis* too.

Lipid metabolism

The biosynthesis of fatty acids was up-regulated (*fabGZ*), while the fatty acids were decreased in the metabolome (heptadecanoate, octadecenoate, hexadecenoate, pentadecanoate). The β-oxidation (*fadABDIJ*) and the fatty acid transporter (*fadL*) were down-regulated. Interestingly, 2-methylcitrate, an intermediate of the odd-numbered fatty acid degradation was decreased, confirming further a reduced degradation of fatty acid, which was also indicated by the down-regulated glyoxylate cycle (*aceAB*) (figure 3.57). The low levels of fatty acids might be a result of increased membrane synthesis, which corresponds to the up-regulation of the first committed step in the assembly of peptidoglycan (*murA*) and indicates a suppression of cell wall synthesis through Crp. Consistently, also the lipid A biosynthesis was up-regulated (*htrB, lpxD*).

Purine and Pyrimidine metabolism

As mentioned previously, the nucleoside permease (*nupC1*) was up-regulated and the mutant gained the ability to use certain nulceosides as sole carbon source as shown by the phenotyping microarrays (table 3.24). Further, enzymes from synthesis and salvage of pyrimidine ribonucleotides, the CMP kinase, the guanylate kinase and the IMP dehydrognase (*cmk, gmk, guaB*) were up-regulated. The increased recycling of guanine bases probably led to the lack of guanine secretion into the supernatant. The adenylsuccinate synthetase (*purA*) catalyzes the first committed step towards the *de novo*

synthesis of AMP and was also up-regulated. In accordance with this, AMP and GMP were increased in the intracellular metabolome of the *crp* mutant.

However, the phosphopentomutase (*deoB*) was up-regulated, which is involved in purine and pyrimidine degradation, where it catalyzes the conversion of ribose-1-P into ribose-5-P, which is further degraded by the PPP. The phosphopentomutase and the nucleoside transporter were the only genes, regulated alike in the *rovA* (chapter 3.3.9.1) and the *crp* mutant, which indicated importance for the ability to degrade nucleosides (chapter 3.3.2). The only down-regulated enzyme in nucleoside metabolism was the uridine phosphorylase (*udp*), involved in uridine degradation.

Vitamins & Cofactors

The synthesis of the major cofactors was up-regulated, including the dephospho-CoA kinase (*coaE*) for coenzyme A, the first step of riboflavin biosynthesis (*ribB*), aspartate oxidase and NAD synthetase (*nadBE*), both involved in NAD *de novo* biosynthesis.

Further, iron transporters (*fepB, fhuD, afuAB*) and the iron storage protein ferritin (*ftnA*) were up-regulated. The glutamate-1-semialdehyde aminotransferase (*hemL*) was down-regulated. It catalyzes the conversion of glutamate-1-semialdehyd to 5-amino-levulinate, an important precursor for heme and tetrapyrrole biosynthesis. Two enzymes from colanic acid biosynthesis (*manB, ugd*) were down-regulated. Colanic acids are loosely attached exopolysaccharides, produced by many enterobacteria and sometimes associated with biofilm formation (Sutherland 2001).

Virulence & Stress

The absence of Crp led to numerous changes in the regulation of genes that are associated with virulence. The gene of the global virulence regulator RovA, the invasion factor invasin (*invA*), the pH 6 antigen (*psaABEF*), flagellar assembly (*fliMC*) and Yops (*virG, yopD, yopH*) were down-regulated, whereas several subunits of the type VI secretion system (*hcp, icmF, impCGH*) and adhesion factors (*yadEF*) as well as several ribosomal proteins *(rplBCDFIJLMOPQRSTVW, rpmABCDFIJ, rpsABCDEHIJKMN*QRS) were up-regulated.

Further, some stress responses such as the cold shock proteins (*cspBCD*), the acid resistance proteins (*hdeBD*) and also the two-component regulatory system OmpR (*cpxR)* were down-regulated in the mutant. The latter is important for survival of

Y. pseudotuberculosis at acidic pH (Hu et al. 2009). It regulates the expression of urease, which is essential for survival in acidic environment.
It has been shown that Crp is crucial for virulence in YPIII, especially for dissemination into deeper tissue such as liver and spleen (Heroven et al. 2012). This indicates that the ability to consume and degrade a multitude of carbon sources is important in deeper tissue.

3.3.10 Influence of the virulence network on the metabolism

An overview over the identified regulation processes controlled by the investigated regulators is shown in figure 3.60. The TCA cycle was influenced through the deletion of the regulators CsrA, Crp and YmoA but a direct interpretation of the meaning was ambiguous, since it was not clear which regulator directly controls these pathways and which effects were indirect. Nevertheless, the tight control of the central carbon pathways seem to be of extreme significance for the organism, since it can be regulated in response to several influences.
Another metabolic trait, influenced by the virulence regulators, was the uptake of nutrients. The regulators positively affected the uptake of amino acids, indicating them to be important for survival of YPIII in the host. The effects of the factor RovM on the metabolism were minor to the tested conditions and mainly mediated through RovA, which, besides influencing Invasin expression, was involved in growth on nucleosides as sole carbon source. RovA represses several enzymes involved in nucleoside degradation, hindering the wild type to use nucleosides as carbon sources. Further, RovA was involved in the repression of acid resistance and its deletion led to faster adaption to acidic environment. It influenced the degradation of arginine, methionine and asparagine. Especially the regulation of the AST-arginine degradation pathway seemed to be repressed by RovA and might therefore hold special importance for the virulence of YPIII.

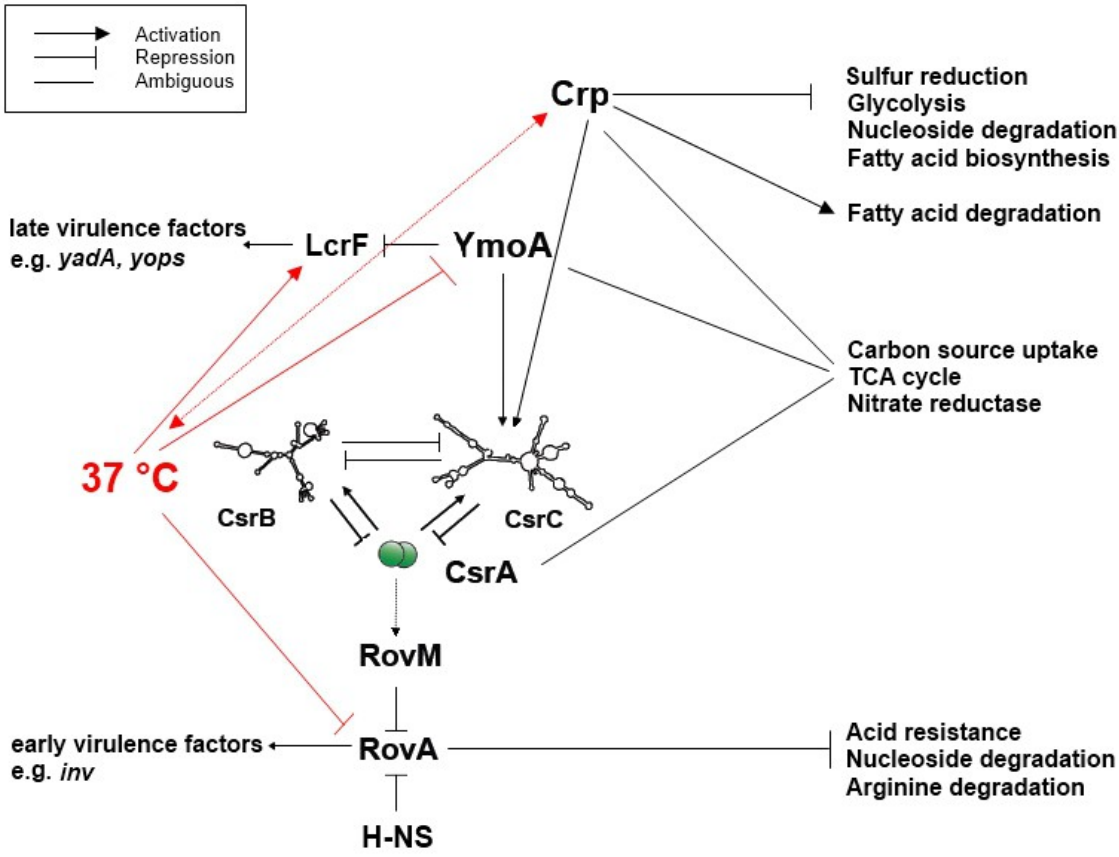

Figure 3.60: Interconnection of the regulatory network controlling expression of virulence factors and metabolism in *Y. pseudotuberculosis*. Adapted from (Heroven & Böhme et al. 2012)

The difference in metabolism between 25 °C and 37 °C was not mediated by RovA and only partly by YmoA, suggesting the presence of another unknown regulator. An influence of Crp on temperature regulation can be suspected. Crp is involved in the requirement of reduced sulfur at 37 °C. The absence of Crp and CsrA had a multitude of similar effects, indicating a close connection of these regulators.

In the previous chapters, several metabolic traits were revealed to be targets for virulence regulators. This included metabolic pathways, whose importance to virulence was known before (e.g. urease). For these, this study provides more information about regulatory events and the influence to several instances of YPIII physiology. Moreover, the analyses identified new metabolic traits, that were not connected to *Yersinia* virulence before (e.g. AST-arginine degradation pathway). These might provide important information for a better understanding of the metabolic site of the infection processes and offer new targets for drug research.

3.4 Unknown compounds in the metabolome of Y. pseudotuberculosis

During this project, several compounds were detected in the metabolome of *Y. pseudotuberculosis* YPIII, that could be reproducibly measured but not identified through mass spectra and retention index comparison. These metabolite derivatives were added to the mass spectra library if they met the following criteria: (I) being reproducible over several measurements, (II) consisting of a mass spectra with sufficient intensity and a clear isotopic pattern and (III) not being caused by contamination.

The intensities of these compounds were monitored over several experiments and the response to the investigated influences (e.g. temperature, growth stage, mutation) were measured. The compounds, that were detected most frequently and showed responses to perturbations of the YPIII metabolome, are shown in table 3.26. The mass spectra and the retention index of the unknown substances were added to the in-house library of the department of bioinformatics and biochemistry at the TU Braunschweig. From prominent peaks in the mass spectra conclusions of the nature of the compounds were drawn, which are also shown in table 3.26.

The compounds unknown_ypy#mse-001_1846.9, unknown_ypy#mse-002_1_2922.4 and unknown_ypy#mse-002_2_2955.1 were also investigated by C. Jäger (Department of Bioinformatics & Biochemistry, TU Braunschweig). For the characterization of selected unknown compounds he compared extracts of YPIII cells grown in [U]-C_{13}-glucose and extracts derivatized with Me-*d3*-OX with standard metabolite extracts (Jäger 2011). He proposed the sum formulas as indicated in table 3.26. Based on the mass spectra, one sum formula with two possible chemical structures was found for unknown_ypy#mse-001_1846.9: 2-methylaconitate from the propanoate metabolism and homoaconitate from the lysine biosynthesis. The compounds unknown_ypy#mse-002_1_2922.4 and unknown_ypy#mse-002_2_2955.1 had an identical mass spectrum and were considered as derivatives from the same substance. The structure was only ambiguously predictable but identified as a trisaccharide (Jäger 2011).

Table 3.26: Unknown components specific for YPIII

Identifier	Retention Index	Prominent Masses	Biological response[5]	Rel. Error [%], (n=6)[6]	Additional Information based on the mass spectra
Unknown#mse-ypy-001_1846.9	1846,9	197; 270; 389	Growth on Glucose ↑ *crp* mutant ↑	19,8	$C_{16}H_{33}O_6Si_3$ (=$C_7H_8O_6$)[7]
Unknown#mse-ypy-002_1_2922.4	2922,4	217; 259	Growth on Glucose ↑ 37°C ↓ *crp, csrA, ymoA* mutant ↑	15,8	$C_{36}H_{81}O_{12}Si_7$ (= $C_{15}H_{26}O_{13}$)[4]
Unknown#mse-ypy-002_2_2955.1	2955,1	217; 259	Growth on Glucose ↑ 37°C ↓ *crp, csrA ymoA* mutant ↑	18,6	$C_{36}H_{81}O_{12}Si_7$ (= $C_{15}H_{26}O_{13}$)[4]
Unknown#mse-ypy-003_1093.7	1093,7	154	*crp* mutant ↓	10,3	
Unknown#mse-ypy-009_1493.0	1493	84; 245	Growth on Glucose ↑ *ymoA, csrA,crp* mutant ↑	6,3	Amino acid derivative
Unknown#mse-ypy-017_1896.2	1896,2	103; 129; 283	37°C ↓ *csrA* mutant ↑	13,2	Phosphate group
Unknown#mse-ypy-021_2090.4	2090,4	117; 197	37 °C ↑ *csrA* mutant ↓	4,3	Amino sugar
Unknown#mse-ypy-023_2128.1	2128,1	117; 129	37°C ↑ *rovA, csrA, ymoA* mutant ↓	7,1	Fatty acid Derivative
Unknown#mse-ypy-036_1981.9	1981,9	103;157; 291	Growth on Glucose ↓ 37 °C ↓ *rovA, crp* & *ymoA* mutant ↓	5,7	Fatty acid Derivative
Unknown#mse-ypy-039_3026.6	3026,6	129; 211; 299	37°C ↓ *rovA* mutant ↓	9,9	Phosphate group

In order to elucidate the nature of the unknown compounds and their role in the metabolism of YPIII further than possible based only on the information of the mass spectra, the means of the metabolic profiles of several experiments were compared. A similar response of metabolites to perturbations indicates a connection in the metabolic network and allows a deduction about the nature of the unknown components through comparison with identified metabolites. A similar attempt based on biological fluctuation used a correlation matrix to uncover metabolic networks (Steuer et al. 2003). However, the method does not generate enough information to specify the role of components in a biological system but only shows very close connections correctly.

5 Compared to the metabolome of YPIII at 25 °C, grown in LB medium

6 Relative Error in the metabolome of YPIII at 25 °C, grown in LB medium

7 As proposed in the thesis of Christian Jäger (Jäger 2011)., sum formula with TMS-groups (=without TMS groups)

On the basis of 194 biological replicates, the means of 36 different conditions were calculated and used to compare the amount of unknown compounds to that of identified metabolites. These 36 conditions included different media, temperature and mutant strains of YPIII. A correlation of reliable significance to other metabolites could be determined for six unknown compounds. The results a presented in form of sections of a SOTA (chapter 2.14.5) in figure 3.61.

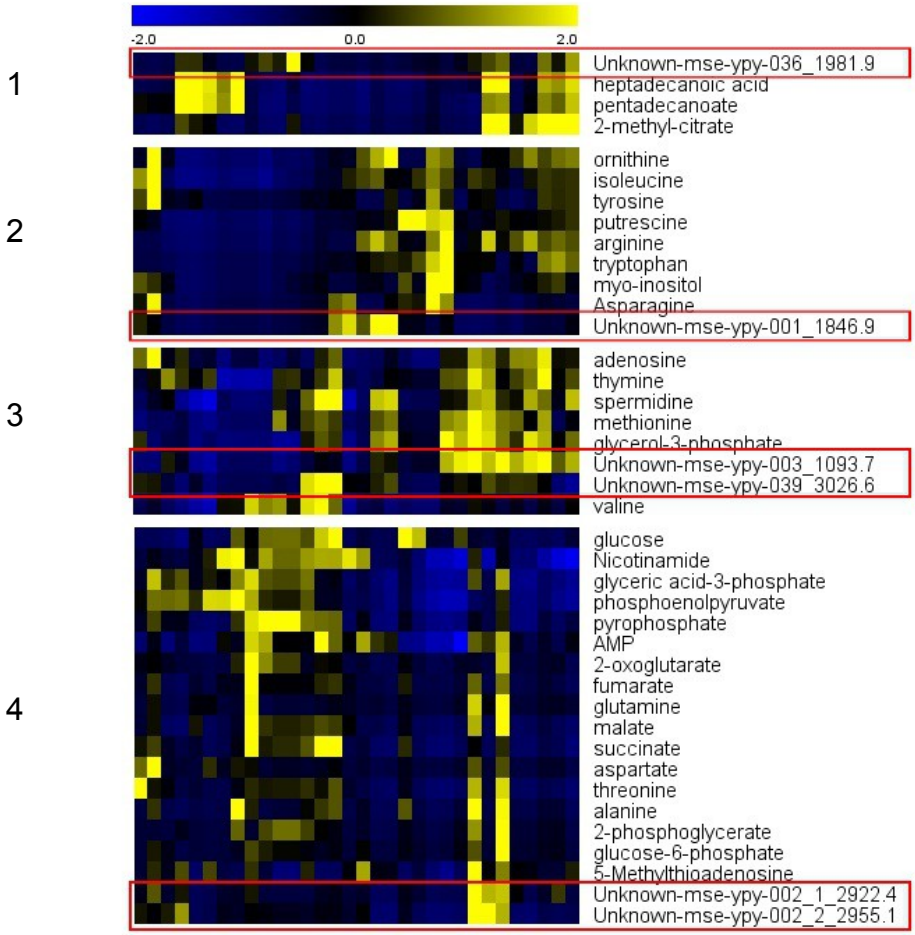

Figure 3.61: Presentation of the correlation of the unknown compounds to known metabolites in form of a self organizing tree algorithm. The analysis was based on 36 samples and 67 metabolites and 10 unknown compounds. For correlation, the Spearman rank correlation was used. The data was z-score normalized. Only sections of the complete analysis are presented for clarity reasons.

For the unknown_ypy#mse-036_1981.9 a similarity to fatty acids was proposed (table 3.26), since the mass spectrum of the component holds fragments associated with fatty acid decomposition (m/z 103, 117, 129). This is further confirmed though the arrangement of the SOTA of the compound into the first cluster together with the compounds of odd-numbered fatty acid metabolism: pentadecanoate, heptadecanoate and

2-methylcitrate, indicating an involvement of the unknown substance in the metabolism of odd-numbered fatty acid metabolism

The structure of unknown_ypy#mse-001_1846.9 has been narrowed down to two proposals based on the mass spectrum, as explained earlier, and is either a component of propanoate degradation or amino acid biosynthesis. Since the concentration profile of the compound beared no similarity to 2-methylcitrate and therefore propanoate metabolism, but rather resembled the amino acids in the second SOTA cluster , it is highly probable that the identity of the unknown is homoaconitate, a compound from lysine biosynthesis, rather than methylaconitate from propanoate metabolism.

In the third cluster the unknown_ypy#mse-003_1093.7 and unknown_ypy#mse-039_3026.6 showed similarities to each other, which indicated that they are derivatives of the same substance. However, the similarity of the unknown compounds to methionine and spermidine indicate an involvement in polyamine biosynthesis.

The unknown_ypy#mse-002_1_2922.4 and unknown_ypy#mse-002_2_2955.1 were already denoted as one substance and their high similarity in the fourth cluster of the SOTA further confirmed this. The concentration profiles resemble that of metabolites from the TCA cycle and the glycolysis (fumarate, malate, succinate, 2-oxoglutarate, glucose-6-P, 2-, 3-phosphoglycerate, PEP), which demonstrates a close connection to the central carbon pathway. Since it is probably a trisaccharide, as mentioned earlier, which is highest concentrated in the metabolome during growth on glucose as carbon source, one can assume a role as carbon storage molecule.

However, a definitive identification of the unknown substances is only possible through the measurements of authentic standards.

4 Summary

The food borne, human pathogenic bacterium *Yersinia pseudotuberculosis* is the next relative of *Yersinia pestis*, the causative agent of the bubonic plague. Several indications were detected in previous studies for metabolic traits that are co-regulated with virulence traits. The identification of metabolic pathways crucial for initiation or establishment of infection is highly desirable as an approach for new drug-targets.

In this study, *Y. pseudotuberculosis* was cultivated for the first time in minimal medium without the addition of vitamins or amino acids, proving the comprehensive synthesizing capacities of the bacterium. The nutrient uptake capabilities were tested in assays for the four major elements C, N, S and P, which were similar to those of other *Enterobacteriaceae* such as *E. coli* and *Salmonella*. The intra- and extracellular metabolome of a batch cultivation of *Y. pseudotuberculosis* was investigated during growth in minimal medium and compared to the metabolome in complex LB medium. The secretion of organic acids was detected during growth in both media and interpreted as indicators for an overflow metabolism during fast proliferation. The growth on glucose led to decreased uptake of the secreted organic acids, suggesting the presence of catabolite repression. An ordered uptake of nutrients from complex medium was observed, in which the bacterium had clear preferences for sugars and certain amino acids. The bacterium was investigated during different growth phases in different media, detecting different growth phase-dependent changes in the metabolites.

Independent from the growth medium, the concentrations of nucleoside and TCA cycle intermediates were decreased in the intracellular metabolome of the stationary phase. On the other hand the amino acid pools increased during low growth rates.

The metabolism of *Y. pseudotuberculosis* was further investigated at the model-temperatures 25 °C and 37 °C, which represent the situation outside and inside the host, respectively. The temperature difference highly influenced the metabolism, exceeding the reactions of other microorganisms. The nutritional requirements were altered in minimal medium at 37 °C, requiring more additives than at 25 °C. A need for reduced sulfur was detected for growth in minimal medium at 37 °C and glucose was not a suitable carbon source. The minimal medium was therefore adjusted to promote growth at 37 °C by adding mannitol and thiosulfate. The metabolome of *Y. pseudotuberculosis* cells grown in LB medium showed only few differences at 37 °C compared to 25 °C. Nearly no differences in

uptake of nutrients was detected, which was supported by the few regulated transporters in the transcriptome. The discrepancy at 37 °C between the extremely reduced utilizable carbon sources in minimal medium and the nearly unaffected uptake of nutrients by the cells in LB medium could be the result of the need for a reducing environment, since reduced sulfur promoted growth. High lactate secretion in both media indicated fermentative metabolism at 37 °C. The intracellular metabolome showed changes in fatty acid composition and indicators for changed membrane composition at higher temperatures. Further increased fatty acid degradation and reduced synthesis was indicated by the transcriptome and the metabolome. The amino acid biosynthesis was also down-regulated at 37 °C and many amino acid pools were reduced. The increased concentration of amino acid degradation products indicated further the use of amino acids as energy and precursor sources in the metabolome of cells grown in minimal and LB medium at 37 °C, while glycolytic degradation was reduced. The cells produced increased virulence factors at 37 °C, which could be observed in the transcriptome by the corresponding up-regulated genes, as well as up-regulated ribosomes and chaperones. A down-regulation of biosynthesis and an up-regulation of defense mechanism against the host immune system is therefore likely induced through temperature elevation.

The influence of virulence regulators RovA, RovM, CsrA, YmoA and Crp was investigated by transcriptome and metabolome analysis with transposon mutant strains deprived of the respective regulation factor. All investigated mutant strains were separated by an hierarchical clustering based on the metabolome data, demonstrating a connection between the investigated regulators and the metabolism. Three mutations influenced growth (Crp, CsrA, YmoA) and uptake of nutrients. The three regulators seemed to influence the important metabolic pathways glycolysis, TCA cycle, fatty acid synthesis and nucleoside metabolism, but a direct interpretation of the meaning was ambiguous, since it was not clear which regulator directly controlled these pathways and which effects were indirect. The regulator RovA was shown to repress the degradation of nucleosides, which might be an important trait for later stages of infection. Further the RovA regulator was involved in the regulation of acid resistance.

The differences in the metabolism of the wild type at the different temperatures was not caused by the temperature-sensing regulators RovA or YmoA, although the temperature-dependent RovA-regulation of Invasin could be confirmed through the transcriptome analysis, as well as the YmoA-dependent regulation of the late virulence factors. However, the metabolic changes observed under the two temperatures 25 °C and 37 °C were not

mediated by these factors. Nevertheless, a possible candidate for the temperature-dependent control of the metabolism was the regulator Crp. The Crp lacking mutant showed several metabolic traits similarly influenced as through the elevation of the temperature such as the fatty acid metabolism and the TCA cycle and the glyoxylate shunt. Strikingly, an involvement of Crp in the need for reduced sulfur at higher temperatures could be demonstrated. Further, similar alterations in the transcriptome and metabolome of the *crp* and *csrA* mutant were measured, indicating overlapping regulatory events.

Specific unknown components were frequently detected in the metabolism of *Y. pseudotuberculosis*, that showed a response to several influences including the mutations of virulence regulators and temperature. Some of them were identified or assigned to a substance class. The majority of these substances held similarities to fatty acids, further demonstrating the importance of these substances to the virulence of *Y. pseudotuberculosis*.

5 Outlook

After a successful establishment of the cultivation of *Y. pseudotuberculosis* in minimal medium at the two model temperatures 25 °C and 37 °C, a more detailed investigation of the metabolism of the bacterium was made possible. During this work several unique metabolic traits were observed, that should gain more research interest, such as the constant secretion of organic acids in all investigated minimal media, which could demonstrate an incomplete degradation of carbon sources, while the concrete mechanism remained unknown. The cause for this observations could be an overflow mechanism or an anaerobic metabolism of *Y. pseudotuberculosis*. Particularly, the high levels of secreted lactate at 37 °C and the corresponding regulated genes indicate an anaerobic functionality of the metabolism at 37 °C. A cultivation, where the percentage of dissolved oxygen in the medium is measured and varied, might be useful to understand this phenomenon. In this context, the cultivation with a C_{13} labeled carbon source might be useful to understand the flux through the metabolism and also the origin of the secreted organic acids.

Further a temperature shift experiment, where the temperature is slowly raised from 25 °C to 37 °C, the metabolome is measured and the oxygen uptake is monitored, would provide insights in the temperature adaption process over a timely manner, which would exceed previous data.

This work further demonstrated the involvement and regulation of the Crp regulator in the changes of metabolism at 37 °C. Besides others, Crp was responsible for some of the increased nutritional requirements at higher temperatures e.g. reduced sulfur. The investigation of the metabolism of a Crp lacking mutant at 37 °C is highly desirable.

Since several pathways showed to be regulated constantly by virulence regulators e.g. the AST arginine degradation, the nucleoside uptake and the fatty acid biosynthesis/degradation, a knock out of genes encoding critical enzymes of these pathways and adjacent investigations of the influence on virulence could elucidate if these pathways are crucial for virulence and therefore interesting approaches for drug targets.

References

Achtman, M. et al., 1999. *Yersinia pestis*, the cause of plague, is a recently emerged clone of Yersinia pseudotuberculosis. *Proceedings of the National Academy of Sciences of the United States of America*, 96(24), pp.14043–8.

Almagro-Moreno, S. & Boyd, E.F., 2009. Insights into the evolution of sialic acid catabolism among bacteria. *BMC evolutionary biology*, 9, p.118.

Ansong, C. et al., 2013. A multi-omic systems approach to elucidating *Yersinia* virulence mechanisms. *Molecular BioSystems*, 9(1), pp.44–54.

Ansong, C. et al., 2009. Global systems-level analysis of Hfq and SmpB deletion mutants in *Salmonella*: implications for virulence and global protein translation. *PloS one*, 4(3), p.e4809.

Athmann, C. et al., 2000. Local pH elevation mediated by the intrabacterial urease of *Helicobacter pylori* cocultured with gastric cells. *The Journal of clinical investigation*, 106(3), pp.339–47.

Baev, M. V, Baev, D., Radek, Agnes Jansco, et al., 2006. Growth of *Escherichia coli* MG1655 on LB medium: monitoring utilization of amino acids, peptides, and nucleotides with transcriptional microarrays. *Applied microbiology and biotechnology*, 71(3), pp.317–22.

Baev, M. V, Baev, D., Radek, Agnes Jancso, et al., 2006. Growth of *Escherichia coli* MG1655 on LB medium: monitoring utilization of sugars, alcohols, and organic acids with transcriptional microarrays. *Applied microbiology and biotechnology*, 71(3), pp.310–6.

Barabási, A.-L. & Oltvai, Z.N., 2004. Network biology: understanding the cell's functional organization. *Nature reviews. Genetics*, 5(2), pp.101–13.

Barnes, P.D. et al., 2006. *Yersinia pseudotuberculosis* disseminates directly from a replicating bacterial pool in the intestine. *The Journal of experimental medicine*, 203(6), pp.1591–601.

Beckering, C., Steil, L. & Weber, M., 2002. Genomewide transcriptional analysis of the cold shock response in *Bacillus subtilis*. *Journal of bacteriology*, 184(22), pp.6395–6402.

Beelen, R., Feldmann, A. & Wijsman, H., 1973. A regulatory gene and a structural gene for alaninase in *Escherichia coli. Mol Gen Genet.*, 121(4), pp.369–74.

Bengoechea, J.A. et al., 2002. Regulatory network of lipopolysaccharide O-antigen biosynthesis in *Yersinia enterocolitica* includes cell envelope-dependent signals. *Molecular microbiology*, 44(4), pp.1045–62.

Bhave, D., III, W.M. & Carroll, K., 2007. Drug targets in *mycobacterial* sulfur metabolism. *Infect disorders drug targets*, 7(2), pp.734–764.

Bligh, E. & Dyer, W., 1959. A rapid method of total lipid extraction and purification. *Can J Biochem Physiol.*, 37(8), pp.911–7.

Bliska, J B, Copass, M.C. & Falkow, S., 1993. The *Yersinia pseudotuberculosi*s adhesin YadA mediates intimate bacterial attachment to and entry into HEp-2 cells. *Infection and immunity*, 61(9), pp.3914–21.

Bochner, B.R., 2009. Global phenotypic characterization of bacteria. *FEMS microbiology reviews*, 33(1), pp.191–205.

Bochner, B.R., Gadzinski, P. & Panomitros, E., 2001. Phenotype microarrays for high-throughput phenotypic testing and assay of gene function. *Genome research*, 11(7), pp.1246–55.

Bohlin, J., Skjerve, E. & Ussery, D.W., 2009. Analysis of genomic signatures in prokaryotes using multinomial regression and hierarchical clustering. *BMC genomics*, 10, p.487.

Bölin, I., Norlander, L. & Wolf-Watz, H., 1982. Temperature-inducible outer membrane protein of *Yersinia pseudotuberculosis* and *Yersinia enterocolitica* is associated with the virulence plasmid. *Infection and immunity*, 37(2), pp.506–12.

Bottone, E.J., 1997. *Yersinia enterocolitica:* the charisma continues. *Clinical microbiology reviews*, 10(2), pp.257–76.

Le Bouguénec, C. & Schouler, C., 2011. Sugar metabolism, an additional virulence factor in enterobacteria. *International journal of medical microbiology : IJMM*, 301(1), pp.1–6.

Bowden, S.D. et al., 2009. Glucose and glycolysis are required for the successful infection of macrophages and mice by *Salmonella enterica serovar typhimurium*. *Infection and immunity*, 77(7), pp.3117–26.

Bradford, M., 1979. A rapid and sensitive method for the quantitation of microgram quantities of protein utilizing the principle of protein-dye binding. *Analytical Biochemistry*, 72(2), pp.248–254.

Bright, G.R. et al., 1987. Fluorescence ratio imaging microscopy: temporal and spatial measurements of cytoplasmic pH. *The Journal of cell biology*, 104(4), pp.1019–33.

Brubaker, B., 2006. *The Prokaryotes* third. M. Dworkin et al., eds., Springer New York.

Brubaker, R.R., 1968. Metabolism of carbohydrates by *Pasteurella pseudotuberculosi*s. *Journal of bacteriology*, 95(5), pp.1698–705.

Brubaker, R.R. & Sulen, a, 1971. Mutations Influencing the Assimilation of Nitrogen by *Yersinia pestis*. *Infection and immunity*, 3(4), pp.580–8.

Buzoleva, L.S. & Somov, G.P., 2003. Adaptation variability of *Yersinia pseudotuberculosis* during long-term persistence in soil. *Bulletin of experimental biology and medicine*, 135(5), pp.456–9.

Carniel, E, 2001. The *Yersinia* high-pathogenicity island: an iron-uptake island. *Microbes and infection / Institut Pasteur*, 3(7), pp.561–9.

Carniel, E, Guilvout, I. & Prentice, M., 1996. Characterization of a large chromosomal "high-pathogenicity island" in biotype 1B *Yersinia enterocolitica*. *Journal of bacteriology*, 178(23), pp.6743–51.

Carniel, E. et al., 2006. *The Prokaryotes* M. Dworkin et al., eds., Springer New York.

Caspi, R. et al., 2010. The MetaCyc database of metabolic pathways and enzymes and the BioCyc collection of pathway/genome databases. *Nucleic acids research*, 38(Database issue), pp.D473–9.

Castanie-Cornet, M. & Penfound, T., 1999. Control of Acid Resistance in *Escherichia coli. Journal of bacteriology*, 181(11).

Cathelyn, J.S. et al., 2006. RovA, a global regulator of *Yersinia pestis*, specifically required for bubonic plague. *Proceedings of the National Academy of Sciences of the United States of America*, 103(36), pp.13514–9.

Cathelyn, J.S. et al., 2007. The RovA regulons of *Yersinia enterocolitica* and *Yersinia pestis* are distinct: evidence that many RovA-regulated genes were acquired more recently than the core genome. *Molecular microbiology*, 66(1), pp.189–205.

Chain, P.S.G. et al., 2004. Insights into the evolution of *Yersinia pestis* through whole-genome comparison with *Yersinia pseudotuberculosis*. *Proceedings of the National Academy of Sciences of the United States of America*, 101(38), pp.13826–31.

Chang, D.-E. et al., 2004. Carbon nutrition of *Escherichia coli* in the mouse intestine. *Proceedings of the National Academy of Sciences of the United States of America*, 101(19), pp.7427–32.

Chauvaux, S. et al., 2007. Transcriptome analysis of *Yersinia pestis* in human plasma: an approach for discovering bacterial genes involved in septicaemic plague. *Microbiology (Reading, England)*, 153(Pt 9), pp.3112–24.

Chromy, B.A. et al., 2005. Proteomic Characterization of *Yersinia pestis* Virulence. *Journal of bacteriology*, 187(23), pp.8172–8180.

Consumer Reports, 2013. What's in the pork? *Consumer Reports magazine*.

Conway, T. & Cohen, P. S., 2006. *Escherichia coli* at the intestinal mucosal surface. In *Virulence mechanisms of bacterial pathogens*. pp. 175–196.

Copeland, A. et al., 2008. *Complete sequence of Yersinia pseudotuberculosis YPIII, direct submission to NCBI Genome,URL:http://www.ncbi.nlm.nih.gov/nuccore/CP000950 , last accessed 13.03.2013*,

Cornelis, G.R., 1998. The *Yersinia* deadly kiss. *Journal of bacteriology*, 180(21), p.5495.

Cronan, J.E. & Rock, C.O., 1996. Biosynthesis of Membrane Lipids. In *Escherichia coli and Salmonella*. pp. 612–631.

Dalebroux, Z.D. et al., 2010. ppGpp conjures bacterial virulence. *Microbiology and molecular biology reviews : MMBR*, 74(2), pp.171–99.

Dersch, P & Isberg, R R, 2000. An immunoglobulin superfamily-like domain unique to the *Yersinia pseudotuberculosis* invasin protein is required for stimulation of bacterial uptake via integrin receptors. *Infection and immunity*, 68(5), pp.2930–8.

Diepold, A. et al., 2010. Deciphering the assembly of the *Yersinia* type III secretion injectisome. *The EMBO journal*, 29(11), pp.1928–40.

Dopazo, J. & Carazo, J.M., 1997. Phylogenetic reconstruction using an unsupervised growing neural network that adopts the topology of a phylogenetic tree. *Journal of molecular evolution*, 44(2), pp.226–33.

Dorman, C.J., 2004. H-NS: a universal regulator for a dynamic genome. *Nature reviews. Microbiology*, 2(5), pp.391–400.

Dreyfus, L. a & Brubaker, R.R., 1978. Consequences of aspartase deficiency in *Yersinia pestis*. *Journal of bacteriology*, 136(2), pp.757–64.

Dube, P. & Handley, S., 2003. The rovA mutant of *Yersinia enterocolitica* displays differential degrees of virulence depending on the route of infection. *Infection and immunity*, 71(6), pp.3512–3520.

Dunn, W.B., Bailey, N.J.C. & Johnson, H.E., 2005. Measuring the metabolome: current analytical technologies. *The Analyst*, 130(5), pp.606–25.

Eckburg, P., Bik, E. & Bernstein, C., 2005. Diversity of the human intestinal microbial flora. *Science*, 308(5728), pp.1635–1638.

Eitel, J. et al., 2005. Cell invasion and IL-8 production pathways initiated by YadA of *Yersinia pseudotuberculosis* require common signalling molecules (FAK, c-Src, Ras) and distinct cell factors. *Cellular microbiology*, 7(1), pp.63–77.

Eitel, J. & Dersch, Petra, 2002. The YadA protein of *Yersinia pseudotuberculosis* mediates high-efficiency uptake into human cells under environmental conditions in which invasin is repressed. *Infection and immunity*, 70(9), p.4880.

Ellison, D.W. et al., 2003. YmoA Negatively Regulates Expression of Invasin from *Yersinia enterocolitica. Journal of bacteriology*, 185(24), pp.7153–7159.

Ellison, D.W., Lawrenz, M.B. & Miller, Virginia L, 2004. Invasin and beyond: regulation of *Yersinia* virulence by RovA. *Trends in microbiology*, 12(6), pp.296–300.

Ellison, D.W. & Miller, Virginia L, 2006. H-NS represses inv transcription in *Yersinia enterocolitica* through competition with RovA and interaction with YmoA. *Journal of bacteriology*, 188(14), pp.5101–12.

Englesberg, E., 1952. The irreversibility of methionine synthesis from cysteine in *Pasteurella pestis*. *Journal of bacteriology*, pp.675–680.

Eppinger, M. et al., 2007. The complete genome sequence of *Yersinia pseudotuberculosis* IP31758, the causative agent of Far East scarlet-like fever. *PLoS genetics*, 3(8), p.e142.

Eylert, E. et al., 2008. Carbon metabolism of *Listeria monocytogenes* growing inside macrophages. *Molecular microbiology*, 69(4), pp.1008–17.

Fabich, A.J. et al., 2008. Comparison of carbon nutrition for pathogenic and commensal *Escherichia coli* strains in the mouse intestine. *Infection and immunity*, 76(3), pp.1143–52.

Feinbaum, R.L. et al., 2012. Genome-wide identification of *Pseudomonas aeruginosa* virulence-related genes using a *Caenorhabditis elegans* infection model. *PLoS pathogens*, 8(7), p.e1002813.

Fiehn, O, 2001. Combining genomics, metabolome analysis, and biochemical modelling to understand metabolic networks. *Comparative and functional genomics*, 2(3), pp.155–68.

Fiehn, Oliver, 2002. Metabolomics--the link between genotypes and phenotypes. *Plant molecular biology*, 48(1-2), pp.155–71.

Flint, H.J. et al., 2007. Interactions and competition within the microbial community of the human colon: links between diet and health. *Environmental microbiology*, 9(5), pp.1101–11.

Foster, J., 2001. Acid stress responses of *Salmonella* and *E. coli:* survival mechanisms, regulation, and implications for pathogenesis. *JOURNAL OF MICROBIOLOGY*, 39(2), pp.89–94.

Fowler, J.M. & Brubaker, R.R., 1994. Physiological basis of the low calcium response in Yersinia pestis. *Infection and immunity*, 62(12), pp.5234–41.

Freter, R., 1983. Human Intestinal Microflora in Health and Diseas. *Academic, New York*, pp.33–54.

Gentleman, R.C. et al., 2004. Bioconductor: open software development for computational biology and bioinformatics. *Genome biology*, 5(10), p.R80.

Glassbrook, N., Beecher, C. & Ryals, J., 2000. Metabolic profiling on the right path. *Nature biotechnology*, 18(11), pp.1142–1143.

Gorden, J. & Small, P.L., 1993. Acid resistance in enteric bacteria. *Infection and immunity*, 61(1), pp.364–7.

Götz, A. et al., 2010. Carbon metabolism of enterobacterial human pathogens growing in epithelial colorectal adenocarcinoma (Caco-2) cells. *PloS one*, 5(5), p.e10586.

Götz, A. & Goebel, W., 2010. Glucose and glucose 6-phosphate as carbon sources in extra- and intracellular growth of enteroinvasive *Escherichia coli* and *Salmonella enterica*. *Microbiology (Reading, England)*, 156(Pt 4), pp.1176–87.

Gutnick, D. et al., 1969. Compounds which serve as the sole source of carbon or nitrogen for *Salmonella typhimurium* LT-2. *Journal of bacteriology*, 100(1), pp.215–219.

Han, Y. et al., 2007. Comparative transcriptomics in *Yersinia pestis*: a global view of environmental modulation of gene expression. *BMC microbiology*, 7, p.96.

Han, Y. et al., 2005. DNA microarray analysis of the heat- and cold-shock stimulons in *Yersinia pestis*. *Microbes and infection / Institut Pasteur*, 7(3), pp.335–48.

Hanegraaf, P.P. & Muller, E.B., 2001. The dynamics of the macromolecular composition of biomass. *Journal of theoretical biology*, 212(2), pp.237–51.

Hanko, V P & Rohrer, J S, 2000. Determination of carbohydrates, sugar alcohols, and glycols in cell cultures and fermentation broths using high-performance anion-exchange chromatography with pulsed amperometric detection. *Analytical biochemistry*, 283(2), pp.192–9.

Hanko, Valoran P & Rohrer, Jeffrey S, 2004. Determination of amino acids in cell culture and fermentation broth media using anion-exchange chromatography with integrated pulsed amperometric detection. *Analytical Biochemistry*, 324(1), pp.29–38.

Hartung, J., Elpelt, B. & Klösener, K.-H., 2005. *Statistik: Lehr- und Handbuch der angewandten Statistik* 14. ed., Oldenbourg Wissenschaftsverlag.

Herbst, K. et al., 2009. Intrinsic thermal sensing controls proteolysis of *Yersinia* virulence regulator RovA. *PLoS pathogens*, 5(5), p.e1000435.

Heroven, A., Böhme, K & Dersch, Petra, 2012. The Csr/Rsm system of *Yersinia* and related pathogens: A post-transcriptional strategy for managing virulence. *RNA biology*, 9(4), pp.379–391.

Heroven, A.K. et al., 2008. A Csr-type regulatory system, including small non-coding RNAs, regulates the global virulence regulator RovA of *Yersinia pseudotuberculosis* through RovM. *Molecular microbiology*, 68(5), pp.1179–95.

Heroven, A.K., Sest, M., et al., 2012. Crp induces switching of the CsrB and CsrC RNAs in *Yersinia pseudotuberculosis* and links nutritional status to virulence. *Frontiers in Cellular and Infection Microbiology*, 2(158).

Heroven, A.K. et al., 2004. RovA is autoregulated and antagonizes H-NS-mediated silencing of invasin and rovA expression in *Yersinia pseudotuberculosis*. *Molecular microbiology*, 53(3), pp.871–88.

Heroven, A.K., Böhme, Katja & Dersch, Petra, 2012. Regulation of virulence gene expression by regulatory RNA elements in *Yersinia pseudotuberculosis*. *Advances in experimental medicine and biology*, 954, pp.315–23.

Heroven, A.K. & Dersch, Petra, 2006. RovM, a novel LysR-type regulator of the virulence activator gene rovA, controls cell invasion, virulence and motility of *Yersinia pseudotuberculosis*. *Molecular microbiology*, 62(5), pp.1469–83.

Herrero, J., Valencia, A. & Dopazo, J., 2001. A hierarchical unsupervised growing neural network for clustering gene expression patterns. *Bioinformatics*, 17(2), pp.126–136.

Higuchi, K. & Carlin, C., 1957. Studies on the nutrition and physiology of *Pasteurella pestis* II. A defined medium for the growth of *Pasteurella pestis*. *Journal of bacteriology*, 75, pp.409–413.

Higuchi, K., Kupferberg, L. & Smith, J.L., 1959. Studies on the nutrition and physiology of *Pasteurella pestis* III . Effects of calcium ions on the growth of virulent and avirulent strains of *Pasteurella pestis*. *Journal of bacteriology*, 77, pp.317–321.

Hiller, K. et al., 2009. MetaboliteDetector: comprehensive analysis tool for targeted and nontargeted GC/MS based metabolome analysis. *Analytical chemistry*, 81(9), pp.3429–39.

Hills, G.M. & Spurr, E.D., 1952. The Effect of Temperature on the Nutritional Requirements of *Pasteurella pestis*. *Microbiological Research*, (1939), pp.64–73.

Hoe, N.P. & Goguen, J.D., 1993. Temperature sensing in *Yersinia pestis*: translation of the LcrF activator protein is thermally regulated. *Journal of bacteriology*, 175(24), pp.7901–9.

Hofreuter, D. et al., 2006. Unique features of a highly pathogenic *Campylobacter jejuni* strain. *Infection and immunity*, 74(8), pp.4694–707.

Hofreuter, D., Novik, V. & Galán, J.E., 2008. Metabolic diversity in *Campylobacter jejuni* enhances specific tissue colonization. *Cell host & microbe*, 4(5), pp.425–33.

Hu, Y. et al., 2010. Characterization of an aspartate-dependent acid survival system in *Yersinia pseudotuberculosis*. *FEBS letters*, 584(11), pp.2311–4.

Hu, Y. et al., 2011. Cra negatively regulates acid survival in *Yersinia pseudotuberculosis. FEMS microbiology letters*, 317(2), pp.190–5.

Hu, Y. et al., 2009. OmpR positively regulates urease expression to enhance acid survival of *Yersinia pseudotuberculosis*. *Microbiology (Reading, England)*, 155(Pt 8), pp.2522–31.

Huang, X. & Lindler, L., 2004. The pH 6 antigen is an antiphagocytic factor produced by *Yersinia pestis* independent of Yersinia outer proteins and capsule antigen. *Infection and immunity*, 72(12), pp.7212–7219.

Igarashi, K. & Kashiwagi, K., 2010. Modulation of cellular function by polyamines. *The international journal of biochemistry & cell biology*, 42(1), pp.39–51.

Isberg, R R & Barnes, P., 2001. Subversion of integrins by enteropathogenic *Yersinia. Journal of cell science*, 114(Pt 1), pp.21–28.

Isberg, R. R., Voorhis, D.L. & Falkow, S., 1987. Identification of invasin: A protein that allows enteric bacteria to penetrate cultured mammalian cells. *Cell*, 50(5), pp.769–778.

Iyer, R., Williams, C. & Miller, C., 2003. Arginine-agmatine antiporter in extreme acid resistance in *Escherichia coli*. *Journal of bacteriology*, 185(22), pp.6556–6561.

Jackson, M.W., Silva-Herzog, E. & Plano, G. V, 2004. The ATP-dependent ClpXP and Lon proteases regulate expression of the *Yersinia pestis* type III secretion system via regulated proteolysis of YmoA, a small histone-like protein. *Molecular microbiology*, 54(5), pp.1364–78.

Jäger, C., 2011. *Entwicklung eines Verfahrens zur Strukturanalyse unbekannter Verbindungen in bakteriellen Zellextrakten*. Technische Universität Braunschweig.

Jermyn, W.S. & Boyd, E.F., 2002. Characterization of a novel *Vibrio* pathogenicity island (VPI-2) encoding neuraminidase (nanH) among toxigenic *Vibrio cholerae* isolates. *Microbiology (Reading, England)*, 148(Pt 11), pp.3681–93.

Jones, B.D., 2005. *Salmonella* invasion gene regulation: a story of environmental awareness. *Journal of microbiology (Seoul, Korea)*, 43, pp.110–7.

Junker, B.H., Klukas, C. & Schreiber, F., 2006. VANTED: a system for advanced data analysis and visualization in the context of biological networks. *BMC bioinformatics*, 7, p.109.

Kaasch, a J. et al., 2012. *Yersinia pseudotuberculosis* bloodstream infection and septic arthritis: case report and review of the literature. *Infection*, 40(2), pp.185–90.

Kawahara, K. et al., 2002. Modification of the Structure and Activity of Lipid A in *Yersinia pestis* Lipopolysaccharide by Growth Temperature. *Infection and immunity*, 70(8), pp.4092–4098.

Kell, D.B., 2004. Metabolomics and systems biology: making sense of the soup. *Current opinion in microbiology*, 7(3), pp.296–307.

Kim, Y.-H. et al., 2005. Proteome response of *Escherichia coli* fed-batch culture to temperature downshift. *Applied microbiology and biotechnology*, 68(6), pp.786–93.

Klein, W., Weber, M.H. & Marahiel, M. a, 1999. Cold shock response of *Bacillus subtilis:* isoleucine-dependent switch in the fatty acid branching pattern for membrane adaptation to low temperatures. *Journal of bacteriology*, 181(17), pp.5341–9.

Knirel, Y.A. et al., 2005. Temperature-Dependent Variations and Intraspecies Diversity of the Structure of the Lipopolysaccharide of *Yersinia pestis*. *Biochemistry*, 44, pp.1731–1743.

De Koning-Ward, T. & Robins-Browne, R., 1997. A novel mechanism of urease regulation in *Yersinia enterocolitica*. *FEMS microbiology letters*, 147, pp.221–226.

De Koning-Ward, T. & Robins-Browne, R., 1996. Analysis of the urease gene complex of members of the genus *Yersinia*. *Gene*, 182(1-2), pp.225–228.

Koning-Ward, T. De & Robins-Browne, R., 1995. Contribution of urease to acid tolerance in *Yersinia enterocolitica*. *Infection and immunity*, 63(10).

Koschack, J., 2008. Standardabweichung und Standardfehler: der kleine, aber feine Unterschied. *ZFA - Zeitschrift für Allgemeinmedizin*, 84(6), pp.258–260.

Kredich, N.M., 1996. Biosynthesis of Cysteine. In F.C. Neidhardt, ed. *Escherichia coli and Salmonella*. ASM Press, pp. 514–524.

Krin, E., Danchin, A. & Soutourina, O., 2010. RcsB plays a central role in H-NS-dependent regulation of motility and acid stress resistance in *Escherichia coli. Research in microbiology*, 161(5), pp.363–71.

Liebeke, M. et al., 2011. A metabolomics and proteomics study of the adaptation of *Staphylococcus aureus* to glucose starvation. *Molecular bioSystems*, 7(4), pp.1241–53.

Lin, J. et al., 1995. Comparative analysis of extreme acid survival in *Salmonella typhimurium*, *Shigella flexneri*, and *Escherichia coli*. *Journal of bacteriology*, 177(14), pp.4097–104.

Lomax, M.S. & Greenberg, G.R., 1968. Characteristics of the deo operon: role in thymine utilization and sensitivity to deoxyribonucleosides. *Journal of bacteriology*, 96(2), pp.501–14.

Lorenz, M.C. & Fink, G.R., 2001. The glyoxylate cycle is required for fungal virulence. *Nature*, 412(6842), pp.83–6.

Majdalani, N., Vanderpool, C.K. & Gottesman, S., 2005. Bacterial small RNA regulators. *Critical reviews in biochemistry and molecular biology*, 40(2), pp.93–113.

Marceau, M., 2005. Transcriptional regulation in *Yersinia*: an update. *Current issues in molecular biology*, 7(2), pp.151–77.

Marcus, E.A. et al., 2005. The Periplasmic alpha-Carbonic Anhydrase Activity of *Helicobacter pylori* Is Essential for Acid Acclimation. *Journal Of Bacteriology*, 187(2), pp.729–738.

Marra, A. & Isberg, RR, 1997. Invasin-dependent and invasin-independent pathways for translocation of *Yersinia pseudotuberculosis* across the Peyer's patch intestinal epithelium. *Infection and immunity*, 65(8), pp.3412–3421.

Martinez-Jéhanne, V. et al., 2009. Role of deoxyribose catabolism in colonization of the murine intestine by pathogenic *Escherichia coli* strains. *Infection and immunity*, 77(4), pp.1442–50.

Maurelli, a T. et al., 1998. "Black holes" and bacterial pathogenicity: a large genomic deletion that enhances the virulence of *Shigella* spp. and enteroinvasive *Escherichia coli*. *Proceedings of the National Academy of Sciences of the United States of America*, 95(7), pp.3943–8.

McKinney, J D et al., 2000. Persistence of *Mycobacterium tuberculosis* in macrophages and mice requires the glyoxylate shunt enzyme isocitrate lyase. *Nature*, 406(6797), pp.735–8.

Mikulskis, a V & Cornelis, G R, 1994. A new class of proteins regulating gene expression in enterobacteria. *Molecular microbiology*, 11(1), pp.77–86.

Miller, J.H., 1992. *A short course in bacterial genetics*, Cold Spring Harbor Laboratory Press.

Mogk, A. et al., 2003. Small heat shock proteins, ClpB and the DnaK system form a functional triade in reversing protein aggregation. *Molecular Microbiology*, 50(2), pp.585–595.

Motin, V.L. et al., 2004. Temporal global changes in gene expression during temperature transition in *Yersinia pestis*. *Journal of bacteriology*, 186(18), p.6298.

Mouriño, M. et al., 1998. Osmolarity modulates the expression of the Hha protein from *Escherichia coli*. *FEMS microbiology letters*, 160(2), pp.225–9.

Mouriño, M. et al., 1996. The Hha protein as a modulator of expression of virulence factors in *Escherichia coli*. *Infection and immunity*, 64(7), pp.2881–4.

Muñoz-Elías, Ernesto J & McKinney, John D, 2006. Carbon metabolism of intracellular bacteria. *Cellular microbiology*, 8(1), pp.10–22.

Nagel, G, Lahrz, A. & Dersch, P, 2001. Environmental control of invasin expression in *Yersinia pseudotuberculosis* is mediated by regulation of RovA, a transcriptional activator of the SlyA/Hor family. *Molecular microbiology*, 41(6), pp.1249–69.

Nanchen, A. et al., 2008. Cyclic AMP-dependent catabolite repression is the dominant control mechanism of metabolic fluxes under glucose limitation in *Escherichia coli*. *Journal of bacteriology*, 190(7), pp.2323–30.

Neidhardt, F., 1963. Effects of environment on the composition of bacterial cells. *Annual Reviews in Microbiology*.

NEIDHARDT, F.C., 1963. EFFECTS OF ENVIRONMENT ON THE COMPOSITION OF BACTERIAL CELLS. F C Neidhardt, ed. *Annual review of microbiology*, 17, pp.61–86.

Neidhardt, F C, Schaechter, J.L. & Ingraham, M., 1990. *Physiology of the bacterial cell: a molecular approach*, Sinauer associates Inc.

Nuorti, J.P. et al., 2004. A widespread outbreak of *Yersinia pseudotuberculosis* O: 3 infection from iceberg lettuce. *Journal of Infectious Deseases*, 189(5), pp.766–74.

O'Donovan, G. a & Neuhard, J., 1970. Pyrimidine metabolism in microorganisms. *Bacteriological reviews*, 34(3), pp.278–343.

Oberhardt, M. a et al., 2008. Genome-scale metabolic network analysis of the opportunistic pathogen *Pseudomonas aeruginosa* PAO1. *Journal of bacteriology*, 190(8), pp.2790–803.

Oldiges, M. et al., 2007. Metabolomics: current state and evolving methodologies and tools. *Applied microbiology and biotechnology*, 76(3), pp.495–511.

Petersen, S. & Young, G., 2002. Essential Role for Cyclic AMP and Its Receptor Protein in *Yersinia enterocolitica* Virulence. *Infection and immunity*, 70(7), pp.3665–3672.

Phadtare, S & Inouye, Masayori, 2001. Role of CspC and CspE in regulation of expression of RpoS and UspA, the stress response proteins in *Escherichia coli*. *Journal of bacteriology*, 183(4), pp.1205–1214.

Phadtare, Sangita & Inouye, Masayori, 2004. Genome-wide transcriptional analysis of the cold shock response in wild-type and cold-sensitive, quadruple-csp-deletion strains of *Escherichia coli*. *Journal of bacteriology*, 186(20), pp.7007–7014.

Phadtare, Sangita, Inouye, Masayori & Severinov, K., 2002. The nucleic acid melting activity of *Escherichia coli* CspE is critical for transcription antitermination and cold acclimation of cells. *The Journal of biological chemistry*, 277(9), pp.7239–45.

Pieper, R. et al., 2009. Temperature and growth phase influence the outer-membrane proteome and the expression of a type VI secretion system in *Yersinia pestis*. *Microbiology (Reading, England)*, 155(Pt 2), pp.498–512.

Poncet, S. et al., 2009. Correlations between carbon metabolism and virulence in bacteria. *Bacterial Sensing and Signaling*, 16, pp.88–102.

Price, S.B., Freeman, M.D. & Yeh, K.S., 1995. Transcriptional analysis of the *Yersinia pestis* pH 6 antigen gene. *Journal of bacteriology*, 177(20), pp.5997–6000.

Prüß, B. et al., 2003. FlhD/FlhC is a regulator of anaerobic respiration and the Entner-Doudoroff pathway through induction of the methyl-accepting chemotaxis protein Aer. *Journal of bacteriology*, 185(2), pp.534–543.

Prüß, B., Markovic, D. & Matsumura, P, 1997. The *Escherichia coli* flagellar transcriptional activator flhD regulates cell division through induction of the acid response gene cadA. *Journal of bacteriology*, 179(11), pp.3818–3821.

Prüss, B.M. et al., 2001. FlhD/FlhC-regulated promoters analyzed by gene array and lacZ gene fusions. *FEMS microbiology letters*, 197(1), pp.91–7.

Pujol, C. & Bliska, J., 2003. The Ability To Replicate in Macrophages Is Conserved between *Yersinia pestis* and *Yersinia pseudotuberculosis*. *Infection and immunity*, 71(10), pp.5892–5899.

Quester, S. & Schomburg, D., 2011. EnzymeDetector: an integrated enzyme function prediction tool and database. *BMC bioinformatics*, 12(1), p.376.

Ramamurthi, K.S. & Schneewind, O., 2002. Type iii protein secretion in *yersinia* species. *Annual review of cell and developmental biology*, 18, pp.107–33.

Rath, D. & Jawali, N., 2006. Loss of expression of cspC, a cold shock family gene, confers a gain of fitness in *Escherichia coli* K-12 strains. *Journal of bacteriology*, 188(19), pp.6780–5.

Ray, K. et al., 2009. Life on the inside: the intracellular lifestyle of cytosolic bacteria. *Nature reviews. Microbiology*, 7(5), pp.333–40.

Rebeil, R. et al., 2004. Variation in lipid A structure in the pathogenic *yersiniae*. *Molecular microbiology*, 52(5), pp.1363–73.

Revell, P. a & Miller, V L, 2000. A chromosomally encoded regulator is required for expression of the *Yersinia enterocolitica inv* gene and for virulence. *Molecular microbiology*, 35(3), pp.677–85.

Richard, H. & Foster, J., 2004. *Escherichia coli* glutamate-and arginine-dependent acid resistance systems increase internal pH and reverse transmembrane potential. *Journal of bacteriology*, 186(18), pp.6032–6041.

Rickman, L. & Scott, C., 2005. Transcription regulators in *Mycobacterium tuberculosis* is required for virulence in mice and controls transcription of the rpfA gene coding for a resuscitation promoting. *Molecular microbiology*, 56(5), pp.1274–1286.

Rohmer, L., Hocquet, D. & Miller, S.I., 2011. Are pathogenic bacteria just looking for food? Metabolism and microbial pathogenesis. *Trends in microbiology*, 19(7), pp.341–8.

Romeo, T., 1998. Global regulation by the small RNA-binding protein CsrA and the non-coding RNA molecule CsrB. *Molecular microbiology*, 29(6), pp.1321–30.

Rosso, M.-L. et al., 2008. Growth of *Yersinia pseudotuberculosis* in human plasma: impacts on virulence and metabolic gene expression. *BMC microbiology*, 8, p.211.

Ruckdeschel, K., Deuretzbacher, A. & Haase, R., 2008. Crosstalk of signalling processes of innate immunity with *Yersinia* Yop effector functions. *Immunobiology*, 213(3-4), pp.261–9.

Sakharkar, K.R., Dhar, P.K. & Chow, V.T.K., 2004. Genome reduction in prokaryotic obligatory intracellular parasites of humans: a comparative analysis. *International journal of systematic and evolutionary microbiology*, 54(Pt 6), pp.1937–41.

Samant, S. et al., 2008. Nucleotide biosynthesis is critical for growth of bacteria in human blood. *PLoS pathogens*, 4(2), p.e37.

Sambrook, J., Fritsch, E.F. & Maniatis, T., 1989. *Molecular Cloning*, Cold Spring Harbor: Cold Spring Harbor Laboratory Press.

Sansonetti, P., 2002. Host-pathogen interactions: the seduction of molecular cross talk. *Gut*, 50 Suppl 3, pp.III2–8.

Schaible, U.E. & Kaufmann, S.H.E., 2005. A nutritive view on the host-pathogen interplay. *Trends in microbiology*, 13(8), pp.373–80.

Schmid, A. et al., 2009. Cross-talk between type three secretion system and metabolism in *Yersinia*. *Journal of Biological*, 284(18), pp.12165–12177.

Schneider, B.L., Kiupakis, a K. & Reitzer, L.J., 1998. Arginine catabolism and the arginine succinyltransferase pathway in *Escherichia coli*. *Journal of bacteriology*, 180(16), pp.4278–86.

Scholz, M et al., 2004. Metabolite fingerprinting: detecting biological features by independent component analysis. *Bioinformatics (Oxford, England)*, 20(15), pp.2447–54.

Scholz, M. & Selbig, J., 2006. Visualization and analysis of molecular data. In Wolfram Weckwerth, ed. *Metabolomics: methods and protocols. Methods in Molecular Biology Series*. New York: Humana Press, pp. 358:87–104.

Severi, E., Hood, D.W. & Thomas, G.H., 2007. Sialic acid utilization by bacterial pathogens. *Microbiology (Reading, England)*, 153(Pt 9), pp.2817–22.

Sezonov, G., Joseleau-Petit, D. & D'Ari, R., 2007. *Escherichia coli* physiology in Luria-Bertani broth. *Journal of bacteriology*, 189(23), pp.8746–9.

Shimada, T. et al., 2011. Novel roles of cAMP receptor protein (CRP) in regulation of transport and metabolism of carbon sources. *PloS one*, 6(6), p.e20081.

Simonet, M, Richard, S. & Berche, P., 1990. Electron microscopic evidence for in vivo extracellular localization of *Yersinia pseudotuberculosis* harboring the pYV plasmid. *Infection and immunity*, 58(3), pp.841–5.

Skaar, E.P., 2010. The battle for iron between bacterial pathogens and their vertebrate hosts. *PLoS pathogens*, 6(8), p.e1000949.

Skorupski, K. & Taylor, R.K., 1997. Cyclic AMP and its receptor protein negatively regulate the coordinate expression of cholera toxin and toxin-coregulated pilus in *Vibrio cholerae*. *Proceedings of the National Academy of Sciences of the United States of America*, 94(1), pp.265–70.

Skurnik, Mikael, 2003. Molecular genetics, biochemistry and biological role of *Yersinia* lipopolysaccharide. *Advances in experimental medicine and biology*, 529, pp.187–97.

Smith, K.S. et al., 1999. Carbonic anhydrase is an ancient enzyme widespread in prokaryotes. *Proceedings of the National Academy of Sciences of the United States of America*, 96(26), pp.15184–9.

Smyth, G., 2004. Linear Models and Empirical Bayes Methods for Assessing Differential Expression in Microarray Experiments. *Statistical Applications in Genetics and Molecular Biology*, 3(1).

Somerville, G. a & Proctor, R. a, 2009. At the crossroads of bacterial metabolism and virulence factor synthesis in *Staphylococci. Microbiology and molecular biology reviews : MMBR*, 73(2), pp.233–48.

Somerville, G.A. et al., 2003. Correlation of Acetate Catabolism and Growth Yield in *Staphylococcus aureus* : Implications for Host-Pathogen Interactions. , 71(8), pp.4724–4732.

Speck, J.J., 1958. The Lobry de Bruyn-Alberda van Ekenstein transformation. *Adv. Carbohydra. Chem*, 13, pp.63–103.

Stanier, R.Y., Palleroni, N.J. & Doudoroff, M., 1966. The aerobic pseudomonads: a taxonomic study. *Journal of general microbiology*, 43(2), pp.159–271.

Stenseth, N.C. et al., 2008. Plague: past, present, and future. *PLoS medicine*, 5(1), p.e3.

Steuer, R. et al., 2003. Observing and interpreting correlations in metabolomic networks. *Bioinformatics*, 19(8), pp.1019–1026.

Strøm, a R. & Kaasen, I., 1993. Trehalose metabolism in *Escherichia coli*: stress protection and stress regulation of gene expression. *Molecular microbiology*, 8(2), pp.205–10.

Suomalainen, M. et al., 2010. Temperature-induced changes in the lipopolysaccharide of *Yersinia pestis* affect plasminogen activation by the pla surface protease. *Infection and immunity*, 78(6), pp.2644–52.

Sutherland, I., 2001. Biofilm exopolysaccharides: a strong and sticky framework. *Microbiology (Reading, England)*, 147(Pt 1), pp.3–9.

Tauxe, R. V, 2004. Salad and pseudoappendicitis: *Yersinia pseudotuberculosis* as a foodborne pathogen. *The Journal of infectious diseases*, 189(5), pp.761–3.

Thomson, N.R. et al., 2006. The complete genome sequence and comparative genome analysis of the high pathogenicity *Yersinia enterocolitica* strain 8081. *PLoS genetics*, 2(12), p.e206.

Timmermans, J. & Van Melderen, L., 2009. Conditional essentiality of the csrA gene in *Escherichia coli*. *Journal of bacteriology*, 191(5), pp.1722–4.

Tran, H.J. et al., 2005. Analysis of RovA, a transcriptional regulator of *Yersinia pseudotuberculosis* virulence that acts through antirepression and direct transcriptional activation. *The Journal of biological chemistry*, 280(51), pp.42423–32.

Tsai, J.C. et al., 2010. The bacterial intimins and invasins: a large and novel family of secreted proteins. *PloS one*, 5(12), p.e14403.

Tsukano, H et al., 1999. *Yersinia pseudotuberculosis* blocks the phagosomal acidification of B10.A mouse macrophages through the inhibition of vacuolar H(+)-ATPase activity. *Microbial pathogenesis*, 27(4), pp.253–63.

Vadyvaloo, V. et al., 2010. Transit through the flea vector induces a pretransmission innate immunity resistance phenotype in *Yersinia pestis*. *PLoS pathogens*, 6(2), p.e1000783.

Valdivia, R.H., 1997. Fluorescence-Based Isolation of Bacterial Genes Expressed Within Host Cells. *Science*, 277(5334), pp.2007–2011.

VanDusen, W.J. et al., 1997. Adenine quantitation in yeast extracts and fermentation media and its relationship to protein expression and cell growth in adenine auxotrophs of *Saccharomyces cerevisiae*. *Biotechnology progress*, 13(1), pp.1–7.

Vemuri, G., Altman, E. & Sangurdekar, D., 2006. Overflow metabolism in *Escherichia coli* during steady-state growth: transcriptional regulation and effect of the redox ratio. *Applied and environmental microbiology*, 72(5), pp.3653–3661.

Vendeville, A. et al., 2005. Making “sense” of metabolism: autoinducer-2, LuxS and pathogenic bacteria. *Nature reviews. Microbiology*, 3(5), pp.383–96.

Viboud, G.I. & Bliska, James B, 2005. Yersinia outer proteins: role in modulation of host cell signaling responses and pathogenesis. *Annual review of microbiology*, 59, pp.69–89.

Villas-Bôas, S. et al., 2007. Data standardization (normalization). In S. G. Villas-Bôas, ed. *METABOLOME ANALYSIS, An Introduction*. New Jersey: John Wiley & Sons, pp. 167–168.

Vogel-Scheel, J. et al., 2010. Requirement of purine and pyrimidine synthesis for colonization of the mouse intestine by *Escherichia coli*. *Applied and environmental microbiology*, 76(15), pp.5181–7.

Wang, Z., Gerstein, M. & Snyder, M., 2009. RNA-Seq: a revolutionary tool for transcriptomics. *Nature Reviews Genetics*, 10(1), pp.57–63.

Wei, B.L. et al., 2001. Positive regulation of motility and flhDC expression by the RNA-binding protein CsrA of *Escherichia coli*. *Molecular microbiology*, 40(1), pp.245–56.

White-Ziegler, C. a & Davis, T.R., 2009. Genome-wide identification of H-NS-controlled, temperature-regulated genes in *Escherichia coli* K-12. *Journal of bacteriology*, 191(3), pp.1106–10.

WHO, 2010. Human plague: review of regional morbidity and mortality, 2004-2009. *Wkly Epidemiol Rec*, 85(6), pp.37–48.

Wortham, B.W. & Oliveira, M.A., 2010. Polyamines are required for the expression of key Hms proteins important for *Yersinia pestis* biofilm formation. *Environmental*, 12(7), pp.2034–2047.

Wortham, B.W., Oliveira, M.A. & Patel, C.N., 2007. Polyamines in Bacteria: Pleiotropic Effects yet Specific Mechanisms. *Advances in experimental medicine and biology*, 603, pp.106–115.

Yamanaka, K. & Inouye, M, 1997. Growth-phase-dependent expression of cspD, encoding a member of the CspA family in *Escherichia coli*. *Journal of bacteriology*.

Yang, Y. et al., 1996. The psa locus is responsible for thermoinducible binding of *Yersinia pseudotuberculosis* to cultured cells. *Infection and immunity*, 64(7), pp.2483–9.

Zhan, L. et al., 2008. The cyclic AMP receptor protein, CRP, is required for both virulence and expression of the minimal CRP regulon in *Yersinia pestis* biovar microtus. *Infection and immunity*, 76(11), pp.5028–37.

Supplementary material

A.1 Supernatant analysis of Y. pseudotuberculosis *grown in glucose minimal medium*

Semiquantitative peak areas (mean: $\bar{x}$, n = 6 biological replicates), relative standard error Se, ratio between values of the exponential/ stationary phase and the p-value of a two-tailed Student's Ttest

Metabolites	$\bar{x}$ (exponential)	Se (exponential) [%]	$\bar{x}$ (stationary)	Se (stationary) [%]	Ratio (stat/exp)	Ttest p-value
2-amino-2-deoxy-gluconate	2218517	4.55	0	0,00	0.00	8,51E-010
2-hydroxy-glutarate	117363	2.75	259516	2,42	2.21	2.00E-09
2-isopropylmalate	33056	12.97	191496	2,66	5.79	3.93E-10
alanine	0	0.00	10919299	4,50		7.56E-10
asparagine	313101	2.71	764646	4,88	2.44	3.41E-07
ethanolamine	114912	3.69	551895	13,97	4.80	2.10E-04
fructose	113618	8.69	0	0,00	0.00	4.32E-07
glucarate-1,4-lactone	1221412	3.43	0	0,00	0.00	5.24E-11
glucose	99740417	9.04	6687	50,15	0.00	6.25E-07
glycerol-3-phosphate	0	0.00	4821	35,94		1.94E-02
glycine	0	0.00	35807	32,73		1.21E-02
hexadecanoate	62307	1.66	59362	4,78	0.95	3.52E-01
hexose_1	177513	3.83	31343	35,04	0.18	5.06E-07
hexose_2	111036	9.84	0	0,00	0.00	1.37E-06
hexose_3	1068339	5.78	31343	35,04	0.03	1.37E-08
hexose_4	249247	10.84	0	0.00	0.00	3.32E-06
lactate	2239312	2.58	4949299	9,64	2.21	2.16E-04
melibiose	79906	4.35	56861	6,34	0.71	5.00E-02
NA_1871.54	515281	5.64	0	0,00	0.00	6.92E-09
NA321	2170659	8.79	0	0,00	0.00	4.84E-07
NA369	528058	10.36	0	0,00	0.00	2.20E-06
NA381	1035824	8.33	103450	22,58	0.10	1.08E-06
NA392	132172	12.84	0	0,00	0.00	1.49E-05
octadecanoate	48557	3.43	44078	3,48	0.91	7.58E-02
oxalate	1334916	3.56	1287238	0,89	0.96	3.53E-01
pentose	44597	3.16	138593	2,36	3.11	1.43E-10
phosphate	88717737	7.69	108198998	6,36	1.22	7.20E-02
pyruvate	393904	2.97	1064214	10,65	2.70	1.55E-04
Unknown#bth-pae-013_1169.8	591907	3.89	607551	2,32	1.03	5.75E-01
Unknown#mse_ypy_1552.88	0	0.00	85737	6,05		1.37E-08
valine	26237	66.33	5768179	5,55	219.85	6.33E-09

A.2 Metabolome analysis of Y. pseudotuberculosis *grown in glucose minimal medium*

Semiquantitative peak areas (mean: $\bar{x}$, n = 6 biological replicates), relative standard error Se, ratio between values of the exponential/ stationary phase and the p-value of a two-tailed Student's Ttest

Metabolites	$\bar{x}$ (exponential)	Se (exponential) [%]	$\bar{x}$ (stationary)	Se (stationary) [%]	Ratio (exp/stat)	Ttest p-value
1,6-anhydro-glucose	412341	5.38	0	0.00	0.00	4.36E-09

Metabolites	$\bar{x}$ (exponential)	Se (exponential) [%]	$\bar{x}$ (stationary)	Se (stationary) [%]	Ratio (exp/stat)	Ttest p-value
2,3-bisphosphoglycerate	1241191	29.31	664802	32.58	0.54	2.03E-01
2,6-diamino-pimelate	403268	4.38	7014	100.00	0.02	1.42E-09
2-amino-2-deoxy-glucose-6-phosphate	158493	43.11	0	0.00	0.00	4.28E-02
2-hydroxy-glutarate	3197239	7.32	93354	72.53	0.03	1.67E-07
2-phosphoglycerate	942344	7.65	371051	29.16	0.39	1.35E-03
3-hydroxy-tetradecanoate	984183	6.12	2052235	6.86	2.09	3.84E-05
5-amino-levulinate	198599	10.68	150727	13.92	0.76	1.40E-01
5-methylthio-adenosine	1599389	4.77	2725152	7.08	1.70	2.91E-04
6-phospho-gluconate	1401678	11.72	2118489	15.97	1.51	8.57E-02
9-(Z)-octadecenoate	361335	17.77	538105	33.60	1.49	3.79E-01
adenine	426495	65.47	1745730	21.74	4.09	1.88E-02
adenosine	394123	22.49	408618	32.65	1.04	9.30E-01
adenosine-3'-monophosphate	368633	8.29	11568	100.00	0.03	7.00E-07
alanine	159354980	4.85	168677160	43.45	1.06	9.02E-01
alanyl-alanine	3752265	5.01	29398269	6.56	7.83	1.15E-07
AMP	21209965	4.82	15005630	5.04	0.71	6.46E-04
asparagine	1361232	6.85	1450546	11.58	1.07	6.52E-01
aspartate	22501671	4.56	20344579	3.62	0.90	1.18E-01
beta-Alanine	259570	31.72	604470	4.53	2.33	2.62E-03
borate	308614	32.91	269085	50.97	0.87	8.22E-01
citrate	636706	3.48	1359551	14.80	2.14	5.10E-03
cysteine	47975	100.00	427884	33.03	8.92	2.91E-02
cytosine	464814	9.13	1163	100.00	0.00	7.03E-07
D235202_2358.8	8716152	4.62	13813353	6.90	1.58	5.98E-04
D256464_2570.76	1459430	5.92	1335873	22.04	0.92	6.96E-01
dodecanoate	676895	5.19	1192893	33.32	1.76	2.25E-01
ethanolamine	2356613	11.65	3863294	15.27	1.64	4.31E-02
fumarate	7424866	9.23	5963928	12.56	0.80	1.81E-01
galactose-6-phosphate	135406	32.50	0	0.00	0.00	1.17E-02
galacturonate-1-phosphate	1210960	3.86	1156457	29.22	0.95	8.76E-01
glucose	2734050	5.37	1813104	8.45	0.66	1.46E-03
glucose-6-phosphate	8182156	12.98	1990369	5.39	0.24	1.73E-04
glutamate	40026346	4.01	59536607	5.12	1.49	2.07E-04
glutamine	28149013	5.20	19088485	10.59	0.68	4.61E-03
glycerate-3-phosphate	11630739	5.72	6807922	9.08	0.59	3.42E-04
glycerol	2152532	9.63	1948089	14.94	0.91	5.80E-01
glycerol-3-phosphate	2367383	10.62	2785254	16.87	1.18	4.51E-01
glycine	7240296	6.63	8375357	10.23	1.16	2.75E-01
guanosine	1107960	22.17	0	0.00	0.00	1.12E-03
guanosine-5-monophosphate	2676762	5.87	2144955	14.99	0.80	1.68E-01
hexadecanoate	2086209	9.45	4229953	8.89	2.03	5.00E-04
homoserine	1783354	3.04	833492	27.86	0.47	2.58E-03
hydrogen sulfide	835044	12.56	1506343	8.85	1.80	2.70E-03
hydroxylamine	30922	26.57	22599	36.56	0.73	4.91E-01
hypoxanthine	1224192	9.03	395906	33.22	0.32	7.01E-04
indole-3-lactate	17325	48.60	28118	30.62	1.62	3.91E-01
inosine	500055	7.39	371173	22.95	0.74	1.95E-01
isoleucine	12090298	14.84	28070964	4.22	2.32	2.23E-05
lactate	82123282	31.97	6620363	27.13	0.08	1.67E-02
lysine	9470645	4.92	95812351	9.36	10.12	2.28E-06
malate	17336233	3.04	11158694	5.80	0.64	2.32E-05
mannose	445187	5.52	826241	11.45	1.86	2.96E-03
mannose-6-phosphate	348244	30.22	106427	23.98	0.31	4.96E-02
NA192001_258	15482843	8.22	1536364	34.93	0.10	1.45E-06
NA203	2218349	17.82	1117409	29.84	0.50	5.91E-02
NA226	3821185	4.33	2351047	9.56	0.62	3.64E-04
n-hexadecenoate	704587	20.73	1258635	35.84	1.79	2.70E-01
Nicotinamide	4317990	3.09	6161064	5.99	1.43	8.47E-04
ornithine	2744342	10.63	1811423	10.63	0.66	2.36E-02
phosphate	16392750	48.82	102489094	5.23	6.25	4.28E-08
phosphoenolpyruvate	1291260	6.81	0	0.00	0.00	4.41E-06
phosphorate monomethyl ester	2673033	10.57	3006977	24.35	1.12	6.79E-01
putrescine	40590181	4.67	49292299	10.54	1.21	1.47E-01
pyroglutamate	16701067	5.10	22382446	8.42	1.34	1.13E-04
pyrophosphate	6320401	8.44	2658960	10.20	0.42	2.06E-02
pyruvate	13985	47.60	1209966	44.89	86.52	5.23E-02
ribose	447284	22.03	0	0.00	0.00	1.08E-03
serine	644605	31.97	569849	60.17	0.88	8.56E-01
similar to Guanine	2412236	8.13	665405	22.55	0.28	3.41E-05
succinate	5398046	8.59	2894871	13.23	0.54	1.94E-03
threonine	8098494	4.94	6258205	5.63	0.77	6.21E-03
tryptophan	1840640	5.66	1264243	63.30	0.69	4.91E-01

Metabolites	$\bar{x}$ (exponential)	Se (exponential) [%]	$\bar{x}$ (stationary)	Se (stationary) [%]	Ratio (exp/stat)	Ttest p-value
tyrosine	10732798	10.01	8622987	5.35	0.80	1.01E-01
Unknown#bth-pae-039_1586.10	1025699	13.97	9018926	5.08	8.79	1.27E-08
Unknown#bth-pae-065_1466.3	2267295	6.98	3243848	7.92	1.43	8.92E-03
unknown#mse_ypy_2290.5	903937	4.02	1073142	27.57	1.19	5.83E-01
unknown#mse-ypy_2359.52	1157691	7.52	2060500	10.46	1.78	3.04E-03
Unknown#mse-ypy-001_1846.10	3074512	5.58	3771992	8.26	1.23	7.84E-02
Unknown#mse-ypy-002_1_2922.5	13667141	3.94	19341905	7.64	1.42	4.77E-03
Unknown#mse-ypy-002_2_2955.2	48536197	4.83	66930413	8.26	1.38	1.20E-02
Unknown#mse-ypy-009_1493.1	2466954	7.28	6150860	7.17	2.49	1.58E-05
Unknown#mse-ypy-017_1896.3	233344	6.97	532185	10.24	2.28	3.71E-04
Unknown#mse-ypy-018_2013.3	293374	8.33	407819	10.22	1.39	3.93E-02
Unknown#mse-ypy-021_2090.5	603797	3.39	308715	12.60	0.51	5.28E-05
Unknown#mse-ypy-026_2236.9	161925	11.63	94262	32.47	0.58	8.91E-02
Unknown#mse-ypy-027_2269.3	783395	6.35	141785	6.56	0.18	1.73E-07
Unknown#mse-ypy-031_1878.9	3848327	12.91	2316949	9.65	0.60	1.85E-02
Unknown#mse-ypy-034_1540.6	5434458	7.24	7446227	11.40	1.37	5.70E-02
Unknown#mse-ypy-036_1981.10	0	0.00	187632	10.70		2.96E-06
Unknown#mse-ypy-038_1545.6	3947684	7.45	5199607	9.76	1.32	5.86E-02
Unknown#mse-ypy-2830.40	3514459	5.61	1270946	14.73	0.36	8.95E-06
Unknown#sst-cgl-078_1847.4	281047	4.90	1619807	8.70	5.76	2.66E-06
Unknown#sst-cgl-116_2331.9	4630126	6.04	5117726	11.46	1.11	4.70E-01
Unknown#sst-cgl-119_2551.5	1411463	6.26	0	0.00	0.00	1.92E-08
Uracil	3071195	17.80	146769	17.77	0.05	3.27E-04
uridine 5'-monophosphate	2972676	8.26	457269	32.31	0.15	5.17E-06
valine	64526745	5.35	158223782	2.72	2.45	1.07E-08
xylulose-5-phosphate	93301	5.46	62091	5.67	0.67	5.08E-04

B.1 Supernatant analysis of Y. pseudotuberculosis *grown in LB medium*

Semiquantitative peak areas (mean: $\bar{x}$, n = 6 biological replicates), relative standard error Se

Metabolite	$\bar{x}$ (t=0 h)	Se (t=0 h)[%]	$\bar{x}$ (t=2.5 h)	Se (t=2.5 h)[%]	$\bar{x}$ (t=5.5 h)	Se (t=5.5 h)[%]	$\bar{x}$ (t=12.0 h)	Se (t=12 h)[%]	$\bar{x}$ (t=15 h)	Se (t=15 h)[%]
2-hydroxy-glutarate	33871	2.20	44593	15.63	67904	11.65	86139	4.42	94391	5.93
3-hydroxybutanoate	414876	1.82	611418	1.14	525182	8.65	428035	5.64	423902	2.83
4-aminobutanoate	28496	3.65	35233	11.13	29241	7.39	18843	5.81	19843	8.02
5-amino-levulinate	156059	2.88	194496	14.46	100005	9.67	4812	50.00	4814	55.22
adenine	45426	2.53	13526	50.72	0	0.00	0	0.00	11975	50.12
adenosine	183430	2.39	41873	19.38	0	0.00	0	0.00	0	0.00
alanine	9146395	6.32	13457815	2.10	10979784	9.76	488941	20.12	120861	55.77
asparagine	826826	2.54	911987	16.74	441788	9.63	39490	22.92	28766	15.64
aspartate	2803186	5.43	2703650	11.94	119874	28.49	53590	7.27	46548	19.51
beta-alanine	2745	3.25	3909	9.91	4249	14.69	3964	5.64	2577	3.68
butylamine	1266777	5.46	1888753	1.94	1609561	10.09	1345985	5.66	1339539	2.98
citrate	85099	4.08	87003	14.58	43184	9.37	0	0.00	0	0.00
cyanamide	509827	8.21	647091	11.24	429576	10.37	251084	11.19	314087	4.27
cysteine	57098	2.64	52187	53.22	32013	50.01	0	0.00	0	0.00
D116201_1172.88	37738	14.40	49415	3.07	45661	10.29	42350	3.30	36151	3.21
diisopropanolamine	91141	4.98	131421	5.76	110315	14.64	75493	3.81	68439	2.00
erythronate	164025	23.06	136636	10.48	92882	7.34	62511	11.30	125104	54.46
ethanolamine	919885	6.92	1450127	0.38	1352284	9.61	1193007	4.75	1241211	4.08
fructose	75132	3.19	0	0.00	0	0.00	0	0.00	0	0.00
fumarate	23156	11.94	96670	22.98	76852	4.06	13456	21.53	14963	10.14
glucose	73184	5.31	105903	16.54	77746	7.66	44624	4.53	46077	10.19
glutamate	2346569	5.81	3338325	3.21	2067952	9.16	3462	19.51	15101	77.12
glycerate	28663	4.16	0	0.00	0	0.00	0	0.00	0	0.00
glycerol	798760	4.26	893902	12.19	39787	21.83	26928	8.30	30427	8.31
glycerol-3-phosphate	52780	2.19	84715	17.41	85445	11.35	63960	6.49	66093	13.99
glycine	1706690	5.05	2456516	1.99	2233915	10.45	167344	14.77	267380	88.99
glycolate	7413	55.06	16754	4.14	14862	5.81	6593	50.01	6237	9.51
guanosine	121148	5.96	94475	50.00	0	0.00	0	0.00	0	0.00
hexadecanoate	55646	3.59	82260	1.03	70955	13.28	79189	5.16	83294	9.70
Hexose_1	91657	7.17	121587	10.71	95302	14.10	55826	6.21	62764	10.75
Hexose_2	3965	1.79	108156	14.98	18219	84.17	12274	90.24	24354	47.36
homocysteine	22411	2.33	11958	0.00	6421	100.00	0	0.00	0	0.00
hydroxylamine	52994	71.04	61856	60.21	55834	50.97	10754	66.19	14562	41.17
hypoxanthine	20255	18.97	69645	33.57	0	0.00	0	0.00	0	0.00

Metabolite	$\bar{x}$ (t=0 h)	Se (t=0 h)[%]	$\bar{x}$ (t=2.5 h)	Se (t=2.5 h)[%]	$\bar{x}$ (t=5.5 h)	Se (t=5.5 h)[%]	$\bar{x}$ (t=12.0 h)	Se (t=12 h)[%]	$\bar{x}$ (t=15 h)	Se (t=15 h)[%]
idose	720316	2.85	137191	35.41	78848	4.57	1974673	4.25	2055297	3.23
inosine	0	0.00	87007	17.56	0	0.00	0	0.00	0	0.00
isoleucine	6190410	6.18	8957711	2.24	7430286	9.73	4081507	50.47	6346609	1.51
lactate	996604	0.46	1449055	8.20	1330300	7.83	452988	1.50	328865	10.86
lactate dimer	34883	2.86	54808	3.93	42644	10.31	34319	5.41	14284	80.94
leucine	510784	11.64	969113	13.78	681775	19.44	404681	15.21	321385	21.05
lysine	5487921	6.12	7826714	3.74	6461955	8.67	4808954	4.87	5111401	4.60
malate	71187	2.62	154787	11.08	155875	11.55	6927	2.54	7177	15.75
maltose	4162342	7.08	5740364	3.15	1348793	56.60	62944	29.77	40993	100.00
mannose	626475	2.81	8808	50.69	0	0.00	0	0.00	0	0.00
methionine sulfoxide	72474	4.06	86167	18.92	62883	9.20	30993	14.03	28789	23.17
myo-inositol	108542	4.43	137062	12.55	106729	8.53	67254	6.48	69984	8.63
NA_1133.83	44509	10.13	67262	3.32	57970	10.73	44307	4.81	39817	8.50
NA_1470.1	105502	33.36	100277	6.95	88679	9.64	95111	4.60	94157	4.25
NA_1705.4	74419	4.88	92580	10.09	68391	8.90	33956	6.25	28407	0.21
NA_2615.1	58379	4.34	78496	18.06	56839	10.68	33115	6.18	33780	11.56
NA100	68981	6.45	94058	3.76	77628	14.58	52692	1.96	54999	9.19
NA106	43928	42.66	90143	3.03	75786	9.28	60967	4.40	61452	5.74
NA109003_(classified_unknown)_1104.97	0	0.00	0	0.00	0	0.00	42658	18.17	49353	7.33
NA114002_(classified_unknown)_1144.3	418346	43.15	832224	1.96	673467	9.53	375377	39.73	564875	4.49
NA137012_(classified_unknown)_1388.87	46087	6.06	66922	4.57	47252	8.23	33102	6.71	32259	5.01
NA184030_(classified_unknown)_1848.26	192468	5.01	261680	14.17	213165	9.77	127476	5.59	133060	8.35
NA192001 (classified unknown)257	98611	3.47	0	0.00	0	0.00	0	0.00	0	0.00
N-acetyl-serine	0	0.00	0	0.00	0	0.00	37423	1.88	37101	2.62
octadecanoate	74838	4.83	113337	3.95	84108	12.75	74761	6.53	77389	10.89
ornithine	266250	37.13	450736	17.82	299797	10.62	158803	42.24	235288	8.51
phenylalanine	4134733	5.80	5783536	4.01	5223949	11.27	3308864	4.71	3466665	3.70
phosphorate	2265265	6.23	3253925	2.42	2533035	9.55	1821682	4.57	1851751	5.30
putrescine	4331	59.14	78080	10.96	89254	14.49	39182	50.88	88018	13.05
pyruvate	0	0.00	239297	13.72	0	0.00	0	0.00	0	0.00
serine	4487211	5.72	4604935	9.83	149597	31.46	70554	20.60	54581	25.07
succinate	96615	2.89	182279	14.24	144758	12.35	3591	29.45	3291	3.48

Metabolite	$\bar{x}$ (t=0 h)	Se (t=0 h)[%]	$\bar{x}$ (t=2.5 h)	Se (t=2.5 h)[%]	$\bar{x}$ (t=5.5 h)	Se (t=5.5 h)[%]	$\bar{x}$ (t=12.0 h)	Se (t=12 h)[%]	$\bar{x}$ (t=15 h)	Se (t=15 h)[%]
threonine	2283512	5.12	2896072	7.63	1328263	10.53	13766	71.62	20653	52.49
thymine	0	0.00	5741	0.00	7050	100.00	16444	0.29	19961	59.26
tryptophan	3392434	4.39	4544126	12.41	3177386	9.91	1759160	7.17	1911849	9.81
tyrosine	6475461	5.23	8763110	6.15	6737901	8.83	3988864	6.54	4365163	7.66
Unknown#bth-pae-013_1169.8	98223	6.50	154512	6.12	120896	9.68	71191	8.11	78528	3.02
Unknown#mse-ypy_1227	314596	2.16	482601	3.24	381719	11.08	298277	4.19	288882	5.61
Unknown#mse-ypy_1381	217455	6.95	318618	4.30	245230	6.79	214040	2.59	200247	5.26
Unknown#mse-ypy_2600	72581	3.65	66371	54.39	0	0.00	0	0.00	0	0.00
Unknown#mse-ypy-004_1302.5	3442	15.14	2107	0.00	477	0.00	598	100.00	1565	100.00
Unknown#mse-ypy-006_1744.2	0	0.00	0	0.00	0	0.00	47828	7.68	45981	50.96
Unknown#mse-ypy-016_1793.3	81528	14.54	91457	13.10	68889	12.82	47707	7.85	70146	22.58
Unknown#sst-cgl-023_1411.8	84682	5.86	119648	7.11	91138	11.93	75795	11.74	72772	4.14
Uracil	65987	6.69	126593	17.34	19211	82.86	15292	9.73	37389	11.93
valine	4978066	7.00	7109717	3.30	6122318	10.30	4957749	2.43	4982196	2.22

B.2 Metabolome analysis of Y. pseudotuberculosis *grown in LB medium*

Semiquantitative peak areas (mean: $\bar{x}$, n = 6 biological replicates), relative standard error Se, ratio between values of the exponential/ stationary phase and the p-value of a two-tailed Student's Ttest

Metabolites	$\bar{x}$ (exponential)	Se (exponential) [%]	$\bar{x}$ (stationary)	Se (stationary) [%]	Ratio (stat/exp)	Ttest p-value
2-aminoadipic-acid	56628	7.29	1607117	8.57	28.38	5.56E-07
2-hydroxy-glutarate	3017829	23.86	368150	9.16	0.12	8.86E-03
2-methyl-citrate	2172903	5.94	2657558	2.76	1.22	1.32E-02
3-amino-propane-1,2-diol	0	0.00	628573	11.01		3.40E-06
3-hydroxybutanoate	7366682	8.08	5741396	15.33	0.78	1.50E-01
3-hydroxy-tetradecanoic-acid	2256478	8.74	3925850	22.12	1.74	7.04E-02
5-methylthio-adenosine	595102	2.45	510221	8.45	0.86	7.48E-02
9-(Z)-octadecenoate	1197514	22.08	175096	5.66	0.15	6.76E-03
adenine	1283272	8.24	1009327	16.57	0.79	1.85E-01
alanine	24532378	12.45	28871949	15.31	1.18	4.28E-01
AMP	12447765	10.13	4767090	12.96	0.38	6.33E-04
asparagine	347064	35.16	1307731	6.32	3.77	1.53E-04
aspartate	5805848	10.00	35702440	10.52	6.15	1.16E-05
beta-alanine	188786	14.93	182141	7.73	0.96	8.48E-01
butylamine	26212345	7.90	19597759	13.65	0.75	7.81E-02
citrate	1013563	5.11	280315	5.31	0.28	5.59E-07
D116201_1172.88	792807	12.23	518338	7.88	0.65	3.85E-02
dodecanoate	952072	4.83	645667	8.38	0.68	1.86E-03
ethanolamine	21520517	7.99	19663374	3.96	0.91	3.83E-01
fructose-1,6-bisphosphate	216245	32.91	641633	15.98	2.97	6.70E-03
fructose-6-phosphate	313842	13.32	44409	41.35	0.14	3.87E-04
fumarate	10441605	15.39	2416720	12.54	0.23	1.56E-03
glucose	2332668	4.46	192779	17.34	0.08	2.31E-08
glucose-6-phosphate	1100220	8.70	676441	6.90	0.61	4.77E-03
glutamate	43998317	8.82	39438786	9.47	0.90	4.25E-01
glutamine	12914873	23.02	2845557	15.48	0.22	1.40E-02
glycerate-3-phosphate	7459576	15.19	6485316	6.93	0.87	4.78E-01
glycerol	4061827	18.25	30512904	16.35	7.51	2.66E-04
glycerol-3-phosphate	1696675	10.96	1409810	31.41	0.83	5.39E-01
glycine	4124037	7.75	1610459	26.42	0.39	9.53E-04
heptadecanoate	0	0.00	681349	19.36		2.86E-04
hexadecanoate	4338753	15.93	1222318	7.39	0.28	2.86E-03
homocysteine	0	0.00	458403	17.95		1.65E-04
homoserine	433578	16.81	685572	10.02	1.58	3.51E-02
inosine	365448	7.18	319727	5.35	0.87	1.97E-01
isoleucine	33647274	8.13	53088669	26.07	1.58	1.65E-01
lactate	28802181	10.85	4202489	18.79	0.15	6.51E-05
lactate dimer	833647	6.47	294272	15.25	0.35	3.76E-05
lysine	64895911	10.28	125466437	3.98	1.93	6.29E-05
malate	8761143	7.30	2245984	13.40	0.26	1.24E-05
myo-inositol	623365	5.34	450666	8.67	0.72	8.04E-03
N,N-dimethylglycine	0	0.00	20440171	18.31		1.90E-04
NA_1133.83	817632	8.13	679696	17.77	0.83	3.22E-01
NA114002_(classified_unknown)_1144.3	9847825	5.84	9045658	11.56	0.92	4.99E-01
NA184	0	0.00	884206	3.96		4.64E-10
NA192001 (classified unknown)257	2849834	8.31	53837489	4.43	18.89	2.18E-09
NA203	3741460	13.52	2400725	6.31	0.64	4.49E-02
NA226	2172903	5.94	1064414	6.79	0.49	5.90E-05
NA411	0	0.00	2730926	32.73		8.07E-03
NA438	0	0.00	972470	11.71		5.66E-06
Nicotinamide	3234292	6.27	2081132	30.25	0.64	9.16E-02
nonanoate	159365	12.74	52729	26.70	0.33	2.54E-03
ornithine	1250209	28.53	10431357	5.57	8.34	2.05E-07
phenylalanine	4614737	44.98	18988005	4.16	4.11	2.07E-04
phosphate	86236452	5.82	66142420	15.73	0.77	9.85E-02
phosphate monomethyl ester	1171640	32.98	1631983	17.85	1.39	3.83E-01
phosphoenolpyruvate	1397560	8.27	1016408	12.46	0.73	5.33E-02
propane-1,3-diamine	183956	14.92	22082	48.07	0.12	6.55E-04
putrescine	79825533	4.83	40483025	6.47	0.51	2.05E-05

Metabolites	$\bar{x}$ (exponential)	Se (exponential) [%]	$\bar{x}$ (stationary)	Se (stationary) [%]	Ratio (stat/exp)	Ttest p-value
Pyroglutamate	15019984	7.56	11676014	9.49	0.78	6.68E-02
pyrophosphate	9487415	15.23	4360523	6.50	0.46	1.14E-02
pyruvate	1298733	12.23	645906	18.74	0.50	1.16E-02
spermidine	1014975	26.56	169784	2.24	0.17	1.95E-02
succinate	12280406	20.22	3301351	11.91	0.27	1.01E-02
succinate-methylester	402684	7.67	493679	13.07	1.23	2.11E-01
threonine	1649626	7.56	1270098	6.03	0.77	3.61E-02
tryptamine	799828	40.04	3255233	8.58	4.07	3.14E-04
tyrosine	14953068	10.01	46831421	5.09	3.13	9.30E-07
Unknown#bth-pae-001_972.8	6176451	10.85	3604294	15.64	0.58	1.87E-02
Unknown#bth-pae-013_1169.8	697950	7.13	950043	6.37	1.36	9.94E-03
Unknown#bth-pae-038_1567.3	0	0.00	653331	14.58		3.34E-05
unknown#mse_ypy-2740	679270	7.37	790868	9.55	1.16	2.36E-01
unknown#mse-ypy_1227	5484213	7.93	4156892	15.91	0.76	1.17E-01
unknown#mse-ypy_1634	1152772	16.36	1425315	14.58	1.24	3.57E-01
unknown#mse-ypy_2152.93	1951520	20.46	995588	10.75	0.51	6.35E-02
unknown#mse-ypy_2359.51	125485	79.43	403817	5.11	3.22	3.44E-02
unknown#mse-ypy_2600	0	0.00	1430884	6.52		3.80E-08
Unknown#mse-ypy-001_1846.9	763946	10.63	440120	9.39	0.58	8.79E-03
Unknown#mse-ypy-002_1_2922.4	2562928	9.05	4081308	11.94	1.59	1.54E-02
Unknown#mse-ypy-002_2_2955.1	6817684	8.76	6286523	9.18	0.92	5.43E-01
Unknown#mse-ypy-004_1302.5	284103	5.70	142812	23.63	0.50	3.12E-03
Unknown#mse-ypy-006_1744.2	2701604	18.48	14039566	4.87	5.20	2.49E-07
Unknown#mse-ypy-009_1493.0	835879	5.71	951271	8.55	1.14	2.34E-01
Unknown#mse-ypy-016_1793.3	1625858	7.55	796968	5.44	0.49	2.37E-04
Unknown#mse-ypy-017_1896.2	655064	6.07	215111	7.76	0.33	5.65E-06
Unknown#mse-ypy-018_2013.2	350739	6.84	204494	5.28	0.58	5.83E-04
Unknown#mse-ypy-019_2018.4	305316	11.87	1961482	7.16	6.42	5.62E-07
Unknown#mse-ypy-020_2054.7	753038	9.80	345246	4.09	0.46	8.07E-04
Unknown#mse-ypy-026_2236.8	81063	17.57	6342	62.35	0.08	1.24E-03
Unknown#mse-ypy-027_2269.2	243183	21.43	165284	14.56	0.68	2.38E-01
Unknown#mse-ypy-028_2276.9	0	0.00	2141970	9.09		6.72E-07
Unknown#mse-ypy-030_2498.7	0	0.00	8630790	9.44		9.31E-07
Unknown#mse-ypy-031_1878.8	5273046	6.54	2943923	15.84	0.56	2.68E-03
Unknown#mse-ypy-034_1540.5	1235985	12.90	833582	14.69	0.67	8.50E-02
Unknown#mse-ypy-036_1981.9	0	0.00	623041	4.73		2.27E-09
Unknown#mse-ypy-037_2590.9	753970	13.41	66799	63.44	0.09	2.54E-04
Unknown#mse-ypy-038_1545.5	3823922	11.90	2793674	5.75	0.73	8.07E-02
Unknown#sst-cgl-023_1411.8	1071294	12.00	891326	12.37	0.83	3.27E-01
Unknown#sst-cgl-053_1708.7	1882961	6.88	1039228	4.65	0.55	3.19E-04
Unknown#sst-cgl-094_2097.4	200052	64.68	844124	5.75	4.22	1.98E-03
Uracil	1552389	20.27	178931	12.66	0.12	3.40E-03
urea	323130	8.52	222167	13.10	0.69	3.32E-02
uridine 5'-monophosphate	2907181	6.34	1086598	7.31	0.37	1.46E-05
valine	35215837	6.69	66856856	12.64	1.90	3.49E-03

C.1 Supernatant analysis of YPIII grown in LB medium at 25 °C and 37 °C

Semiquantitative peak areas (mean: $\bar{x}$, n = 6 biological replicates), relative standard error Se

Metabolite	x (M blank)	Se (M blank) [%]	$\bar{x}$ (25 °C 3 h)	Se (25 °C , 3 h) [%]	$\bar{x}$ (25 °C, 5.5 h)	Se (25 °C, 5.5 h) [%]	$\bar{x}$ (25 °C, 9.5 h)	Se (25 °C, 9.5 h) [%]	$\bar{x}$ (25 °C, 14.5 h)	Se (25 °C, 14.5 h) [%]	$\bar{x}$ (25 °C, 23.5 h)	Se (25 °C, 23.5 h) [%]	$\bar{x}$ (37 °C, 3 h)	Se (37 °C, 3 h)) [%]	$\bar{x}$ (37 °C, 5.5 h)	Se (37 °C, 5.5 h) [%]	$\bar{x}$ (37 °C, 9.5 h)	Se (37 °C, 9.5 h) [%]	$\bar{x}$ (37 °C, 14.5 h)	Se (37 °C, 14.5 h) [%]	$\bar{x}$ (37 °C, 23.5 h)	Se (37 °C, 23.5 h) [%]
1,8-diamino-octane	127030	18.70	106144	50.03	94235	50.11	34339	100.00	0	0.00	0	0.00	0	0.00	0	0.00	0	0.00	0	0.00	0	0.00
1-O-methyl-, alpha-galactopyranoside	121337	1.73	123999	1.13	117496	1.19	116662	2.62	78135	44.49	114284	0.63	116775	1.81	119442	1.71	114648	2.75	112295	1.38	118136	0.82
2-hydroxy-glutarate	22484	1.52	23636	2.66	31409	4.06	78955	1.37	83348	2.43	90875	2.34	11936	88.44	24558	1.18	29483	4.40	48521	3.86	50802	2.84
3-amino-1,2,4-triazole	29223	1.04	31849	0.92	28585	2.91	27142	6.43	24190	3.78	25472	3.45	27456	4.53	28753	3.52	25579	6.11	19241	31.36	23387	9.48
3-hydroxybutanoate	0	0.00	0	0.00	0	0.00	0	0.00	0	0.00	0	0.00	0	0.00	0	0.00	13330	8.18	15506	1.44	14774	4.95
3-methyl-2-oxopentanoate	0	0.00	0	0.00	0	0.00	6082	5.85	7974	21.64	8309	2.24	2381	100.00	0	0.00	7809	7.30	8778	4.44	14592	0.89
3-phenyllactate	0	0.00	0	0.00	0	0.00	0	0.00	0	0.00	0	0.00	0	0.00	14298	100.00	0	0.00	59916	8.38	103238	4.39
4-aminobutanoate	25720	2.18	25768	1.48	25459	1.26	24821	0.59	24079	2.17	24508	0.46	24099	4.62	24292	1.97	25042	2.30	26611	1.22	26334	1.70
4-hydroxybutanoate	0	0.00	0	0.00	0	0.00	0	0.00	25790	13.86	56837	3.76	0	0.00	0	0.00	24263	22.92	79852	6.22	132155	3.67
5-amino-levulinate	215613	1.90	201546	1.02	184105	2.55	0	0.00	0	0.00	0	0.00	193044	2.03	148141	12.66	0	0.00	0	0.00	0	0.00
5-methoxy-tryptamine	14497	50.87	16324	50.10	15288	50.13	0	0.00	0	0.00	0	0.00	0	0.00	0	0.00	0	0.00	0	0.00	0	0.00
adenine	61379	50.06	27030	51.10	0	0.00	0	0.00	0	0.00	0	0.00	0	0.00	0	0.00	0	0.00	0	0.00	0	0.00
adenosine	110734	1.65	31595	4.24	10092	5.38	5813	50.58	4257	50.46	0	0.00	48088	19.81	10793	2.79	8350	5.85	9386	11.06	8857	6.86
alanine	4400809	5.94	4584816	2.11	4460961	0.85	1743720	10.99	0	0.00	0	0.00	4230304	4.13	4431915	1.52	3439915	1.90	254774	22.15	193722	13.40
allo-threonine	14019	1.88	12722	1.25	11697	7.42	10844	7.80	3800	37.59	3467	7.15	11942	1.00	12332	3.13	11088	5.31	9650	7.46	21319	51.20
alpha,alpha-trehalose	0	0.00	0	0.00	0	0.00	0	0.00	0	0.00	0	0.00	0	0.00	0	0.00	14126	40.57	627	100.00	0	0.00
arginine	21345	24.21	19332	1.99	21997	11.41	9739	51.52	10917	33.53	13739	31.98	16995	14.42	15367	13.59	14775	36.21	17594	7.31	12488	30.86
asparagine	528556	1.15	487264	1.44	435771	0.74	243346	2.76	118395	4.40	36919	4.71	425534	0.55	313477	5.66	30518	5.97	24548	9.24	18539	4.79
aspartate	1758283	3.95	1262901	1.85	34020	2.90	44197	23.49	27273	1.73	25439	0.94	1009371	0.25	43122	5.44	63125	3.35	95534	2.18	156493	2.62
beta-Alanine	1463	13.80	1691	8.42	2910	6.23	4420	17.29	7301	64.78	6955	82.66	1978	6.39	5363	26.71	13544	5.80	10189	37.67	21784	2.55
citrate	85593	3.79	52833	4.28	47097	4.54	0	0.00	0	0.00	0	0.00	76105	6.15	83088	2.45	0	0.00	0	0.00	14404	51.06
cysteine	36930	6.32	34239	2.51	31855	1.72	23839	1.72	21140	4.94	14934	51.67	38367	14.08	30858	0.08	23880	2.77	21829	2.00	20540	0.97
D116201_1172.88	29858	0.71	26706	0.43	28060	3.01	27633	4.62	26852	5.44	24807	2.82	24570	3.20	25187	11.10	27038	3.22	26229	1.66	26794	3.34
Diethanolamine	30077	50.34	12824	100.00	39319	4.74	0	0.00	0	0.00	8012	100.00	20692	100.00	33388	50.33	27162	11.98	0	0.00	0	0.00
dihydrouracil	29099	4.84	26936	4.90	24846	3.17	18819	1.36	17257	5.40	17078	2.63	18591	23.00	20669	2.49	18553	2.15	17731	2.59	17568	3.04
erythritol	7131	16.95	6555	41.43	5943	12.71	2015	38.04	1748	13.53	473	100.00	10061	23.52	9526	6.23	11992	10.93	10535	37.26	4109	16.25
ethanolamine	753241	3.08	806973	1.82	944075	0.28	1146232	0.11	1176913	0.57	1198004	1.71	782275	5.60	967713	2.15	1263460	2.42	1374820	1.32	1388603	0.83
fructose	73490	1.85	0	0.00	0	0.00	0	0.00	0	0.00	0	0.00	0	0.00	0	0.00	0	0.00	0	0.00	2324	100.00
fumarate	14627	96.67	74329	13.71	154465	3.12	30842	10.32	33591	9.08	31104	10.99	194798	35.44	356823	9.86	424760	3.46	275744	4.36	346808	4.56
glucose	141651	6.93	95575	1.23	97714	1.67	85902	2.35	81336	3.95	87839	0.68	96584	1.75	98865	1.22	95348	5.05	92401	1.18	94123	1.32
glutamate	4158931	3.08	4125269	1.47	3430767	0.61	0	0.00	0	0.00	0	0.00	3827129	0.32	2614350	16.36	0	0.00	0	0.00	0	0.00

Metabolite	x (M blank)	Se (M blank) [%]	$\bar{x}$ (25 °C 3 h)	Se (25 °C , 3 h) [%]	$\bar{x}$ (25 °C, 5.5 h)	Se (25 °C, 5.5 h) [%]	$\bar{x}$ (25 °C, 9.5 h)	Se (25 °C, 9.5 h) [%]	$\bar{x}$ (25 °C, 14.5 h)	Se (25 °C, 14.5 h) [%]	$\bar{x}$ (25 °C, 23.5 h)	Se (25 °C, 23.5 h) [%]	$\bar{x}$ (37 °C, 3 h)	Se (37 °C, 3 h)) [%]	$\bar{x}$ (37 °C, 5.5 h)	Se (37 °C, 5.5 h) [%]	$\bar{x}$ (37 °C, 9.5 h)	Se (37 °C, 9.5 h) [%]	$\bar{x}$ (37 °C, 14.5 h)	Se (37 °C, 14.5 h) [%]	$\bar{x}$ (37 °C, 23.5 h)	Se (37 °C, 23.5 h) [%]
glycerate	13473	6.53	0	0.00	0	0.00	0	0.00	0	0.00	0	0.00	13625	3.07	11598	13.24	0	0.00	0	0.00	0	0.00
glycerol	704752	4.87	607690	1.01	38859	1.91	36020	1.02	33310	4.44	39260	3.64	352361	39.95	35256	2.48	39464	7.92	38011	10.15	45489	8.17
glycerol-3-phosphate	91231	2.50	116948	2.25	157667	1.03	174386	2.11	114461	49.05	183275	1.71	110216	6.11	159811	3.49	184884	2.03	192308	2.01	194441	1.14
glycine	2482841	6.48	2573140	1.20	2652738	1.02	2973252	1.63	0	0.00	0	0.00	2318011	5.72	2552199	3.00	1782390	13.08	0	0.00	37188	55.86
glycolate	0	0.00	0	0.00	0	0.00	7362	50.00	2926	100.00	0	0.00	0	0.00	6141	52.12	0	0.00	0	0.00	0	0.00
guanine	14613	28.91	18208	7.15	8650	6.84	0	0.00	35608	13.45	69053	4.07	31316	60.51	18615	22.57	34733	23.31	79769	6.61	153734	7.84
hexadecanoate	53051	2.68	44110	5.47	48436	2.21	43640	11.80	41599	2.82	46279	9.19	43890	3.09	41902	2.68	48049	3.99	45510	3.34	45788	2.75
hexose_1	896682	3.17	163366	17.10	124165	0.79	113728	2.59	101891	5.03	110442	6.90	134485	4.06	122886	5.35	100781	4.24	116833	6.10	115859	6.83
hexose_2	586077	1.69	0	0.00	0	0.00	38075	52.06	83729	3.49	80791	12.13	14112	100.00	8425	100.00	0	0.00	0	0.00	0	0.00
histidine	51917	18.41	50001	8.76	49636	0.61	20185	13.38	10476	3.63	10649	2.05	39444	35.76	39819	11.96	51598	10.56	54949	5.53	52261	11.02
homocysteine	25865	5.25	29876	2.24	43070	10.38	24293	7.43	17002	2.57	10288	9.48	35256	15.39	52200	3.25	44637	3.05	40497	7.12	38289	9.75
homoserine	2769	9.21	4099	26.42	7454	16.56	2969	5.95	2504	8.05	2386	17.40	2342	2.31	3564	35.53	3527	10.13	4868	5.42	3770	30.98
hydroxylamine	24627	2.42	22924	4.52	24038	9.05	17107	4.56	19799	14.67	17682	11.44	12565	58.64	16646	10.99	15669	18.62	21902	11.06	9851	38.92
hypoxanthine	20004	3.58	81046	2.49	74966	4.36	0	0.00	0	0.00	37029	2.62	97993	24.49	93834	13.54	0	0.00	32927	12.28	88036	7.27
isoleucine	3907207	7.03	4038783	1.27	3871400	0.22	3690103	1.24	3681433	3.08	3814342	1.59	3716161	4.22	3880580	2.27	2617669	40.47	3874121	1.81	3770421	2.23
lactate	635938	4.92	691832	4.65	774940	4.93	734264	3.28	442631	5.44	250264	0.59	422310	87.48	912346	3.18	753530	1.12	641497	1.50	585398	2.39
leucine	5470438	6.50	5714897	1.29	5678761	1.11	5527005	1.35	5465802	3.16	5659501	1.18	5260475	5.16	5628033	1.83	5796858	2.08	5787791	1.86	5747314	1.85
lysine	5842241	6.37	6066236	1.25	5951096	0.04	5849443	0.78	5065755	2.78	5222406	0.38	5576372	4.81	5948667	1.87	6298042	1.24	6370487	1.64	6397796	1.07
malate	13436	4.07	27742	1.50	55214	1.32	4645	28.90	1696	25.32	1930	21.14	39031	2.29	117469	10.34	300610	3.14	269290	1.89	167738	1.35
maleamate	44506	12.95	58288	23.68	33537	11.93	39935	6.74	41750	12.61	37960	11.29	69347	13.10	57172	33.56	35567	8.92	36865	16.44	40307	6.92
mannitol	5662	4.36	8402	5.35	7369	13.33	4312	34.58	5390	9.76	4354	35.27	5653	21.27	5875	5.23	2765	44.80	5954	6.51	4153	11.83
mannose	6910	3.56	445	100.00	0	0.00	420	100.00	0	0.00	0	0.00	0	0.00	0	0.00	0	0.00	688	100.00	0	0.00
methionine	1393385	3.49	1393566	1.41	1310691	2.36	1254325	1.03	1227732	5.58	1500240	1.14	1313174	0.48	1335584	0.88	1134064	3.58	1113814	0.65	1126270	1.67
methionine sulfoxide	55505	6.50	63412	2.67	61330	3.95	46505	3.69	47779	46.96	73300	41.87	61651	13.51	58291	2.17	47210	8.23	52285	45.61	61396	31.05
myo-inositol	98760	3.53	101074	2.80	102239	1.02	99416	1.62	92660	2.32	75113	3.11	92634	5.26	99677	1.72	99257	2.51	100804	1.77	100047	1.82
NA_1141.88	101412	2.54	107884	4.37	101479	4.91	98378	2.59	92740	3.34	94161	3.64	102607	4.63	107896	6.75	108410	6.36	77961	32.72	101067	7.45
NA_1703.1	18984	1.62	18276	2.11	22063	15.63	24106	7.89	21242	2.98	20267	25.67	15840	10.24	29282	18.38	14646	24.29	24571	10.71	21911	9.12
NA_1705.4	58324	17.00	48062	24.49	51850	20.79	68414	22.72	59186	18.50	47616	14.18	74117	2.28	77876	11.83	60877	9.41	55585	15.59	64419	4.96
NA_2615.1	70926	4.99	78127	0.49	72455	5.35	75899	7.13	70986	7.41	72622	4.67	70882	2.14	77393	6.70	72599	3.65	69705	2.62	71463	1.99
NA106	38106	44.21	56124	2.41	44311	23.39	50012	1.28	48534	2.33	49859	4.69	35080	38.99	51081	2.24	52531	4.06	54877	2.79	51632	2.53
NA114002_(classified_unknown)_1144.3	573980	7.04	594962	5.82	617753	2.67	664644	5.43	653642	8.02	663080	4.28	554339	0.22	597631	3.58	602765	1.42	282349	54.56	423951	48.94
NA137012_(classified_unknown)_1388.87	51251	5.51	50667	2.47	45785	2.32	49598	5.37	46635	3.83	45333	3.22	50796	7.22	53805	3.50	51702	3.23	49216	0.77	48680	0.69
NA148018_1493.54	179942	77.38	131335	69.09	52185	33.82	39657	18.53	61991	24.84	45340	11.52	48733	20.53	44092	13.71	57808	18.39	63766	14.32	55425	11.53
NA155015_1545.6	32092	1.43	36466	5.05	32951	4.40	38749	3.40	32323	20.41	33551	10.83	33436	5.67	35465	7.03	42451	12.16	37859	5.61	39830	11.64
NA161011_1619.12	67151	14.66	63384	1.92	58511	7.16	51187	3.10	51433	4.53	51159	2.86	68635	12.39	60094	19.61	53319	1.63	47505	2.16	54237	3.58
NA178025_1797.31	49045	27.86	72549	6.54	61997	2.59	34280	6.76	41127	15.82	45651	14.07	67758	5.77	34910	14.26	30911	9.16	29171	4.98	29851	1.17
NA184	29220	5.64	27085	2.58	26469	3.51	26206	2.37	25717	5.96	25239	7.60	30763	10.16	28345	4.69	24629	5.97	22998	6.67	40803	19.92
NA184030_(classified	314518	4.40	284402	3.13	262700	1.78	244311	2.63	245202	4.83	267833	0.88	292912	6.53	266105	1.69	242643	2.57	254956	2.25	283466	6.09

Metabolite	x (M blank)	Se (M blank) [%]	$\bar{x}$ (25 °C 3 h)	Se (25 °C , 3 h) [%]	$\bar{x}$ (25 °C, 5.5 h)	Se (25 °C, 5.5 h) [%]	$\bar{x}$ (25 °C, 9.5 h)	Se (25 °C, 9.5 h) [%]	$\bar{x}$ (25 °C, 14.5 h)	Se (25 °C, 14.5 h) [%]	$\bar{x}$ (25 °C, 23.5 h)	Se (25 °C, 23.5 h) [%]	$\bar{x}$ (37 °C, 3 h)	Se (37 °C, 3 h)) [%]	$\bar{x}$ (37 °C, 5.5 h)	Se (37 °C, 5.5 h) [%]	$\bar{x}$ (37 °C, 9.5 h)	Se (37 °C, 9.5 h) [%]	$\bar{x}$ (37 °C, 14.5 h)	Se (37 °C, 14.5 h) [%]	$\bar{x}$ (37 °C, 23.5 h)	Se (37 °C, 23.5 h) [%]
_unknown)_1848.26																						
NA192001 (classified unknown)257	88020	3.39	39505	5.26	34139	3.85	33944	2.98	29292	6.30	32174	3.69	38693	5.46	35204	2.41	322609	90.38	292101	89.47	41729	19.17
NA201002 (classified unknown)312	93313	27.96	75034	20.99	30420	65.92	0	0.00	0	0.00	0	0.00	36596	26.26	0	0.00	0	0.00	0	0.00	9792	100.00
NA203	36723	6.15	27843	6.19	27281	15.76	69646	28.04	78537	15.85	89754	0.66	26791	3.17	49060	3.67	47613	4.68	39669	28.64	63150	0.62
NA289	1407	100.00	2950	51.99	1985	51.10	852	52.21	568	57.30	293	100.00	2719	31.02	669	100.00	0	0.00	0	0.00	0	0.00
NA341	0	0.00	0	0.00	0	0.00	25337	51.03	29657	10.14	47219	5.42	0	0.00	0	0.00	0	0.00	0	0.00	0	0.00
NA344	61580	2.09	50984	2.96	37645	3.61	4459	100.00	0	0.00	0	0.00	41370	12.60	12552	50.49	0	0.00	0	0.00	0	0.00
NA369	72348	3.38	0	0.00	0	0.00	0	0.00	0	0.00	0	0.00	23440	100.00	0	0.00	0	0.00	0	0.00	0	0.00
NA374	8635	12.79	0	0.00	0	0.00	0	0.00	0	0.00	0	0.00	7827	38.04	0	0.00	0	0.00	0	0.00	0	0.00
NA489	75775	10.72	92090	6.24	93860	3.01	74771	2.15	71613	2.52	83218	2.65	87004	7.95	73689	5.64	82369	5.75	86420	7.07	80632	15.75
NA547	24786	15.85	34529	3.67	22038	50.26	27768	11.56	20286	50.92	35536	3.91	36438	9.20	33125	5.51	33966	3.27	31395	2.71	32334	9.79
NA570	2571956	5.78	2525337	1.57	1326940	4.44	24099	32.40	41091	8.36	39514	3.42	2287558	2.35	1465383	16.91	39322	10.04	45873	5.36	42504	5.63
NA663	84332	2.67	98357	3.42	73682	20.54	86707	3.27	85104	4.67	97242	5.01	83820	6.57	90258	11.42	84525	9.64	94999	2.37	103586	3.33
NA78	141337	4.85	141202	8.89	115714	3.69	131955	3.98	137171	4.29	129214	5.06	139084	7.80	129054	9.96	112957	2.37	124035	7.19	132094	4.39
N-acetylneuraminate	30738	8.59	33890	5.07	0	0.00	0	0.00	533	100.00	0	0.00	29145	17.98	0	0.00	0	0.00	0	0.00	0	0.00
N-acetyl-serine	63416	23.81	34696	9.78	32867	12.15	40536	2.16	39421	8.43	38331	12.12	53000	34.35	39185	6.26	77449	1.54	80116	4.05	84270	1.25
n-hexadecenoate	0	0.00	6190	100.00	7036	100.00	12189	100.00	9755	100.00	37768	4.25	7136	100.00	0	0.00	0	0.00	0	0.00	0	0.00
Nicotinamide	26840	6.19	0	0.00	0	0.00	0	0.00	0	0.00	0	0.00	13342	100.00	8022	100.00	0	0.00	0	0.00	9391	100.00
octadecanoate	55370	1.29	46915	4.03	41601	0.81	38061	1.18	38286	6.06	37416	2.50	44736	4.50	39290	4.24	40295	2.05	41505	2.87	41714	2.40
ornithine	244559	2.65	229318	2.21	239309	2.20	261097	2.05	232224	4.20	226330	0.11	229350	2.10	257678	3.05	1286879	82.07	216289	1.02	203783	2.19
phenylacetate	0	0.00	0	0.00	0	0.00	0	0.00	0	0.00	0	0.00	0	0.00	0	0.00	0	0.00	0	0.00	244006	4.25
phenylalanine	3182048	2.93	3177898	2.01	3456802	1.35	2835920	0.66	2811854	3.02	2876941	0.03	3045816	2.57	3346279	1.23	2843074	1.24	2822325	1.53	2526534	5.79
phenylpyruvate	0	0.00	0	0.00	0	0.00	0	0.00	55762	5.11	85259	1.13	0	0.00	0	0.00	75950	7.31	89043	50.75	108656	76.98
phosphate	2290064	47.83	3291706	2.31	3159847	1.83	3090093	0.79	3023949	2.77	2174284	45.78	3141449	4.41	3221768	1.07	3297373	1.32	3345841	1.99	3359743	2.02
proline	2312569	4.75	2190068	0.51	1357916	2.00	0	0.00	0	0.00	0	0.00	1108425	81.28	1480695	10.78	0	0.00	0	0.00	0	0.00
putrescine	21558	1.80	78182	4.13	75953	1.31	94097	1.60	113792	2.25	299203	5.07	104179	1.19	139309	11.42	442515	10.34	862251	3.47	2330865	2.25
pyroglutamate	4227325	7.73	4371389	2.13	4287051	0.77	4019733	1.74	3270708	2.85	845745	0.54	4050699	6.95	4240560	1.64	4293734	0.99	4087076	1.33	2657470	49.88
pyrophosphate	0	0.00	6247	100.00	2528	100.00	1258	100.00	614	100.00	12402	26.54	7518	12.76	4912	51.28	5940	51.18	7312	55.11	8209	54.00
pyruvate	0	0.00	136062	4.18	0	0.00	0	0.00	0	0.00	0	0.00	245553	16.99	189208	51.37	0	0.00	0	0.00	0	0.00
ribose	3639	7.61	1066	100.00	0	0.00	0	0.00	0	0.00	0	0.00	3852	11.56	2694	50.03	0	0.00	0	0.00	0	0.00
serine	2356961	4.24	1738117	2.72	49844	4.58	45693	5.04	29514	6.89	19283	1.53	1839493	8.16	48252	12.50	45796	3.27	33332	5.07	29487	5.16
spermidine	34498	3.36	34078	4.11	42686	9.24	38250	10.22	29551	8.14	32190	8.16	32245	25.25	39577	7.22	39575	8.33	38948	6.07	42934	12.83
succinate	71466	2.65	102145	1.64	178122	0.81	2192	42.19	2604	2.34	1720	25.80	114984	8.42	222537	4.18	150028	3.95	114713	2.86	121599	0.46
sucrose	60844	3.49	61654	3.81	59325	1.75	56833	2.87	54788	1.33	62244	2.49	56749	5.86	55877	3.00	61051	3.49	61165	2.77	56667	3.83
threonine	1133375	4.10	1099894	1.27	872147	2.32	0	0.00	0	0.00	0	0.00	1044961	1.94	891639	3.74	0	0.00	0	0.00	0	0.00
thymine	3595	84.03	10678	50.86	18812	13.13	24412	16.34	32838	11.31	39909	7.51	15031	4.62	22785	11.32	26056	14.87	38155	8.99	38727	0.62

Metabolite	x (M blank)	Se (M blank) [%]	$\bar{x}$ (25 °C 3 h)	Se (25 °C , 3 h) [%]	$\bar{x}$ (25 °C, 5.5 h)	Se (25 °C, 5.5 h) [%]	$\bar{x}$ (25 °C, 9.5 h)	Se (25 °C, 9.5 h) [%]	$\bar{x}$ (25 °C, 14.5 h)	Se (25 °C, 14.5 h) [%]	$\bar{x}$ (25 °C, 23.5 h)	Se (25 °C, 23.5 h) [%]	$\bar{x}$ (37 °C, 3 h)	Se (37 °C, 3 h)) [%]	$\bar{x}$ (37 °C, 5.5 h)	Se (37 °C, 5.5 h) [%]	$\bar{x}$ (37 °C, 9.5 h)	Se (37 °C, 9.5 h) [%]	$\bar{x}$ (37 °C, 14.5 h)	Se (37 °C, 14.5 h) [%]	$\bar{x}$ (37 °C, 23.5 h)	Se (37 °C, 23.5 h) [%]
tryptophan	1039714	9.81	1118808	4.55	1086675	3.68	1514283	3.68	1578278	1.41	1673693	2.53	843495	24.66	835631	4.39	820972	7.36	777397	3.88	528618	11.28
tyrosine	2262069	3.51	2125236	1.56	1990539	0.84	1619310	0.31	1568489	1.84	1637662	0.88	1983799	2.20	1951197	1.12	1595523	2.37	1602114	2.06	1594001	1.25
Unknown#bth-pae-013_1169.8	85144	4.24	105486	3.14	95808	8.93	89455	1.38	76723	4.99	77122	3.90	94029	0.66	100434	7.60	103699	8.86	99677	4.04	102125	4.04
Unknown#bth-pae-065_1466.2	59981	23.14	82452	5.22	110471	16.90	74995	6.75	0	0.00	0	0.00	49391	100.00	47637	50.11	48900	50.39	0	0.00	0	0.00
Unknown#mse-ypy-004_1302.5	1915	100.00	3193	100.00	2192	100.00	0	0.00	0	0.00	0	0.00	7679	6.27	4755	50.79	0	0.00	2693	100.00	0	0.00
Unknown#mse-ypy-006_1744.2	70990	16.81	3358	47.53	4771	22.82	36176	8.44	97046	6.39	166243	3.10	6682	63.09	6540	27.34	40883	13.00	76073	3.05	91110	4.82
Unknown#mse-ypy-019_2018.4	12952	3.03	14960	12.33	15695	8.10	13048	3.07	13895	4.26	19271	2.57	17230	2.16	16605	2.03	14856	3.02	20860	2.09	23323	4.43
Unknown#mse-ypy-028_2276.9	0	0.00	0	0.00	0	0.00	0	0.00	0	0.00	17181	10.88	0	0.00	0	0.00	0	0.00	0	0.00	0	0.00
Unknown#mse-ypy-036_1981.9	36037	74.16	14840	1.33	8744	5.55	50010	69.85	8220	28.50	11132	4.10	13547	4.73	14798	1.46	6827	8.55	12253	1.86	12247	3.60
Unknown#sst-cgl-009_1250.2	85281	31.38	64330	4.32	123987	5.07	64436	5.67	60591	5.46	62576	5.57	81187	55.44	79993	30.82	64000	8.21	59859	3.56	891475	60.08
uracil	77161	9.16	103335	2.22	63458	13.93	0	0.00	23919	5.99	73574	3.29	132030	2.10	91336	9.40	22953	19.92	56046	5.05	131157	3.97
uridine	12023	9.24	7327	8.30	912	100.00	0	0.00	0	0.00	0	0.00	3293	100.00	807	100.00	1409	51.59	1994	59.31	666	100.00
valine	3965955	6.12	4181900	1.39	4211799	0.98	4391328	0.89	4363736	3.05	4644364	0.36	3873316	3.09	4132712	2.11	4323475	2.51	4627665	2.49	4492268	2.98
xanthine	21724	8.72	20811	6.76	14284	7.13	939	10.06	1125	3.04	1279	3.69	19673	20.93	20258	6.52	20831	13.40	15895	28.23	19039	8.46

C.2 Intracellular metabolome analysis in LB medium at 37 °C and 25 °C

Semiquantitative peak areas (mean: $\bar{x}$, n = 9 biological replicates), relative standard error Se

Metabolites	$\bar{x}$ (25 °C exp)	Se (25 °C exp) [%]	$\bar{x}$ (25 °C stat)	Se (25 °C stat) [%]	$\bar{x}$ (37 °C exp)	Se (37 °C exp) [%]	$\bar{x}$ (37 °C stat)	Se (37 °C stat) [%]
1-methyl-hydantoin	1434391	0.11	567817	0.08	1340938	0.18	624104	0.09
1-Octadecanol	71529	0.27	166586	0.28	44728	0.07	220928	0.18
3-hydroxypyridine	3365329	0.14	2383950	0.05	3406266	0.10	2111116	0.08
3-hydroxytetradecanoate	63086	0.13	70421	0.16	88417	0.07	131494	0.13
5'-Methylthioadenosine	46221	0.08	360464	0.26	158628	0.24	156356	0.25
9-(E)-octadecenoate	330143	0.18	67329	0.13	73967	0.14	15455	0.62
adenine	8224551	0.14	8090933	0.07	11081632	0.10	8834858	0.12
adenosine	319543	0.40	130296	0.28	721472	0.23	225730	0.27
allo-threonine	62233	0.20	250053	0.10	0	0	101356	0.21
alpha,alpha-trehalose	0	0	0	0	749168	0.22	0	0
AMP	1175020	0.18	2238096	0.05	2479936	0.15	4444226	0.09
arginine	186064	0.73	920600	0.29	178967	0.26	2823678	0.16
Asparagine	147836	0.65	698514	0.39	138422	0.40	616867	0.25
aspartate	195857	0.09	4693714	0.29	221211	0.25	1679333	0.36
butyro-1,4-lactam	5565266	0.50	3390232	0.24	8119989	0.19	3667530	0.18
Cadaverin	2120114	0.52	7341436	0.16	1614800	0.13	18191494	0.15
citrate	340328	0.08	548470	0.05	173659	0.39	497308	0.12
cytosine	4159223	0.13	6180985	0.07	5484862	0.09	6572952	0.10
D116201_1172.88	2329531	0.22	709951	0.17	1327425	0.24	591590	0.14
Erythritol	202950	0.43	373604	0.16	290322	0.27	961350	0.14
ethanolamine	97741202	0.15	32136650	0.14	58408295	0.22	25670986	0.13
fumarate	234729	0.15	212707	0.17	426006	0.24	702650	0.15
glucose	696596	0.37	359726	0.09	234749	0.33	332641	0.08
glutamate	5569861	0.24	29122365	0.04	6012795	0.27	2550725	0.60
Glutamine	621136	0.32	1125807	0.26	384300	0.46	130222	0.13
Glutarate	440421	0.38	781321	0.11	445406	0.20	2015392	0.13
glycerate	102257	0.20	149071	0.25	70156	0.27	456333	0.18
glycerate-3-phosphate	581946	0.17	1628688	0.05	108401	0.29	1464788	0.15
glycerol	3371904	0.22	960018	0.41	1839676	0.33	753472	0.33
glycerol-3-phosphate	3507313	0.16	1180476	0.11	1255159	0.11	546184	0.28
glycine	1402554	0.20	394838	0.07	976579	0.08	454608	0.14
guanine	1874510	0.12	1989801	0.05	2090937	0.12	2148767	0.08
heptadecanoate	164850	0.68	528881	0.11	0	0	608812	0.14
hexadecanoate	6271481	0.15	1303857	0.08	7041348	0.13	1193914	0.15
hydroxyglutarate	88936	0.69	341814	0.45	23772	0.27	82867	0.69
hydroxylamine	2067191	0.16	561510	0.17	1200471	0.20	436605	0.17
isoleucine	4037275	0.31	15921450	0.13	7445570	0.12	15602564	0.07
leucine	15894286	0.18	26835254	0.13	15874263	0.16	23734771	0.08
lumichrome	5402038	0.17	1601359	0.21	4068437	0.20	3646215	0.13
lysine	8080161	0.08	76324521	0.03	9861652	0.10	94684562	0.09
malate	884688	0.20	94692	0.20	775990	0.27	243390	0.10
methionine	0	0	1356370	0.06	126533	0.46	544213	0.22
myo-inositol	201586	0.30	940871	0.34	66456	0.34	1034444	0.18
NA_2019.3	2448541	0.18	5064307	0.03	3770699	0.06	6217845	0.04
NA102	2797164	0.17	2776884	0.10	2351822	0.12	1964314	0.06
NA106	3835998	0.15	1180670	0.14	2498472	0.20	975286	0.11
NA114002_(classified_unknown)_1144.3	20571429	0.16	16258721	0.11	16128175	0.14	10921781	0.09
NA341	0	0	856121	0.11	0	0	869299	0.16
NA407	496143	0.22	683408	0.10	1099530	0.27	675219	0.10
NA76	1162528	0.21	575803	0.11	828840	0.23	595288	0.08
NA86	510857	0.15	154271	0.19	350556	0.19	170354	0.26
n-hexadecenoate	46248848	0.18	9142051	0.11	19127405	0.11	4848501	0.24
Nicotinamide	861393	0.28	2131171	0.20	2953489	0.27	5708572	0.12
nicotinate	0	0	0	0	0	0	319306	0.14
octadecanoate	1421290	0.16	546727	0.15	991523	0.18	399311	0.12
ornithine	165402	0.38	3347859	0.06	231127	0.38	3802748	0.09
pantothenate	0	0	116221	0.03	13054	0.44	18844	0.66
pentadecanoate	744263	0.13	1007487	0.09	0	0	1295464	0.15
phenylalanine	1638225	0.49	4077188	0.15	3512462	0.15	3825739	0.07
phosphate monomethyl ester	3916982	0.25	396861	0.06	160038	0.15	400513	0.12
phosphoenolpyruvate	252057	0.57	808714	0.37	65061	0.29	1061000	0.20
phosphorate	154355653	0.14	46643061	0.26	82933214	0.28	38327980	0.24

Metabolites	$\bar{x}$ (25 °C exp)	Se (25 °C exp) [%]	$\bar{x}$ (25 °C stat)	Se (25 °C stat) [%]	$\bar{x}$ (37 °C exp)	Se (37 °C exp) [%]	$\bar{x}$ (37 °C stat)	Se (37 °C stat) [%]
putrescine	114358843	0.11	147870764	0.13	141361872	0.12	215200233	0.02
pyroglutamate	29047354	0.20	73463801	0.02	21799602	0.21	58154460	0.10
serine	122286	0.40	301443	0.27	102822	0.18	659111	0.15
sorbitol	215703	0.11	92671	0.19	200659	0.13	117315	0.17
spermidine	413480	0.12	2266436	0.27	920008	0.10	1451444	0.11
succinate	271332	0.17	55890	0.09	110835	0.14	104044	0.22
succinate-methylester	285851	0.10	0	0	533420	0.06	0	0
tetradecanoate	12119757	0.13	4060000	0.07	15285887	0.09	4819731	0.13
threonine	143445	0.47	157934	0.04	202537	0.30	60243	0.28
thymine	2704717	0.10	6988602	0.06	4030157	0.13	8487694	0.09
Tryptamine	429014	0.67	1346136	0.34	402761	0.24	2698872	0.18
Tryptophan	811693	0.50	3474643	0.31	1352861	0.29	8274328	0.19
tyrosine	0	0	12757143	0.04	1775556	0.32	7900559	0.11
Unknown#bth-pae-013_1169.8	1126355	0.67	1176667	0.09	1152097	0.29	1239821	0.05
Unknown#bth-pae-038_1567.3	0	0	0	0	0	0	457787	0.16
Unknown#cja-ppu-009_1882.25	387687	0.48	883304	0.09	691676	0.22	1538330	0.12
Unknown#mse-ypy-001_1846.9	118667	0.15	55975	0.03	125236	0.09	303084	0.17
Unknown#mse-ypy-002_1_2922.4	0	0	240991	0.06	246729	0.21	693753	0.10
Unknown#mse-ypy-002_2_2955.1	0	0	957328	0.10	1012035	0.28	3696206	0.11
Unknown#mse-ypy-007_1315.2	13961276	0.23	4743790	0.17	9358399	0.20	3119381	0.20
Unknown#mse-ypy-016_1793.3	5882751	0.32	1003259	0.52	1344458	0.47	1592508	0.40
Unknown#mse-ypy-019_2018.4	0	0	284862	0.02	0	0	145442	0.26
Unknown#mse-ypy-023_2128.1	0	0	224688	0.23	382645	0.11	518374	0.12
Unknown#mse-ypy-028_2276.9	0	0	624949	0.15	0	0	0	0
Unknown#mse-ypy-039_3026.6	1488094	0.12	769470	0.13	1517696	0.14	92807	0.93
Unknown#sst-cgl-001_1746.7	0	0	0	0	0	0	1605711	0.14
Unknown#sst-cgl-008_1248.7	0	0	0	0	1139106	0.15	0	0
uracil	5495219	0.11	2794885	0.06	5474760	0.11	2711045	0.11
urea	530877	0.22	202049	0.15	279542	0.23	259981	0.14
uridine	52407	0.23	38900	0.33	84650	0.22	61650	0.15
valine	5902274	0.37	38821409	0.06	9189596	0.16	25132850	0.09

C.3 Temperature dependent genes (37 °C vs. 25 °C)

Only significant changes (37 °C/ 25 °C > 1.8-fold) are shown as $\log_2$ fold ratios. The genes encoding proteins participating in the metabolism are indicated in the category class.

Gene ID	Gene locus	$\log_2$ Fold Change	Description	Category-Class
YPK_2200		5,23	hypothetical protein YPK_2200	
YPK_1731		3,55	conserved hypothetical protein	
pYV0025		3,47	putative outer membrane virulence protein	
pYV0054	yopD	3,15	putative Yop negative regulation/targeting component	
pYV0058	lcrG	3,05	putative Yop regulator	
pYV0055	yopB	3,03	putative Yop targeting protein	
pYV0067		2,96	type III secretion system ATPase	
pYV0065	yopN. lcrE	2.95	putative membrane-bound Yop targeting protein	
pYV0094	yopH	2,77	putative protein-tyrosine phosphatase Yop effector	
pYV0056	*lcrH, sycD*	2,73	low calcium response protein H	
pYV0057	*lcrV*	2,64	putative V antigen	
pYV0064	*tyeA*	2,53	putative Yop secretion and targeting protein	
pYV0040		2,34	yop targeting protein YopK, YopQ	
pYV0002		2,28	hypothetical protein	
pYV0077		2,22	hypothetical protein	

Gene ID	Gene locus	Log_2 Fold Change	Description	Category-Class
YPK_3421	*ydjJ*	2,1	Alcohol dehydrogenase zinc-binding domain protein	
pYV0024	*sycE, yerA*	2,09	putative yopE chaperone	
YPK_4004		2,08	conserved hypothetical protein	
YPK_4005		1,98	protein of unknown function UPF0261	
pYV0032	*sopA*	1,83	putative plasmid partitioning transcription repressor	
pYV0001	*ypkA*	1,79	putative targeted effector protein kinase	
pYV0039		1,79	putative transposase	
pYV0063	*sycN*	1,79	putative type III secretion protein	
YPK_1610	*gutB*	1,71	alcohol dehydrogenase	Metabolism
pYV0078	*yscB*	1,6	hypothetical protein	
YPK_3422	*rpiB*	1,6	ribose-5-phosphate isomerase B	Metabolism
pYV0044		1,56	hypothetical protein	
pYV0031	*sopB*	1,54	plasmid-partitioning protein	
pYV0068	*yscO*	1,53	putative type III secretion protein	
YPK_3035		1,53	conserved hypothetical protein	
pYV0079	*yscC*	1,52	putative type III secretion protein	
YPK_1960		1,48	conserved hypothetical protein	
YPK_3420		1,42	short-chain dehydrogenase/reductase SDR	
YPK_0012	*ibpB*	1,34	heat shock chaperone IbpB	
YPK_0011	*ibpA*	1,33	heat shock protein IbpA	
YPK_2199		1,27	conserved hypothetical protein	
pYV0084		1,25	putative type III secretion protein	
YPK_0762	*gntP*	1,22	gluconate:H+ symporter	
YPK_2198		1,15	conserved hypothetical protein	
YPK_1611		1,13	ribose transport system substrate-binding protein	
pYV0026		1,11	hypothetical protein	
YPK_3727	*rpsO*	1,08	30S ribosomal protein S15	
YPK_3203		1,07	conserved hypothetical protein	
pYV0062	*yscX*	1,05	putative type III secretion protein	
YPK_3594	*dnaK*	1,04	molecular chaperone Dank	
YPK_2197		1,02	conserved hypothetical protein	
YPK_3228	*ybaW*	1,02	thioesterase superfamily protein	Metabolism
YPK_3389	*cybC*	1,01	cytochrome b562	
YPK_3309	*fadE*	1	acyl-CoA dehydrogenase	Metabolism
YPK_3216	*ybaY*	0,96	putative lipoprotein	
YPK_3933	*fadB*	0,95	multifunctional fatty acid oxidation complex subunit alpha	Metabolism
YPK_4131	*cpxP*	0,92	periplasmic stress adaptor protein CpxP	
YPK_0031		0,89	conserved hypothetical protein	
pYV0089	*yscM, lcrQ*	0,88	putative type III secretion regulatory	
pYV0007		0,86	putative replication transcriptional regulator	
YPK_2023		0,86	translation initiation factor Sui1	
YPK_2295		0,85	hypothetical protein	
YPK_2474	*cspC*	0,85	cold shock-like protein CspC	
YPK_3418		0,83	dihydroxyacetone kinase	Metabolism
YPK_4214	*asnA*	0,83	asparagine synthetase AsnA	Metabolism
YPK_1959		0,82	hypothetical protein YPK_1959	
YPK_0273	*tusC*	0,8	sulfur relay protein TusC	
YPK_1388	*napB*	-0,8	citrate reductase cytochrome c-type subunit	Metabolism
YPK_3632	*osmY*	-0,8	periplasmic protein	
YPK_3243	*cyoC*	-0,81	cytochrome o ubiquinol oxidase subunit III	Metabolism
YPK_2969	*sdhB*	-0,82	succinate dehydrogenase iron-sulfur subunit	Metabolism
YPK_2096	*gapA*	-0,83	glyceraldehyde-3-phosphate dehydrogenase, type I	Metabolism
YPK_2219		-0,84	hypothetical protei	
YPK_2955	*pal*	-0,84	peptidoglycan-associated outer membrane lipoprotein	
YPK_0437	*yghU*	-0,85	putative glutathione S-transferase YghU	
YPK_0303	*secY*	-0,86	preprotein translocase subunit SecY	
YPK_2947	*psiF*	-0,86	PsiF repeat protein	
YPK_0287	*rpsS*	-0,87	30S ribosomal protein S19	

Gene ID	Gene locus	Log_2 Fold Change	Description	Category-Class
YPK_0305	*rpsM*	-0,88	30S ribosomal protein S13	
YPK_0308	*rpoA*	-0,88	DNA-directed RNA polymerase subunit alpha	
YPK_1877	*slyB*	-0,88	outer membrane lipoprotein SlyB	
YPK_3425	*rpoS*	-0,89	RNA polymerase sigma factor RpoS	
YPK_4108		-0,9	conserved hypothetical protein	
YPK_2970	*sdhA*	-0,91	succinate dehydrogenase flavoprotein subunit	Metabolism
YPK_4035	*trxA*	-0,91	thioredoxin	
YPK_1397	*ygiW*	-0,93	conserved hypothetical protein	
YPK_0486	*gabD*	-0,94	succinic semialdehyde dehydrogenase	Metabolism
YPK_1876	*rovA*	-0,94	transcriptional regulator SlyA	
YPK_2018		-0,94	protein of unknown function DUF466	
YPK_2967	*sucB*	-0,94	dihydrolipoamide succinyltransferase	Metabolism
YPK_2236		-0,95	conserved hypothetical protein	
YPK_3590	*rpsT*	-0,95	30S ribosomal protein S20	
YPK_3631		-0,95	protein of unknown function DUF1328	
YPK_0302	*rplO*	-0,96	50S ribosomal protein L15	
YPK_0335	*rplK*	-0,96	50S ribosomal protein L11	
YPK_4153	*rpmG*	-0,96	50S ribosomal protein L33	
YPK_3364	*rpsP*	-0,97	30S ribosomal protein S16	
YPK_2074	*hns*	-0,98	global DNA-binding transcriptional dual regulator H-NS	
YPK_0306	*rpsK*	-0,99	30S ribosomal protein S11	
YPK_1428	*ptsH*	-0,99	PTS system phosphohistidinoprotein-hexose phosphotransferase subunit Hp	
YPK_2022	*osmB*	-1,02	osmotically inducible lipoprotein OsmB	
YPK_3353	*yfiA*	-1,03	ribosome-associated inhibitor A	
YPK_2123	*minE*	-1,04	cell division topological specificity factor MinE	
YPK_0293	*rplN*	-1,05	50S ribosomal protein L14	
YPK_0504	*yhbH*	-1,06	putative sigma(54) modulation protein	
YPK_1268	*ail*	-1,06	virulence-related outer membrane protein	
YPK_0035	*sodA*	-1,07	superoxide dismutase	
YPK_0649	*ribB*	-1,07	3.4-dihydroxy-2-butanone 4-phosphate synthase	Metabolism
YPK_2068	*oppC*	-1,07	peptide/nickel transport system permease protein	
YPK_3816	*frdD*	-1,08	fumarate reductase subunit D	Metabolism
YPK_0348	*rsd*	-1,09	anti-RNA polymerase sigma 70 factor	
YPK_4221		-1,1	F0F1 ATP synthase subunit C	Metabolism
YPK_1867		-1,11	hypothetical protein YPK_1867	
YPK_3645		-1,11	hypothetical protein YPK_3645	
YPK_0120	*uspA*	-1,12	UspA domain-containing protein	
YPK_0248	*crp*	-1,13	cAMP-regulatory protein	
YPK_1001	*cynT*	-1,14	carbonic anhydrase	Metabolism
YPK_2363	*wrbA*	-1,14	TrpR binding protein WrbA	
YPK_2968	*kgd*	-1,18	2-oxoglutarate dehydrogenase E1 component	Metabolism
YPK_0039	*fdoH*	-1,19	formate dehydrogenase subunit beta	Metabolism
YPK_1682	*rpmF*	-1,19	50S ribosomal protein L32	
YPK_0365	*aceA*	-1,2	isocitrate lyase	Metabolism
YPK_0040	*fdoI*	-1,21	formate dehydrogenase-O subunit gamma	Metabolism
YPK_1823	*rplT*	-1,22	50S ribosomal protein L2	
YPK_2972	*sdhC*	-1,24	succinate dehydrogenase cytochrome b556 large membrane subunit	Metabolism
YPK_0278	*tuf*	-1,25	elongation factor Tu	
YPK_1725		-1,25	conserved hypothetical protein	
YPK_2069	*oppB*	-1,28	oligopeptide transporter permease	
YPK_1822	*rpmI*	-1,29	50S ribosomal protein L35	
YPK_3798		-1,31	hypothetical protein YPK_3798	
YPK_2966	*sucC*	-1,33	succinyl-CoA synthetase subunit beta	Metabolism

Gene ID	Gene locus	Log_2 Fold Change	Description	Category-Class
YPK_4014		-1,33	hypothetical protein YPK_4014	
YPK_3922		-1,34	protein of unknown function DUF485	
YPK_1826	*ihfA*	-1,37	integration host factor subunit alpha	
YPK_3921	*acs*	-1,37	acetyl-CoA synthetase	Metabolism
YPK_2229	*argD*	-1,38	bifunctional succinylornithine transaminase/acetylornithine transaminase	Metabolism
YPK_0246		-1,4	hypothetical protein YPK_0246	
YPK_3820		-1,41	hypothetical protein YPK_3820	
YPK_2704		-1,42	conserved hypothetical protein	
YPK_0547		-1,45	protein of unknown function DUF883 ElaB	
YPK_1932		-1,46	hypothetical protein YPK_1932	
YPK_2465	*manY*	-1,51	PTS system mannose/fructose/sorbose family IIC subunit	Metabolism
YPK_3548		-1,52	hypothetical protein YPK_3548	
YPK_2235	*phoH*	-1,53	hypothetical protein	
YPK_1520	*fabB*	-1,54	3-oxoacyl-(acyl carrier protein) synthase I	Metabolism
YPK_2429	*invA*	-1,54	Invasin region 3	
YPK_2373		-1,55	conserved hypothetical protein	
YPK_2466	*manZ*	-1,55	PTS system mannose-specific transporter subunit IID	Metabolism
YPK_3923	*actP*	-1,58	acetate permease	
YPK_2062		-1,59	conserved hypothetical protein	
YPK_3368	*luxS*	-1,6	S-ribosylhomocysteinase	Metabolism
YPK_3010	*gltI*	-1,63	glutamate and aspartate transporter subunit	
YPK_1326		-1,65	hypothetical protein	
YPK_2667	*ihfB*	-1,65	integration host factor subunit beta	
YPK_2185		-1,72	conserved hypothetical protein	
YPK_0332	*tuf*	-1,77	elongation factor Tu	
YPK_2070	*oppA*	-1,79	peptide/nickel transport system substrate-binding protein	
YPK_0166		-1,87	protein of unknown function DUF1471	
YPK_3764		-1,88	hypothetical protein YPK_3764	
YPK_2483		-1,93	hypothetical protein YPK_2483	
YPK_2694	*cspD*	-2,03	cold-shock DNA-binding domain-containing protein	
YPK_1617		-2,14	conserved hypothetical protein	
YPK_2879		-2,28	Transglycosylase-associated protein	
YPK_1375	*afuA*	-2,38	iron(III) transport system substrate-binding protein	
YPK_1854	*lpp*	-2,51	murein lipoprotein	
YPK_4249	*rpmH*	-2,57	50S ribosomal protein L34	
YPK_3563	*hcp*	-2,61	type VI secretion system secreted protein Hcp	
YPK_2649	*ompF*	-2,72	outer membrane pore protein F	
YPK_2630	*ompA*	-3,09	outer membrane protein A	
YPK_3031	*cspE*	-3,19	cold shock protein CspE	
YPK_2441		-3,64	conserved hypothetical protein	

D.1 Time-resolved supernatant analysis in minimal medium at 37 °C

Semiquantitative peak areas (mean: $\bar{x}$, n = 4), relative standard error Se

Metabolite	x (M blank)	Se (M blank) [%]	$\bar{x}$ (25 °C 15 h)	Se (25 °C, 15 h) [%]	$\bar{x}$ (25 °C, 19 h)	Se (25 °C, 19 h) [%]	$\bar{x}$ (25 °C, 22 h)	Se (25 °C, 22 h) [%]	$\bar{x}$ (25 °C, 30 h)	Se (25 °, 30 h) [%]	$\bar{x}$ (37 °C, 17 h)	Se (37 °C, 17 h) [%]	$\bar{x}$ (37 °C, 20 h)	Se (37 °C, 20 h)) [%]	$\bar{x}$ (37 °C, 23 h)	Se (37 °C, 23 h) [%]	$\bar{x}$ (37 °C, 31 h)	Se (37 °C, 31 h) [%]
2-hydroxybutanoate	0	0.00	0	0.00	0	0.00	0	0.00	0	0.00	0	0.00	0	0.00	12713	100.00	66131	6.77
2-hydroxy-glutarate	10164	100.00	142627	4.29	316406	7.74	286730	9.97	174820	8.74	1245581	6.88	1427430	11.37	1732445	4.56	1903502	1.67
2-isopropylmalate	0	0.00	38399	4.80	119384	1.91	107367	7.88	62068	8.78	0	0.00	0	0.00	0	0.00	0	0.00
2-methyl-malate	0	0.00	9028	33.55	33438	11.10	34865	11.65	25940	5.26	48855	4.24	64737	4.22	88642	2.85	105492	2.24
3-hydroxybutanoate	0	0.00	19057	7.80	37795	7.58	38380	5.72	35329	9.13	18066	16.69	25686	12.58	31466	5.61	39486	6.21
alanine	0	0.00	0	0.00	0	0.00	0	0.00	0	0.00	0	0.00	0	0.00	0	0.00	40216	8.60
beta-Alanine	0	0.00	0	0.00	1726	68.42	2182	43.01	767	66.01	2727	39.31	3388	47.48	3649	34.64	12125	9.46
citrate	0	0.00	0	0.00	0	0.00	0	0.00	0	0.00	11682	10.28	13299	2.96	19219	10.13	2814	100.00
erythritol	36897	7.19	27877	1.73	37511	9.49	35635	7.87	0	0.00	34087	8.27	32699	2.26	41290	4.74	43695	2.96
ethanolamine	823121	1.03	575097	9.11	1139554	6.88	1176992	3.91	1207972	2.23	293768	9.67	320489	4.34	555811	10.91	451938	3.57
galactose	98877627	7.71	21344465	57.77	14340	70.53	12863	100.00	0	0.00	29963201	27.97	29913308	15.50	19012547	3.23	13538	74.06
glycerol	24080	51.26	5873	100.00	11064	58.71	21133	8.68	24355	2.82	8410	58.00	8166	57.74	22146	10.04	18388	5.64
glycerol-3-phosphate	0	0.00	3047	58.12	0	0.00	0	0.00	0	0.00	4924	35.77	6925	16.63	10870	46.51	0	0.00
hexadecanoate	0	0.00	0	0.00	0	0.00	4428	100.00	4916	100.00	17216	37.39	14657	11.88	2523	100.00	8052	60.61
idose	105553	21.55	64819	59.29	0	0.00	0	0.00	0	0.00	13516	33.46	13556	24.78	0	0.00	0	0.00
isoleucine	0	0.00	0	0.00	0	0.00	95433	12.97	129433	3.51	0	0.00	0	0.00	0	0.00	76693	8.21
lactate	391179	70.56	1440380	4.77	1392671	1.97	735618	20.96	271329	48.06	9470832	6.60	12385305	4.78	22526669	2.86	24932344	10.42
malate	0	0.00	0	0.00	0	0.00	0	0.00	0	0.00	0	0.00	0	0.00	1323	100.00	6572	8.16
mannitol	98170736	7.38	41914815	6.94	119804	34.79	146588	28.66	182594	2.36	37131028	12.53	33579276	5.58	20356277	20.62	97517	33.44
phosphate	163947704	7.63	73676540	4.00	88841413	5.69	84437369	7.03	84168669	3.53	52858989	16.24	53679251	6.46	77398116	6.07	50825460	5.22
pyroglutamate	147789	53.19	62168	35.49	118645	13.94	127310	17.70	119534	19.00	109171	30.73	100649	19.55	108265	15.75	111502	25.76
pyruvate	0	0.00	39014	34.13	0	0.00	0	0.00	0	0.00	311349	10.49	306680	4.45	648833	10.46	63060	33.88
succinate	0	0.00	6445	33.47	12433	23.85	12286	12.63	11518	24.88	7776	66.07	7668	17.66	16964	11.80	13716	53.10
Unknown#bth-pae-013_1169.8	370622	14.44	106928	4.84	139871	10.40	150582	6.14	143459	2.87	103101	21.23	92103	8.92	130069	11.42	82492	2.48
Unknown#bth-pae-019_1282.2	0	0.00	0	0.00	0	0.00	0	0.00	0	0.00	37193	36.97	29581	58.09	0	0.00	0	0.00
Unknown#bth-pae-035_1530.4	0	0.00	0	0.00	0	0.00	0	0.00	0	0.00	0	0.00	0	0.00	0	0.00	21041	12.56
Unknown#sst-cgl-009_1250.2	0	0.00	0	0.00	0	0.00	0	0.00	0	0.00	888	100.00	1872	62.31	4858	36.06	9821	1.46
Uracil	0	0.00	5151	100.00	0	0.00	34695	35.07	36901	46.05	26063	57.05	21887	39.07	28791	12.90	20249	12.81
valine	0	0.00	0	0.00	62117	100.00	495744	8.35	772908	3.33	0	0.00	0	0.00	0	0.00	0	0.00

Metabolite	x (M blank)	Se (M blank) [%]	$\bar{x}$ (25 °C 15 h)	Se (25 °C, 15 h) [%]	$\bar{x}$ (25 °C, 19 h)	Se (25 °C, 19 h) [%]	$\bar{x}$ (25 °C, 22 h)	Se (25 °C, 22 h) [%]	$\bar{x}$ (25 °C, 30 h)	Se (25 °, 30 h) [%]	$\bar{x}$ (37 °C, 17 h)	Se (37 °C, 17 h) [%]	$\bar{x}$ (37 °C, 20 h)	Se (37 °C, 20 h)) [%]	$\bar{x}$ (37 °C, 23 h)	Se (37 °C, 23 h) [%]	$\bar{x}$ (37 °C, 31 h)	Se (37 °C, 31 h) [%]
xylose	0	0.00	11990	4.21	19796	2.79	17560	5.22	15719	4.74	0	0.00	0	0.00	0	0.00	0	0.00

D.2 Time-resolved intracellular metabolome analysis in minimal medium at 37 °C

Semiquantitative peak areas (mean: $\bar{x}$, n = 4), relative standard error Se

Metabolite	$\bar{x}$ (25 °C 15 h)	Se (25 °C, 15 h) [%]	$\bar{x}$ (25 °C, 19 h)	Se (25 °C, 19 h) [%]	$\bar{x}$ (25 °C, 22 h)	Se (25 °C, 22 h) [%]	$\bar{x}$ (25 °C, 30 h)	Se (25 °, 30 h) [%]	$\bar{x}$ (37 °C, 17 h)	Se (37 °C, 17 h) [%]	$\bar{x}$ (37 °C, 20 h)	Se (37 °C, 20 h)) [%]	$\bar{x}$ (37 °C, 23 h)	Se (37 °C, 23 h) [%]	$\bar{x}$ (37 °C, 31 h)	Se (37 °C, 31 h) [%]
1,6-anhydro-glucose	2907	14.06	0	0.00	0	0.00	0	0.00	3738	13.68	3582	7.39	2949	20.39	0	0.00
2-aminoadipic-acid	1323	8.95	1977	10.86	1668	9.23	13690	19.86	1290	5.80	1115	5.00	1101	18.29	4706	9.32
2-hydroxy-glutarate	2053	24.45	2673	6.00	5126	26.57	2047	42.22	43315	17.57	38799	9.91	27889	19.14	17186	20.17
2-methyl-malate	0	0.00	0	0.00	0	0.00	0	0.00	0	0.00	0	0.00	18682	63.35	27241	5.19
2-oxoglutarate	28792	36.59	6530	48.96	3647	29.86	1878	78.96	22319	23.66	10720	9.82	1588	74.70	341	52.91
2-phenylacetamide	0	0.00	0	0.00	0	0.00	0	0.00	0	0.00	0	0.00	2488	9.01	0	0.00
2-phosphoglycerate	1895	49.88	126	19.07	125	23.15	5258	85.66	2434	27.93	2501	6.53	1511	43.29	1934	96.94
3-hydroxy-dodecanoate	4150	3.50	5102	10.99	4535	12.91	3893	11.04	6195	8.83	5476	5.11	7166	12.41	7276	7.67
3-hydroxypyridine	9217	8.84	10782	19.42	9694	16.36	10747	21.09	7018	10.11	6958	9.32	7480	27.53	3131	35.71
5-methylthio-adenosine	4410	30.79	7836	34.36	7157	3.65	10191	29.37	6151	29.73	2877	36.24	9729	44.10	7853	17.52
6-phospho-gluconate	29670	41.16	185783	9.91	88002	24.46	65866	54.93	118785	32.80	78859	33.38	26690	38.90	22076	68.01
9-(E)-octadecenoate	28658	23.80	68387	3.53	34150	21.56	23999	15.35	8040	17.03	1866	13.60	8502	9.97	21567	15.29
9-(Z)-hexadecenoate	45287	17.65	49356	8.39	35499	17.24	31424	11.32	19078	17.49	11954	13.83	39804	10.67	62216	11.29
adenine	199287	15.16	232980	14.03	306465	15.96	285651	22.21	163726	11.35	165092	10.72	240905	35.63	134803	8.91
adenosine	2569	25.43	5159	14.37	11950	28.76	13394	81.89	5508	35.82	3230	26.07	11906	69.14	3613	38.15
alanine	49698	47.81	10866	23.94	27877	77.76	5921	21.80	40358	50.27	35975	50.37	233441	16.21	50833	32.95
alanyl-alanine	0	0.00	40212	70.80	8314	100.00	7430	48.12	0	0.00	0	0.00	242334	8.32	0	0.00
allo-threonine	14438	24.90	160891	5.13	19360	7.56	7725	12.69	32830	14.23	27701	8.96	27968	20.19	3031	45.82
AMP	54467	24.99	99769	47.95	80803	29.45	84537	23.11	213730	34.11	133100	8.84	131812	48.45	91753	22.89
aspartate	67093	46.67	45984	12.22	45984	15.67	34693	8.20	26161	11.65	23204	11.78	16703	19.76	7293	14.35
beta-Alanine	0	0.00	5387	77.90	17180	28.59	20749	16.27	2741	27.28	4928	33.09	2175	47.68	1132	57.99
citrate	256495	13.74	315859	30.25	78997	12.02	37917	20.27	275655	12.77	193274	6.14	231372	14.38	9664	17.81
cysteine	4618	35.53	8889	27.33	5954	52.58	4372	21.24	0	0.00	0	0.00	0	0.00	0	0.00
cytosine	127928	16.33	237198	12.76	204003	16.26	226541	41.80	123235	8.10	102673	11.75	148045	46.90	121458	7.86
decanoate	2861	10.76	4932	14.05	3040	23.75	2039	34.15	2444	30.04	1704	15.87	5124	20.75	10105	3.05
dodecanoate	56977	3.25	76447	8.80	52842	8.63	66142	4.37	9253	17.17	8134	4.18	23038	9.03	38860	6.91

Metabolite	$\bar{x}$ (25 °C 15 h)	Se (25 °C, 15 h) [%]	$\bar{x}$ (25 °C, 19 h)	Se (25 °C, 19 h) [%]	$\bar{x}$ (25 °C, 22 h)	Se (25 °C, 22 h) [%]	$\bar{x}$ (25 °C, 30 h)	Se (25 °, 30 h) [%]	$\bar{x}$ (37 °C, 17 h)	Se (37 °C, 17 h) [%]	$\bar{x}$ (37 °C, 20 h)	Se (37 °C, 20 h)) [%]	$\bar{x}$ (37 °C, 23 h)	Se (37 °C, 23 h) [%]	$\bar{x}$ (37 °C, 31 h)	Se (37 °C, 31 h) [%]
ethanolaminephosphate	89428	10.67	185077	27.50	139947	10.18	93637	15.33	197174	17.77	131207	10.61	138848	12.04	92795	20.81
fumarate	25103	9.31	18789	26.95	6880	19.55	3517	14.69	30610	20.26	22598	7.92	20904	12.23	2614	16.63
glucose	52214	6.40	16165	14.66	15219	24.18	5857	18.35	88543	10.16	78394	8.52	62652	14.76	9943	28.25
glucose-6-phosphate	0	0.00	0	0.00	5465	40.19	0	0.00	13389	41.65	6556	25.47	3381	20.85	3662	49.08
glutamate	5835942	7.53	7324204	0.05	5782067	7.64	2951143	10.80	6071915	4.13	5446933	2.65	1762566	6.50	368332	18.41
glycerate	1229	10.10	1371	19.07	1982	10.55	1985	46.29	941	37.15	1038	11.54	1829	28.74	1011	37.76
glycerate-3-phosphate	85380	10.71	39454	4.17	57125	12.58	61612	3.00	79400	9.64	64795	5.92	71808	13.97	7191	27.09
glycerol-3-phosphate	220238	9.63	243499	4.78	217267	12.05	160751	5.71	158844	9.87	129187	5.09	123289	19.46	41613	17.01
glycine	369553	27.51	652918	22.00	355773	28.01	223906	12.58	125745	9.53	129869	8.57	166335	12.44	51326	22.36
guanine	29334	21.82	31987	15.82	33233	13.73	35350	7.35	28694	3.85	30214	15.44	30325	11.75	14578	35.07
heptadecanoate	5125	30.47	17725	7.88	9111	34.04	3342	67.43	1553	49.59	2696	57.97	558	86.19	5546	16.70
homoserine	0	0.00	8713	12.92	0	0.00	0	0.00	0	0.00	0	0.00	0	0.00	0	0.00
lactate	0	0.00	0	0.00	0	0.00	0	0.00	143405	37.09	192543	20.63	232788	26.36	952823	20.83
leucine	140256	9.81	228988	8.75	219017	9.58	221839	7.95	69655	2.78	72968	2.05	67099	5.41	47555	10.11
lysine	19950	26.64	14713	16.54	12029	16.61	63420	13.51	188550	25.03	224043	6.16	254713	15.52	266915	28.99
malate	53086	21.32	21644	30.28	4100	3.28	2567	14.52	63467	19.84	45542	6.16	45590	13.23	1761	17.71
methionine	14758	15.56	47382	2.48	37185	10.15	26637	5.37	16481	8.42	12561	5.89	12624	16.60	1963	34.13
NA_1067.1	0	0.00	0	0.00	30003	58.69	0	0.00	65461	72.92	73247	70.19	17497	100.00	540810	13.47
NA_1643	7876	17.48	9937	8.78	11347	8.61	11777	9.02	19922	19.51	16806	5.10	16636	8.09	16147	17.71
NA_2019.3	21036	12.36	27965	12.30	23413	8.54	18957	13.79	49371	8.81	45721	5.63	42021	2.52	35603	4.69
NA_2600.6	48460	37.84	62031	23.60	55767	18.28	62746	27.69	76358	17.97	55524	16.55	79637	29.20	67237	14.98
NA185	0	0.00	0	0.00	0	0.00	0	0.00	2288	76.35	10696	35.84	25706	3.04	51147	3.20
NA192001 (classified unknown)257	2930134	27.94	363796	57.30	1190670	50.29	165218	26.29	4267013	34.52	4379980	22.81	1990295	29.03	154429	31.97
NA276	29911	45.01	30524	11.90	0	0.00	0	0.00	76441	23.59	62401	32.70	36858	55.64	0	0.00
NA411	0	0.00	176502	15.38	0	0.00	0	0.00	0	0.00	0	0.00	0	0.00	0	0.00
NA459	2306	41.05	20032	17.00	53140	28.27	48964	20.70	3649	61.00	0	0.00	0	0.00	51797	25.04
N-acetyl-serine	24250	20.01	46242	32.44	28216	13.24	19480	23.18	73550	9.57	67959	15.86	29051	24.88	8729	71.04
nicotinamide	34164	33.78	46826	9.07	40943	10.27	31513	21.95	125591	21.01	91942	6.22	98772	25.88	52839	12.27
nicotinate	12448	22.38	25157	9.12	21300	21.96	11970	12.98	35300	1.53	40224	9.08	44641	17.65	30201	10.69
norvaline	0	0.00	0	0.00	0	0.00	0	0.00	130923	13.26	142711	3.21	154148	9.19	0	0.00
oleate methyl ester	14045	27.52	21017	28.40	18764	12.95	10692	37.06	0	0.00	0	0.00	0	0.00	0	0.00
orotate	0	0.00	0	0.00	0	0.00	0	0.00	21046	25.25	15293	9.21	0	0.00	0	0.00
phenylalanine	0	0.00	0	0.00	8806	14.06	8293	18.36	0	0.00	0	0.00	0	0.00	0	0.00
phosphoenolpyruvate	24091	13.12	15200	17.29	17639	14.43	15583	4.57	14342	17.91	11475	14.79	14564	12.31	1524	38.62
putrescine	15728	31.31	53598	30.49	1841	58.93	0	0.00	0	0.00	0	0.00	0	0.00	0	0.00
pyroglutamate	1525465	10.82	2512228	14.62	1576004	11.84	819687	16.50	1396766	13.50	1034461	5.35	627482	19.10	280034	7.00
pyrophosphate	47776	9.25	41876	3.33	38788	25.72	34388	14.48	222514	20.55	179120	6.88	85081	8.36	16930	17.75
pyruvate	3309	18.59	7545	89.77	6036	32.80	4308	58.75	45146	18.67	55332	43.62	22134	17.19	693	62.19
ribose	1637	2.20	2259	18.67	1967	11.11	2004	9.11	1824	12.71	1545	9.20	1969	14.32	2923	13.77

Metabolite	$\bar{x}$ (25 °C 15 h)	Se (25 °C, 15 h) [%]	$\bar{x}$ (25 °C, 19 h)	Se (25 °C, 19 h) [%]	$\bar{x}$ (25 °C, 22 h)	Se (25 °C, 22 h) [%]	$\bar{x}$ (25 °C, 30 h)	Se (25 °, 30 h) [%]	$\bar{x}$ (37 °C, 17 h)	Se (37 °C, 17 h) [%]	$\bar{x}$ (37 °C, 20 h)	Se (37 °C, 20 h)) [%]	$\bar{x}$ (37 °C, 23 h)	Se (37 °C, 23 h) [%]	$\bar{x}$ (37 °C, 31 h)	Se (37 °C, 31 h) [%]
serine	63326	18.98	68487	4.30	228630	72.81	114506	5.93	65549	30.19	84096	6.54	119224	6.72	31269	31.92
sorbitol-6-phosphate	7343	25.88	8628	28.09	14044	26.68	4917	36.43	71227	24.29	45572	19.10	38138	23.94	6702	29.33
spermidine	45711	39.99	152813	13.71	161321	19.18	135945	16.99	33373	12.81	35304	29.97	21110	30.68	26687	42.84
succinate	103709	26.58	60600	46.98	21397	36.56	10855	19.85	48513	11.08	44246	8.73	52743	19.92	4388	5.52
succinic-acid-methylester	26072	10.58	22832	17.42	9322	13.91	5186	20.56	16966	23.60	11624	17.88	6737	27.25	1089	36.70
tetradecanoate	122328	9.43	154484	10.03	132948	14.24	173211	3.77	87509	9.16	62230	10.68	74863	8.99	87338	10.73
threonine	12413	29.13	163191	13.73	18048	12.52	6323	8.92	27593	14.01	23050	13.41	24676	11.99	1368	39.97
thymine	172630	14.62	230496	10.38	242118	12.89	291067	28.92	197233	8.10	174233	10.62	240371	39.60	142752	1.85
tyrosine	16276	27.41	6198	26.80	71654	8.14	108871	10.90	14919	39.13	6178	33.77	7049	40.16	2678	57.88
Unknown#bth-pae-030_1454.4	47244	13.15	31137	14.10	54363	12.74	70008	21.24	33351	17.48	38702	19.56	54149	28.55	17713	34.60
Unknown#bth-pae-036_1549.1	42000	14.98	63522	11.73	57264	17.49	63403	27.71	42357	12.42	38693	16.70	39059	40.74	27973	9.68
Unknown#bth-pae-039_1586.9	0	0.00	0	0.00	0	0.00	0	0.00	51970	14.43	37917	8.43	54632	10.14	0	0.00
Unknown#mse-ypy-002_1_2922.4	17384	32.88	37940	51.24	21183	16.15	41037	17.82	17405	33.07	10031	9.64	12092	50.30	7933	16.07
Unknown#mse-ypy-002_2_2955.1	174935	20.34	252135	26.13	181545	8.86	308159	17.04	135913	30.18	83668	8.44	73766	37.19	56045	14.62
Unknown#mse-ypy-003_1093.7	48079	11.19	56108	11.59	83068	18.60	62354	23.38	53423	15.16	60330	9.31	68517	20.25	48911	9.34
Unknown#mse-ypy-009_1493.0	7402	12.96	10796	4.67	10959	3.75	15619	16.93	11456	19.56	9008	13.09	10324	28.72	5865	13.64
Unknown#mse-ypy-012_1604.97	1131	18.87	1339	11.86	2204	40.35	2779	52.29	1361	31.33	1063	15.94	1065	27.69	4861	82.03
Unknown#mse-ypy-017_1896.2	13207	17.57	14633	22.13	10425	10.70	11554	11.65	3105	29.72	3696	33.48	3986	13.73	2796	22.36
Unknown#mse-ypy-020_2054.7	0	0.00	0	0.00	0	0.00	0	0.00	862	33.57	1802	16.37	2014	21.93	0	0.00
Unknown#mse-ypy-021_2090.4	3605	10.72	1093	50.20	0	0.00	0	0.00	8251	18.93	6678	14.74	7072	19.15	0	0.00
Unknown#mse-ypy-023_2128.1	26474	29.44	69756	10.44	40794	17.08	51415	17.09	62982	20.94	58102	19.18	200630	14.37	578353	7.36
Unknown#mse-ypy-036_1981.9	0	0.00	1410	3.88	3128	14.29	2032	15.97	0	0.00	0	0.00	0	0.00	0	0.00
Unknown#mse-ypy-039_3026.6	154221	33.90	285532	35.39	282295	20.65	221984	13.61	23747	20.95	9125	9.76	6061	25.30	9287	46.58
Unknown#sst-cgl-001_1746.7	37922	6.24	45721	10.99	33675	35.04	19940	39.18	81854	9.56	65035	4.62	54685	4.99	30186	13.98
Unknown#sst-cgl-111_2282.3	15704	33.92	42500	17.42	41849	3.41	20937	40.87	41121	18.71	19786	38.88	29324	14.95	21744	34.49
Uracil	55670	13.15	55784	7.77	61030	10.69	69344	21.32	54720	5.42	47618	6.44	62276	23.74	36388	8.96
valine	388317	20.31	2465131	3.20	1795462	10.16	903356	3.29	253488	12.08	151854	5.19	174041	13.32	65215	23.54
xylulose-5-phosphate	1195	23.67	1128	29.81	414	26.69	360	27.32	3518	15.40	3287	7.70	1857	25.64	873	16.96

E.1 Transcriptome analyses of the Y. pseudotuberculosis *mutant strains YP3, YP72, YP53, YP50, YP89*

Only significant changes (mutant/ wild type > 1.8-fold) are shown as $\log_2$ fold ratios for every mutant strain. The genes encoding proteins participating in the metabolism are indicated in the category class.

Gene ID	Gene locus	YP89 (crp-)	YP53 (csrA-)	YP50 (ymoA-)	YP72 (rovM-)	YP3 (rovA-)	Description	Category-Class
pYptb0001	*rep*	-1.78		-1.84			plasmid replication protein	
pYptb0003				0.83	1.7		hypothetical protein	
pYptb0007	*triD*			-0.84			type IV secretion system protein VirB5	
pYptb0010	*eex*	-0.97		-1.1			hypothetical protein	
pYptb0011	*triE*			-0.88			type IV secretion system protein VirB6	
pYptb0017	*kikA*			-0.93			hypothetical protein	
pYptb0019				-0.87			hypothetical protein	
pYptb0024		-0.88		-1.54			hypothetical protein (DUF1891 motif)	
pYptb0033				-0.89			hypothetical protein	
pYptb0043				-1.06	-1.03		hypothetical protein	
pYV0001				1.41			putative targeted effector protein kinase (YopO)	
pYV0002	*sycO*			1.91			putative type III secretion chaperone	
pYV0007		-1.4					replication protein	
pYV0011				0.89			transposase remname	
pYV0013	*yadA*			1.13			YadA domain-containing protein	
pYV0017		-0.86		1.42			putative resolvase	
pYV0018				1.08			transposase IS3/IS911 family protein	
pYV0019				0.91			putative transposase	
pYV0024	*sycE; yerA*	-0.82		1.87			putative YopE chaperone	
pYV0025	*yopE*			3.04			putative outer membrane virulence protein	
pYV0026			-0.87				hypothetical protein	
pYV0027			-1				hypothetical protein	
pYV0033				-0.89			hypothetical protein	
pYV0039				2.06			putative transposase	
pYV0040	*yopK; yopQ*			2.57			yop targeting protein YopK; YopQ	
pYV0041	*yopT*			-0.82			yop targeted effector YopT	Metabolism
pYV0044				2.28			hypothetical protein	
pYV0045				1.52			hypothetical protein	
pYV0046				1			putative transposase remnant	
pYV0047	*yopM*			1.99			Type III secretion system leucine rich repeat protein	
pYV0048				1.37			hypothetical protein	
pYV0049				2.04			hypothetical protein	
pYV0052				1.48			putative transposase	
pYV0054	*yopD*	-0.9		2.24			putative Yop negative regulation/targeting component	
pYV0055	*yopB*			2.49			putative Yop targeting protein; Secretion system effector C (SseC) like family	
pYV0056	*lcrH; sycD*			2.55			low calcium response protein H; chaperone	
pYV0057	*lcrV*			3.16			putative V antigen	
pYV0058	*lcrG*			2.88			putative Yop regulator	
pYV0059	*lcrR*			1.95			type III secretion system regulator	
pYV0060	*lcrD; yscV*			1.07			putative membrane-bound Yop protein	
pYV0061	*yscY*			1.27			putative type III secretion protein	
pYV0062	*yscX*			1.11			putative type III secretion protein	
pYV0063	*sycN*			1.06	-0.96		putative type III secretion protein	
pYV0064	*tyeA*			1.09			putative Yop secretion and targeting protein	
pYV0065	*yopN; lcrE*			1.71			putative membrane-bound Yop targeting protein	
pYV0067	*yscN*			1.91			type III secretion system ATPase	
pYV0068	*yscO*			1.51			putative type III secretion protein	
pYV0069	*yscP*			1.3			putative type III secretion protein	
pYV0070	*yscQ*			1.15			type III secretion system protein	
pYV0071	*yscR*			1.02			type III secretion system protein	

Gene ID	Gene locus	YP89 (crp-)	YP53 (csrA-)	YP50 (ymoA-)	YP72 (rovM-)	YP3 (rovA-)	Description	Category-Class
pYV0072	*yscS*			1.16			putative type III secretion protein	
pYV0073	*yscT*			1.03			putative type III secretion protein	
pYV0074	*yscU*			1.03			putative type III secretion protein	
pYV0075	*virG;yscW*	-0.82	0.88	2.86			putative Yop targeting lipoprotein	
pYV0076	*lcrF; virF*			2.44			putative thermoregulatory protein	
pYV0077	*yscA*			3.26			hypothetical protein yscA in Y. enterocolitica	
pYV0078	*yscB*			3.17			YscB family type III secretion system chaperone	
pYV0079	*yscC*	-1.09		2.46			putative type III secretion protein	
pYV0080	*yscD*			2.21			putative type III secretion protein	
pYV0081	*yscE*			2.99			putative type III secretion protein	
pYV0082	*yscF*			3.07			putative type III secretion protein	
pYV0083	*yscG*			2.39			putative type III secretion protein	
pYV0084	*yscH*	1.2		1.87			putative type III secretion protein	
pYV0085	*yscI; lcrO*			2.3			putative type III secretion protein	
pYV0086	*yscJ; ylpB*			2.06			putative type III secretion lipoprotein	
pYV0087	*yscK*			1.95			putative type III secretion protein	
pYV0088	*yscL*			2.31			type III secretion system protein	
pYV0089	*yscM; lcrQ*	-1.11	0.96	2.13			putative type III secretion regulatory	
pYV0090	*lcrS*			1.69			putative transposase; Pfam: Transposase_8	
pYV0091				2.05		-0.84	putative transposase	
pYV0092				2.67			putative transposase;Pfam: rve	
pYV0093	*tnpA*			2.19			putative transposase	
pYV0094	*yopH*	-0.92		2.52			putative protein-tyrosine phosphatase Yop effector	
pYV0097				1.18			hypothetical protein	
pYV0098	*yopP; yopJ*			3.89			putative targeted effector protein; YopJ protease family	Metabolism
pYV0099				2.55	0.88		hypothetical protein	
YPK_0011	*ibpA*			2.99			heat shock protein IbpA	
YPK_0012	*ibpB*		1.14	2.4			heat shock chaperone IbpB	
YPK_0013	*yidE*	-1.24	-1.49				hypothetical protein	
YPK_0025	*yiaF*	2.5	1.99				putative lipoprotein	
YPK_0031				0.8			hypothetical protein	
YPK_0035	*sodA*		-0.91				superoxide dismutase	
YPK_0037	*fdoG*	-1.32	-0.89				formate dehydrogenase; alpha subunit	Metabolism
YPK_0043	*selB*		-0.92				selenocysteinyl-tRNA-specific translation factor	
YPK_0044				1.12			hypothetical protein	
YPK_0045				1.13			hypothetical protein	
YPK_0046					-0.91		hypothetical protein	
YPK_0051		4.03		2.66			fimbrial protein	
YPK_0052	*yqiG*			0.88			fimbrial biogenesis outer membrane usher protein	
YPK_0053		0.8		1.26	1.03		pili assembly chaperone	
YPK_0054	*ybgO*			0.86			fimbrial protein	
YPK_0062	*hsdM?*			1.09			hypothetical protein	
YPK_0064		-1.46		1.05			hypothetical protein	
YPK_0065				0.9			N4/N6-methyltransferase family protein	
YPK_0066				0.89			transposase IS3/IS911 family protein	
YPK_0077	*hutH*	1.51		-1.01			histidine ammonia-lyase	Metabolism
YPK_0078	*hutT*		-1.02	-1.06			amino acid permease-associated region	
YPK_0081	*uhpA*	-0.97	-0.85				two component LuxR family transcriptional regulator	
YPK_0107	*yapE*			-0.97			outer membrane autotransporter	
YPK_0109					-0.81		hypothetical protein	
YPK_0116	*opdA*	1.05		0.92			oligopeptidase A	Metabolism
YPK_0117	*yhiQ*			0.86			putative methyltransferase	
YPK_0120	*uspA*	-3.49	-1.1	-1.04			universal stress protein A	
YPK_0121	*uspB*		-1.13	-1.05			universal stress protein UspB	
YPK_0130		1.72	1.08				ribokinase-like domain-containing protein	
YPK_0131		-1.05					two component transcriptional regulator	
YPK_0132			-0.88				hypothetical protein	
YPK_0136	*gntK*					0.89	carbohydrate kinase	Metabolism
YPK_0138				-0.81	-0.91		hypothetical protein	
YPK_0145	*invC*			0.82			adhesin/invasin	
YPK_0149	*glgC*			-0.8			glucose-1-phosphate adenylyltransferase	Metabolism
YPK_0150	*glgA*	0.81					glycogen synthase	Metabolism
YPK_0151	*glgP*	1.86		-0.99			starch phosphorylase	Metabolism
YPK_0154				1.09			hypothetical protein	

Gene ID	Gene locus	YP89 (crp-)	YP53 (csrA-)	YP50 (ymoA-)	YP72 (rovM-)	YP3 (rovA-)	Description	Category-Class
YPK_0155				1.06			hypothetical protein	
YPK_0159	*glpE*		-0.92				thiosulfate sulfurtransferase	
YPK_0161	*malP*			0.86			starch phosphorylase	Metabolism
YPK_0162	*malQ*		-0.95				4-alpha-glucanotransferase	Metabolism
YPK_0166			-1.01				hypothetical protein	
YPK_0169	*feoA*					-0.9	ferrous iron transport protein A	
YPK_0174	*pckA*	1.05					phosphoenolpyruvate carboxykinase	Metabolism
YPK_0175	*hslO*			0.87			HSP33-like chaperonin	
YPK_0176	*hslR*			0.98			ribosome-associated heat shock protein Hsp15	
YPK_0184				-1.25			hypothetical protein	
YPK_0200				-0.98			hypothetical protein	
YPK_0238	*tsgA*	-0.88					hypothetical protein	
YPK_0240			-0.91				LacI family transcription regulator	
YPK_0248	*crp*	-2.83					cAMP-regulatory protein	
YPK_0250				0.87	-1.1		hypothetical protein	
YPK_0251				1.15			Hcp1 family type VI secretion system effector	
YPK_0252				1.45			hypothetical protein	
YPK_0253				1.37			hypothetical protein	
YPK_0257		0.81					lysine exporter protein LysE/YggA	
YPK_0269			-1.02		-0.8		SlyX protein	
YPK_0270	*fkpA*		0.94				FKBP-type peptidyl-prolyl cis-trans isomerase	
YPK_0273				-0.93			sulfur relay protein TusC	
YPK_0274				-0.84			sulfur transfer complex subunit TusB	
YPK_0276	*rpsG*			1.35			30S ribosomal protein S7	
YPK_0277	*fusA*			0.82			elongation factor G	
YPK_0278	*tuf*	1					elongation factor Tu	
YPK_0280	*bfd*	-1.3	-1.87				bacterioferritin-associated ferredoxin	
YPK_0281	*bfr*		-1.29	-1.18			bacterioferritin	
YPK_0282	*rpsJ*	1.57		1.23			ribosomal protein S10	
YPK_0283	*rplC*	1.67		0.94			50S ribosomal protein L3	
YPK_0284	*rplD*	1.67		0.98			50S ribosomal protein L4	
YPK_0285	*rplW*	1.61		0.95			50S ribosomal protein L23	
YPK_0286	*rplB*	1.5		0.96			50S ribosomal protein L2	
YPK_0287	*rpsS*	1.28		0.93			30S ribosomal protein S19	
YPK_0288	*rplV*	1.49		1.02			50S ribosomal protein L22	
YPK_0289	*rpsC*	1.14		1.1			30S ribosomal protein S3	
YPK_0290	*rplP*	1.11		1.08			50S ribosomal protein L16	
YPK_0291	*rpmC*	1.36		1.21			50S ribosomal protein L29	
YPK_0292	*rpsQ*	1.24		1.26			30S ribosomal protein S17	
YPK_0294	*rplX*			0.92			50S ribosomal protein L24	
YPK_0296	*rpsN*	0.94		0.82			30S ribosomal protein S14	
YPK_0297	*rpsH*	0.82					30S ribosomal protein S8	
YPK_0298	*rplF*	0.92					50S ribosomal protein L6	
YPK_0299	*rplR*	1.26		0.9			50S ribosomal protein L18	
YPK_0300	*rpsE*	1.09		1.01			30S ribosomal protein S5	
YPK_0301	*rpmD*	1.46		1.03			50S ribosomal protein L30	
YPK_0302	*rplO*	1.36					50S ribosomal protein L15	
YPK_0303	*secY*	1.47		1.03			preprotein translocase subunit SecY	
YPK_0304	*rpmJ*	1.51		0.86			50S ribosomal protein L36	
YPK_0305	*rpsM*	1.48		0.92			30S ribosomal protein S13	
YPK_0306	*rpsK*	1.47					30S ribosomal protein S11	
YPK_0307	*rpsD*	1.59					30S ribosomal protein S4	
YPK_0308	*rpoA*	1.61		1.07			DNA-directed RNA polymerase subunit alpha	
YPK_0309	*rplQ*	1.8		1.15			50S ribosomal protein L17	
YPK_0328	*coaA*			0.85			pantothenate kinase	Metabolism
YPK_0333	*secE*	0.86					preprotein translocase subunit SecE	
YPK_0334	*nusG*	0.88					transcription antitermination protein NusG	
YPK_0335	*rplK*			1.03			50S ribosomal protein L11	
YPK_0336	*rplA*			0.81			50S ribosomal protein L1	
YPK_0337	*rplJ*	0.96					50S ribosomal protein L10	
YPK_0338	*rplL*	0.94		0.89			50S ribosomal protein L7/L12	
YPK_0341	*rpoC*	0.89					DNA-directed RNA polymerase subunit beta	
YPK_0348	*rsd*	-0.85		-0.94			anti-RNA polymerase sigma 70 factor	
YPK_0354	*hupA*	-0.88					DNA-binding protein HU-alpha	
YPK_0356	*purD*			-1.18			phosphoribosylamine-glycine ligase	Metabolism
YPK_0364	*aceB*	-1.11	-2.06				malate synthase	Metabolism
YPK_0365	*aceA*	-0.95	-2.29				isocitrate lyase	Metabolism
YPK_0366	*aceK*		-1.42				isocitrate dehydrogenase kinase/phosphatase	
YPK_0367	*iclR*	-1.01	-0.92				ranscriptional repressor IclR	

Gene ID	Gene locus	YP89 (crp-)	YP53 (csrA-)	YP50 (ymoA-)	YP72 (rovM-)	YP3 (rovA-)	Description	Category-Class
YPK_0376	*malG*		-0.93	0.88			maltose transporter permease	
YPK_0377	*malF*		-1.11				maltose transporter membrane protein	
YPK_0378	*malE*		-1.83	2.02			maltose ABC transporter periplasmic protein	
YPK_0379	*amyA*		-1.08	2.04			glycosidase	
YPK_0380	*malK*		-1.09	2.23			maltose/maltodextrin transporter ATP-binding protein	
YPK_0381	*lamB*		-2.82	2.96			maltoporin	
YPK_0382	*malM*		-1.45	1.41			maltose regulon periplasmic protein	
YPK_0384		1.09	0.99				hypothetical protein	
YPK_0385	*hcp*	0.95	1.61	0.8			Hcp1 family type VI secretion system effector	
YPK_0386	*impB*		1.14	1.45			type VI secretion protein	
YPK_0387	*impC*		1.38	1.23			EvpB family type VI secretion protein	
YPK_0388				0.98			type VI secretion system protein	
YPK_0396		-0.93					fis family transcriptional regulator	
YPK_0399					0.94		type VI secretion protein IcmF	
YPK_0402		-0.95		-0.85			hypothetical protein	
YPK_0404				0.97			hypothetical protein	
YPK_0411				1.24			hypothetical protein	
YPK_0426	*yjcD*			-1.1			xanthine/uracil/vitamin C permease	
YPK_0427			1.23				transposase mutator type	
YPK_0431		-1.65					carbohydrate ABC transporter periplasmic-binding protein	
YPK_0442	*cspa1*			1.61			cold-shock DNA-binding domain-containing protein	
YPK_0443	*cspa1*			1.45			cold-shock DNA-binding domain-containing protein	
YPK_0444	*cspa1*			1.04			cold-shock DNA-binding domain-containing protein	
YPK_0445	*pcp*		-2.49	-0.81			17 kDa surface antigen	
YPK_0446		-0.86					beta-lactamase domain-containing protein	
YPK_0452	*fis*	1.79		0.95			DNA-binding protein fis	
YPK_0453		0.97					tRNA-dihydrouridine synthase B	
YPK_0458	*accC*	0.83					acetyl-CoA carboxylase biotin carboxylase subunit	Metabolism
YPK_0464	*yhdA; csrD*			-0.86			regulatory protein CsrD	
YPK_0465	*mreB*	1.11					rod shape-determining protein MreB	
YPK_0467	*mreD*				-0.84		rod shape-determining protein MreD	
YPK_0475				0.85			hypothetical protein	
YPK_0478	*tcaC*			0.96			virulence plasmid 65kDa B protein	
YPK_0479	*tcaB*			1.47			toxin subunit (insecticidal)	
YPK_0480	*tcaA*			1.41			virulence protein (insecticidal)	
YPK_0483		0.92					hypothetical protein	
YPK_0486	*gabD*		-0.87				succinic semialdehyde dehydrogenase	Metabolism
YPK_0487			-0.98				guanine-specific ribonuclease N1 and T1	
YPK_0492			-0.84				cytochrome b562	
YPK_0494	*treC*	1.81		1.04			trehalose-6-phosphate hydrolase	Metabolism
YPK_0495	*treB*	1.7	0.84	1.24			trehalose(maltose)-specific PTS system components IIBC	Metabolism
YPK_0497		3.46	3.22		-1.12		hypothetical protein	
YPK_0502		0.82					hypothetical protein	
YPK_0504	*yhbH*			-1.38			putative sigma(54) modulation protein	
YPK_0512	*yrbF*	1.52					putative ABC transporter ATP-binding protein YrbF	
YPK_0513	*yrbE*	1.6					hypothetical protein	
YPK_0514	*yrbD*	1.39					hypothetical protein	
YPK_0515	*yrbC*	1.94					toluene tolerance family protein	
YPK_0516		2.03					putative anti-sigma B factor antagonist	
YPK_0518	*murA*	1					UDP-N-acetylglucosamine 1-carboxyvinyltransferase	Metabolism
YPK_0524	*rplM*	0.85	0.8	1.02			50S ribosomal protein L13	
YPK_0525	*rpsI*	0.94	0.9	0.85			30S ribosomal protein S9	
YPK_0533	*arcB*	-1.1	-0.85				aerobic respiration control sensor protein ArcB	Metabolism
YPK_0534	*elbB*		-0.81	-0.88			isoprenoid biosynthesis protein with amidotransferase-like domain	
YPK_0535	*mtgA*		-0.81				monofunctional biosynthetic peptidoglycan transglycosylase	Metabolism
YPK_0536		1.02	0.97				hypothetical protein	
YPK_0545		0.88					hypothetical protein	
YPK_0547				-0.93			protein of unknown function DUF883 ElaB	
YPK_0558	*sstT*	-2.65	-1.12				serine/threonine transporter SstT	

Gene ID	Gene locus	YP89 (crp-)	YP53 (csrA-)	YP50 (ymoA-)	YP72 (rovM-)	YP3 (rovA-)	Description	Category-Class
YPK_0563	*fadH*	-0.95					NADH:flavin oxidoreductase/NADH oxidase	
YPK_0564		-1.91		-1.64	0.9		acid-resistance membrane protein	
YPK_0569	*terX*		-0.85				stress protein	
YPK_0571					0.82		polypeptide-transport-associated domain-containing protein	
YPK_0572	*fhaB*			-1.47			filamentous haemagglutinin outer membrane protein	
YPK_0578		-1.33		-1.18			hypothetical protein	
YPK_0581				0.99			hypothetical protein	
YPK_0582				0.9			putative adhesin/hemolysin	
YPK_0585	*chvB?*			0.96			hypothetical protein	
YPK_0586	*togA?*			0.95			ABC transporter related	
YPK_0593	*bglX*			0.98			beta-glucosidase	Metabolism
YPK_0598		-0.87	-0.96				hypothetical protein	
YPK_0602				0.92			YheO domain-containing protein	
YPK_0603	*tdcF*			0.93			endoribonuclease L-PSP	
YPK_0604				1.08			endoribonuclease L-PSP	
YPK_0611	*yrhA*			1			hypothetical protein	
YPK_0612				1.49			hypothetical protein	
YPK_0621				-0.96			hypothetical protein	
YPK_0626		-0.84					hypothetical protein	
YPK_0631		-1.69	-3.08	-1.79			hypothetical protein	
YPK_0634	*rpoD*	0.83	-0.82	0.84			RNA polymerase sigma factor RpoD	
YPK_0636	*rpsU*			1.16			30S ribosomal protein S21	
YPK_0638	*plsY*	-0.81					putative glycerol-3-phosphate acyltransferase PlsY	Metabolism
YPK_0649	*ribB*	0.9		-0.83			3;4-dihydroxy-2-butanone 4-phosphate synthase	Metabolism
YPK_0651		-1.08					glutathionylspermidine synthase	
YPK_0652		-1.14					hypothetical protein	
YPK_0663	*plsC*	1.4					1-acyl-sn-glycerol-3-phosphate acyltransferase	Metabolism
YPK_0664		0.88					hypothetical protein	
YPK_0665	*sufI*	1.12					repressor protein for FtsI	
YPK_0667	*dkgA*	0.86					2;5-diketo-D-gluconate reductase A	
YPK_0668	*yqhD*		-0.91				iron-containing alcohol dehydrogenase	
YPK_0687	*cpaA*			0.92			peptidase A24A prepilin type IV	
YPK_0692	*cpbD*			1.24			fibronectin type III domain-containing protein	
YPK_0693	*chiC*			0.97			glycoside hydrolase family protein	
YPK_0694	*smfA*			1.44			fimbrial protein	
YPK_0695	*papC*		-1.35				fimbrial biogenesis outer membrane usher protein	
YPK_0696	*papD*		-1.19				pili assembly chaperone	
YPK_0697		-0.9	-1.01				fimbrial protein	
YPK_0698	*fepB; fhuD*	1.38		1.23			iron-enterobactin transporter periplasmic binding protein	
YPK_0699				1.34			hypothetical protein	
YPK_0703	*flhB*			1.68			flagellar biosynthesis protein FlhB	
YPK_0724				1.08			hypothetical protein	
YPK_0725				1.58			putative transcriptional regulator; CadC	
YPK_0727				0.81			hypothetical protein	
YPK_0736	*slyB; pcp*	-1.22					outer membrane lipoprotein SlyB	
YPK_0751	*irp2*	-1.18		-1.69			amino acid adenylation domain-containing protein	
YPK_0759		-1.57		0.95			hypothetical protein	
YPK_0767				1.96			hypothetical protein	
YPK_0768				1.71			hypothetical protein	
YPK_0769				2.29	-1.11		hypothetical protein	
YPK_0770				0.93			YD repeat-containing protein	
YPK_0771				1.87		0.8	hypothetical protein	
YPK_0772				2.13			rhs protein	
YPK_0773				2.05			hypothetical protein	
YPK_0774				0.92			hypothetical protein	
YPK_0775				2.29	-0.82		hypothetical protein	
YPK_0776				2.02			hypothetical protein	
YPK_0777				1.15			hypothetical protein	
YPK_0789		1.9	1.35	1.26	-0.9		intradiol ring-cleavage dioxygenase	
YPK_0792	*yspI; ytbI*	-0.88		1.38			autoinducer synthesis protein	
YPK_0794				0.87			lipoprotein	
YPK_0795	*insA*			0.88			insertion element protein	
YPK_0797				0.83			hypothetical protein	

Gene ID	Gene locus	YP89 (crp-)	YP53 (csrA-)	YP50 (ymoA-)	YP72 (rovM-)	YP3 (rovA-)	Description	Category-Class
YPK_0806				-0.88			peptidase M23B	
YPK_0807		-1.66					hypothetical protein	
YPK_0809		-1.08		-1			hypothetical protein	
YPK_0812	*rbsB*	-1.02	-0.86				ribose transport system substrate-binding protein	
YPK_0817				-0.81			hypothetical protein	
YPK_0844				0.94			hypothetical protein	
YPK_0851	*epd*		-1				erythrose 4-phosphate dehydrogenase	Metabolism
YPK_0854	*mscS2*	0.84					MscS mechanosensitive ion channel	
YPK_0856	*yggE*		1.43	-0.88			hypothetical protein	
YPK_0858	*rpiA*	-0.88					ribose-5-phosphate isomerase A	Metabolism
YPK_0859	*serA*			-0.93			D-3-phosphoglycerate dehydrogenase	Metabolism
YPK_0869	*gcvP*			-0.88			glycine dehydrogenase	Metabolism
YPK_0870			-0.99		-1.19		hypothetical protein	
YPK_0871	*yadF*	2.48	2	1.02			YadA domain-containing protein	
YPK_0873	*hlyIII*		-0.93				hemolysin III family channel protein	
YPK_0884				1.38			hypothetical protein	
YPK_0890					-0.83		putative relication initiation protein	
YPK_0892	*gpa*			-1			replication gene A	
YPK_0898					-0.95		putative capsid scaffolding protein	
YPK_0915			1.03				tail assembly chaperone GP38	
YPK_0919					2.4		hypothetical protein	
YPK_0924	*lysS*	0.86					lysyl-tRNA synthetase	
YPK_0953			1				hypothetical protein	
YPK_0954			1.14				hypothetical protein	
YPK_0955			1.03				colicin D	
YPK_0962			-0.96				hypothetical protein	
YPK_0963					1.86		hypothetical protein	
YPK_0998				0.92			outer membrane autotransporter	
YPK_0999				1.18			hypothetical protein	
YPK_1000		-0.89					hypothetical protein	
YPK_1001	*mig5*	-3.36	-2.56	-1.92		-0.87	carbonic anhydrase	Metabolism
YPK_1003					-1.07		general secretion pathway protein C	
YPK_1007	*gspG*			1.11			general secretion pathway protein G	
YPK_1010	*gspJ*				1.04		general secretion pathway protein J	
YPK_1011	*gspK*			0.91			general secretion pathway protein K	
YPK_1012	*gspL*			1.07	1.43		general secretion pathway protein L	
YPK_1013				1.8			hypothetical protein	
YPK_1014	*gspO*			1.9			prepilin peptidase	Metabolism
YPK_1016		-1.26		-0.87			transcriptional regulator; CadC	
YPK_1017				1.37			hypothetical protein	
YPK_1018	*tsr; cheD*			1.08			methyl-accepting chemotaxis sensory transducer	
YPK_1019		1					hypothetical protein	
YPK_1020		0.98					beta-lactamase domain-containing protein	
YPK_1037		-1.2					hypothetical protein	
YPK_1040		0.82					prepilin peptidase dependent protein-like protein	
YPK_1042	*ptrA*	1					peptidase M16 domain-containing protein	Metabolism
YPK_1056				-0.81			hypothetical protein	
YPK_1062		-0.83	-1.2	-0.94			hypothetical protein	
YPK_1063	*dapD*	-1.26	-0.95				2;3;4;5-tetrahydropyridine-2;6-carboxylate N-succinyltransferase	Metabolism
YPK_1066	*rpsB*	1.02	0.8	1			30S ribosomal protein S2	
YPK_1067	*tsf*	0.81					elongation factor Ts	
YPK_1071	*uppS*			-0.85			undecaprenyl diphosphate synthase	Metabolism
YPK_1073	*rseP*	0.92					regulator of sigma E protease	Metabolism
YPK_1074	*yaeT*	1.05					outer membrane protein assembly factor YaeT	
YPK_1076	*lpxD*	1.1					UDP-3-O-[3-hydroxymyristoyl] glucosamine N-acyltransferase	Metabolism
YPK_1077	*fabZ*	0.95					(3R)-hydroxymyristoyl-ACP dehydratase	Metabolism
YPK_1085		-0.92					cytochrome c class I	
YPK_1090	*cutF; nlpE*		0.84				copper homeostasis protein (lipoprotein)	
YPK_1111					-1.58		urate catabolism protein	
YPK_1122	*yicN*			1.04			hypothetical protein	
YPK_1123				0.92			hypothetical protein	
YPK_1124	*cspB*			1.16			cold-shock DNA-binding domain-containing protein	
YPK_1126	*oppB*			-0.97			peptide/nickel transport system permease protein	
YPK_1128	*oppD*		-0.89				ABC transporter related	

Gene ID	Gene locus	YP89 (crp-)	YP53 (csrA-)	YP50 (ymoA-)	YP72 (rovM-)	YP3 (rovA-)	Description	Category-Class
YPK_1131	*ureA*	-1.09		1.07	1.51	-0.82	urease subunit gamma	Metabolism
YPK_1132	*ureB*	-0.97			1.36		urease subunit beta	Metabolism
YPK_1133	*ureC*	-0.87	-0.96		1.3	-0.9	urease subunit alpha	Metabolism
YPK_1134	*ureE*			0.89	0.97		urease accessory protein UreE	
YPK_1135	*ureF*				0.95		urease accessory protein UreF	
YPK_1136	*ureG*				1.08		urease accessory protein UreG	
YPK_1137	*ureD*				0.89		urease accessory protein UreD	
YPK_1139	*nixA*		-0.81				high-affinity nickel-transporter	
YPK_1140	*hdeB*	-0.89	-0.91	-0.99	0.96	-1.06	acid-resistance protein	
YPK_1141	*kch*		-1.82				voltage-gated potassium channel	
YPK_1144	*celA*	-1.18					PTS system; cellobiose-specific IIB component	
YPK_1153				-0.83			hypothetical protein	
YPK_1168		0.86	0.87				UreA amidolyase related protein	
YPK_1174	*grcA*		-1.2				autonomous glycyl radical cofactor GrcA	
YPK_1181	*nadB*	0.98					L-aspartate oxidase	Metabolism
YPK_1182	*rpoE*			-1.69			RNA polymerase sigma factor RpoE	
YPK_1183	*rseA*			-0.98			anti-RNA polymerase sigma factor SigE	
YPK_1202					1.06		VRR-NUC domain-containing protein	
YPK_1207		-1.77		-1.49			hypothetical protein	
YPK_1210		-0.9		-1.17			XRE family transcriptional regulator	
YPK_1222				-1.09			hypothetical protein	
YPK_1223		-1		-0.83			hypothetical protein	
YPK_1234					2.36		hypothetical protein	
YPK_1236					-0.89		hypothetical protein	
YPK_1238					1.65		hypothetical protein	
YPK_1244		-1.48	-1	-1.68			hypothetical protein	
YPK_1261	*nadE*	0.81					NAD+ synthetase	Metabolism
YPK_1262	*glnB*	0.98					nitrogen regulatory protein P-II 1	
YPK_1265	*glyA*			-0.94			serine hydroxymethyltransferase	
YPK_1267		1.06		-0.89			hypothetical protein	
YPK_1268	*ailA*	1.29		-1.02			virulence-related outer membrane protein	
YPK_1275	*iscR*	-1.14	1.25				DNA-binding transcriptional regulator IscR	
YPK_1276	*iscS*	-1.14	0.93				cysteine desulfurase	Metabolism
YPK_1277	*nifU*	-0.92					scaffold protein	
YPK_1289	*ndk*	-1.73					nucleoside diphosphate kinase	Metabolism
YPK_1293	*ispG*	1.08					4-hydroxy-3-methylbut-2-en-1-yl diphosphate synthase	Metabolism
YPK_1296	*yfgL*	1.03					outer membrane protein assembly complex subunit YfgL	
YPK_1298			-0.83				auxin efflux carrier	
YPK_1302	*guaB*	0.84		-0.92			inosine 5'-monophosphate dehydrogenase	Metabolism
YPK_1304				1.8			Hcp1 family type VI secretion system effector	
YPK_1306				-0.95			hypothetical protein	
YPK_1309				0.91			hypothetical protein	
YPK_1311		-1.29		-1.5			hypothetical protein	
YPK_1312				0.97			hypothetical protein	
YPK_1322		-1.04					hypothetical protein	
YPK_1326		-0.87	-1.28	-1.05			hypothetical protein	
YPK_1332	*mdtA*			-1.01			putative multidrug efflux transporter MdtA	
YPK_1347	*pstB*			-0.82			phosphate ABC transporter	
YPK_1349	*speG*			0.87			diamine N-acetyltransferase	Metabolism
YPK_1351	*purI*			-1.1			phosphoribosylaminoimidazole synthetase	
YPK_1354	*hda*	-1.15					DNA replication initiation factor	
YPK_1358		-0.88					hypothetical protein	
YPK_1359				0.9			hypothetical protein	
YPK_1364	*purC*			-1.11			phosphoribosylaminoimidazole-succinocarboxamide synthase	Metabolism
YPK_1365				-1.21			hypothetical protein	
YPK_1375	*afuA*	-2.71	1.52				iron(III) transport system substrate-binding protein	
YPK_1376	*afuB*	-1.33	1.25				iron(III) transport system permease protein	
YPK_1377		-1.33	1.12				ABC transporter related	
YPK_1381					-0.9		hypothetical protein	
YPK_1384	*narP*			0.88	0.91		nitrate/nitrite response regulator NarP	
YPK_1385	*napF*	-0.87	1.23	0.84	-1.08		ferredoxin-type protein NapF	Metabolism
YPK_1386	*napD*	-0.8	1.2	0.95	-1.41		assembly protein for periplasmic nitrate reductase	Metabolism
YPK_1387	*napA*			0.88			nitrate reductase catalytic subunit	Metabolism
YPK_1388	*napB*		1.06	0.95	-1.06		citrate reductase cytochrome c-type subunit	Metabolism
YPK_1389	*napC*		0.92	0.9			cytochrome c-type protein NapC	Metabolism
YPK_1392		0.9					hypothetical protein	

Gene ID	Gene locus	YP89 (crp-)	YP53 (csrA-)	YP50 (ymoA-)	YP72 (rovM-)	YP3 (rovA-)	Description	Category-Class
YPK_1394				1.05			putative acetyltransferase	
YPK_1397	*ygiW*	-0.87		-1			hypothetical protein	
YPK_1400	*nanA*			1.79			N-acetylneuraminate lyase	Metabolism
YPK_1408	*cysP*	1.2		-0.93			thiosulfate transporter subunit	
YPK_1409	*cysU*	1.21					sulfate/thiosulfate transporter subunit	
YPK_1410	*cysW*	0.98					sulfate/thiosulfate transporter permease subunit	
YPK_1411	*cysA*	1.73					sulfate/thiosulfate transporter subunit	
YPK_1412	*cysM*	1.15					cysteine synthase B	
YPK_1413				0.98			hypothetical protein	
YPK_1424	*cpxR*	-0.81					two-component system; OmpR family; response regulator	
YPK_1427	*ptsI*		-0.82				phosphoenolpyruvate-protein phosphotransferase	
YPK_1428	*ptsH*		-1.04				phosphohistidinoprotein-hexose phosphotransferase component of PTS system (HPr)	
YPK_1429	*cysK*	1.63	0.88				cysteine synthase A	Metabolism
YPK_1430	*cysZ*	2.12	1.33				putative sulfate transport protein CysZ	
YPK_1438	*nupC(1)*	1.53				1.48	nucleoside transporter	
YPK_1449	*csgG*	-1.24		2.27			curli production assembly/transport component CsgG	
YPK_1450				1.86			putative lipoprotein	
YPK_1451				2.02			hypothetical protein	
YPK_1459				1.03			Hcp1 family type VI secretion system effector	
YPK_1462	*sfuB*				0.93		binding-protein-dependent transport systems inner membrane component	
YPK_1465		-0.88					LuxR family transcriptional regulator	
YPK_1468				-0.87			hypothetical protein	
YPK_1475	*fimA*		1.03	1.78			major type 1 subunit fimbrin (pilin)	
YPK_1478				3.47			fimbrial protein	
YPK_1479	*impB*			1.3			type VI secretion system protein ImpB	
YPK_1480	*impC*			1.32			type VI secretion system protein ImpC	
YPK_1481			1.01	2.48			type VI secretion system secreted protein Hcp	
YPK_1483	*impJ*			0.81			type VI secretion system protein ImpJ	
YPK_1487				0.84			hypothetical protein	
YPK_1489	*impE*			0.96			type VI secretion system protein ImpE	
YPK_1490	*impF*			0.91			type VI secretion system protein ImpF	
YPK_1492	*phnA*	-1.41	-0.97	-1.46			alkylphosphonate utilization operon protein PhnA	Metabolism
YPK_1506	*fadL*	-2.06					long-chain fatty acid outer membrane transporter	
YPK_1507				-0.84			hypothetical protein	
YPK_1508	*fadI*	-1.02					acetyl-CoA acyltransferase	
YPK_1509	*fadJ*	-0.84	0.8				multifunctional fatty acid oxidation complex subunit alpha	
YPK_1510		-1.14					hypothetical protein	
YPK_1520	*fabB*		-0.95	-0.85			3-oxoacyl-(acyl carrier protein) synthase I	Metabolism
YPK_1522	*smfA*			1.38			fimbrial protein	
YPK_1534	*cvpA*			-1.01			colicin V production protein	
YPK_1535	*purF*			-0.86			amidophosphoribosyltransferase	Metabolism
YPK_1537			-0.81		-0.96		hypothetical protein	
YPK_1538	*hisJ*	-1.38	-1.22	-0.87	-0.86		histidine transport system substrate-binding protein	
YPK_1539	*hisQ*	-0.98	-1		-1.03		polar amino acid ABC transporter; inner membrane subunit	
YPK_1544	*yfcE*	1.09					phosphodiesterase	
YPK_1545		1.05	0.87				NUDIX hydrolase	
YPK_1546	*ulaA*			0.82			PTS system; ascorbate-specific IIC component	Metabolism
YPK_1547	*sgaB*			0.92			PTS system; ascorbate-specific IIB component	Metabolism
YPK_1548	*cmtB*			0.94			PTS system; ascorbate-specific IIA component	Metabolism
YPK_1553			-0.98				hypothetical protein	
YPK_1559	*rovM*	1.92		0.89	-1.87		LysR family transcriptional regulator	
YPK_1574				1.1			hypothetical protein	
YPK_1575	*idnK*			1.16			gluconokinase	Metabolism
YPK_1576	*idnO*			1.57			gluconate 5-dehydrogenase	
YPK_1581					1.92		hypothetical protein	
YPK_1585	*elaB*		1.39				protein of unknown function DUF883 ElaB	

Gene ID	Gene locus	YP89 (crp-)	YP53 (csrA-)	YP50 (ymoA-)	YP72 (rovM-)	YP3 (rovA-)	Description	Category-Class
YPK_1586					1.52		protein RhiA	
YPK_1589	*menD*	-0.87		-1.21			2-succinyl-5-enolpyruvyl-6-hydroxy-3-cyclohexene-1-carboxylate synthase	Metabolism
YPK_1591	*menB*		-0.98				naphthoate synthase	Metabolism
YPK_1592	*menC*		-0.93				O-succinylbenzoate synthase	Metabolism
YPK_1593	*menE*		-0.92				O-succinylbenzoic acid-CoA ligase	Metabolism
YPK_1597	*mcp*			-0.94			methyl-accepting chemotaxis protein	
YPK_1598	*glnQ*					0.83	glutamine ABC transporter ATP-binding protein	
YPK_1600	*glnH*		-0.86		-1.17	0.99	glutamine transport system substrate-binding protein	
YPK_1601		-1.58					hypothetical protein	
YPK_1602	*dps*	-0.81	-0.81	-1.01		-1.13	DNA starvation/stationary phase protection protein Dps	
YPK_1606	*ompX; ailD*	2.79	2.82	1.01			outer membrane protein X	
YPK_1609				1.67			hypothetical protein	
YPK_1611	*rbsB*		-0.82				monosaccharide-transporting ATPase	
YPK_1612		-1.05		-1.08			ABC transporter related	
YPK_1614	*lacI*	-1.03		0.82			LacI family transcription regulator	
YPK_1616	*ttuC; dmlA*		-0.93				tartrate dehydrogenase	Metabolism
YPK_1618	*yeaV*		-1.06				putative transporter	
YPK_1619			-2.66		-1.03		Rieske (2Fe-2S) domain-containing protein (putative dioxygenase alpha subunit)	
YPK_1620	*yeaX*		-1.07				ferredoxin	
YPK_1623				0.83			hypothetical protein	
YPK_1625				0.86			hypothetical protein	
YPK_1640				0.81			hypothetical protein	
YPK_1642		-0.94					hypothetical protein	
YPK_1644			1.24	1.2			CRISPR-associated Cas1 family protein	
YPK_1645			0.94	0.84			CRISPR-associated helicase Cas3 family protein	
YPK_1646			0.86	0.99			CRISPR-associated Csy1 family protein	
YPK_1648				1.17			CRISPR-associated Csy3 family protein	
YPK_1655	*ypsR; sdiA; yenR*			0.85			LuxR family transcriptional regulator	
YPK_1658	*cvrA*			0.87			cell volume regulation protein A	
YPK_1659				-0.81			hypothetical protein	
YPK_1660					0.86		glucans biosynthesis protein C	
YPK_1665	*htrB*	1.1					lipid A biosynthesis lauroyl acyltransferase	Metabolism
YPK_1666			-0.93				hypothetical protein	
YPK_1671			1.02				LuxR family transcriptional regulator	
YPK_1674	*dinI*		1.41				DNA damage-inducible protein I	
YPK_1681		1.3					hypothetical protein	
YPK_1682	*rpmF*	1.31					50S ribosomal protein L32	
YPK_1686	*fabG*	1.7					3-ketoacyl-(acyl-carrier-protein) reductase	Metabolism
YPK_1691	*tdk*			-0.9			thymidylate kinase	Metabolism
YPK_1694	*ptsG*			0.8			PTS system; glucose-specific IIB component	
YPK_1701				-1.41			hypothetical protein	
YPK_1704					-1.1		hypothetical protein	
YPK_1705	*ycfJ*		2.17				hypothetical protein	
YPK_1725		-1.15					hypothetical protein	
YPK_1729		-0.89					hypothetical protein	
YPK_1731				1.41			hypothetical protein	
YPK_1738		1.34	3.65				hypothetical protein	
YPK_1740	*cspC?; cspA?*	-1.2	1.58	2.06			cold-shock DNA-binding domain-containing protein	
YPK_1741		-0.89					hypothetical protein	
YPK_1744	*mgtB*	-1.98	-1.13	-2.2			Mg2+-importing ATPase	
YPK_1745	*flhD*	-2.65	-0.98	1.51			transcriptional activator FlhD	
YPK_1746	*flhC*	-2.45	-1.06	1.11			transcriptional activator FlhC	
YPK_1747	*motA*		-1.02				flagellar motor protein MotA	
YPK_1748	*motB*		-0.88				flagellar motor protein MotB	
YPK_1750	*cheW*	-0.97	-1.24				purine-binding chemotaxis protein	
YPK_1751				0.81			putative integral membrane protein	
YPK_1760	*cwlA; xlyA; xlyB*	0.95	1.14				N-acetylmuramyl-L-alanine amidase	
YPK_1761		3.21	3.01		-0.97		YadA domain-containing protein	
YPK_1762		1.35	1.53	0.99			hypothetical protein	
YPK_1763		0.88	1.14				hypothetical protein	

Gene ID	Gene locus	YP89 (crp-)	YP53 (csrA-)	YP50 (ymoA-)	YP72 (rovM-)	YP3 (rovA-)	Description	Category-Class
YPK_1765		-1.06	-1.21				hypothetical protein	
YPK_1770		-0.97					hypothetical protein	
YPK_1778		1.03		1.09			spore coat U domain-containing protein	
YPK_1786	*fimA*			1.86			fimbrial protein	
YPK_1795	*gltP*			1.02			sodium:dicarboxylate symporter	
YPK_1803	*kduD1*			-0.8			2-deoxy-D-gluconate 3-dehydrogenase	Metabolism
YPK_1806			1.21				transposase mutator type	
YPK_1807			0.88				transposase	
YPK_1811		1.41					fructosamine kinase	
YPK_1813	*yfeC*	-0.81		-1.5			manganese/iron transport system permease protein	
YPK_1815	*yfeA*		-0.84				manganese/iron transport system substrate-binding protein	
YPK_1818		-2.06					hypothetical protein	
YPK_1822	*rpmI*	1.2		0.8			50S ribosomal protein L35	
YPK_1823	*rplT*	1.58		0.84			50S ribosomal protein L20	
YPK_1826	*ihfA*			-0.94			integration host factor subunit alpha	
YPK_1841	*aroH*	0.91					phospho-2-dehydro-3-deoxyheptonate aldolase	Metabolism
YPK_1842		-1.09					hypothetical protein	
YPK_1843	*ppsA*		-0.86	-0.9			phosphoenolpyruvate synthase	Metabolism
YPK_1844		1.26					putative inner membrane protein	
YPK_1846	*ydiI*			-0.92			thioesterase superfamily protein	
YPK_1855	*pykF*	1.47					pyruvate kinase	Metabolism
YPK_1858	*cfa*		-1.07				cyclopropane fatty acyl phospholipid synthase	
YPK_1862	*purR*			-1.3			DNA-binding transcriptional repressor PurR	
YPK_1863	*sodB*		-1.22	-0.87			superoxide dismutase	
YPK_1864		1.02					NLP/P60 protein	
YPK_1869	*gloA*	-0.89					lactoylglutathione lyase	Metabolism
YPK_1870	*sepC*		-0.98				rhs family protein-like protein	
YPK_1876	*rovA*	-3.16		-1.43	1.73	-3.04	transcriptional regulator SlyA	
YPK_1877	*slyB*		0.89				17 kDa surface antigen	
YPK_1878	*anmK*	-1.2	-0.93				anhydro-N-acetylmuramic acid kinase	
YPK_1879		-0.81					hypothetical protein	
YPK_1883	*gst*			-1.29			glutathionine S-transferase	Metabolism
YPK_1884			-1.01				hypothetical protein	
YPK_1885			-1.18				hypothetical protein	
YPK_1902	*tyrR*	-0.84					DNA-binding transcriptional regulator TyrR	
YPK_1903	*tpx*	0.89		-0.91			thiol peroxidase	
YPK_1917	*hslJ*	1.11	0.98				heat shock protein HslJ	
YPK_1918	*ldhA*	-1.07					D-lactate dehydrogenase	Metabolism
YPK_1926			0.88				hypothetical protein	
YPK_1927			0.92				XRE family transcriptional regulator	
YPK_1942	*pntB*			-0.9			NAD(P) transhydrogenase subunit beta	Metabolism
YPK_1947				0.85			hypothetical protein	
YPK_1949	*ilvN*			-1.15			acetolactate synthase 1 regulatory subunit	
YPK_1950	*ilvB*	-0.8					acetolactate synthase catalytic subunit	
YPK_1951		1.88	4.83				hypothetical protein	
YPK_1953	*srfB*			1.12			putative virulence factor SrfB	
YPK_1954				0.95			hypothetical protein	
YPK_1959				-0.95			hypothetical protein	
YPK_1963	*rbsB*		-1.1				ribose transport system substrate-binding protein	
YPK_1966					1.57		hypothetical protein	
YPK_1971				1.02			hypothetical protein	
YPK_1974	*aldH2*		-0.99				aldehyde dehydrogenase	
YPK_1975		-1.27	-0.91				fis family GAF modulated sigma54 specific transcriptional regulator	
YPK_1976	*ydfG*	-1.25					3-hydroxy acid dehydrogenase	
YPK_1977		-0.85					hypothetical protein	
YPK_1978		-0.81	1.94				hypothetical protein	
YPK_1980	*bioD*			1.29			putative dithiobiotin synthetase	Metabolism
YPK_1981	*mlc*	-1.08					ROK family protein	
YPK_1987			0.86				hypothetical protein	
YPK_1989		-3.5					hypothetical protein	
YPK_1990		-3.52					hypothetical protein	
YPK_1994		0.86					hypothetical protein	
YPK_1996	*araC*	-1.45					DNA-binding transcriptional regulator AraC	
YPK_1999	*araF*	-1.1					L-arabinose transport system substrate-binding protein	
YPK_2014				-0.88			NAD-dependent epimerase/dehydratase	
YPK_2017	*cstA*	-1.21	-0.98	-1.05			carbon starvation protein CstA	

Gene ID	Gene locus	YP89 (crp-)	YP53 (csrA-)	YP50 (ymoA-)	YP72 (rovM-)	YP3 (rovA-)	Description	Category-Class
YPK_2018		-1.67	-1.06	-1.23			hypothetical protein	
YPK_2022	*osmB*	-0.91					lipoprotein	
YPK_2030	*acnA*		-0.88				aconitate hydratase	Metabolism
YPK_2032	*cysB*	-0.98		-1.09			transcriptional regulator CysB	
YPK_2048				-1.08			transport-associated	
YPK_2049	*ompW*		-2.1	-1.19			outer membrane protein W	
YPK_2059		-1.05			1.32		hypothetical protein	
YPK_2060				1.05			hypothetical protein	
YPK_2061	*ailB*		1.2	1	1.03		virulence-related outer membrane protein	
YPK_2065				1.21			hypothetical protein	
YPK_2066	*oppF*		-1.06	-0.83			peptide/nickel transport system ATP-binding protein	
YPK_2067	*oppD*	-0.82	-0.91				peptide/nickel transport system ATP-binding protein	
YPK_2068	*oppC*	-1	-0.96				peptide/nickel transport system permease protein	
YPK_2069	*oppB*	-1.1	-0.89				peptide/nickel transport system permease protein	
YPK_2070	*oppA*	-2.07	-1.45	-0.9			peptide/nickel transport system substrate-binding protein	
YPK_2072	*adhE*		-0.84	0.97			bifunctional acetaldehyde-CoA/alcohol dehydrogenase	
YPK_2073	*tdk*			0.98			thymidine kinase	Metabolism
YPK_2077	*ugd*	-0.97		-1.05			UDPglucose 6-dehydrogenase	
YPK_2090		-0.81					hypothetical protein	
YPK_2094		-0.94					hypothetical protein	
YPK_2095	*msrB*	-1.15					peptide-methionine (R)-S-oxide reductase	
YPK_2096	*gapA*			1.03			glyceraldehyde-3-phosphate dehydrogenase; type I	Metabolism
YPK_2099				-0.81			hypothetical protein	
YPK_2100	*prkA*			-0.84			putative serine protein kinase	
YPK_2101				-1.24			hypothetical protein	
YPK_2107	*dadA*	-2.26		-1.66			D-amino acid dehydrogenase small subunit	Metabolism
YPK_2116				2.04			major facilitator transporter	
YPK_2125	*fadD*	-3.63					long-chain acyl-CoA synthetase	Metabolism
YPK_2126	*slp*		-1.16	-0.83			Slp family outer membrane lipoprotein	
YPK_2153	*cutC*		0.82				copper homeostasis protein CutC	
YPK_2156	*HlyA*	-2.6	-1.92	-2.09			hemolysin	
YPK_2157	*HlyB*			-1.19			hemolysin activation/secretion protein??	
YPK_2161	*rimJ*	0.86					ribosomal-protein-S5-alanine N-acetyltransferase	
YPK_2164			-0.87				cytoplasmic chaperone TorD family protein	
YPK_2185		-4.07	-1.12	-0.88			hypothetical protein	
YPK_2197		1.09	1.8	1.12			hypothetical protein	
YPK_2198		1.11	1.66				hypothetical protein	
YPK_2199		1.26	1.83	0.94			hypothetical protein	
YPK_2200		1.01	0.86	1.31		-1.19	hypothetical protein	
YPK_2205				0.9			Sel1 domain-containing protein	
YPK_2219		-1.32	-0.87				hypothetical protein	
YPK_2222	*hutI*	0.89					imidazolonepropionase	Metabolism
YPK_2224	*ompC2*			1.11			porin	
YPK_2225	*astE*		-0.98		-0.97	1.17	succinylglutamate desuccinylase	Metabolism
YPK_2226	*astB*		-1.21		-1.19	1.02	succinylarginine dihydrolase	Metabolism
YPK_2227	*astD*		-1.1		-1.38	1.13	succinylglutamic semialdehyde dehydrogenase	Metabolism
YPK_2228	*astA*		-1.19	-0.89	-1.21	1.09	arginine succinyltransferase	Metabolism
YPK_2229	*argD*		-1.62	-1.1	-2.14	1.38	bifunctional succinylornithine transaminase/acetylornithine transaminase	Metabolism
YPK_2239	*pgaC*		-1.61				N-glycosyltransferase PgaC	
YPK_2240	*pgaB*		-0.81				polysaccharide deacetylase	
YPK_2242		-0.98		-1.17			peptidase M24	
YPK_2245			-0.81				redoxin domain-containing protein	
YPK_2251			-1.38				hypothetical protein	
YPK_2252	*ftr1*	-0.93					high-affinity iron transporter	
YPK_2253			-1.13	-0.98			major facilitator transporter	
YPK_2254			-0.87				glutaminase	
YPK_2260		0.88					amidohydrolase 2	
YPK_2269	*fimZ*		-0.98				two component LuxR family transcriptional regulator	
YPK_2275				1.08			hypothetical protein	
YPK_2282				-1.34	-0.85		hypothetical protein	
YPK_2283				-0.98			hypothetical protein	
YPK_2290				-1.04			hypothetical protein	

Gene ID	Gene locus	YP89 (crp-)	YP53 (csrA-)	YP50 (ymoA-)	YP72 (rovM-)	YP3 (rovA-)	Description	Category-Class
YPK_2291			1.05	1.11			transposase	
YPK_2293				0.92			hypothetical protein	
YPK_2294		-0.98					hypothetical protein	
YPK_2295		-0.93					hypothetical protein	
YPK_2307	*intT*	-0.92		0.86			integrase family protein	
YPK_2308				1.01			hypothetical protein	
YPK_2309		-0.96					hypothetical protein	
YPK_2310		-0.89					XRE family transcriptional regulator	
YPK_2354	*pgsA*		-0.83				CDP-diacylglycerol--glycerol-3-phosphate 3-phosphatidyltransferase	Metabolism
YPK_2355	*uvrC*	0.83		0.82			excinuclease ABC subunit C	
YPK_2356	*uvrY*	0.98		0.95			two-component system; NarL family; invasion response regulator UvrY	
YPK_2357				0.84			hypothetical protein	
YPK_2361	*cycA*				-0.84	0.81	D-alanine/D-serine/glycine permease	
YPK_2363	*wrbA*		-1.15	-1.27			TrpR binding protein WrbA	
YPK_2367	*putP*		1.37				sodium/proline symporter	
YPK_2368			1.09				hypothetical protein	
YPK_2371				-1.09			hypothetical protein	
YPK_2378	*fliZ*			1.19			flagella biosynthesis protein FliZ	
YPK_2379				1.05			hypothetical protein	
YPK_2380	*fliA*		-1.24	0.86			flagellar biosynthesis sigma factor	
YPK_2381	*fliC*	-1.27	-1.46	-1.08			flagellin	
YPK_2383	*fliS*			0.87			flagellar protein FliS	
YPK_2384	*fliT*			1.39			flagellar biosynthesis protein FliT	
YPK_2385				1.29			AraC family transcriptional regulator	
YPK_2388				0.95			death on curing protein	
YPK_2390	*fliE*		-0.81	1.33			flagellar hook-basal body protein FliE	
YPK_2391	*fliF*			0.99			flagellar MS-ring protein	
YPK_2392	*fliG*			0.82			flagellar motor switch protein G	
YPK_2393	*fliH*			1.07			flagellar assembly protein H	
YPK_2395	*fliJ*			0.86	-0.92		flagellar biosynthesis chaperone	
YPK_2396	*fliK*			0.81			flagellar hook-length control protein FliK	
YPK_2398	*fliL*			0.82			flagellar FliL protein	
YPK_2399	*fliM*	-0.81					flagellar motor switch protein FliM	
YPK_2400	*fliN*			0.91			flagellar motor switch protein FliN/FliY	
YPK_2401	*fliO*			0.91			flagellar protein FliO/FliZ	
YPK_2402	*fliP*			0.95			flagellar biosynthetic protein FliP	
YPK_2403	*fliQ*			0.83			flagellar biosynthetic protein FliQ	
YPK_2405				1.34			hypothetical protein	
YPK_2406				1.46			hypothetical protein	
YPK_2410		-0.87		-1.01			simple sugar transport system substrate-binding protein	
YPK_2412		-1.37		-1.4			hypothetical protein	
YPK_2413		-0.89		-0.95			short chain dehydrogenase	
YPK_2417	*flgJ*			0.88			flagellar protein FlgJ	
YPK_2418	*flgI*			0.95			flagellar P-ring protein precursor FlgI	
YPK_2419	*flgH*			0.89			flagellar L-ring protein precursor FlgH	
YPK_2420	*flgG*		-0.84				flagellar basal-body rod protein FlgG	
YPK_2421	*flgF*			0.81			flagellar basal-body rod protein FlgF	
YPK_2422	*flgE*			1.26			flagellar hook protein FlgE	
YPK_2423	*flgD*			1.31			flagellar basal-body rod modification protein FlgD	
YPK_2424	*flgC*		-1.05	1.06			flagellar basal-body rod protein FlgC	
YPK_2425	*flgB*		-1.12	1.05			flagellar basal body rod protein FlgB	
YPK_2426	*flgA*			0.86			flagella basal body P-ring formation protein FlgA	
YPK_2429	*invA*	-2.4				-1.87	invasin region 3	
YPK_2430	*flhE*			0.84			flagellar protein FlhE	
YPK_2437	*copC*	-0.86					copper resistance protein CopC	
YPK_2438	*ftnA*	1.17	0.88	-0.82			ferroxidase	Metabolism
YPK_2441				-1.01			hypothetical protein	
YPK_2443		-0.9	-0.94				hypothetical protein	
YPK_2444	*yqfB*	-0.85	-1				hypothetical protein	
YPK_2447	*purT*			-1.14			phosphoribosylglycinamide formyltransferase 2	Metabolism
YPK_2451	*sdaA*	-1.14		1.44			L-serine dehydratase 1	Metabolism
YPK_2464	*manX*	-0.89					PTS system mannose/fructose/sorbose family IIB subunit	
YPK_2465	*manY*		-0.87	-0.96			PTS system mannose/fructose/sorbose family IIC subunit	
YPK_2466	*manZ*	-0.88	-1.1	-0.98			mannose-specific PTS system protein IID	
YPK_2470		1.53	1.92				diguanylate cyclase with PAS/PAC sensor	

Gene ID	Gene locus	YP89 (crp-)	YP53 (csrA-)	YP50 (ymoA-)	YP72 (rovM-)	YP3 (rovA-)	Description	Category-Class
YPK_2471				2.59			hypothetical protein	
YPK_2474	*cspC*	-1.49					cold shock-like protein CspC	
YPK_2475		-1.61					hypothetical protein	
YPK_2481		0.98	0.94				hypothetical protein	
YPK_2482			-0.95				hypothetical protein	
YPK_2483		-4.22	-2.57	-0.94			hypothetical protein	
YPK_2485				0.96			hypothetical protein	
YPK_2486			-0.84	1	-0.81		hypothetical protein	
YPK_2488		1.15					protein of unknown function RIO1	
YPK_2489				-0.85			YCII-related	
YPK_2500				0.97			hypothetical protein	
YPK_2501				0.89			hypothetical protein	
YPK_2502		-1.01					polysaccharide deacetylase	
YPK_2503		-1.32					major facilitator transporter	
YPK_2506	*lldD*		-1.1				L-lactate dehydrogenase	Metabolism
YPK_2507			-1.33	-0.89			hypothetical protein	
YPK_2508		-1.27	-1.11	-0.85			mandelate racemase/muconate lactonizing protein	
YPK_2509		-1.03	-0.98				5-oxopent-3-ene-1;2;5-tricarboxylate decarboxylase	
YPK_2510		-1.1	-0.99				short-chain dehydrogenase/reductase SDR	
YPK_2512		-0.92					major facilitator transporter	
YPK_2518		-0.9					hypothetical protein	
YPK_2522		-1.33	-1				hypothetical protein	
YPK_2530	*hisA*		-0.85				phosphoribosylformimino-5-aminoimidazole carboxamide ribotide isomerase	Metabolism
YPK_2531	*hisF*		-0.81				imidazole glycerol phosphate synthase subunit HisF	Metabolism
YPK_2537	*galU*			0.92			UTP-glucose-1-phosphate uridylyltransferase	
YPK_2544	*alcC*	-1.25					IucA/IucC family protein	
YPK_2549		1.24	0.94				integral membrane protein TerC	
YPK_2555				0.91			hypothetical protein	
YPK_2561	*cdd*					2.6	cytidine deaminase	Metabolism
YPK_2564	*mglC*	-0.83					methyl-galactoside transport system permease protein	
YPK_2565	*mglA*	-1.14		0.94			methyl-galactoside transport system ATP-binding protein	
YPK_2566	*mglB*	-2.64					methyl-galactoside transport system substrate-binding protein	
YPK_2573			1.14	1.1	1.48		hypothetical protein	
YPK_2574			1.01	1.77	0.88		hypothetical protein	
YPK_2576				1.26			ABC transporter related	
YPK_2577				1.2			radical SAM domain-containing protein	
YPK_2582				2.24			hypothetical protein	
YPK_2602	*fabD*			0.98			putative acyltransferase	Metabolism
YPK_2603	*acpP*			1.84			putative acyl carrier protein	
YPK_2604				1.23			hypothetical protein	
YPK_2605	*fabG7*			1.03			short-chain dehydrogenase/reductase SDR	
YPK_2606				0.82			polyketide biosynthesis enoyl-CoA hydratase	
YPK_2609	*fabG*	-1.01		-1.55			3-oxoacyl-[acyl-carrier protein] reductase	Metabolism
YPK_2610	*fabB*			0.82			3-oxoacyl-[acyl-carrier-protein] synthase I	Metabolism
YPK_2611	*fabZ*			0.83			3R-hydroxymyristoyl ACP dehydrase	Metabolism
YPK_2613	*fabG5?*			0.83			short-chain dehydrogenase/reductase SDR	
YPK_2615	*cnf1*	0.95		3.22			cytotoxic necrotizing factor	
YPK_2619	*acyP*			-1.03			acylphosphatase	Metabolism
YPK_2621	*hspQ*			0.87			hemimethylated DNA binding protein	
YPK_2628	*tfoX*		0.9				DNA transformation protein and related proteins	
YPK_2637		0.87	0.81				hypothetical protein	
YPK_2641	*rlmL*		0.81				23S rRNA m(2)G2445 methyltransferase	
YPK_2643		-1.05	1.38				hypothetical protein	
YPK_2644	*pyrD*		1.15				dihydroorotate oxidase	Metabolism
YPK_2649	*ompF/ ompC2*	-2.34					porin	
YPK_2650	*aspC*		1.7	-0.89			aspartate aminotransferase	
YPK_2652			0.98				beta-lactamase domain-containing protein	
YPK_2660	*kdsB*		0.83				3-deoxy-manno-octulosonate cytidylyltransferase	Metabolism
YPK_2661			1.1				hypothetical protein	
YPK_2662	*cspB*		0.94				cold-shock DNA-binding domain-containing protein	
YPK_2663		-0.95					hypothetical protein	
YPK_2664	*lpxK*		1				tetraacyldisaccharide 4'-kinase	Metabolism

Gene ID	Gene locus	YP89 (crp-)	YP53 (csrA-)	YP50 (ymoA-)	YP72 (rovM-)	YP3 (rovA-)	Description	Category-Class
YPK_2667	*ihfB*		0.98				integration host factor subunit beta	
YPK_2668	*rpsA*	2.2					30S ribosomal protein S1	
YPK_2669	*cmk*	1.73	1.72				cytidylate kinase	Metabolism
YPK_2670	*aroA*	0.81	1.18				3-phosphoshikimate 1-carboxyvinyltransferase	Metabolism
YPK_2671	*serC*		1.57				phosphoserine aminotransferase	Metabolism
YPK_2672	*yadC*			1.07			hypothetical protein	
YPK_2673	*yadB*			0.93			hemagluttinin domain-containing protein	
YPK_2674	*ansB*			1.02		0.98	L-asparaginase II	Metabolism
YPK_2676	*focA*			0.93			formate transporter	
YPK_2677	*pflB*			0.93			formate acetyltransferase	Metabolism
YPK_2678					1.03		glycosyl transferase family protein	
YPK_2681	*serS*	0.94	1.08				seryl-tRNA synthetase	
YPK_2687	*trxB*		0.81				thioredoxin reductase	Metabolism
YPK_2691	*infA*		1.4	0.84			translation initiation factor IF-1	
YPK_2692	*clpA*		1.25				ATP-dependent Clp protease ATP-binding subunit ClpA	
YPK_2693	*clpS*		1.01				ATP-dependent Clp protease adaptor protein ClpS	
YPK_2694	*cspD*	-3.46		-1.81			cold-shock DNA-binding domain-containing protein	
YPK_2695	*macB*		0.98				macrolide transporter ATP-binding/permease protein	
YPK_2696	*macA*		1.17				macrolide transporter subunit MacA	
YPK_2703	*poxB*		0.92				pyruvate dehydrogenase	Metabolism
YPK_2709	*pheA2*		1.47				chorismate mutase	
YPK_2710	*artP*		1.21				arginine transport system ATP-binding protein	
YPK_2711	*artI*		1.25				arginine transport system substrate-binding protein	
YPK_2712	*artQ*		0.92				arginine transporter permease subunit ArtQ	
YPK_2714	*artJ*		0.84				hypothetical protein	
YPK_2722				-1.19			hypothetical protein	
YPK_2723				-1.15	-0.89		hypothetical protein	
YPK_2729	*potG*			-1.06			putrescine transporter ATP-binding subunit	
YPK_2733	*grxA*		1.52				glutaredoxin 1	
YPK_2735		0.9	1.94				membrane protein	
YPK_2736		0.85	1.32				undecaprenyl pyrophosphate phosphatase	
YPK_2739	*sdaC*	-1.04	1.08	1.93			serine transporter	
YPK_2740	*dacC*		1.19				serine-type D-Ala-D-Ala carboxypeptidase	Metabolism
YPK_2746		0.87	1.67				HAD family hydrolase	
YPK_2751	*fhuD*	0.99	0.89				periplasmic binding protein	
YPK_2752	*lysP*	2.69	3.04				lysine transporter	
YPK_2753			0.8				hypothetical protein	
YPK_2754			1.05				putative DNA-binding transcriptional regulator	
YPK_2756	*nfo*		1.17				endonuclease IV	
YPK_2758	*psaB*	-1.17		1.33	0.99		pili assembly chaperone	
YPK_2759	*psaA*	-2.04	1.71	1.44	1.51	-1.31	pH 6 antigen precursor (antigen 4) (adhesin)	
YPK_2760	*psaF*	-2.09	1.53	1.15	0.96	-1.37	hypothetical protein	
YPK_2761	*psaE*	-3.53	1.58	1.19	1.12	-2.93	transcriptional regulator; CadC	
YPK_2762	*fruA*	-1.35	1.95	-0.81			fructose-specific PTS system IIBC component	Metabolism
YPK_2763	*fruK*	-0.95	1.93				1-phosphofructokinase	Metabolism
YPK_2764	*fruB*	-1.06	1.98				bifunctional fructose-specific PTS IIA/HPr protein	Metabolism
YPK_2767		-1.4		-0.91			simple sugar transport system ATP-binding protein	
YPK_2778	*uxuA*	-1.09	0.92				mannonate dehydratase	Metabolism
YPK_2781				0.99			hypothetical protein	
YPK_2784	*spr*	-2.31	1.97				lipoprotein Spr	Metabolism
YPK_2786	*yejA*		0.97				extracellular solute-binding protein	
YPK_2790			0.86				hypothetical protein	
YPK_2791			1				hypothetical protein	
YPK_2795	*rplY*		1.4	0.84			50S ribosomal protein L25	
YPK_2796	*ndpA*		1.05				nucleoid-associated protein NdpA	
YPK_2797	*yejL*		0.87				hypothetical protein	
YPK_2798	*yejM*		0.92				sulfatase	
YPK_2801			1.28				hypothetical protein	
YPK_2802			1.29				colicin D	
YPK_2804		-0.93	2.1	0.84			hypothetical protein	
YPK_2805	*bglA*		1.55				6-phospho-beta-glucosidase	Metabolism
YPK_2806			1.21				hypothetical protein	

Gene ID	Gene locus	YP89 (crp-)	YP53 (csrA-)	YP50 (ymoA-)	YP72 (rovM-)	YP3 (rovA-)	Description	Category-Class
YPK_2808			2.03				tail assembly chaperone GP38	
YPK_2809			2.37				putative bacteriophage tail fiber protein	
YPK_2810			2.29				putative bacteriophage protein GP48	
YPK_2811			2.25				baseplate J family protein	
YPK_2812			2.07	-1.31			GP46 family protein	
YPK_2813			2.06				phage baseplate assembly protein V	
YPK_2814			1.84				Mu P family protein	
YPK_2815			1.58				DNA circulation family protein	
YPK_2816			1.81				hypothetical protein	
YPK_2817			3.21				putative bacteriophage protein	
YPK_2818			3.47				hypothetical protein	
YPK_2819			3.48				Mu tail sheath family protein	
YPK_2820			3.6				putative bacteriophage protein	
YPK_2821			3.04				hypothetical protein	
YPK_2822			3.05				hypothetical protein	
YPK_2827			0.8	-1.5			antitermination Q family protein	
YPK_2830	*msgA*		0.92				DinI family protein	
YPK_2836	*ampH*	1.09	1.61				beta-lactam binding protein AmpH	
YPK_2839	*ompC*	0.97	2.45	0.97			outer membrane porin protein C	
YPK_2843	*rcsB*	0.95	1.42	0.94			transcriptional regulator RcsB	
YPK_2845			0.97				hypothetical protein	
YPK_2846	*gyrA*		1.19				DNA gyrase subunit A	
YPK_2852	*cinA*		0.97				competence damage-inducible protein A	
YPK_2854	*yfaZ*	1.69	2.2		-1.02		YfaZ family protein	
YPK_2855	*katA*		-0.82	-1.03			catalase	Metabolism
YPK_2860	*LdcC*		2.66		2.65	-0.81	arginine decarboxylase	Metabolism
YPK_2861	*adiC*		2.68		2.68		arginine:agmatine antiporter	
YPK_2863			1.09				ABC transporter related	
YPK_2864	*yehW; opuBB*		0.81				osmoprotectant transport system permease protein	
YPK_2865	*osmF; opuBC*		1.37				osmoprotectant transport system substrate-binding protein	
YPK_2866	*sseA*		0.86				3-mercaptopyruvate sulfurtransferase	Metabolism
YPK_2867	*ddc*	1.96	1.45				aromatic-L-amino-acid decarboxylase	Metabolism
YPK_2868		2.26	2.24		-0.98		hypothetical protein	
YPK_2873	*livK*			-0.99			branched-chain amino acid transport system substrate-binding protein	
YPK_2874				1.31			hypothetical protein	
YPK_2875	*phnE2*				-0.91		phosphonate ABC transporter	
YPK_2879			1.1	-1.14			hypothetical protein	
YPK_2880			1.24				hypothetical protein	
YPK_2885	*pbpG*			0.88			D-alanyl-D-alanine endopeptidase	Metabolism
YPK_2888				1.11			hypothetical protein	
YPK_2892			1.61	1.33	1.12		hypothetical protein	
YPK_2893			1.78	1.74	1.58		hypothetical protein	
YPK_2894			1.51	1.75	1.52		hypothetical protein	
YPK_2908	*hydH; zraS*			-0.84			signal transduction histidine kinase; nitrogen specific; NtrB	Metabolism
YPK_2918			1.36				hypothetical protein	
YPK_2920	*moaD*				0.84		molybdenum cofactor biosynthesis protein D	
YPK_2922	*moaA*		0.85				molybdenum cofactor biosynthesis protein A	
YPK_2933	*pgl*		0.93				6-phosphogluconolactonase	Metabolism
YPK_2940	*modF*		1.17				putative molybdenum transport ATP-binding protein ModF	
YPK_2947	*psiF*			-0.91			PsiF repeat-containing protein	
YPK_2949	*aroG*		1.41				3-deoxy-7-phosphoheptulonate synthase	Metabolism
YPK_2953	*nadA*		0.82				quinolinate synthetase	Metabolism
YPK_2954	*ybgF*	1.04	1.09				tol-pal system protein YbgF	
YPK_2955	*pal*		1.25				peptidoglycan-associated outer membrane lipoprotein	
YPK_2956	*tolB*	0.82	2.15				translocation protein TolB	
YPK_2959	*tolQ*		0.83				colicin uptake protein TolQ	
YPK_2960	*ybgC*		1.13				acyl-CoA thioester hydrolase YbgC	
YPK_2962					1.18		cyd operon protein YbgT	
YPK_2963	*cydB*				1.06		cytochrome d ubiquinol oxidase; subunit II	Metabolism
YPK_2964	*cydA*	-1.09					cytochrome bd ubiquinol oxidase subunit I	Metabolism
YPK_2965	*sucD*	-0.99	1.34	-0.82			succinyl-CoA synthetase subunit alpha	Metabolism
YPK_2966	*sucC*	-1.12	1.54				succinyl-CoA synthetase subunit beta	
YPK_2967	*sucB*	-1.5	1.29				dihydrolipoamide succinyltransferase	Metabolism
YPK_2968	*sucA; kgd*	-1.39	1.77				2-oxoglutarate dehydrogenase E1 component	Metabolism
YPK_2969	*sdhB*	-1.77	1.48				succinate dehydrogenase iron-sulfur subunit	
YPK_2970	*sdhA*	-1.6	2.04				succinate dehydrogenase flavoprotein subunit	

Gene ID	Gene locus	YP89 (crp-)	YP53 (csrA-)	YP50 (ymoA-)	YP72 (rovM-)	YP3 (rovA-)	Description	Category-Class
YPK_2971	*sdhD*	-1.74	1.75	-0.86			succinate dehydrogenase cytochrome b556 small membrane subunit	
YPK_2972	*sdhC*	-1.86	1.85				succinate dehydrogenase cytochrome b556 large membrane subunit	
YPK_2973	*gltA*		1.13				citrate synthase	Metabolism
YPK_2974	*grpE*		1.17	1.41			GrpE protein	
YPK_2976	*RecN*		2.58				DNA repair protein RecN (Recombination protein N)	
YPK_2977	*smpA*		1.77				hypothetical protein	
YPK_2980	*smpB*		1.46				SsrA-binding protein	
YPK_2984			1.1				hypothetical protein	
YPK_2985					-0.82		hypothetical protein	
YPK_2990	*fldA*	-0.84	0.82				flavodoxin FldA	
YPK_2991	*fur*		0.93				Fur family transcriptional regulator; ferric uptake regulator	
YPK_2994	*glnS*		1.11				glutaminyl-tRNA synthetase	
YPK_2996	*nagE*	-1.17	-0.81	-0.84			PTS system, N-acetylglucosamine-specific IIC component	Metabolism
YPK_3001	*asnB*			-0.88			asparagine synthetase B	Metabolism
YPK_3002				-0.87			hypothetical protein	
YPK_3005	*miaB*		1.86				tRNA-i(6)A37 thiotransferase enzyme MiaB	
YPK_3006			0.85				PhoH family protein	
YPK_3007	*ybeY*		0.81				putative metalloprotease	
YPK_3010	*gltI*	-4.31	-1.69	-2.16			glutamate and aspartate transporter subunit	
YPK_3011	*gltJ*	-1.45	-1.09	-0.82			polar amino acid ABC transporter; inner membrane subunit	
YPK_3012	*gltK*	-1.01	-1.03	-0.86			polar amino acid ABC transporter; inner membrane subunit	
YPK_3013	*gltL*	-1.09	-0.86				ABC transporter related	
YPK_3014				-1.06			hypothetical protein	
YPK_3015	*leuS*		1.19				leucyl-tRNA synthetase	Metabolism
YPK_3016	*lptE; rlpB*	1.3	1.62				LPS-assembly lipoprotein RlpB	
YPK_3019	*ybeB*		0.95				hypothetical protein	
YPK_3020	*ybeA*		0.89				rRNA large subunit methyltransferase	
YPK_3024	*dacA*		1.02				D-alanyl-D-alanine carboxypeptidase fraction A	Metabolism
YPK_3025			0.85	0.92			hypothetical protein	
YPK_3028	*tatE*	1.27	1.3				twin arginine translocase protein A	
YPK_3031	*cspE*			-0.8			cold shock protein CspE	
YPK_3035		-2.88	-1.43		-0.83		hypothetical protein	
YPK_3038		-1			1.09		hypothetical protein	
YPK_3040	*iolE*	-1.03		-0.87			xylose isomerase domain-containing protein	Metabolism
YPK_3041	*iolC*	-0.82					5-dehydro-2-deoxygluconokinase	Metabolism
YPK_3044	*rbsA*	-1.08					ribose transport system ATP-binding protein	
YPK_3045	*rbsB*	-1.19		-0.91			ribose transport system substrate-binding protein	
YPK_3046	*idhA; iolG*	-1.18					inositol 2-dehydrogenase	Metabolism
YPK_3048	*iolD*	-1.24					3D-(3;5/4)-trihydroxycyclohexane-1;2-dione hydrolase	Metabolism
YPK_3049	*mmsA; iolA*	-1.44		-0.89			methylmalonate-semialdehyde dehydrogenase	Metabolism
YPK_3055	*ner; nlp; sfsB*		0.96				putative transcriptional regulator	
YPK_3057			0.99				hypothetical protein	
YPK_3060			2.6	2.57			Hcp1 family type VI secretion system effector	
YPK_3061			2.28	2.42	-1.08		hypothetical protein	
YPK_3062			2.36	2.34			hypothetical protein	
YPK_3070			1.07				hypothetical protein	
YPK_3071			0.86				hypothetical protein	
YPK_3072	*bglX*		0.86				beta-glucosidase	Metabolism
YPK_3084				-1.11			CDP-alcohol phosphatidyltransferase	
YPK_3087			0.81				hypothetical protein	
YPK_3089			0.81				hypothetical protein	
YPK_3091				0.92			tail assembly chaperone GP38	
YPK_3092				0.99			hypothetical protein	
YPK_3096			1.11				hypothetical protein	
YPK_3097			1.47				hypothetical protein	
YPK_3100			1.1				minor tail family protein	
YPK_3101			1.26				hypothetical protein	
YPK_3104			0.89				hypothetical protein	
YPK_3105			0.99				hypothetical protein	

Gene ID	Gene locus	YP89 (crp-)	YP53 (csrA-)	YP50 (ymoA-)	YP72 (rovM-)	YP3 (rovA-)	Description	Category-Class
YPK_3106			1.12				hypothetical protein	
YPK_3108			2.8				DinI family protein	
YPK_3109	*dinI*		2.42				DinI family protein	
YPK_3118				0.98			phage-related membrane protein	
YPK_3119			0.93				hypothetical protein	
YPK_3120		0.94	1.32				putative bacteriophage protein	
YPK_3121		0.88	1.55				hypothetical protein	
YPK_3122		1.1	1.44				Mu tail sheath family protein	
YPK_3123		0.99	1.38				hypothetical protein	
YPK_3134				-0.88			hypothetical protein	
YPK_3142			0.84				hypothetical protein	
YPK_3146			1.18				hypothetical protein	
YPK_3148		-1.23	-1.01	-1			hypothetical protein	
YPK_3151			1.03				hypothetical protein	
YPK_3152	*cysS*		0.9				cysteinyl-tRNA synthetase	
YPK_3153	*ppiB*		1.56				peptidyl-prolyl cis-trans isomerase B (rotamase B)	
YPK_3160			0.86				short chain dehydrogenase	
YPK_3161	*ybbN*		1.08	0.97			putative thioredoxin	
YPK_3162			1.32				band 7 protein	
YPK_3163		-0.9	1.24	-1.05			hypothetical protein	
YPK_3166	*ybaP*		1.05				GumN family protein	
YPK_3167			1.11				hypothetical protein	
YPK_3169						0.93	hypothetical protein	
YPK_3177	*fepE*			1.9			ferric enterobactin transport protein FepE	
YPK_3178	*manB*	-0.86		1.67			phosphomannomutase	Metabolism
YPK_3179	*gne*			1.75			NAD-dependent epimerase/dehydratase	
YPK_3180	*wbyL*			1.75			glycosyltransferase	Metabolism
YPK_3181	*manC*			1.41			mannose-1-phosphate guanylyltransferase	Metabolism
YPK_3182	*fcl*			1.22			GDP-L-fucose synthase	Metabolism
YPK_3183	*gmd*			1.2			GDP-mannose 4;6-dehydratase	Metabolism
YPK_3184	*wbyK*			1.26			mannosyltransferase	Metabolism
YPK_3185	*wzy*			0.93			O-antigen biosynthesis protein Wxy	
YPK_3187		-0.92					glycosyl transferase family protein	
YPK_3189	*ddhC*	-0.93		0.92			CDP-6-deoxy-D-xylo-4-hexulose-3-dehydrase	Metabolism
YPK_3192	*ddhD*	-1.11					CDP-4-dehydro-6-deoxyglucose reductase	Metabolism
YPK_3195	*htpG*			1.35			molecular chaperone HtpG	
YPK_3196	*recR*			0.89			recombination protein RecR	
YPK_3203		-1.48	-0.81				hypothetical protein	
YPK_3205	*ychN*	-0.9					DsrE family protein	
YPK_3212			1.11	2.5			hypothetical protein	
YPK_3213			0.94	3.16			hypothetical protein	
YPK_3214	*ymoA*		0.95	-0.94			hemolysin expression-modulating protein	
YPK_3215	*ybaZ*			1.73			methylated-DNA-protein-cysteine methyltransferase	
YPK_3216	*ybaY*	0.89			-0.83	0.88	putative lipoprotein	
YPK_3218				-2.11			hypothetical protein	
YPK_3219	*amtB*			-2.62			ammonium transporter; Amt family	
YPK_3220	*glnK*			-2.04			nitrogen regulatory protein P-II 2	
YPK_3228	*ybaW; tesC*	-1.78					thioesterase superfamily protein	Metabolism
YPK_3229	*ybaV*		0.92				helix-hairpin-helix repeat-containing competence protein ComEA	
YPK_3231	*hupB*		0.83				transcriptional regulator HU subunit beta	
YPK_3232	*lon*	0.85		1.02			ATP-dependent Lon protease	Metabolism
YPK_3233	*clpX*			0.88			ATP-dependent Clp protease ATP-binding subunit ClpX	
YPK_3234	*clpP*			0.88			ATP-dependent Clp protease; protease subunit	Metabolism
YPK_3235	*tig*			0.86			trigger factor	
YPK_3236				0.89			hypothetical protein	
YPK_3237	*bolA*			-0.82			transcriptional regulator BolA	
YPK_3240		-0.96				0.83	hypothetical protein	
YPK_3241	*cyoA*	-1.2					cytochrome o ubiquinol oxidase subunit II	Metabolism
YPK_3242	*cyoB*	-1.27					cytochrome o ubiquinol oxidase; subunit I	Metabolism
YPK_3269	*ggt*	1.46			-0.83	1.2	gamma-glutamyltranspeptidase	
YPK_3270				-0.95			short chain dehydrogenase	
YPK_3271	*malZ*	1.17					alpha-glucosidase	Metabolism
YPK_3279	*yajF; mak*	-0.92					fructokinase	Metabolism
YPK_3281	*yaiE*	-2.16	-0.91	-1.05			hypothetical protein	
YPK_3283				0.93			putative methyltransferase	
YPK_3284	*yafE*			1.34			methyltransferase type 11	

Gene ID	Gene locus	YP89 (crp-)	YP53 (csrA-)	YP50 (ymoA-)	YP72 (rovM-)	YP3 (rovA-)	Description	Category-Class
YPK_3285		-0.85		1.04			hypothetical protein	
YPK_3289	*crl*	-0.99		-1.19			DNA-binding transcriptional regulator Crl	
YPK_3291	*gpt;gpp;gxu*			0.86			xanthine-guanine phosphoribosyltransferase	Metabolism
YPK_3292				0.86			putative holin protein	
YPK_3293	*cpbD*	-1.12		1.31			chitin-binding domain-containing protein	
YPK_3298		-1.21					hypothetical protein	
YPK_3301	*nqrE*	-0.87					Na(+)-translocating NADH-quinone reductase subunit E	
YPK_3303	*nqrC*	-1.04					Na(+)-translocating NADH-quinone reductase subunit C	
YPK_3304	*nqrB*	-0.88					Na(+)-translocating NADH-quinone reductase subunit B	
YPK_3305	*nqrA*	-1.39					Na(+)-translocating NADH-quinone reductase subunit A	
YPK_3312	*rscA; hmwA*			0.86			filamentous haemagglutinin outer membrane protein	
YPK_3321	*mtnB*		-0.86				methylthioribulose-1-phosphate dehydratase	Metabolism
YPK_3323	*yafV*			-0.94			hypothetical protein	
YPK_3349	*clpB*			1.25			ATP-dependent Clp protease ATP-binding subunit ClpB	
YPK_3353	*yfiA*	-1.17					ribosome-associated inhibitor A	
YPK_3361	*rplS*	1.3	0.91	0.86			50S ribosomal protein L19	
YPK_3362	*trmD*	0.96		0.9			tRNA (guanine-N(1)-)-methyltransferase	
YPK_3363	*rimM*			1.03			16S rRNA-processing protein RimM	
YPK_3364	*rpsP*			1			small subunit ribosomal protein S16	
YPK_3368	*luxS*			-0.88			S-ribosylhomocysteinase	Metabolism
YPK_3369	*gshA*	1.51					glutamate-cysteine ligase	Metabolism
YPK_3370	*yqaA*	1.64					hypothetical protein	
YPK_3371	*yqaB*	1.83	0.9				fructose-1-phosphatase	
YPK_3372	*csrA*		-3.31				carbon storage regulator	
YPK_3388	*katY*		-2.34	-1.02			catalase/peroxidase HPI	Metabolism
YPK_3389	*cybC*		-1.75				cytochrome b562	
YPK_3390	*cybB*		-0.94	0.89			cytochrome b561	
YPK_3394	*dmsA*		-0.82				anaerobic dimethyl sulfoxide reductase subunit A	
YPK_3397	*fucR*	-1.04		1.01			DeoR family transcriptional regulator; L-fucose operon activator	
YPK_3398		-0.81		1.55			carbohydrate ABC transporter periplasmic-binding protein	
YPK_3399				0.99			simple sugar transport system ATP-binding protein	
YPK_3400				0.86			monosaccharide-transporting ATPase	
YPK_3401				1.16			monosaccharide-transporting ATPase	
YPK_3402	*sgbU*			1.5			putative L-xylulose 5-phosphate 3-epimerase	Metabolism
YPK_3403	*sgbK; lyxK*			1.19			L-xylulokinase	Metabolism
YPK_3404	*fumA*	-0.91					fumarate hydratase; class I	Metabolism
YPK_3406	*map*	-1.02					methionine aminopeptidase; type I	Metabolism
YPK_3407			-0.91				acetyltransferase	
YPK_3411	*yhjA*		-0.99				cytochrome-c peroxidase	
YPK_3423		-1.3		-1.21			hypothetical protein	
YPK_3425	*rpoS*			-1.18			RNA polymerase sigma factor RpoS	
YPK_3427	*pcm*	0.82					protein-L-isoaspartate O-methyltransferase	
YPK_3432	*ftsB*	-0.81					cell division protein FtsB	
YPK_3434	*cysC*	0.86					adenylylsulfate kinase	Metabolism
YPK_3435	*cysN*	1.25					sulfate adenylyltransferase subunit 1	Metabolism
YPK_3436	*cysD*	1.34					sulfate adenylyltransferase subunit 2	Metabolism
YPK_3437	*cysG*	0.98					uroporphyrin-III C-methyltransferase	Metabolism
YPK_3438		-1.09	0.88				YcfA family protein	
YPK_3439		-0.93	0.93				hypothetical protein	
YPK_3440	*cysH*	1.65					phosphoadenosine phosphosulfate reductase	Metabolism
YPK_3441	*cysI*	1.75					sulfite reductase subunit beta	Metabolism
YPK_3442	*cysJ*	1.25					sulfite reductase subunit alpha	Metabolism
YPK_3445	*sodC*	0.84		-1.2			superoxide dismutase	
YPK_3446	*eno*	1.03					phosphopyruvate hydratase	Metabolism
YPK_3449	*relA*	0.84					GTP pyrophosphokinase	Metabolism
YPK_3450		0.87					hypothetical protein	
YPK_3452	*htrA*	1.06	1.47				serine endoprotease	Metabolism
YPK_3459	*hemL*	-0.89					glutamate-1-semialdehyde aminotransferase	Metabolism
YPK_3472	*panB*			-1			3-methyl-2-oxobutanoate hydroxymethyltransferase	Metabolism
YPK_3474	*panD*		-0.95				aspartate 1-decarboxylase	Metabolism

Gene ID	Gene locus	YP89 (crp-)	YP53 (csrA-)	YP50 (ymoA-)	YP72 (rovM-)	YP3 (rovA-)	Description	Category-Class
YPK_3486	*yacL*		-0.82				hypothetical protein	
YPK_3490	*aceF*		-0.91				pyruvate dehydrogenase E2 component (dihydrolipoamide acetyltransferase)	Metabolism
YPK_3491	*aceE*		-0.83				pyruvate dehydrogenase subunit E1	
YPK_3499	*hofB*			-0.89			protein transport protein HofB	
YPK_3502		0.88					hypothetical protein	
YPK_3503	*coaE*	0.92					dephospho-CoA kinase	Metabolism
YPK_3504	*yacF*			-0.85			hypothetical protein	
YPK_3505		1.21					hypothetical protein	
YPK_3529	*fruR*		-0.84				DNA-binding transcriptional regulator FruR	
YPK_3530	*ilvH*			-0.83			acetolactate synthase 3 regulatory subunit	Metabolism
YPK_3534				-1.36			hypothetical protein	
YPK_3549		3.06	2.76		-1.18		hypothetical protein	
YPK_3550		1.6	2.89		0.83		type VI secretion protein IcmF	
YPK_3551		2	3.57				hypothetical protein	
YPK_3552		2.51	3.94	0.96			type VI secretion protein	
YPK_3553		2.33	3.89	0.86			putative lipoprotein	
YPK_3554		2.31	3.77				hypothetical protein	
YPK_3555		2.38	3.96	0.81			hypothetical protein	
YPK_3556		1.75	3.34				pentapeptide repeat-containing protein	
YPK_3557		1.8	3.61				pentapeptide repeat-containing protein	
YPK_3558	*vgrG5*	2.4	4.09	0.99			type VI secretion system Vgr family protein	
YPK_3559	*clpB*	1.8	2.97				type VI secretion ATPase	
YPK_3560	*impH*	2.07	3.24				type VI secretion protein	
YPK_3561	*impG*	2.41	3.85				type VI secretion protein	
YPK_3562		3.26	4.41	1.07	-1.23		type VI secretion system protein ImpF	
YPK_3563		1.89	1.8		-1.78		type VI secretion system secreted protein Hcp	
YPK_3564	*impC*	3.35	4	1.25	-1.02	0.81	type VI secretion system protein ImpC	
YPK_3565		2.88	4	1.26	-1.03	0.81	type VI secretion protein	
YPK_3566		2.66	4.43	1.34	-1		ImpA domain-containing protein	
YPK_3567		3.26	4.3	1.44	-1.55		hypothetical protein	
YPK_3576				1.68			hypothetical protein	
YPK_3577				1.16	-1.3		hypothetical protein	
YPK_3579	*yjjB*			0.97			hypothetical protein	
YPK_3580	*yjjP*			1.09			hypothetical protein	
YPK_3582	*carB*			-0.98			carbamoyl phosphate synthase large subunit	Metabolism
YPK_3583	*carA*			-0.83			carbamoyl phosphate synthase small subunit	Metabolism
YPK_3585	*ispH*	0.94					4-hydroxy-3-methylbut-2-enyl diphosphate reductase	Metabolism
YPK_3590	*rpsT*			1.07			30S ribosomal protein S20; small subunit	
YPK_3593	*dnaJ*			1.52			chaperone protein DnaJ	
YPK_3594	*dnaK*			1.63			molecular chaperone DnaK	
YPK_3595	*yaaH*			0.98			hypothetical protein	
YPK_3599	*talB*			-0.8			transaldolase B	Metabolism
YPK_3607	*creA*	2.21	1.31				hypothetical protein	
YPK_3608		1.81	1.05				hypothetical protein	
YPK_3624	*deoD*		-0.85			2.58	purine nucleoside phosphorylase	Metabolism
YPK_3625	*deoB*	0.87		-0.96		1.76	phosphopentomutase	Metabolism
YPK_3626	*deoA*					1.96	thymidine phosphorylase	Metabolism
YPK_3627	*deoC*					2.5	deoxyribose-phosphate aldolase	Metabolism
YPK_3628	*nupC(2)*					1.34	nucleoside transporter	
YPK_3631			0.94	-0.82			hypothetical protein	
YPK_3632	*osmY*	0.93	1.69	-0.92			periplasmic protein	
YPK_3638	*hmsT*		-0.87				diguanylate cyclase	
YPK_3648	*lsrK*			0.94			autoinducer-2 (AI-2) kinase	
YPK_3649	*lsrR*			1.22			DeoR family transcriptional regulator	
YPK_3653	*lsrB*	-0.81	-1.04	0.89			autoinducer AI-2 ABC transporter	
YPK_3654	*lsrF*		-0.87	1.12			aldolase; putative autoinducer-2 (AI-2)	
YPK_3655	*yneC*	-1.03	-0.99	1.13			autoinducer-2 (AI-2) modifying protein LsrG	
YPK_3656			1.87				hypothetical protein	
YPK_3657	*pstA*			0.82			PTS system; fructose-specific IIA-like component	
YPK_3658	*frwC*			0.82			putative fructose-like permease EIIC subunit 2	
YPK_3659	*frwB*			0.94			putative fructose-like phosphotransferase EIIB subunit 2	
YPK_3673	*hsdS*			-0.86			restriction modification system DNA specificity subunit	
YPK_3674	*hsdR*	-1.07		-1.54			HsdR family type I site-specific deoxyribonuclease	
YPK_3705		-0.81					hypothetical protein	
YPK_3706		-0.85					multiple sugar transport system ATP-binding	

Gene ID	Gene locus	YP89 (crp-)	YP53 (csrA-)	YP50 (ymoA-)	YP72 (rovM-)	YP3 (rovA-)	Description	Category-Class
							protein	
YPK_3707		-1.06					multiple sugar transport system permease protein	
YPK_3709		-0.87					extracellular solute-binding protein	
YPK_3710				1.17			hypothetical protein	
YPK_3711				0.92			heparinase II/III family protein	
YPK_3713	*yhbS*		-0.83				GCN5-related N-acetyltransferase	
YPK_3720				0.84			hypothetical protein	
YPK_3721			0.84				hypothetical protein	
YPK_3724	*deaD*	2.9		0.83			ATP-dependent RNA helicase DeaD	
YPK_3725	*nlpI*		-0.94				lipoprotein NlpI	
YPK_3730	*infB*			0.92			translation initiation factor IF-2	
YPK_3732				0.92	0.83		hypothetical protein	
YPK_3736	*hflB*			0.95			ATP-dependent metalloprotease	Metabolism
YPK_3737	*rrmJ*			1.01			23S rRNA methyltransferase J	
YPK_3739	*greA*		0.84				transcription elongation factor GreA	
YPK_3749		-0.89					hypothetical protein	
YPK_3756	*rpmA*	0.96		1.08			50S ribosomal protein L27	
YPK_3757	*rplU*			1.25			50S ribosomal protein L21	
YPK_3761	*mdh*	-1.72	-1.12	-0.88			malate dehydrogenase	Metabolism
YPK_3763		2.43				0.87	hypothetical protein	
YPK_3773				-1.11			hypothetical protein	
YPK_3774	*ytfJ*		0.91				hypothetical protein	
YPK_3775	*cysQ*	1.12		-1.2			adenosine-3'(2');5'-bisphosphate nucleotidase;CysQ	
YPK_3776	*cpdB*					0.89	2';3'-cyclic-nucleotide 2'-phosphodiesterase	Metabolism
YPK_3779	*ytfB*	0.86					hypothetical protein	
YPK_3781	*rplI*	0.93		1.04			50S ribosomal protein L9	
YPK_3782	*rpsR*	1.06		1.19			30S ribosomal protein S18	
YPK_3783	*priB*	1.04		0.87			primosomal replication protein N	
YPK_3784	*rpsF*			1.06			30S ribosomal protein S6	
YPK_3788	*aidB*	-1.31	-1.01	-1.12			isovaleryl CoA dehydrogenase	
YPK_3793	*purA*	1.01	-0.97				adenylosuccinate synthetase	Metabolism
YPK_3795	*hflC*	0.9					FtsH protease regulator HflC	
YPK_3796	*hflK*	0.95					FtsH protease regulator HflK	
YPK_3797	*hflX*	0.94					putative GTPase HflX	
YPK_3813	*frdA*	-1.12	-1.43	-0.87			fumarate reductase flavoprotein subunit	
YPK_3814	*frdB*	-1.31	-1.51				fumarate reductase iron-sulfur subunit	
YPK_3815	*frdC*	-1.43	-1.65	-0.93			fumarate reductase subunit C	
YPK_3816	*frdD*	-1.39	-1.61	-1.06			fumarate reductase subunit D	
YPK_3822	*groEL*			0.85			chaperonin GroEL	
YPK_3823	*groES*			0.89			co-chaperonin GroES	
YPK_3824	*fxsA*			1.02			cytoplasmic membrane protein	
YPK_3825	*aspA*	-2.1					aspartate ammonia-lyase	Metabolism
YPK_3835					-0.87		hypothetical protein	
YPK_3836				1.57			hypothetical protein	
YPK_3837					1.03		hypothetical protein	
YPK_3838	*insB*			0.89			IS1 transposase; InsB	
YPK_3841	*rhaR*	-1.11	-0.95				L-rhamnose operon transcriptional activator RhaR	
YPK_3848	*fucO*			-0.92			lactaldehyde reductase	
YPK_3850	*ssb*		-0.82				single-strand DNA-binding protein	
YPK_3852			-0.92	-1.43			hypothetical protein	
YPK_3857	*pspG*	-1.37	1.16		1.16	-0.9	phage shock protein G	
YPK_3859	*zur*		-0.93				zinc uptake transcriptional repressor	
YPK_3863	*ubiA*	0.97					4-hydroxybenzoate octaprenyltransferase	Metabolism
YPK_3866				0.86			berberine/berberine domain-containing protein	
YPK_3867			1.92				hypothetical protein	
YPK_3868				0.89			hypothetical protein	
YPK_3869	*fimC1*			1.05			putative periplasmic; fimbrial chaperone protein	
YPK_3870	*fimD1*			0.99			fimbrial biogenesis outer membrane usher protein	
YPK_3871				1.58			hypothetical protein	
YPK_3879		0.99					hypothetical protein	
YPK_3880		1.13	0.98				hypothetical protein	
YPK_3882		0.97					hypothetical protein	
YPK_3884	*metF*	2.14	2.08	0.8			methylenetetrahydrofolate reductase	
YPK_3886	*chuX*		0.81				hypothetical protein	
YPK_3888	*hemP*			2.04			hemin uptake protein	
YPK_3890	*hmuS*		1.73				hemin-degrading family protein	
YPK_3891	*hmuT*		1.34				iron complex transport system substrate-	

Gene ID	Gene locus	YP89 (crp-)	YP53 (csrA-)	YP50 (ymoA-)	YP72 (rovM-)	YP3 (rovA-)	Description	Category-Class
							binding protein	
YPK_3892	*hmuU*		1.31				iron complex transport system permease protein	
YPK_3894	*metC*			1.3			cystathionine beta-lyase	Metabolism
YPK_3895	*sdaC1*			0.96			putative transmembrane serine transport protein	
YPK_3897	*yedF*			1.24			hypothetical protein	
YPK_3898	*yedE*			0.83			putative inner membrane protein	
YPK_3900	*yscT*	-1.59		-1.83			type III secretion protein SpaR/YscT/HrcT	
YPK_3920	*gltP*			1.08			glutamate/aspartate:proton symporter	
YPK_3921	*rcs; acsA*	-1.81	-0.96	-0.81			acetyl-CoA synthetase	Metabolism
YPK_3922		-2.01	-1.81	-0.99			hypothetical protein	
YPK_3923	*actP*	-1.92	-1.8	-1.03			acetate permease	
YPK_3926				1.25			transposase IS3/IS911 family protein; helix-turn-helix; fis-type	
YPK_3933	*fadB*	-1.86					multifunctional fatty acid oxidation complex subunit alpha	
YPK_3934	*fadA*	-1.79					3-ketoacyl-CoA thiolase	
YPK_3936	*ubiD*	-1.63	-0.8	-1.57			3-octaprenyl-4-hydroxybenzoate decarboxylase	Metabolism
YPK_3942	*tatA*	-0.86	-1.16				twin arginine-targeting protein translocase	
YPK_3949						2.15	protein tyrosine/serine phosphatase	
YPK_3950	*udp*	-1.12	-1.04	-0.99		2.46	uridine phosphorylase	Metabolism
YPK_3952	*metE*		-1.02		-1.37	-1.05	5-methyltetrahydropteroyltriglutamate-homocysteine S-methyltransferase	Metabolism
YPK_3963					-0.82		hypothetical protein	
YPK_3976	*rpoH*	0.87					RNA polymerase factor sigma-32	
YPK_3982				1.03			hypothetical protein	
YPK_3983		-0.87		1.26			hypothetical protein	
YPK_3993				1.32			hypothetical protein	
YPK_3994				0.89			putative sugar phosphatase	
YPK_4015	*cyaA*	1.52		-0.83			adenylate cyclase	Metabolism
YPK_4034	*rho*	0.9					transcription termination factor Rho	
YPK_4042	*fimA*			1.1			fimbrial protein	
YPK_4047				-0.83	-1.13		colicin immunity protein/pyocin immunity protein	
YPK_4049				0.98			hypothetical protein	
YPK_4050		-0.95		-1.38			S-type pyocin domain-containing protein	
YPK_4053		-1.42		-0.99			hypothetical protein	
YPK_4076	*fabR*	-0.93					DNA-binding transcriptional repressor FabR	
YPK_4080				-0.81			putative peroxiredoxin/glutaredoxin family protein	
YPK_4084	*hasD*			0.92			type I secretion system ATPase	
YPK_4085	*hasA*		1.17	3.01			heme-binding A family protein	
YPK_4089	*argC*	1.04					N-acetyl-gamma-glutamyl-phosphate reductase	Metabolism
YPK_4098	*rpmE*			0.92			50S ribosomal protein L31	
YPK_4103	*hslV*			1.54			ATP-dependent protease peptidase subunit	Metabolism
YPK_4104	*hslU*			1.27			ATP-dependent protease ATP-binding subunit HslU	
YPK_4106	*rraA*		-0.97	-0.87			ribonuclease activity regulator protein RraA	
YPK_4107		3	4.04	1.36	-1.15		hypothetical protein	
YPK_4108		2.06	2.56	1.06			hypothetical protein	
YPK_4111	*yiiU*	1.13	0.9				hypothetical protein	
YPK_4112	*glpF*	-0.87		0.81			MIP family channel protein	
YPK_4131	*cpxP*		1.95				periplasmic stress adaptor protein CpxP	
YPK_4144	*tdh*	-0.87					threonine 3-dehydrogenase	Metabolism
YPK_4145	*kbl*	-1.42					2-amino-3-ketobutyrate coenzyme A ligase	Metabolism
YPK_4153	*rpmG*			0.85			50S ribosomal protein L33	
YPK_4154	*rpmB*	0.85	0.95	1.02			50S ribosomal protein L28	
YPK_4169		-0.89		-0.81			hypothetical protein	
YPK_4171		-0.95					hypothetical protein	
YPK_4176	*gmk*	0.92					guanylate kinase	Metabolism
YPK_4184		0.94					thioesterase domain-containing protein	
YPK_4185	*dtd*	0.99					D-tyrosyl-tRNA(Tyr) deacylase	
YPK_4186	*rbn*	1.38					ribonuclease BN	
YPK_4187		2.49	2.79				phosphatase	
YPK_4189	*glnA*			-2.57			glutamine synthetase	Metabolism
YPK_4190	*glnL*			-1.23	-0.86		nitrogen regulation protein NR(II)	Metabolism
YPK_4191	*glnG*			-1.15			nitrogen regulation response regulator GlnG	
YPK_4196	*dsbA*	0.84					thiol:disulfide interchange protein DsbA	
YPK_4208		-1.37					hypothetical protein	
YPK_4209	*rbsK*	-2.29	-0.8				ribokinase	Metabolism

Gene ID	Gene locus	YP89 (crp-)	YP53 (csrA-)	YP50 (ymoA-)	YP72 (rovM-)	YP3 (rovA-)	Description	Category-Class
YPK_4210	*rbsD*	-2.4	-0.81				D-ribose pyranase	
YPK_4214	*asnA*			-1.09			asparagine synthetase AsnA	Metabolism
YPK_4218	*gidB*			0.83			16S rRNA methyltransferase GidB	
YPK_4219	*atpI*	-0.93					F0F1 ATP synthase subunit I	Metabolism
YPK_4221	*atpE*	-0.91					F0F1 ATP synthase subunit C	Metabolism
YPK_4222	*atpF*	-0.92					F0F1 ATP synthase subunit B	Metabolism
YPK_4229	*glmS*	1.02					glucosamine-fructose-6-phosphate aminotransferase	Metabolism
YPK_4231	*pstS*		-0.85				phosphate ABC transporter periplasmic substrate-binding protein PstS	
YPK_4237		1.02	0.97	-0.88			polar amino acid ABC transporter	
YPK_4242				0.95			hypothetical protein	
YPK_4243		-0.82					hypothetical protein	
YPK_4247	*yidD*			0.97			hypothetical protein	
YPK_4248	*rnpA*			0.97			ribonuclease P protein component	
YPK_4249	*rpmH*			0.91			50S ribosomal protein L34	

E.2 Supernatant analyses of the mutant strains

Semiquantitative peak areas (mean: $\bar{x}$, n = 3 biological replicates), relative standard error Se

Metabolite	$\bar{x}$ (Medium)	Se (Medium) [%]	$\bar{x}$ (YPIII (wt))	Se (YPIII (wt)) [%]	$\bar{x}$ (YP89 (*crp*$^-$))	Se (YP89 (*crp*$^-$)) [%]	$\bar{x}$ (YP53 (*csrA*$^-$))	Se (YP53 (*csrA*$^-$)) [%]	$\bar{x}$ (YP3 *(rovA*$^-$*))*	Se (YP3 *(rovA*$^-$*))* [%]	$\bar{x}$ (YP72 *(rovM*$^-$*))*	Se (YP72 *(rovM*$^-$*))* [%]	$\bar{x}$ (YP50 *(ymoA*$^-$*))*	Se (YP72 *(rovM*$^-$*))* [%]
3-methyl-2-oxopentanoate	0	0.00	1604	20.56	0	0.00	427	0.00	1666	4.48	1958	15.28	2899	9.74
adenine	25601	3.35	2504	100.00	2485	22.66	2443	61.67	8197	30.30	10768	21.30	5248	37.43
adenosine-3',5'-cyclic-monophosphate	14882	15.65	2204	48.63	5681	15.18	7498	54.90	2184	26.71	2440	4.64	7572	44.57
AMP	0	0.00	0	0.00	8248	14.45	0	0.00	0	0.00	0	0.00	0	0.00
beta-Alanine	50	100.00	61	100.00	6413	12.97	104	58.42	79	100.00	0	0.00	717	39.78
alanine	3163444	2.05	2211	100.00	3515865	4.34	2428835	10.14	2330	100.00	48659	13.33	267487	4.87
altrose	351248	2.95	11497	22.26	22789	29.76	18927	17.49	19593	14.32	20718	20.95	14240	49.82
arginine	20691	1.22	15371	6.43	21354	8.46	13827	9.13	14267	3.25	16203	1.06	14907	8.89
asparagine	331114	0.94	29514	7.59	214536	7.27	10490	11.63	6439	5.32	84553	10.79	45985	4.56
aspartate	1454306	1.28	0	0.00	0	0.00	29782	0.00	12943	100.00	0	0.00	0	0.00
3-hydroxybutanoate	1508	0.79	1495	16.82	2933	9.43	1890	23.35	1544	1.92	1885	35.09	1968	13.40
4-aminobutanoate	16205	3.15	12651	7.33	17937	6.91	13962	10.47	12658	7.64	13102	8.31	14703	4.87
4-hydroxybutanoate	0	0.00	12217	8.74	734	59.54	363	100.00	8695	5.12	12260	4.95	1557	59.50
citrate	34866	4.11	0	0.00	41832	9.33	14505	62.12	0	0.00	0	0.00	0	0.00
diethylene glycol	0	0.00	217	100.00	265	52.88	235	57.76	487	51.26	0	0.00	0	0.00
erythritol	3287	5.58	0	0.00	3984	10.59	2858	16.87	0	0.00	0	0.00	0	0.00
fructose	8020	4.22	0	0.00	0	0.00	450	0.00	0	0.00	0	0.00	0	0.00
fumarate	3769	0.00	6506	8.23	84409	8.55	12584	42.06	5984	51.42	7968	19.46	6550	8.41
hexose_1	41654	10.27	37599	5.79	42474	4.17	34840	9.70	35764	1.51	37610	8.01	35192	6.48
glucose	46303	3.10	40050	2.49	40608	3.41	36084	9.74	33156	2.39	41351	7.14	37414	4.53
glutamate	3994958	1.77	0	0.00	2380667	3.25	588943	0.00	0	0.00	0	0.00	0	0.00
2-hydroxy-glutarate	9665	1.76	27011	10.41	11287	4.72	9348	12.27	22755	10.28	31291	8.22	32634	5.25
glycerate	3976	6.49	0	0.00	0	0.00	0	0.00	0	0.00	0	0.00	0	0.00
glycerol	289472	3.56	13097	3.98	14236	14.80	12413	8.87	18912	6.47	105213	57.01	14907	5.47
glycerol-3-phosphate	35631	6.68	65082	10.52	64829	2.82	67094	10.84	63323	5.16	70850	6.29	63162	7.81
glycine	1816337	1.22	0	0.00	4047135	4.86	3409998	15.46	0	0.00	0	0.00	2172164	14.67
glycylglycine	13705	4.24	0	0.00	0	0.00	2052	0.00	0	0.00	0	0.00	0	0.00
guanine	2602	50.15	8441	10.20	510	100.00	1525	57.75	7845	12.39	11734	9.70	3821	34.75
guanosine	50782	3.42	0	0.00	0	0.00	0	0.00	0	0.00	0	0.00	0	0.00
hexadecanoate	16581	2.86	13004	2.61	15217	1.57	13109	5.61	13035	9.52	11696	10.30	12730	2.10
histidine	72018	7.83	0	0.00	83467	5.71	48494	17.72	0	0.00	0	0.00	2339	58.53
homocysteine	4259	6.17	3897	10.51	8069	8.12	4057	11.22	1309	21.65	6840	8.19	1385	10.24
homoserine	2069	54.39	0	0.00	4193	5.89	3381	18.57	0	0.00	0	0.00	0	0.00

Metabolite	$\bar{x}$ (Medium)	Se (Medium) [%]	$\bar{x}$ (YPIII (wt))	Se (YPIII (wt)) [%]	$\bar{x}$ (YP89 (*crp*$^-$))	Se (YP89 (*crp*$^-$)) [%]	$\bar{x}$ (YP53 (*csrA*$^-$))	Se (YP53 (*csrA*$^-$)) [%]	$\bar{x}$ (YP3 *(rovA*$^-$*))*	Se (YP3 *(rovA*$^-$*))* [%]	$\bar{x}$ (YP72 *(rovM*$^-$*))*	Se (YP72 *(rovM*$^-$*))* [%]	$\bar{x}$ (YP50 *(ymoA*$^-$*))*	Se (YP72 *(rovM*$^-$*))* [%]
idose	104831	2.87	0	0.00	0	0.00	5422	0.00	0	0.00	0	0.00	0	0.00
inosine	4975	23.70	0	0.00	0	0.00	0	0.00	0	0.00	0	0.00	0	0.00
myo-inositol	61734	2.49	53269	5.11	63948	6.56	54956	8.62	50148	5.12	50268	4.79	58402	1.32
isoleucine	4298397	1.78	5165159	1.18	5626545	3.34	4234943	9.61	5026878	1.52	4974568	4.23	5272235	1.78
lactate	218891	2.97	136823	7.34	233544	4.87	235628	8.71	142671	0.94	138856	5.80	206186	2.04
lysine	3725680	0.74	3455573	2.80	3771450	4.22	3250560	6.37	3555765	0.94	3426620	2.91	3701307	2.36
malate	5264	2.62	0	0.00	45754	6.01	9333	0.00	0	0.00	0	0.00	0	0.00
maltose	1767977	1.95	0	0.00	5138	0.00	820	0.00	0	0.00	0	0.00	0	0.00
mannitol	3279	12.95	11892	76.32	3188	7.99	2289	19.51	3127	10.80	3138	11.39	2927	10.16
methionine sulfoxide	20671	7.86	10674	18.98	18825	2.23	16552	11.96	37391	7.08	24484	13.46	15820	49.31
NA_1421.09	19327	2.80	15422	3.44	18478	8.10	15900	8.69	16195	4.15	14964	5.18	15966	2.21
NA_1705.4	6376	50.43	0	0.00	11061	4.16	9199	15.98	0	0.00	0	0.00	2242	100.00
NA_2615.1	30840	14.64	28406	1.40	29011	2.28	25593	8.94	24941	7.65	25336	7.00	21102	20.78
NA114002_(classified_unknown)_1144.3	686066	2.75	697336	5.59	664240	3.82	666805	6.45	786197	3.94	705853	1.55	673343	6.02
NA161011_1619.12	21354	23.92	19935	3.34	18339	8.70	16243	8.18	20272	6.09	21682	5.86	18612	12.66
NA184030_(classified_unknown)_1848.26	61743	9.57	58010	12.57	59636	4.18	54513	3.51	62721	6.36	47366	9.03	58284	5.21
NA186026_1867.48	32552	2.49	29615	9.71	32114	3.18	30222	13.44	29129	6.17	35958	16.36	28363	4.87
NA374	0	0.00	0	0.00	7456	30.34	0	0.00	0	0.00	0	0.00	0	0.00
NA570	686944	49.22	24841	30.25	17212	16.53	16741	5.33	20737	27.56	14049	6.13	15229	25.47
NA663	5170	13.97	4543	3.94	4176	6.48	4041	9.96	3297	33.38	4294	22.78	4080	16.13
NA78	34971	3.66	32220	3.94	31115	4.61	28522	8.68	29370	5.92	31239	2.90	29739	1.42
nicotinamide	5877	8.65	0	0.00	0	0.00	0	0.00	0	0.00	0	0.00	85	100.00
octadecanoate	32183	4.07	19241	10.19	23965	5.05	21239	7.61	21007	5.02	19900	13.74	20322	5.19
ornithine	85630	0.90	78088	3.59	87882	6.13	74168	9.98	71767	3.75	76792	6.30	69347	6.37
phenylalanine	1875718	1.81	1439833	3.57	1895634	5.20	1495010	7.77	1419933	0.44	1517666	3.48	1570109	2.47
proline	1383576	1.76	0	0.00	0	0.00	163019	0.00	0	0.00	0	0.00	0	0.00
N-acetyl-putrescine	21709	3.20	0	0.00	0	0.00	6320	57.76	0	0.00	0	0.00	0	0.00
putrescine	2644	100.00	59547	7.15	34569	5.12	481984	15.15	69714	15.85	95881	8.41	680588	1.70
pyroglutamate	7075738	1.55	0	0.00	5656667	7.04	5478549	8.87	103061	0.00	0	0.00	836812	100.00
hexose_2	61941	3.00	18656	5.52	17445	7.04	17185	9.53	21975	7.69	21083	14.75	17244	2.26
serine	1397960	1.29	4535	10.28	10770	2.82	7657	8.54	3438	13.33	5289	10.68	7536	3.13
spermidine	10504	3.57	5162	9.64	8312	7.19	8334	11.04	6399	10.16	6543	7.69	6983	4.80
succinate	75171	3.79	0	0.00	229268	8.06	25054	0.00	0	0.00	0	0.00	5039	33.40
sucrose	16902	5.23	12579	14.16	16225	9.19	12461	16.57	13549	8.45	14183	8.80	13882	3.75
allo-threonine	1508	60.21	0	0.00	2489	11.73	2040	17.45	0	0.00	0	0.00	794	23.72
threonine	896108	0.44	0	0.00	402922	9.76	282007	45.97	0	0.00	0	0.00	0	0.00
thymine	0	0.00	8427	10.90	6942	12.94	4709	15.88	12793	10.27	9758	9.19	8680	5.68
tryptophan	134279	6.44	90685	14.06	118698	1.91	100646	11.85	98058	8.35	94997	8.77	131227	24.35
tyrosine	1290436	1.69	896725	4.90	1204326	3.04	1060667	7.54	904703	2.07	940909	6.76	991782	1.31

Metabolite	$\bar{x}$ (Medium)	Se (Medium) [%]	$\bar{x}$ (YPIII (wt))	Se (YPIII (wt)) [%]	$\bar{x}$ (YP89 (*crp*$^-$))	Se (YP89 (*crp*$^-$)) [%]	$\bar{x}$ (YP53 (*csrA*$^-$))	Se (YP53 (*csrA*$^-$)) [%]	$\bar{x}$ (YP3 (*rovA*$^-$))	Se (YP3 (*rovA*$^-$)) [%]	$\bar{x}$ (YP72 (*rovM*$^-$))	Se (YP72 (*rovM*$^-$)) [%]	$\bar{x}$ (YP50 (*ymoA*$^-$))	Se (YP72 (*rovM*$^-$)) [%]
Unknown#bth-pae-013_1169.8	15520	19.82	24816	6.87	37123	15.64	25846	5.34	27993	19.63	23566	12.61	25525	7.63
Unknown#bth-pae-065_1466.2	45482	4.28	0	0.00	70244	6.89	56118	12.85	0	0.00	0	0.00	33071	4.66
Unknown#mse-ypy-006_1744.2	12688	26.53	26488	7.86	3563	5.10	14504	31.10	27285	1.13	35566	3.25	31959	7.73
Unknown#mse-ypy-019_2018.4	6087	2.66	7724	5.41	7092	1.71	5515	8.26	7459	2.49	6651	6.06	6884	5.81
Unknown#mse-ypy-026_2236.8	1957	7.41	0	0.00	0	0.00	0	0.00	0	0.00	0	0.00	0	0.00
Unknown#mse-ypy-028_2276.9	0	0.00	4127	29.71	2533	13.25	0	0.00	8443	5.94	101	100.00	1245	60.51
Unknown#mse-ypy-036_1981.9	28	100.00	912	52.25	2238	5.81	0	0.00	1568	3.70	1372	15.41	593	21.54
Unknown#sst-cgl-028_1478.9	0	0.00	0	0.00	283	17.41	0	0.00	0	0.00	0	0.00	0	0.00
Uracil	43706	2.03	19270	16.87	49882	5.36	15319	16.86	20132	14.62	25169	5.13	14600	5.70
uridine	6898	3.87	0	0.00	0	0.00	0	0.00	0	0.00	0	0.00	0	0.00
valine	4965498	1.25	5496481	4.67	6021676	3.56	4827364	8.63	5682823	1.49	5416431	3.09	6047610	1.07
xanthine	9474	7.07	0	0.00	0	0.00	0	0.00	0	0.00	0	0.00	0	0.00

E.3 Intracellular metabolome analyses of the mutant strains

Semiquantitative peak areas (mean: $\bar{x}$, n = 6 biological replicates), relative standard error Se. The abbreviation n.d. marks metabolites that were not detected in the respective samples

Metabolite	$\bar{x}$ (YP89 (*crp*$^-$))	Se (YP89 (*crp*$^-$)) [%]	$\bar{x}$ (YPIII (wt))	Se (YPIII (wt)) [%]	$\bar{x}$ (YP53 (*csrA*$^-$))	Se (YP53 (*csrA*$^-$)) [%]	$\bar{x}$ (YPIII (wt))	Se (YPIII (wt)) [%]	$\bar{x}$ (YP3 (*rovA*$^-$))	Se (YP3 (*rovA*$^-$)) [%]	$\bar{x}$ (YPIII (wt))	Se (YPIII (wt)) [%]	$\bar{x}$ (YP72 (*rovM*$^-$))	Se (YP72 (*rovM*$^-$)) [%]	$\bar{x}$ (YPIII (wt))	Se (YPIII (wt)) [%]	$\bar{x}$ (YP50 (*ymoA*$^-$))	Se (YP72 (*rovM*$^-$)) [%]	$\bar{x}$ (YPIII (wt))	Se (YPIII (wt)) [%]
1-methyl-hydantoin	674417	16.04	733685	19.09	n.d.		n.d.		n.d.		n.d.		n.d.		n.d.		n.d.		n.d.	
hexose_1	n.d.		n.d.		28742	7.55	17622	14.74	n.d.		n.d.		n.d.		n.d.		n.d.		n.d.	
2-aminoadipate	n.d.		n.d.		n.d.		n.d.		61130	11.51	0		n.d.		n.d.		n.d.		n.d.	
2'-deoxyadenosine	n.d.		n.d.		n.d.		n.d.		253553	33.78	138997	27.47	44606	42.23	58595	24.31	n.d.		n.d.	
2'-deoxyguanosine	n.d.		n.d.		n.d.		n.d.		902880	12.69	1178093	7.34	n.d.		n.d.		n.d.		n.d.	
2-deoxy-ribose	n.d.		n.d.		n.d.		n.d.		476807	27.26	394607	33.43	n.d.		n.d.		n.d.		n.d.	
2-hydroxy-glutarate	n.d.		n.d.		n.d.		n.d.		23230	11.32	16593	8.67	29882	12.52	21119	26.61	n.d.		n.d.	
2-methyl-citrate	0		5012307	4.35	4686345	27.64	1360132	37.31	1851319	13.48	1895213	7.80	5848656	6.19	5356406	4.43	5916287	7.43	7248604	6.26
2-oxo-isocaproate	n.d.		n.d.		65894	14.49	136702	14.63	221755	7.19	156747	7.09	203932	27.01	146062	12.86	126018	18.36	121762	16.63
3-cyanopyridine	n.d.		n.d.		1360099	7.99	728497	15.08	n.d.		n.d.		n.d.		n.d.		n.d.		n.d.	
3-hydroxybenzoate	n.d.		n.d.		n.d.		n.d.		n.d.		n.d.		n.d.		n.d.		n.d.		n.d.	
3-hydroxypyridine	603480	9.05	628969	7.28	1549656	11.85	1037153	15.98	n.d.		n.d.		1309111	8.50	1210877	11.37	n.d.		n.d.	
4-aminobutanoate	54601	17.19	84207	12.45	22936	23.32	39176	5.73	103234	11.26	72047	13.41	44629	7.41	58553	11.70	n.d.		n.d.	

Metabolite	$\bar{x}$ (YP89 (*crp*$^-$))	Se (YP89 (*crp*$^-$)) [%]	$\bar{x}$ (YPIII (wt))	Se (YPIII (wt)) [%]	$\bar{x}$ (YP53 (*csrA*$^-$))	Se (YP53 (*csrA*$^-$)) [%]	$\bar{x}$ (YPIII (wt))	Se (YPIII (wt)) [%]	$\bar{x}$ (YP3 *(rovA*$^-$*))*	Se (YP3 *(rovA*$^-$*))* [%]	$\bar{x}$ (YPIII (wt))	Se (YPIII (wt)) [%]	$\bar{x}$ (YP72 *(rovM*$^-$*))*	Se (YP72 *(rovM*$^-$*))* [%]	$\bar{x}$ (YPIII (wt))	Se (YPIII (wt)) [%]	$\bar{x}$ (YP50 *(ymoA*$^-$*))*	Se (YP72 *(rovM*$^-$*))* [%]	$\bar{x}$ (YPIII (wt))	Se (YPIII (wt)) [%]
4-hydroxybenzoate	n.d.		n.d.		109222	65.78	1112250	21.43	983598	33.32	419002	80.73	453766	55.43	877264	17.80	n.d.		n.d.	
4-oxobutanoate	205491	38.48	432779	75.43	n.d.		n.d.		n.d.		n.d.		n.d.		n.d.		n.d.		n.d.	
5,6-dihydrothymine	n.d.		n.d.		220321	12.79	142261	17.03	n.d.		n.d.		n.d.		n.d.		n.d.		n.d.	
5-methylhydantoin	855225	13.84	861228	16.58	n.d.		n.d.		3497057	26.99	2165993	12.55	n.d.		n.d.		1183586	9.62	1018902	11.29
5-methylthio-adenosine	290059	5.19	316098	13.14	228278	10.14	290750	2.69	360392	4.70	386593	8.84	222856	3.09	186720	6.93	347992	5.20	331588	9.23
6-(Z)-octadecenoate	523611	12.87	1236434	5.06	1745494	6.55	1768638	17.87	1395151	19.49	2379244	8.64	2288357	3.54	2394245	6.35	2115723	14.58	3021600	10.67
6-deoxy-mannose	1849698	7.69	1920472	12.30	n.d.		n.d.		n.d.		n.d.		1052973	7.94	1100892	10.27	n.d.		n.d.	
9-(Z)-hexadecenoate	1309469	11.97	2573913	6.47	6153965	12.10	3576602	12.09	4204190	15.31	4846811	11.03	6389373	12.19	5987287	25.21	4688978	12.35	4673775	7.19
9-(Z)-hexadecenoate methyl ester	n.d.		n.d.		n.d.		n.d.		679133	8.98	482427	32.03	n.d.		n.d.		n.d.		n.d.	
adenine	12074472	8.60	13041680	9.77	23551305	7.90	24129710	8.98	24137086	6.83	26169969	9.72	26501111	10.28	22722065	8.66	16880618	6.72	17204017	5.63
adenosine	388909	14.65	367412	18.73	779355	25.48	612442	7.72	984376	12.84	902317	39.56	608533	18.45	598983	12.75	457109	28.93	265708	18.84
alanyl-alanine	6108963	20.69	0		n.d.		n.d.		n.d.		n.d.		n.d.		n.d.		n.d.		n.d.	
allo-threonine	n.d.		n.d.		n.d.		n.d.		36988	26.25	109338	40.08	n.d.		n.d.		n.d.		n.d.	
AMP	5433170	3.35	4316239	3.19	2888918	13.50	3510056	14.30	6843711	10.58	7144177	7.32	3548376	11.39	4314820	7.39	6442667	7.78	6836728	6.12
arginine	859911	1.94	620273	6.02	529811	9.05	1310133	8.90	430917	7.08	1156600	12.80	701553	10.36	1623101	11.85	1036671	3.89	1108508	7.99
asparagine	158239	7.58	53119	20.73	n.d.		n.d.		n.d.		n.d.		n.d.		n.d.		28903	14.17	60681	14.58
aspartate	524969	11.71	334452	28.77	n.d.		n.d.		858230	13.60	913898	22.95	953635	9.74	534804	9.98	28513	5.81	90181	5.07
benzene-1,2,4-triol	n.d.		n.d.		41385	21.31	59579	25.03	n.d.		n.d.		n.d.		n.d.		n.d.		n.d.	
beta-alanyl-lysine	466918	18.12	828109	14.91	n.d.		n.d.		1392843	5.54	1622437	13.59	661565	5.38	550467	13.63	521470	8.60	1277094	12.02
cysteamine	n.d.		n.d.		n.d.		n.d.		n.d.		n.d.		241329	22.50	422976	64.61	115110	5.52	61958	42.78
cytidine-2',3'-cyclic-monophosphate	n.d.		n.d.		n.d.		n.d.		n.d.		n.d.		n.d.		n.d.		30382	26.19	17561	30.58
cytosine	6821710	10.09	7632781	12.59	9530995	11.09	7798744	6.98	10815980	7.89	9985089	12.48	9615168	4.08	9235403	2.42	6681724	9.85	5064042	5.67
D200302_2009.31	n.d.		n.d.		2594428	3.83	986450	6.43	n.d.		n.d.		929666	5.91	1063171	7.14	1285498	4.16	1304240	8.60
D228685_2290.54	3338582	3.78	5062016	7.08	5143257	5.28	3681003	8.96	n.d.		n.d.		3003866	10.16	3487468	12.37	5826202	4.12	6226949	5.38
D235202_2358.7	4738376	4.97	1579288	2.13	n.d.		n.d.		n.d.		n.d.		n.d.		n.d.		n.d.		n.d.	
diethanolamine	n.d.		n.d.		n.d.		n.d.		2600565	83.47	1658467	65.24	n.d.		n.d.		n.d.		n.d.	
dodecanol	n.d.		n.d.		115306	17.51	282905	53.62	n.d.		n.d.		72748	16.26	77677	14.53	n.d.		n.d.	
ethanolamine	21344627	10.73	26252786	6.46	n.d.		n.d.		n.d.		n.d.		n.d.		n.d.		n.d.		n.d.	
ethanolaminephosphate	1253986	7.88	1626045	12.45	1135725	10.38	979918	21.55	2660667	12.43	2953482	11.70	1108794	9.75	1265782	13.25	2750529	18.55	1937758	9.26
fructose-1,6-bisphosphate	41310	9.93	11741	28.89	n.d.		n.d.		n.d.		n.d.		n.d.		n.d.		5553	47.59	28289	18.14
fumarate	178726	7.70	236203	7.90	201063	6.72	422762	7.45	556553	3.76	417943	4.43	580542	2.68	466350	3.73	221335	6.34	439023	4.98
glucoheptonate-1,4-lactone	n.d.		n.d.		3139635	7.72	1272016	14.90	n.d.		n.d.		n.d.		n.d.		837145	3.31	835584	3.99
glucono-1,5-lactone	n.d.		n.d.		n.d.		n.d.		68671	9.02	71214	13.85	n.d.		n.d.		n.d.		n.d.	
glucose	831279	6.66	1040086	5.61	4588948	7.56	2964298	10.54	916249	23.05	1130769	26.46	1762029	12.78	1587579	9.36	858023	9.03	781632	7.93
glucose-6-phosphate	n.d.		n.d.		31063	13.91	24134	32.76	74907	18.46	32336	37.51	32901	24.78	29053	25.43	n.d.		n.d.	
glutamate	25389319	10.24	4622654	11.76	5663991	11.64	7073753	9.59	14364063	12.93	8812912	8.56	15076883	4.92	8601071	8.70	n.d.		n.d.	

Metabolite	$\bar{x}$ (YP89 (*crp*$^-$))	Se (YP89 (*crp*$^-$)) [%]	$\bar{x}$ (YPIII (wt))	Se (YPIII (wt)) [%]	$\bar{x}$ (YP53 (*csrA*$^-$))	Se (YP53 (*csrA*$^-$)) [%]	$\bar{x}$ (YPIII (wt))	Se (YPIII (wt)) [%]	$\bar{x}$ (YP3 *(rovA*$^-$*))*	Se (YP3 *(rovA*$^-$*))* [%]	$\bar{x}$ (YPIII (wt))	Se (YPIII (wt)) [%]	$\bar{x}$ (YP72 *(rovM*$^-$*))*	Se (YP72 *(rovM*$^-$*))* [%]	$\bar{x}$ (YPIII (wt))	Se (YPIII (wt)) [%]	$\bar{x}$ (YP50 *(ymoA*$^-$*))*	Se (YP72 *(rovM*$^-$*))* [%]	$\bar{x}$ (YPIII (wt))	Se (YPIII (wt)) [%]
glutamine	987207	6.07	379998	12.64	n.d.		n.d.		960309	13.84	237664	8.72	323904	7.19	237463	14.15	n.d.		n.d.	
glutarate	n.d.		n.d.		n.d.		n.d.		35106	50.63	133903	91.20	49991	77.50	69874	74.56	15825	42.94	30053	55.23
glyceraldehyde	n.d.		n.d.		n.d.		n.d.		n.d.		n.d.		n.d.		n.d.		53448	46.56	25773	20.99
glycerate	n.d.		n.d.		n.d.		n.d.		40505	27.87	6390	48.54	18108	7.21	20206	11.52	n.d.		n.d.	
glycerate-3-phosphate	601125	3.17	230938	8.66	13726	77.36	67225	20.17	367114	11.87	159566	12.00	56109	20.68	85275	4.95	291582	8.17	302723	10.42
glycerol	7438691	33.67	6562644	45.74	n.d.		n.d.		n.d.		n.d.		n.d.		n.d.		n.d.		n.d.	
glycerol-3-phosphate	5751698	13.08	7213042	8.76	13712611	10.56	12227458	10.23	16388422	15.72	15787615	17.14	18511278	14.28	13932679	25.22	14194349	13.26	14712072	10.73
glycine	5204776	17.62	1263787	27.60	443645	15.59	88591	22.23	1650579	8.00	1247325	11.38	633993	6.90	578589	9.68	25421	7.89	165862	76.52
glycyl-phenylalanine	n.d.		n.d.		n.d.		n.d.		17351285	9.68	1877402	11.43	n.d.		n.d.		n.d.		n.d.	
guanine	2567500	9.44	2715970	14.71	4420129	14.86	4172901	5.25	4603912	18.94	4985520	5.19	4755519	12.81	4474492	4.11	2440328	4.00	2160980	9.87
guanosine	n.d.		n.d.		2556538	18.38	1807042	4.93	3275126	13.13	2256901	23.79	1272712	21.72	1607498	10.49	n.d.		n.d.	
guanosine-3',5'-cyclic-monophosphate	n.d.		n.d.		n.d.		n.d.		203353	16.29	258343	17.68	n.d.		n.d.		133510	21.13	149457	11.78
guanosine-5-monophosphate	28150800	4.30	14882295	16.32	367871	16.49	9113335	11.68	6306960	21.53	13165485	11.89	8516620	5.33	7600646	14.76	2896947	5.77	11317918	12.11
heptadecanoate	990576	25.08	4376868	7.12	1478200	8.11	11146712	7.10	8619465	10.82	12441966	11.11	8718911	9.44	8097008	8.00	5345156	4.98	7577996	4.34
homocysteine	n.d.		n.d.		n.d.		n.d.		68723	15.67	34450	26.76	n.d.		n.d.		n.d.		n.d.	
homoserine	n.d.		n.d.		n.d.		n.d.		n.d.		n.d.		n.d.		n.d.		43648	8.91	97242	22.77
hydroquinone	n.d.		n.d.		355491	12.68	318711	17.33	n.d.		n.d.		n.d.		n.d.		n.d.		n.d.	
hydroxylamine	970995	10.04	990853	7.61	n.d.		n.d.		n.d.		n.d.		n.d.		n.d.		n.d.		n.d.	
hypoxanthine	n.d.		n.d.		193720	9.68	130771	26.54	n.d.		n.d.		175738	24.00	186116	23.68	103013	11.60	76838	8.79
IMP	582331	25.91	573439	34.18	n.d.		n.d.		2574607	38.32	1942927	19.69	n.d.		n.d.		2035217	29.91	1295403	19.10
isoleucine	8221248	13.41	10430799	16.21	8443291	6.65	12660987	6.08	9087108	9.41	7161364	10.90	18732871	4.41	15476560	7.40	15012883	11.27	18842504	7.51
itaconate	n.d.		n.d.		11883023	7.88	8496801	5.74	6941576	17.75	5528728	18.08	8647901	3.25	9414053	7.06	n.d.		n.d.	
lactate	n.d.		n.d.		n.d.		n.d.		n.d.		n.d.		728601	28.08	747759	40.66	n.d.		n.d.	
leucine	7984197	12.68	10118341	21.76	11226925	9.74	17719478	10.37	23170958	10.03	24901427	11.91	25235642	5.51	24779278	7.58	31659658	17.28	33843711	13.70
lysine	4337792	12.21	5293325	20.56	44119794	9.80	57354586	19.20	37604135	7.95	55246268	6.56	57203808	7.60	41731591	9.10	7615766	14.15	8312538	11.75
malate	172138	17.96	244875	12.26	89572	17.32	269336	7.59	655707	10.99	395664	9.52	457827	6.65	305398	4.11	129135	6.11	372211	11.56
maleate	n.d.		n.d.		380781	50.46	258834	27.10	n.d.		n.d.		190080	16.45	195250	26.55	n.d.		n.d.	
mannitol	n.d.		n.d.		n.d.		n.d.		n.d.		n.d.		n.d.		n.d.		20044430	13.62	23435323	16.53
methionine	310987	8.34	664649	22.98	872788	4.85	1746950	7.73	4199170	5.74	2679414	7.75	2166524	2.93	2158976	3.64	1844715	12.32	1873896	8.68
myo-inositol	55821	21.91	126433	9.78	36992	9.78	161392	8.34	284251	7.90	184651	9.05	221223	3.07	38046	45.69	329389	8.19	324161	14.43
NA_1175.82	n.d.		n.d.		n.d.		n.d.		n.d.		n.d.		n.d.		n.d.		n.d.		n.d.	
NA_2019.3	831852	3.69	790782	6.32	n.d.		n.d.		n.d.		n.d.		n.d.		n.d.		n.d.		n.d.	
NA102	600216	9.18	746656	17.31	n.d.		n.d.		n.d.		n.d.		n.d.		n.d.		n.d.		n.d.	
NA114002_1144.3	16706638	8.80	14457756	6.43	n.d.		n.d.		n.d.		n.d.		n.d.		n.d.		n.d.		n.d.	
NA135011_1366.01	398740	12.82	137597	14.48	134867	6.77	255461	8.62	521776	7.45	462885	17.17	268304	9.08	235262	7.88	n.d.		n.d.	
NA162008_1636.84	1507808	20.92	0		n.d.		n.d.		n.d.		n.d.		n.d.		n.d.		1710493	14.12	191422	83.48
NA163015_1642.75	197243	15.75	0		158050	13.76	84569	10.93	n.d.		n.d.		n.d.		n.d.		137375	8.86	74564	10.53
NA164	n.d.		n.d.		1687759	5.32	1209634	7.11	n.d.		n.d.		n.d.		n.d.		n.d.		n.d.	

Metabolite	$\bar{x}$ (YP89 (*crp*$^-$))	Se (YP89 (*crp*$^-$)) [%]	$\bar{x}$ (YPIII (wt))	Se (YPIII (wt)) [%]	$\bar{x}$ (YP53 (*csrA*$^-$))	Se (YP53 (*csrA*$^-$)) [%]	$\bar{x}$ (YPIII (wt))	Se (YPIII (wt)) [%]	$\bar{x}$ (YP3 *(rovA*$^-$*))*	Se (YP3 *(rovA*$^-$*))* [%]	$\bar{x}$ (YPIII (wt))	Se (YPIII (wt)) [%]	$\bar{x}$ (YP72 *(rovM*$^-$*))*	Se (YP72 *(rovM*$^-$*))* [%]	$\bar{x}$ (YPIII (wt))	Se (YPIII (wt)) [%]	$\bar{x}$ (YP50 *(ymoA*$^-$*))*	Se (YP72 *(rovM*$^-$*))* [%]	$\bar{x}$ (YPIII (wt))	Se (YPIII (wt)) [%]
NA184030_1848.26	n.d.		n.d.		n.d.		n.d.		n.d.		n.d.		n.d.		n.d.		n.d.		n.d.	
NA226	2879440	9.70	4792105	4.53	6532019	8.43	7859567	8.75	8101450	7.75	6851975	4.05	8887985	8.67	8481666	5.24	6475111	8.62	6876328	5.04
NA229001428	0		980094	14.99	n.d.		n.d.		n.d.		n.d.		n.d.		n.d.		1161332	5.91	1429191	9.42
NA250	1022846	4.73	997812	2.76	n.d.		n.d.		1650701	9.90	2763777	4.66	1041663	6.54	977177	6.91	2037398	4.66	1898506	3.97
NA284	107404	6.42	195943	7.28	297517	5.25	476143	5.66	n.d.		n.d.		n.d.		n.d.		n.d.		n.d.	
NA349	61333	28.51	173926	10.50	369604	6.10	158902	7.16	216161	4.76	213870	8.85	184836	7.20	194611	9.57	n.d.		n.d.	
NA377	n.d.		n.d.		n.d.		n.d.		103074	13.96	189146	7.79	202260	15.69	141815	14.59	178222	11.26	164489	7.06
NA411	6669729	8.22	4679678	25.08	1682373	6.69	6479283	5.24	10817795	13.16	7650303	25.71	1220503	13.17	8894474	5.78	n.d.		n.d.	
NA438	114523	22.37	260250	8.61	0		241550	7.91	22580	15.26	399328	12.02	288005	7.22	348098	4.26	3187	100.00	404770	12.35
NA451	n.d.		n.d.		n.d.		n.d.		n.d.		n.d.		n.d.		n.d.		22788	100.00	606440	12.81
NA501	n.d.		n.d.		n.d.		n.d.		n.d.		n.d.		n.d.		n.d.		1059571	5.55	1454509	4.03
NA524	n.d.		n.d.		1960914	16.60	947804	8.31	n.d.		n.d.		1177252	3.97	1054544	23.48	n.d.		n.d.	
NA66	n.d.		n.d.		17945	11.41	22417	15.25	n.d.		n.d.		n.d.		n.d.		n.d.		n.d.	
NA668	n.d.		n.d.		1205846	22.55	1376976	27.66	n.d.		n.d.		1244266	30.35	1286857	10.36	n.d.		n.d.	
NA690	n.d.		n.d.		1253801	9.73	996533	14.50	n.d.		n.d.		n.d.		n.d.		n.d.		n.d.	
NA695	n.d.		n.d.		2046859	16.90	2551591	16.58	n.d.		n.d.		n.d.		n.d.		n.d.		n.d.	
NA76	748412	4.00	805120	5.41	1569567	6.66	1682573	7.69	n.d.		n.d.		2364704	6.13	1923797	6.45	780126	9.29	799790	5.19
NA86	141769	12.69	202604	25.32	n.d.		n.d.		n.d.		n.d.		n.d.		n.d.		n.d.		n.d.	
n-hexadecenoate	4974056	45.38	2865321	93.94	863683	15.12	3318714	76.21	n.d.		n.d.		4016600	47.92	4864612	42.74	n.d.		n.d.	
nicotinamide	n.d.		n.d.		750065	18.22	322074	15.92	1345479	29.16	1758393	29.61	357913	20.72	617353	18.66	n.d.		n.d.	
nicotinate	n.d.		n.d.		265699	12.04	241678	14.86	163616	25.06	286156	33.82	290115	5.47	164341	16.06	n.d.		n.d.	
ornithine	5145491	9.69	2712857	13.72	1783459	6.91	4048517	8.55	1155270	10.93	3479346	11.23	944357	11.43	2253692	14.89	3880347	9.03	3814480	9.75
ornithine-1,5-lactam	n.d.		n.d.		820238	5.61	612940	6.62	n.d.		n.d.		545504	4.72	591051	5.72	n.d.		n.d.	
oxalate	n.d.		n.d.		106053	76.40	104128	77.63	n.d.		n.d.		n.d.		n.d.		n.d.		n.d.	
pentadecanoate	0		2736143	5.12	1248856	5.55	6396988	9.97	5759384	8.72	10340754	9.18	4109061	6.22	3844950	6.67	2866609	3.32	4361539	6.05
phenylalanine	4511936	12.42	4699569	15.93	901261	12.81	1998768	16.17	3627931	9.72	2233609	9.28	9752384	8.55	7591782	7.37	2699393	17.91	2316227	11.05
phenylethylamine	n.d.		n.d.		118753	9.05	94734	11.27	n.d.		n.d.		77786	25.24	86031	20.22	45494	13.96	31807	12.38
phosphoenolpyruvate	183796	11.84	64504	13.50	n.d.		n.d.		142933	12.44	89072	13.10	n.d.		n.d.		81605	12.18	126730	18.47
phosphate monomethyl ester	476940	1.58	474555	4.20	408043	12.39	432367	4.40	842959	6.93	723403	11.63	641498	5.82	628277	4.72	566506	10.84	661698	2.99
putrescine	60807166	7.96	66160336	7.34	74898146	13.78	55821417	9.47	71114634	22.27	80134160	33.58	54927417	10.55	64223230	10.84	79063941	13.90	80994124	16.05
pyroglutamate	32965259	7.68	13219481	10.76	12996915	10.22	11563178	8.90	17185633	14.00	14370570	10.20	21849360	17.95	15444901	7.59	n.d.		n.d.	
pyrophosphate	575142	25.82	834319	33.98	n.d.		n.d.		n.d.		n.d.		n.d.		n.d.		268492	30.22	799792	19.37
pyruvate	n.d.		n.d.		171970	32.77	123115	25.31	n.d.		n.d.		n.d.		n.d.		n.d.		n.d.	
ribose	3054	31.53	1	58.64	n.d.		n.d.		n.d.		n.d.		n.d.		n.d.		n.d.		n.d.	
serine	30197	32.61	9694	52.82	n.d.		n.d.		n.d.		n.d.		4278907	63.25	2414413	56.02	7445648	94.96	16972091	56.86
sorbitol	13952892	9.22	14625636	8.12	29457235	8.41	18724925	25.44	n.d.		n.d.		34127776	21.35	19183555	29.59	n.d.		n.d.	
spermidine	1934681	7.98	3809420	5.61	5417788	13.24	3905431	10.42	6119325	6.04	6611165	8.77	3629676	6.75	3718317	6.62	6703830	6.19	7670662	3.81
succinate-methylester	123852	34.39	640272	2.94	230071	27.56	579843	6.53	914104	17.40	831333	11.75	1134922	6.28	987528	7.17	n.d.		n.d.	
threonine	251218	14.88	65491	19.18	n.d.		n.d.		106569	9.69	70488	19.36	41484	33.64	39093	15.48	n.d.		n.d.	

Metabolite	$\bar{x}$ (YP89 (*crp*$^-$))	Se (YP89 (*crp*$^-$)) [%]	$\bar{x}$ (YPIII (wt))	Se (YPIII (wt)) [%]	$\bar{x}$ (YP53 (*csrA*$^-$))	Se (YP53 (*csrA*$^-$)) [%]	$\bar{x}$ (YPIII (wt))	Se (YPIII (wt)) [%]	$\bar{x}$ (YP3 *(rovA*$^-$*))*	Se (YP3 *(rovA*$^-$*))* [%]	$\bar{x}$ (YPIII (wt))	Se (YPIII (wt)) [%]	$\bar{x}$ (YP72 *(rovM*$^-$*))*	Se (YP72 *(rovM*$^-$*))* [%]	$\bar{x}$ (YPIII (wt))	Se (YPIII (wt)) [%]	$\bar{x}$ (YP50 *(ymoA*$^-$*))*	Se (YP72 *(rovM*$^-$*))* [%]	$\bar{x}$ (YPIII (wt))	Se (YPIII (wt)) [%]
thymine	7479876	9.45	8313404	10.76	12466139	15.66	11774912	10.58	18152444	20.44	16382966	11.16	13871468	8.44	13992360	2.96	11928814	6.73	8939944	8.80
tridecanoate	n.d.		n.d.		n.d.		n.d.		2906737	3.52	3005233	10.56	n.d.		n.d.		n.d.		n.d.	
tryptamine	n.d.		n.d.		n.d.		n.d.		528152	14.73	919392	8.81	n.d.		n.d.		n.d.		n.d.	
tryptophan	1535218	16.15	1853475	32.95	n.d.		n.d.		1813230	19.44	1563661	18.82	1756072	9.78	1565575	14.92	3552591	14.63	4022371	13.10
tyrosine	5597157	5.49	5772702	8.65	n.d.		n.d.		n.d.		n.d.		6936127	5.69	6511524	5.75	6778137	8.25	10295774	8.50
Unknown#bth-pae-035_1530.4	619843	3.42	506285	7.12	1550879	2.95	1276173	4.18	n.d.		n.d.		820894	9.98	682718	6.37	583331	12.54	572053	4.70
Unknown#bth-pae-036_1549.1	803315	10.57	825872	14.42	n.d.		n.d.		794900	12.01	942575	24.70	n.d.		n.d.		1103923	10.76	691737	10.61
Unknown#bth-pae-039_1586.9	1463468	11.63	1677878	8.75	2268027	6.96	1757910	8.86	n.d.		n.d.		n.d.		n.d.		n.d.		n.d.	
unknown#mse-ypy_2600	n.d.		n.d.		n.d.		n.d.		1569284	40.92	55893	68.40	n.d.		n.d.		n.d.		n.d.	
Unknown#mse-ypy-001_1846.9	2250498	6.72	217293	22.98	n.d.		n.d.		n.d.		n.d.		n.d.		n.d.		n.d.		n.d.	
Unknown#mse-ypy-002_1_2922.4	3627635	9.15	566605	16.87	633084	15.62	315606	17.89	284885	19.74	399660	14.26	540701	8.32	606295	11.69	2355622	5.67	782849	15.88
Unknown#mse-ypy-002_2_2955.1	21579569	7.73	1601106	24.62	n.d.		n.d.		n.d.		n.d.		322085	27.58	594019	21.26	n.d.		n.d.	
Unknown#mse-ypy-003_1093.7	5292944	12.35	5792183	11.66	10460928	10.36	12916148	6.81	15245782	11.49	10937189	4.97	10504213	7.87	11101820	10.89	4719031	15.33	6111473	10.34
Unknown#mse-ypy-006_1744.2	n.d.		n.d.		n.d.		n.d.		1861467	11.56	2968791	8.15	3468890	5.42	3178324	11.29	1727762	9.36	3034741	4.68
Unknown#mse-ypy-008_1437.2	n.d.		n.d.		1168086	9.62	1095125	8.99	n.d.		n.d.		n.d.		n.d.		n.d.		n.d.	
Unknown#mse-ypy-009_1493.0	1969097	8.04	469619	7.19	866314	9.37	679223	6.30	594442	7.39	508689	4.38	712092	7.01	692239	5.66	1730551	5.61	813191	6.29
Unknown#mse-ypy-016_1793.3	n.d.		n.d.		n.d.		n.d.		n.d.		n.d.		1950346	79.53	2165221	70.13	n.d.		n.d.	
Unknown#mse-ypy-017_1896.2	1003297	18.23	1348247	16.55	4067917	7.75	1864381	14.19	n.d.		n.d.		1996566	10.28	1979434	11.36	n.d.		n.d.	
Unknown#mse-ypy-018_2013.2	n.d.		n.d.		526077	5.25	557420	5.98	765797	3.82	820024	4.08	726595	3.35	684176	5.81	637116	5.03	724989	6.50
Unknown#mse-ypy-019_2018.4	0		507665	6.73	n.d.		n.d.		n.d.		n.d.		n.d.		n.d.		n.d.		n.d.	
Unknown#mse-ypy-021_2090.4	n.d.		n.d.		97311	7.98	104297	6.76	149267	13.03	134997	9.22	157094	7.41	127547	5.41	145710	6.47	162244	4.23
Unknown#mse-ypy-022_2109.5	780212	10.40	970186	15.25	1348129	2.78	825290	13.53	n.d.		n.d.		774305	12.47	710409	9.13	n.d.		n.d.	
Unknown#mse-ypy-	1729255	8.33	1227545	18.98	973513	12.28	6982631	10.11	2945885	8.86	4951357	11.13	6457904	3.75	5802421	10.14	1232434	4.97	2826646	7.11

Metabolite	$\bar{x}$ (YP89 (*crp*$^-$))	Se (YP89 (*crp*$^-$)) [%]	$\bar{x}$ (YPIII (wt))	Se (YPIII (wt)) [%]	$\bar{x}$ (YP53 (*csrA*$^-$))	Se (YP53 (*csrA*$^-$)) [%]	$\bar{x}$ (YPIII (wt))	Se (YPIII (wt)) [%]	$\bar{x}$ (YP3 *(rovA*$^-$*))*	Se (YP3 *(rovA*$^-$*))* [%]	$\bar{x}$ (YPIII (wt))	Se (YPIII (wt)) [%]	$\bar{x}$ (YP72 *(rovM*$^-$*))*	Se (YP72 *(rovM*$^-$*))* [%]	$\bar{x}$ (YPIII (wt))	Se (YPIII (wt)) [%]	$\bar{x}$ (YP50 *(ymoA*$^-$*))*	Se (YP72 *(rovM*$^-$*))* [%]	$\bar{x}$ (YPIII (wt))	Se (YPIII (wt)) [%]
023_2128.1																				
Unknown#mse-ypy-026_2236.8	202276	26.47	423849	15.23	n.d.		n.d.		150196	18.21	128058	20.95	n.d.		n.d.		123957	9.39	364866	30.40
Unknown#mse-ypy-028_2276.9	434986	16.30	577994	22.61	n.d.		n.d.		337123	11.96	456489	16.67	n.d.		n.d.		114308	23.31	534226	11.84
Unknown#mse-ypy-030_2498.7	2029657	14.82	1441914	15.18	n.d.		n.d.		1423593	40.43	883459	31.88	n.d.		n.d.		637389	10.57	1896382	19.16
Unknown#mse-ypy-036_1981.9	71912	10.08	129737	5.67	0		84435	7.43	61130	11.51	136178	14.53	157532	7.21	164727	4.26	64271	12.83	206293	7.07
Unknown#mse-ypy-037_2590.9	n.d.		n.d.		n.d.		n.d.		n.d.		n.d.		n.d.		n.d.		118908	5.30	106141	6.08
Unknown#mse-ypy-039_3026.6	n.d.		n.d.		3471964	13.56	3364720	13.84	3095927	15.73	5201820	10.47	2900665	11.51	3453521	13.39	4280588	9.26	3877625	9.93
Unknown#mse-ypy-2830.39	n.d.		n.d.		n.d.		n.d.		430532	9.12	360966	20.69	n.d.		n.d.		299567	17.65	277190	19.01
Unknown#sst-cgl-028_1478.9	n.d.		n.d.		207513	15.25	201759	16.24	n.d.		n.d.		n.d.		n.d.		n.d.		n.d.	
Unknown#sst-cgl-094_2097.4	938669	3.39	877497	9.24	n.d.		n.d.		n.d.		n.d.		n.d.		n.d.		n.d.		n.d.	
Uracil	3756481	9.44	4051962	9.11	10930919	6.58	9413397	7.21	9156466	8.57	7946501	8.25	9781806	4.86	9533693	9.65	6861684	7.21	5937531	7.03
urea	n.d.		n.d.		n.d.		n.d.		865334	20.03	796617	10.27	1061306	30.14	1024699	16.37	n.d.		n.d.	
valine	12557250	12.95	20395284	9.78	12512341	8.67	20771372	7.59	33438316	5.66	28969474	6.60	26434373	3.27	24551673	8.70	10473637	11.96	17128254	13.19

*E.4 Scatterplots of the metabolic profiles of the mutant strains YP3 (*rovA$^-$*) vs. the wild type strain YPIII*

Scatterplot of the metabolic profiles of the mutant strain YP3 (*rovA*$^-$) vs. the wild type strain YPIII

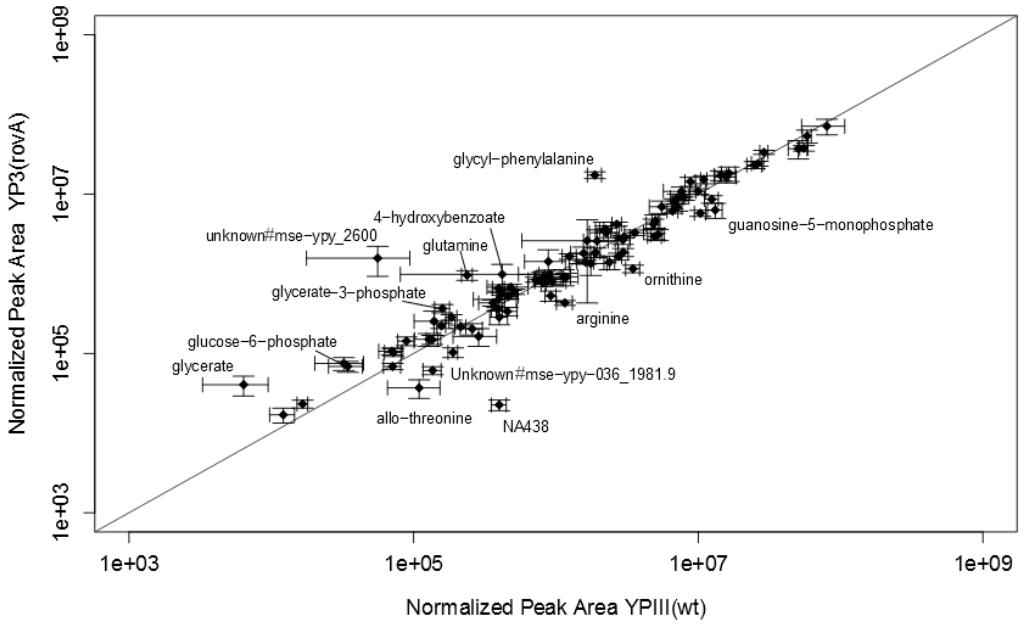

Scatterplot of the metabolic profiles of the mutant strain YP72 (*rovM*$^-$) vs. the wild type strain YPIII

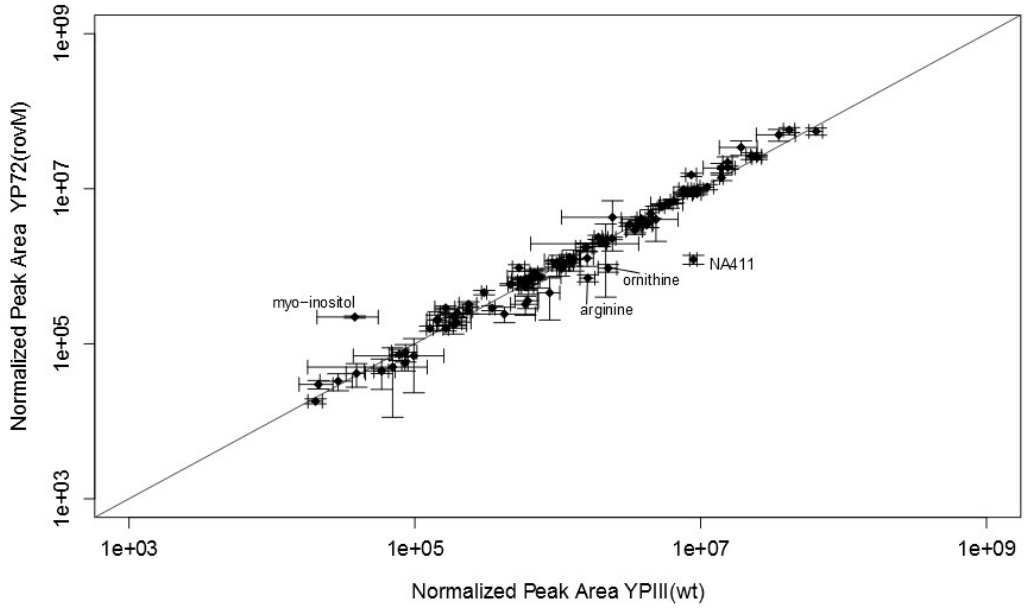

Scatterplot of the metabolic profiles of the mutant strain YP89 (*crp*$^-$) vs. the wild type strain YPIII

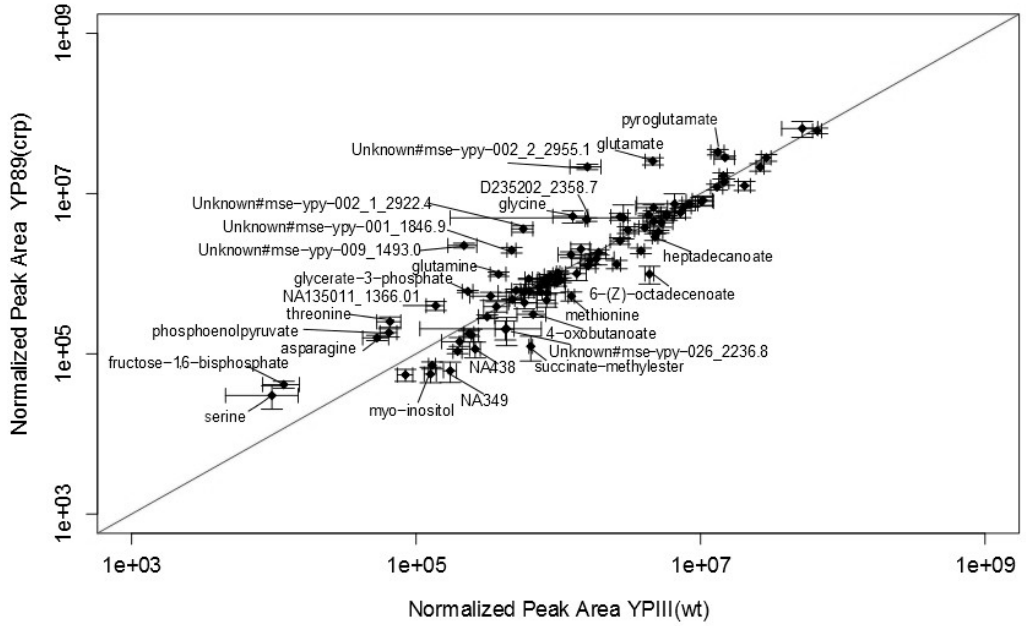

Danksagung

Zur Entstehung dieser Arbeit haben viele Personen beigetragen, bei denen ich mich an dieser Stelle aufrichtig bedanken möchte, auch wenn es zu viele sind, um sie alle namentlich zu nennen. Bei Herrn Prof Dietmar Schomburg möchte ich mich für die Möglichkeit an diesem spannenden Thema zu arbeiten und meine Doktorarbeit in seiner Arbeitsgruppe anzufertigen bedanken Außerdem gilt mein Dank Frau Prof. Petra Dersch, für die Übernahme des Zweitgutachtens, die freundliche Betreuung und die fachlichen Anregungen. Ein herzlichen Dank auch an Herrn Prof. Dieter Jahn für die unkomplizierte Bereitschaft den Vorsitz der Prüfungskommission zu übernehmen.

Besonders bei Dr. Kerstin Schmidt-Hohagen möchte ich mich bedanken, für die viele Hilfe bei der Korrektur dieser Arbeit und die stetige Bereitschaft zu Diskussion, außerdem bei Dr. Ann Kathrin Heroven, für die gute Zusammenarbeit und die freundliche Unterstützung.

Ein großer Dank gebührt auch den aktuellen und ehemaligen Mitgliedern in der Arbeitsgruppe für fruchtvolle Diskussionen, Hilfestellung, soziale Zerstreuung, und die Erweiterung meines Horizontes. Insbesondere bedanke ich mich bei Ingrid Hartwig für die gemeinsame Arbeit an *Yersinia*, sowie ganz besonders bei Dr. Christian Jäger, Dr. Christian Scherling und Dr. Lorenz Reimer, die viel für meine Weiterbildung getan haben.

Ein sehr großer Dank gilt meinen Eltern für ihr Vertrauen, den unerschütterlichen Rückhalt, und die Möglichkeit meinen eigenen Weg suchen zu können. Ich möchte mich auch bei meiner erweiterten Familie Kamila, Anita und Lina bedanken, die mich sehr glücklich durch ihre Freundschaft und ihre Hilfe machen. Und ganz besonders will ich mich bei Jan-Erik bedanken, für die unglaubliche Unterstützung und vor allem dafür, dass er mein Leben so viel schöner macht.